

The author(s) shown below used Federal funds provided by the U.S. Department of Justice and prepared the following final report:

Document Title: Reducing Uncertainty of Quantifying the Burning Rate of Upholstered Furniture

Author: Marc L. Janssens

Document No.: 239050

Date Received: July 2012

Award Number: 2010-DN-BX-K221

This report has not been published by the U.S. Department of Justice. To provide better customer service, NCJRS has made this Federally-funded grant final report available electronically in addition to traditional paper copies.

Opinions or points of view expressed are those of the author(s) and do not necessarily reflect the official position or policies of the U.S. Department of Justice.

SOUTHWEST RESEARCH INSTITUTE®

6220 CULEBRA RD. 78238-5166 • P.O. DRAWER 28510 78228-0510 • SAN ANTONIO, TEXAS, USA • (210) 684-5111 • WWW.SWRI.ORG
CHEMISTRY AND CHEMICAL ENGINEERING DIVISION
FIRE TECHNOLOGY DEPARTMENT
WWW.FIRE.SWRI.ORG
FAX (210) 522-3377



REDUCING UNCERTAINTY OF QUANTIFYING THE BURNING RATE OF UPHOLSTERED FURNITURE

FINAL REPORT
Consisting of 207 Pages

SwRI® Project No. 01.15998
Award No.: 2010-DN-BX-K221
Period of Performance: October 1, 2010 – March 31, 2012
Final Report Date: May 31, 2012

Prepared for:

National Institute of Justice, OJP
810 Seventh Street N.W.
Washington, DC 20531

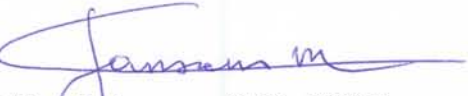
This project was supported by Award No. 2010-DN-BX-K221, awarded by the National Institute of Justice, Office of Justice Programs, U.S. Department of Justice. The opinions, findings, and conclusions or recommendations expressed in this publication/program/exhibition are those of the author(s) and do not necessarily reflect those of the Department of Justice.

Performed by:


Marc L. Janssens (Principal Investigator)
Christina Gomez
Jason P. Huczek
Kristopher J. Overholt

David M. Ewan
Marcelo M. Hirschler
Robert L. Mason
J. Marshall Sharp

Prepared by:


Marc L. Janssens, Ph.D., FSFPE
Senior Engineer
Center for Nuclear Waste Regulatory Analyses

Approved by:


Matthew S. Blais, Ph.D.
Director
Fire Technology Department

This report is for the information of the client. It may be used in its entirety for the purpose of securing product acceptance from duly constituted approval authorities. This report shall not be reproduced except in full, without the written approval of SwRI. Neither this report nor the name of the Institute shall be used in publicity or advertising.



ABSTRACT

The goal of this project was to develop guidelines on how to best estimate the burning rate of upholstered furniture and quantify/optimize the uncertainty of the predictions. This uncertainty consists of an aleatory and an epistemic component. The focus was on the epistemic component, which is often the largest of the two components and the hardest to quantify. Primary sources of epistemic uncertainty of the heat release rate (HRR) of upholstered furniture are the lack of knowledge of the ignition scenario and limited understanding of enclosure effects.

To accomplish the project goal two series of full-scale furniture and room calorimeter tests were performed. The first series was a parametric study involving 79 full-scale fire tests on upholstered furniture mockups. The primary objective of these tests was to quantify ignition scenario (including incendiary) and enclosure effects on the HRR of upholstered furniture. The test matrix was partly based on fractional factorial designs.

Small-scale tests were performed to obtain fire properties of the two fabrics and six padding materials and specific fabric-padding combinations used in the construction of the mockups. Tests were conducted in the Cone Calorimeter (ASTM E 1354) and the Microscale Combustion Calorimeter (ASTM D 7309). In addition, specimens of the six padding materials were tested to verify their compliance (or non-compliance) with CA TB 117.

The predictive capability of three upholstered furniture burning rate models (referred to as Babrauskas, Babrauskas 2, and CBUF) was determined based on the results of the parametric study and small-scale test data for the mockup materials. One of the three models (Babrauskas) was slightly modified to improve agreement between calculated and measured HRR. In addition, an attempt was made to use the field fire model Fire Dynamics Simulator (FDS) to better account for the effect of the exact location of the ignition source on flame spread over the seating surface.

The compartment fire models Consolidated Model of Fire Growth and Smoke Transport and FDS were used to determine how the use of the upholstered furniture burning rate models (compared to the use of measured HRR data) affect the accuracy of temperature and heat flux estimates in the room.

Twenty-two sets of used upholstered furniture were obtained for the second series of full-scale tests. Twenty-seven full-scale room fire tests were conducted on at least one item in each set. A reduced number of Cone Calorimeter and Microscale Combustion Calorimeter tests were performed on the soft components. Specimens of the padding materials were tested to verify their non-compliance with CA TB 117.

The small- and full-scale test data on the used furniture (components) were used to assess the predictive capability of the aforementioned upholstered furniture burning rate models. In this case the models significantly underpredicts the peak HRR. The Babrauskas model, with a fabric factor of 0.4 and a padding factor of 0.8, gave the best agreement ($R^2 = 0.72$), but the calculated peak heat release had to be increased by 50% (and burning time reduced by 33%). The accuracy of the Babrauskas model needs refinement and more work is needed to improve the predictions. It will take some time to conduct the additional analysis and in the meantime it is suggested that an alternative approach involving a sensitivity analysis be used.

The results and report of this study will be made available to the fire investigation community over the Internet. Video DVDs were created as training materials that will give arson investigators the opportunity to witness the full-scale fire tests a posteriori and help them develop a better understanding of fire dynamics in upholstered furniture fires.

TABLE OF CONTENTS

	PAGE
1 EXECUTIVE SUMMARY	1
2 INTRODUCTION.....	8
2.1 STATEMENT OF THE PROBLEM	8
2.2 LITERATURE REVIEW	9
2.3 RATIONALE FOR THE RESEARCH	23
3 METHODS.....	24
3.1 OVERVIEW	24
3.2 FULL-SCALE EXPERIMENTAL SETUP	26
3.3 FULL-SCALE FURNITURE MOCKUP TESTS.....	32
3.4 SMALL-SCALE FURNITURE MOCKUP TESTS.....	44
3.5 MODELING OF MOCKUP FURNITURE TESTS	45
3.6 FULL-SCALE USED FURNITURE TESTS	46
3.7 SMALL-SCALE USED FURNITURE TESTS	47
3.8 MODELING OF USED FURNITURE TESTS.....	48
4 RESULTS.....	49
4.1 TEST ID STRING.....	49
4.2 FURNITURE MOCKUP TESTS	50
4.3 MODELING OF MOCKUP FURNITURE TESTS	64
4.4 USED FURNITURE TESTS.....	70
4.5 MODELING OF USED FURNITURE TESTS.....	73
5 CONCLUSIONS	76
5.1 DISCUSSION OF FINDINGS	76
5.2 IMPLICATIONS FOR POLICY AND PRACTICE.....	80
5.3 IMPLICATIONS FOR FURTHER RESEARCH	81
6 REFERENCES	82
6.1 CODES AND STANDARDS	82
6.2 CITED REFERENCES	85
7 DISSEMINATION OF RESEARCH FINDINGS.....	89
7.1 PUBLICATIONS AND PRESENTATIONS.....	89
7.2 DATA	90
7.3 VIDEO	90

Appendix A: Mathematical Modeling of Compartment Fires

Appendix B: Experimental Methods and Measurement Uncertainty Calculations

Appendix C: Upholstered Furniture Burning Rate Correlations and Models

Appendix D: Pictures of Used Furniture Obtained for Testing

Appendix E: Triangular HRR Approximations for Fractional Factorial Design Analysis

Appendix F: Tukey Multiple Comparisons

Appendix G: Burning Rate Predictions for Open Calorimeter Mockup Tests

Appendix H: Burning Rate Predictions for Fractional Factorial Design Tests

Appendix I: Burning Rate Predictions for Remaining Room Calorimeter Mockup Tests

Appendix J: Burning Rate Predictions for Used Furniture Tests

LIST OF TABLES

	PAGE
Table 1. Averages and Standard Deviations for the Used Furniture Tests.....	7
Table 2. Characteristics of Ignition Sources for Upholstered Furniture.....	10
Table 3. Results Reported by Tu and Mitler.	12
Table 4. Chair Materials Used in Cleary et al. Study.	13
Table 5. Ignition Sources Used in Cleary et al. Study.....	13
Table 6. Cleary et al. Study PHRR Results.	14
Table 8. Chair Materials in CBUF Study with EN-1021-2 Source.	16
Table 9. CBUF PHRRs for Medium Intensity Ignition Sources.	16
Table 10. CBUF Results with Non FR Chair and FR Chair.....	17
Table 11. Results from Study by Babrauskas et al.	19
Table 12. Results from Study by Parker et al.	20
Table 13. Results from CBUF Ventilation Effect Study.	22
Table 14. Distance of Tree TCs above the Floor or below the Door Header.	28
Table 15. Fabrics and Padding Materials for Mockup Cushions.....	33
Table 16. Open Calorimeter Mockup Tests.....	42
Table 17. Possible One-Third Fractions of a 3 ³ Factorial Experiment.	44
Table 18. Details of the Fractional Factorial Experiments.	44
Table 19. Additional Room Calorimeter Tests on Mockups.	45
Table 20. Selected Cone Calorimeter Test Data for Mockup Specimens.	45
Table 21. Details of the Used Furniture Sets Obtained for Testing.....	47
Table 22. Selected Cone Calorimeter Test Data for Used Furniture Specimens.....	48
Table 23. System for Composing and Deciphering the Test ID String.	49
Table 24. List of Open Calorimeter Mockup Tests.	50
Table 25. List of Fractional Factorial Design Tests.	57
Table 26. Response Variables for 1-Seat Sofa Triangular HRR Approximations.	58
Table 27. Response Variables for 3-Seat Sofa Triangular HRR Approximations.	59
Table 28. ANOVA Results.....	60
Table 29. List of Open Calorimeter Mockup Tests.	61
Table 31. Used Furniture Data to Construct HRR Curves for Sensitivity Analysis.....	79

LIST OF FIGURES

	PAGE
Figure 1. Enclosure Effects in CBUF Study.	21
Figure 3. Plan View of Test Room.	28
Figure 4. 1-Seat Sofa Mockup Placed on Scale prior to Testing.	29
Figure 5. TC Tree above Specimen and Wall Heat Flux Meters.	29
Figure 6. Back Corner in Test Room Opposite Specimen.	30
Figure 7. Doorway TC Tree Moved to the Side for Easy Room Access.	30
Figure 8. Test Shortly after Ignition with Small Flame.	31
Figure 9. Test on 1-Seat Sofa near Peak Burning.	31
Figure 10. HRR of Liquid Pool Fire Ignition Sources.	35
Figure 11. Locations of Small Burner Flame (B), S = Top, F = Front, B= Back.	35
Figure 12. Small Flame Ignition Source Applied to Top (BS).	36
Figure 13. Small Flame Ignition Source Applied to Front Bottom (BF).	36
Figure 14. Small Flame Ignition Source Applied to Back (BB).	37
Figure 15. Locations of Large Burner Flame (C), S = Top, F = Front, B= Back.	37
Figure 16. Large Flame Ignition Source Applied to Top (CS).	38
Figure 17. Front Bottom Large Flame Ignition Source prior to Ignition (CF).	38
Figure 18. Large Flame Ignition Source Applied to Front Bottom (CF).	39
Figure 19. Locations of Liquid Pool Fire (A), S = Top, F = Front, B= Back.	39
Figure 20. Gasoline Distributed over Seat Cushion (AS).	40
Figure 21. Liquid Pool Fire Applied to Top (AS).	40
Figure 22. Gasoline Distributed over Ceramic Fiber Blanket (AF)	41
Figure 23. Liquid Pool Fire Applied to Front Bottom (AS).	41
Figure 24. Measurement Uncertainty of 1-Seat Sofa Mockup HRR.	51
Figure 25. HRR Repeatability for a 1-Seat Sofa Ignited by a Large Flame.	52
Figure 26. HRR Repeatability for a 1-Seat Sofa Ignited by a Small Flame.	52
Figure 27. SOM123CS1 during Large Burner Flame Exposure.	53
Figure 28. SOM123CS1: Flames Spread from Ignited Side to the Other Side.	54
Figure 29. Effect of Ignition Source Location on HRR of a 3-Seat Sofa.	54
Figure 30. SOM123CS2: Flames Spread from Center to Both Sides.	55
Figure 31. Triangular Approximation of HRR Curve.	58
Figure 32. Enclosure Effect on HRR for Large Flame Ignition Source.	62
Figure 33. Enclosure Effect on HRR for Small Flame Ignition Source.	63
Figure 34. Effect of Small Flame Location on HRR of 1-Seat Sofa.	63
Figure 35. Effect of Small Flame Location on HRR of 1-Seat Sofa.	64
Figure 36. Calculated vs. Measured PHRR for All Mockup Tests (All Models).	66
Figure 37. Calculated vs. Measured PHRR for All Mockup Tests (Babrauskas).	66
Figure 38. Calculated vs. Measured PHRR for All Mockup Tests (Babrauskas 2).	67
Figure 39. Calculated vs. Measured PHRR for All Mockup Tests (CBUF).	67
Figure 40. Measured vs. Calculated HRR (LRM123AF1).	68
Figure 41. CFAST HGL Temperature Predictions (LRM123AF1).	69

Figure 42. Measured vs. Calculated HRR (LRM123BC1).	69
Figure 43. CFAST HGL Temperature Predictions (Small Flame Ignition).	70
Figure 45. Effect of Ignition Source Strength on HRR of a 1-Seat Sofa.....	72
Figure 46. Measurement Uncertainty of the HRR of a Used 1-Seat Sofa.....	73
Figure 47. Calculated vs. Measured PHRR for Used Furniture (All Models).	74
Figure 48. Calculated vs. Measured PHRR for Used Furniture (Babrauskas).	74
Figure 49. Calculated vs. Measured PHRR for Used Furniture (Babrauskas 2).	75
Figure 50. Calculated vs. Measured PHRR for Used Furniture (CBUF).	75
Figure 51. Calculated vs. Measured PHRR (Babrauskas Adjusted).	76
Figure 52. Snapshot of Video of Test LRU161AS1.....	90

1 EXECUTIVE SUMMARY

The reconstruction of residential fires very often requires reliable estimates of the heat release rate (HRR) of upholstered furniture. This is true regardless of whether a CFD code, a zone model, or another type of analysis is used.

Under ideal circumstances, identical items to those involved in the fire are available. The necessary data can then be obtained from experiments in a furniture calorimeter and some small scale tests. However, even in this case, the test data is subject to uncertainty. The sources of this uncertainty include, for example, measurement errors (aleatory uncertainty) and unknown ignition scenario (epistemic uncertainty).

It is usually not possible to obtain undamaged items for furniture calorimeter testing, but it is more likely that enough specimens are available for small-scale testing. The extent of small scale testing that can be performed depends on the quantity of material that is available. If there is enough for Cone Calorimeter (ASTM E1354) tests, it may be possible to predict the burning behavior of the furniture item with reasonable accuracy. More often, there are no specimens available for Cone Calorimeter tests, but enough material for Microflow Combustion Calorimeter (ASTM D 7309) tests. This calorimeter provides limited information about the heat release characteristics of the material that may be helpful in reducing the uncertainty of burning rate estimates of an upholstered furniture item.

The worst case is when small-scale tests cannot be performed due to lack of funding, time, and/or test material. In this case, the best that the investigator can do is to determine the general characteristics of the furniture item(s) involved in the fire based on a detailed survey of the fire scene and interviews with people who have some intimate knowledge about the furniture and to estimate the HRR based on literature data for items that are similar (taking into account the unreliability of fact witnesses). However, if a test reported in the literature used an ignition scenario that is inconsistent with that postulated for the fire under investigation, the use of literature data may not be justified without some adjustments. In addition, there are virtually no HRR data in the literature for upholstered furniture ignited with an accelerant.

The goal of this project was to develop guidelines for each of these situations on how to best estimate the burning rate of upholstered furniture and quantify/optimize the uncertainty of the predictions. This uncertainty consists of an aleatory and an epistemic

component. The first component is uncertainty due to random variation while the second is uncertainty due to lack of (complete) knowledge. Aleatory uncertainty can be estimated using standard mathematical techniques. Quantifying epistemic uncertainty, which is often (by far) the larger of the two uncertainty components, is much more difficult. Primary sources of epistemic uncertainty of the HRR of upholstered furniture include the lack of knowledge of the ignition scenario and limited understanding of enclosure effects. The focus of this study is on these two sources of uncertainty.

Two series of full-scale tests were conducted in this project. Except for the first 19 tests which were conducted directly under the calorimeter hood, the furniture specimen was placed in a $4.65 \times 3.43 \times 2.43$ m (L \times W \times H) compartment of light wood-frame construction covered with two layers of ½-in. type X gypsum board on the inside. The furniture item was placed on a scale in a corner opposite a 0.74-m wide and 2.0-m high doorway located in the center of one of the short walls of the room. The HRR of the specimen was measured based on the oxygen consumption technique. Thermocouples (TC) were distributed throughout the compartment and in the doorway to characterize the thermal environment in the room during the tests. Schmidt-Boelter heat flux gauges were used to measure the heat flux to the floor and to the walls in the vicinity of the test specimen. Video footage and photographic documentation was obtained for every test.

The first series of full-scale tests consisted of 79 tests on CA TB 133 upholstered furniture mockups. The mockup cushions were constructed with one of two fabrics (non-FR treated cotton and FR-treated cotton) and one of six padding materials (three types of polyurethane foam, a chloroprene latex foam and two types of polyester fiberfill). Although most of the tests were performed on 1- and 3-seat sofa mockups, a limited number of tests were also performed on chair and 2-seat sofa mockups. The tests on the 1- and 3-seat sofa mockups included two fractional factorial designs to assess the effect of the padding material (low density [LD] polyurethane foam, high density [HD] polyurethane foam, and CA TB 117 compliant foam), ignition source (small flame, large gas burner flame, and liquid pool fire), and ignition source location (seat top, front bottom, and back). The non-FR cotton fabric was used in all fractional factorial design tests. The main conclusions of the mockup tests are as follows:

- The repeatability of furniture calorimeter tests with a large flame ignition source is very good. For example, based on four repeat tests the coefficient of variance of the

peak HRR (PHRR) at the 95% confidence level was found to be approximately 8%. This is comparable to the measurement uncertainty of the PHRR, which for most items that were tested was determined to be between 8% and 9%.

- The time to the onset of a self-propagating fire was found to be considerably more variable in repeat tests with a small flame ignition source. Compared to the tests with a large flame ignition source the PHRR was also found to be more variable, although the effect on PHRR was not as pronounced.
- The HRR of a triple seat sofa is very sensitive to the location on the top surface where the ignition source is applied. The PHRR for a 3-seat sofa ignited with a large flame ignition source (CA TB 133) in the center was approximately 2.5 times the peak observed for ignition of one of the side cushions (approximately 1000 kW vs. 400 kW). A similar trend was observed for the small flame applied at the center versus the corner (approximately 1300 kW vs. 600 kW).
- The fractional factorial experiments indicated that the type of ignition source is a significant factor affecting the ignition delay (t_0). In terms of the effect on t_0 , there is no significant difference between the large burner flame and the liquid pool fire, but the small flame ignition source results in a significant increase of t_0 .
- The fractional factorial experiments also showed that the PHRR is strongly affected by the padding material (the average peak for CA TB 117 foam is significantly lower in particular for the 1-seat sofas that were tested).
- Back ignition generally resulted in a shorter ignition delay, but a slower fire growth rate and lower PHRR.
- Finally, comparison of heat release data of items tested directly under the hood versus in a room indicated that enclosure effects were negligible. However, the PHRRs in these tests were between 200–500 kW, which is well below that required for room flashover.

Small-scale tests were performed to obtain fire properties of the two fabrics and six padding materials and specific fabric-padding combinations used in the construction of the mockups. Tests were conducted in the Cone Calorimeter (ASTM E 1354) and the Microscale Combustion Calorimeter (ASTM D 7309). In addition, specimens of the six padding materials were tested to verify their compliance (or non-compliance) with CA TB 117.

The predictive capability of three upholstered furniture burning rate models (referred to as Babrauskas, Babrauskas 2, and CBUF) was determined based on the results of the parametric study and small-scale test data for the upholstery materials (Cone Calorimeter and Microscale Combustion Calorimeter). The Babrauskas model is briefly described below.

Based on the results of furniture flammability studies conducted at NIST in the early 1980s, Babrauskas observed that many upholstered furniture items have HRR versus time graphs that are triangular in shape. This observation formed the basis for a simple model to predict PHRR (top of the triangle) and burning time (triangle base width) on the basis of generic characteristics of the furniture item. According to the model, PHRR can be estimated from

$$\dot{Q}_{\max} = 210 [FF][PF][CM][FC][SF]$$

where

$$\dot{Q}_{\max} = \text{PHRR (kW);}$$

$$FF = \text{Fabric factor;}$$

1.0 for thermoplastic fabrics (e.g. polyolefin)

0.4 for cellulosic fabrics (e.g. cotton)

0.25 for PVC or polyurethane film-type coverings

$$PF = \text{Padding factor;}$$

1.0 for polyurethane foam, latex foam, or mixed materials

0.4 for cotton batting or neoprene foam

$$CM = \text{Combustible mass (kg);}$$

$$FC = \text{Frame combustibility factor.}$$

1.66 for non-combustible frames

0.58 for melting plastic

0.30 for wood

0.18 for charring plastic

SF = Style factor; and

1.5 for ornate convoluted shapes

1.2–1.3 for intermediate shapes

1.0 for plain, primarily rectilinear construction

The triangle base width (burn time) is estimated by

$$t_b = \frac{[FM][CM]\Delta h_c}{\dot{Q}_{\max}}$$

where

t_b = Burn time (s);

FM = Frame material factor; and

1.8 for metal or plastic frames

1.3 for wood frames

Δh_c = Effective heat of combustion for the fuel item (kJ/kg).

The advantage of this model is that the HRR can be estimated based on some generic characteristics of the furniture item, the total combustible mass and the effective heat of combustion of the soft materials (fabric and padding materials). Only a few grams of material are needed to measure the latter in an oxygen bomb calorimeter or the Microflow Combustion Calorimeter. The heat of combustion can also be estimated with reasonable accuracy from tabulated values.

To improve agreement between calculated and measured PHRR, the Babrauskas model was modified by using adjusted PF values for the different types of padding materials that were tested. Following the adjustment, this model gave the best matching predictions of PHRR for the mockup tests.

An attempt was also made to use the field fire model FDS (Fire Dynamics Simulator) to better account for the effect of the exact location of the ignition source on flame spread over the seating surface. Although the FDS model is the most advanced of the four because it is based on physics rather than a correlation, it has some unique challenges that could not be fully addressed. As a result the FDS model consistently underpredicts the HRR curve.

The zone fire model Consolidated Model of Fire Growth and Smoke Transport (CFAST) and field fire model FDS were also used to determine how the use of the upholstered furniture burning rate models (compared to the use of measured HRR data for the item) affects the accuracy of Hot Gas Layer (HGL) temperature and heat flux estimates in the room. It was determined that both compartment fire models predict the HGL temperature with remarkable accuracy when the measured HRR is specified. This implies that the accuracy of the CFAST and FDS HGL temperature predictions depends on how well the burning rate model predictions agree with the actual HRR.

Twenty-two sets of used upholstered furniture were obtained. The second series of full-scale tests involved 27 items of the used upholstered furniture. At least one item from each set was tested. A reduced number of Cone Calorimeter and Microscale Combustion Calorimeter tests were performed on the soft component materials. Specimens of the padding materials were tested to verify their non-compliance with CA TB 117.

The small- and full-scale test data on the used furniture (components) were used to assess the predictive capability of the aforementioned upholstered furniture burning rate models. In this case the models significantly underpredicts the PHRR. The Babrauskas model, with a fabric factor of 0.4 and a padding factor of 0.8, gave the best agreement ($R^2 = 0.72$), but the calculated peak heat release had to be increased by 50% (and burning time reduced by 33%). The accuracy of the Babrauskas model needs refinement and more work is needed to improve the predictions. It will take some time to conduct the additional analysis and in the meantime the alternative approach described below may be used.

Epistemic uncertainty can indirectly be accounted for by conducting a parametric analysis. Such an analysis could, for example, consist of a series of simulations to determine the effect of different ignition scenarios and furniture sizes. The averages and standard deviations from the used furniture tests in Table 1 can be used to guide such a sensitivity study. Heat release curves can be constructed based on the values in this table, assuming that the ignition delay and PHRR are only affected by the ignition scenario and the furniture size

(1-, 2-, or 3-seat), respectively. With a specified PHRR, the base of the triangle can be determined using the estimated mass of the item, a soft combustible mass fraction of 27% (based on average component weights measured for the items used to prepare the specimens for small-scale testing) and a heat of combustion of the soft furnishings of approximately 23 MJ/kg.

Table 1. Averages and Standard Deviations for the Used Furniture Tests.

Sofa Size	Mass (kg)	PHRR (kW)	Ignition Source	Ignition Delay (s)
1-Seat	33.7 ± 11.3	1455 ± 401	Accelerant	71 ± 55
2-Seat	39.4 ± 6.1	1726 ± 113	Small Flame Center	435 ± 214
3-Seat	67.2 ± 17.5	2073 ± 356	Small Flame Corner	171 ± 52

The results and report of this study and any papers presented at conferences will be made available to the fire investigation community over the Internet. This includes a database that resulted from this work. The database can serve as a central repository for other relevant data that are now at many places in different formats.

Video DVDs were created as training materials that will give arson investigators the opportunity to witness the full-scale fire tests a posteriori. Video plots are included with information on the enclosure temperature and HRR, which will help arson investigators develop an understanding of fire dynamics in upholstered furniture fires.

The upholstered furniture burning rate models that were explored in this study, without adjustments, appear to significantly under-predict the HRRs that were measured for used furniture. For example, the Babrauskas model has a bias of 0.66, which means that, on average, the model under-predicts the PHRR for the used furniture by 34%. In addition, the standard error after removing the bias is 518 kW, which is rather high given that the range of measured PHRRs for the used sofas is 893–2446 kW. Additional research is needed to understand what the fundamental reasons are for these discrepancies and how the predictive capability of the burning rate models can be improved.

Three of the four burning rate models that were considered assume that the HRR vs. time curve of upholstered furniture is approximately triangular in shape. Some of the HRR data that was obtained for used furniture items puts the validity of this assumption in question. It is suggested to explore other curve shapes to fit the data, for example a t^2 fire growth stage followed by a period of steady burning at PHRR and a linear decay.

The FDS furniture flame spread and burning model shows the most promise because it is based on physics and not on correlations. As such, this model has the potential of being capable of accounting for ignition source strength, source location, and enclosure effects. However, more work is needed to address the challenges that were encountered in our initial attempts at using FDS to model furniture fires. More specifically a more detailed algorithm is needed to predict opposed-flow flame spread at sub-grid scale. In addition, better method need to be developed to account for thickness and heat flux effects.

2 INTRODUCTION

2.1 STATEMENT OF THE PROBLEM

According to the National Fire Protection Association (NFPA), in 2005–2009 fires beginning with upholstered furniture accounted for 19% of home fire deaths (Ahrens, 2011). According to the same source, upholstered furniture is a major contributor to flame spread in homes. Therefore, it is very likely that in the reconstruction of a residential fire scene, the investigator will need to estimate the contribution of upholstered furniture to the development of the fire. Compartment fire modeling is a powerful tool that can greatly facilitate the fire investigator’s job in making this assessment¹ (Icove and DeHaan, 2004, Janssens, 2000). However, fire modeling also has some significant limitations that are often not recognized.

In a paper published 15 years ago, Babrauskas examined the question whether compartment fire models are good enough for Fire Safety Engineering (Babrauskas, 1996). He concluded that the main limitation of compartment fire models is that they generally are not capable of predicting fire growth, but only suitable for calculating the consequences of a user specified fire. Since the publication of Babrauskas’ paper, significant progress has been made in our ability to model the fire; but, realistically, even now, it can only be done for relatively simple cases such as, for example, liquid fuel spill fires. To account for the contribution from complex objects such as chairs or sofas, the current practice still is to rely on user-specified heat release versus time curves. This implies that the uncertainty of results from computer simulations of fires that involve upholstered furniture largely depends on the accuracy of the time-varying HRR data specified by the investigator.

¹ The two types of compartment fire models that are commonly used in fire reconstruction are briefly described in Appendix A.

There are an almost infinite number of variations in upholstered furniture shapes, styles, frame types, and material combinations. Consequently, the chance that heat release data from prior testing are available for a chair or sofa that was involved in a fire is very close to zero. In fact, the more general problem of limited availability of material data for input into fire models was identified in a report of a recent study for the National Institute of Justice (NIJ) to assess the near- and long-term needs for state and local law enforcement involved in fire and explosion investigations and forensic analyses (Chasteen, 2008), hereafter referred to as the *NIJ Needs Assessment Report*.

In addition, the HRR of an upholstered chair or sofa not only depends on the materials involved and the design of the furniture, but also on the severity and location of the ignition source and the size of the enclosure where the item is located (Krasny, Parker and Babrauskas, 2001). These factors (greatly) add to the uncertainty of estimated HRRs of upholstered furniture as there is limited quantitative information available on how to account for their effects.

2.2 LITERATURE REVIEW

A detailed review of the literature was conducted with a focus on studies of ignition scenario and enclosure effects on the burning rate of upholstered furniture. The results of the review are summarized below.

2.2.1 Ignition Scenario Effects

Back in the 1970s, it was established that upholstered furniture represented a potentially serious concern: a single item can yield a fire severe enough to take the room to flashover (Babrauskas, 1979). Following this understanding, several European researchers, especially in the United Kingdom, conducted extensive series of studies using a variety of ignition sources, often on various types of mock-ups. The primary objective of these studies was to investigate the severity and characteristics of potential furniture ignition sources.

As an example of this type of work, a study by Benisek and Phillips found that matches were more likely to ignite the upholstery substrate when placed near, rather than in, the crevice between the seat and back cushion (Benisek and Phillips, 1978). However, the rate of flame spread was more rapid when ignition was in the crevice. The butane flame burner results were not affected by position. Many more examples exist. Perhaps one of the most interesting

studies was a review in 1987 by Paul and Christian, which describes in great detail a wide variety of standard flaming ignition sources that can be used (Paul and Christian, 1987).

A key result of these studies was the first attempt at developing a flaming ignition standard for upholstered furniture composite systems in the United Kingdom: British Standard (BS) 5852. This test uses a variety of butane flames and wood cribs as ignition sources, and it tests a combination of fabric and padding, made up into two standard cushions: bottom and back. However, the test actually evaluates padding materials under standard fabrics and fabrics with standard padding materials. Details of the flaming ignition sources in this test and of some others are shown in Table 2.

Table 2. Characteristics of Ignition Sources for Upholstered Furniture.

Source	THR* (kJ)	Flame Height (mm)	Heat Output (kW)	Exposure Time (s)	Description
EN 1021 -2	1.5	35	0.1	15	Butane gas burner
BS 5852 #1	2	35	0.1	20	Butane gas burner
BS 5852 #2	12	145	0.3	40	Butane gas burner
BS 5852 #3	46	240	0.7	70	Butane gas burner
BS 5852 #4	142	150–245	1.0	ca. 180	Wood crib 8.5 g
CBUF Low 1	153	N/A	1.7	90	Small square propane
BS 5852 #5	285	250–335	1.9	ca. 200	Wood crib 17 g
CBUF Low 2	522	N/A	5.8	90	Small square propane
Mitler/Tu	600	N/A	10.0	60	Propane gas burner
BS 5852 #6	1040	250–350	2.6	ca. 350	Wood crib 60 g
Cleary TB 133	1300	N/A	16.3	80	Square propane burner
CA TB 133 Gas	1550	N/A	19.3	80	Square propane burner
CA TB 133 Paper	1680	N/A	N/A	ca. 380	Newspaper 90 g
Michigan Roll	2000	N/A	30.9	N/A	Newspaper 130-160 g
BS 5852 #7	2110	345–490	6.4	ca. 390	Wood crib 126 g
School Bus Test	2300	N/A	33.8	N/A	Newspaper 200 g
CA TB 129	3200	N/A	17.8	180	T propane burner
CBUF gas	3600	N/A	30.0	120	Square propane burner
CBUF BR1	4800	N/A	40.0	120	Square propane burner
CBUF BR3	5400	N/A	30.0	180	Square propane burner
CBUF BR4	6000	N/A	20.0	300	Square propane burner
NFPA 286 Early	12000	N/A	40.0	300	Box propane burner
NFPA 286 Late	96000	N/A	160.0	600	Box propane burner

*THR = Total heat release, i.e., product of heat output and exposure time.

In the early stages of ignition source development, paper ignition sources were very common. However it was later discovered that they suffer from poor repeatability/reproducibility and they have; therefore, mostly been replaced by gas burners of various types. In some cases, studies were conducted to replace a paper source by a representative gas burner source. A typical example is the work at the National Bureau of Standards (NBS, currently the National Institute of Standards and Technology or NIST) on the paper bag used for the California Technical Bulletin (CA TB) 133 test (Ohlemiller and Villa, 1990). However, some paper ignition sources are still being used today, primarily because of the ease with which such sources can be employed. The results of such tests tend to divide tested materials and products into two categories: those that pass and those that fail, based on simple criteria. The two most widely used examples in the U.S. in the early 21st century are the Michigan Roll test for mattresses (described in ASTM F 1085 and in ASTM F 1870) and the school bus seating test (National Safety Council). Some of the implications of such testing were discussed by Hirschler (Hirschler, 1997, 2004, 2005).

The ignition sources in Table 2 can be characterized into four classes: low THR (EN 1021-2, BS 5852 gas burners and crib #4, CBUF Low 1; less than 200 kJ), medium THR (BS 5852 crib #5 through CA TB 133; less than 2 MJ), high THR (Michigan Roll, BS 5852 crib #7 through CBUF gas; less than 4 MJ), and very high THR (CBUF BR and NFPA 286 sources).

As a result of these initial studies, it was determined that the type of ignition source and its location on the item of upholstered furniture (or mockup) is critical to the following: (a) whether ignition occurs, (b) how long it takes for ignition to occur, (c) whether a self-propagating fire occurs, and (d) how long it takes for a self-propagating fire to develop.

Following this initial work, several studies were conducted to investigate the effect of ignition source and location on the heat release of full scale upholstered furniture; details follow. One study was conducted at NIST in 1992 (Mittler and Tu, 1994). The tests were performed in a furniture calorimeter, under a hood, where HRR and species production rates were obtained. Unfortunately details of the study were never published (only an abstract exists, which was published after completion of a subsequent NIST study). The authors conducted 12 full scale burns on 3 types of chairs. All chairs were of similar design but different composition. They used one ignition source placed at four locations, namely (1) the center of the chair seat cushion, (2) the lower center of the chair front, (3) the lower center of

the chair side, and (4) the lower center of the chair back. The ignition source was a 10-kW propane gas tube burner applied to the chair for 60 s. The authors found that the PHRR was independent of ignition location. However, the time at which the peak occurred could vary widely with location of the ignition source. Generally, ignition of the seat cushion gave the quickest peak. The authors concluded that most of the differences in the heat release curves for varying ignition sources may simply be a consequence of the effect of location. It must be noted; however, that this study used a single ignition source while only varying the ignition source location. Results were presented for only one chair, constructed with melamine-treated polyurethane foam. The authors noted that ignition almost did not occur when the source was placed at the lower center of the chair back (which is an area that often has very little padding). Results are presented in Table 3. Since the ignition source was of medium intensity, it is reasonable to conclude that the variability in PHRR is more a function of experimental variability (repeatability).

Table 3. Results Reported by Tu and Mitler.

Ignition Source Location	PHRR (kW)	Time to PHRR (s)
Center of chair seat cushion	1237	820
Lower center of chair front	1349	880
Lower center of chair side	1346	1280
Lower center of chair back	1271	2520
Average	1301	1375

A more comprehensive study was conducted at NIST in 1992 (Cleary, Ohlemiller and Villa, 1992, 1994). In this study, a set of upholstered chairs constructed from five different fabric/foam combinations was subjected to a variety of ignition sources suggested by fire statistics. The key objective of the study was to predict fire hazard by a zone model technique. The materials used for the chairs are shown in Table 4 and the ignition sources used are given in Table 5.

The tests were performed in a furniture calorimeter, under a hood, where HRR and species production rates were obtained. All the chairs had the same geometric configuration and were custom manufactured for the study by a commercial manufacturer. The chair frame was composed of a mixture of hard wood structural elements and plywood panels, with the latter utilized in such places as the tops of the chair arms and the front panel below the seat cushion. The seat was supported by a platform spring of steel wire. The polyurethane foam, present in all of the chairs, was a conventional non fire-retarded material with a nominal

density of 24 kg/m³ (1.5 lb/ft³). One of the chairs (type B) incorporated a wrap of polyester batting around the foam cushions; this was avoided in the others, despite its market popularity, in order to simplify the number of interacting materials. Another one of the chairs (type A) had a comparable wrap of cotton batting around the foam cushions and along the inner surface of the chair arms. This wrap, in combination with the rather light-weight cotton fabric, rendered this chair type uniquely ignitable by a smoldering cigarette. The cotton batting was nominally non-fire retarded but there were some indications during the experiments of a slight boric acid presence.

Table 4. Chair Materials Used in Cleary et al. Study.

Chair	Filling	Wrap	Cover
A	Non FR Polyurethane	Non FR Cotton Batting Overwrap	Non FR 100% Cotton Fabric No Back Coating 10-12 oz/yd ²
B	Non FR Polyurethane	Non FR Polyester Batting Overwrap	63% Nylon, 26% Polyolefin and 11% Acrylic Fabric Latex Back coating
C	Non FR Polyurethane	None	100% Polyolefin Fabric Latex Back Coating
D	Non FR Polyurethane	None	Acrylic Fabric Rayon/Cotton Backing
E	Non FR Polyurethane	None	Expanded Vinyl Fabric

Table 5. Ignition Sources Used in Cleary et al. Study.

No.	Label	Description
1	C	A smoldering cigarette
2	M	A match-like flame (BS 5852 #1)
3	L	An incandescent lamp (55 W reflective tungsten halogen spot light)
4	H	A space heater (2 quartz tubes; 1500 W and 120 V)
5	B	CA TB 133 gas burner, with lower gas flow rate: 11 l/min

The ignition sources used were all of low intensity except for the CA TB 133 burner (used with a gas flow rate of 11 l/min instead of the standard 13 l/min). The study concluded that none of the ignition scenarios examined consistently yielded the greatest potential hazard for all chair types tested when ignition and sustained burning was achieved. They recommended that the fire hazard of upholstered furniture for residential use be assessed on the basis of resistance to small flame and cigarette ignition combined with PHRR and time to peak subsequent to ignition by a strong source such as the CA TB 133 equivalent gas burner.

The data obtained (based on the published graphs) are shown in Table 6. The authors concluded that, “for any chair type, the time to the PHRR depended on the ignition sequence, but the magnitude of the peak did not, within the scatter of the data for any given chair”. In actual fact, these conclusions are based on data for three chairs and two burners, CA TB 133 and BS 5852 #1. No comparisons are possible for chairs A and E because the BS 5852 #1 igniter was unable to ignite the chairs, which were the best performers (the only ones with HRRs that never exceeded 1 MW). Interestingly, in the case of chair A the cigarette ignition caused the highest HRR.

Table 6. Cleary et al. Study PHRR Results.

PHRR (kW)	Chair	Igniter	PHRR (kW)	Chair	Igniter
560	A	Cigarette	1121	D	BS 5852 #1
557	A	Cigarette	1337	D	BS 5852 #1
423	A	Radiant Heater	988	D	Lamp
404	A	Radiant Heater	1275	D	Lamp
452	A	CA TB 133	1332	D	Radiant Heater
459	A	CA TB 133	985	D	Radiant Heater
1270	B	BS 5852 #1	1120	D	CA TB 133
1123	B	BS 5852 #1	1236	D	CA TB 133
1605	B	Radiant Heater	826	E	Radiant Heater
1200	B	Radiant Heater	723	E	Radiant Heater
1418	B	CA TB 133	701	E	CA TB 133
1472	B	CA TB 133	580	E	CA TB 133
1256	C	BS 5852 #1	N/A	N/A	N/A
1132	C	BS 5852 #1	N/A	N/A	N/A
1167	C	Radiant Heater	N/A	N/A	N/A
980	C	Radiant Heater	N/A	N/A	N/A
1297	C	CA TB 133	N/A	N/A	N/A
1300	C	CA TB 133	N/A	N/A	N/A

Overall, the conclusions regarding the lack of effect of ignition source on PHRR are somewhat debatable as the PHRR with the CA TB 133 burner seems to have been somewhat higher than those with the match burner in two out the three tests where comparisons are possible, namely chairs B and C (see the average PHRR values in Table 7). However, the differences seem to be small.

Table 7. Cleary et al. Study Analysis.

PHRR (kW)	Chair	Igniter	Average PHRR (kW)
1270	B	BS 5852 #1	1197
1123	B	BS 5852 #1	
1418	B	CA TB 133	1445
1472	B	CA TB 133	
1256	C	BS 5852 #1	1194
1132	C	BS 5852 #1	
1297	C	CA TB 133	1299
1300	C	CA TB 133	
1121	D	BS 5852 #1	1229
1337	D	BS 5852 #1	
1120	D	CA TB 133	1178
1236	D	CA TB 133	
988	D	Lamp	1132
1275	D	Lamp	
1332	D	Radiant Heater	1159
985	D	Radiant Heater	

In the early to mid-1990s a comprehensive study of the problem of upholstered furniture fires was conducted in Europe (Sundström, 1996). This study, referred to as CBUF (Combustion Behaviour of Upholstered Furniture), involved a series of experiments to evaluate the effect of ignition source and location. All the experiments were performed in a furniture calorimeter with six chairs. Table 8 shows information on the materials used in these chairs.

Initially experiments were conducted with a match size burner (EN 1021-2, similar to the BS 5852 #1, except that the application period was 15 s instead of 20 s). No heat release was measured in these tests and the results were simply ignition (for two chairs) or no ignition (for four chairs). One anomaly was found: one chair did not ignite in full scale with the EN 1021-2 source but did ignite in the EN 1021-2 mockup test. Information on EN 1021-2 performance is also shown in Table 8.

Subsequent tests used a small propane square ring burner (115 × 115 mm in size) that delivered either 1.7 kW for 90 s or 5.8 kW for 90 s and the CBUF propane burner (30 kW for 120 s). The burners were applied to the junction of the seat cushion and the armrest. The shapes of the HRR versus time curves were very similar for all three ignition conditions, but the peaks occurred at different times when measured from time of ignition. However, when

the times to a “self-propagating fire” (which the CBUF project defines as a HRR of 400 kW) were measured from the time of “sustained ignition” (which this project defines as the moment when a HRR of 50 kW first occurs), they were very similar, regardless of the ignition source. CBUF assumes detectable fires to be about 50-kW size and that below this HRR, the occupants of the room may not notice a fire if their attention is directed somewhere else. With this assumption, the ignition source would become unimportant for estimates of escape times if the times to a “self-propagating fire” are all the same. The results in Table 9 appear to validate the assumption and also suggest that the ignition source has a very low effect on the PHRR, although the experimental scatter seems high to draw clear conclusions.

Table 8. Chair Materials in CBUF Study with EN-1021-2 Source.

Chair	Filling	Wrap	Cover	Ignition
1:5	CMHR Foam Seat FR Polyester Back	FR Polyester Fiberfill	Acrylic Pile Fabric FR Back-Coated Cellulose Ground	No
1:6	HR Foam	None	Leather	No
1:8	Polyether Foam	Non FR Polyester Fiberfill	Non FR Polyester	Yes
1:9	CMHR Foam	FR Polyester Fiberfill	FR Cotton	No
1:12	Polyether Foam	Non FR Polyester Fiberfill	Non FR Polyester	Yes
1:19	HR Foam	None	FR Polyester	No*

* Item ignited in EN 1021-2 mockup

Table 9. CBUF PHRRs for Medium Intensity Ignition Sources.

Chair	CBUF Low Intensity 1		CBUF Low Intensity 2		CBUF Burner	
	PHRR (kW)	Time 50–400 kW (s)	PHRR (kW)	Time 50–400 kW (s)	PHRR (kW)	Time 50–400 kW (s)
1:5	N/A	N/A	N/A	N/A	730	395
1:6	N/A	N/A	1250	115	1140	135
1:8	N/A	N/A	1640	50	1430	35
1:9	N/A	N/A	516	1220	510	1335
1:12	1000	45	N/A	N/A	670	40
1:19	1100	50	N/A	N/A	980	55

The CBUF project included another series of pertinent tests. In this series they used two chairs, which are simply described as FR chair and Non FR chair. The data presented indicates that this description is actually incorrect (the FR PHRR is higher than the non-FR PHRR) and the opposite should have been the designation. These two chairs were exposed to four ignition sources, namely the CBUF ignition source and three others, of higher power.

The results for PHRR and total heat released (with the designations corrected) are shown in Table 10. This is the sole study that clearly suggests no effect of ignition source on PHRR. It should be noted; however, that all of the ignition sources used in this study were of high or very high intensity.

Table 10. CBUF Results with Non FR Chair and FR Chair.

Ignition Source	Non FR PHRR (kW)	FR PHRR (kW)	Non FR THR (MJ)	FR THR (MJ)
BR1	1043	504	348	130
BR2	1182	463	369	122
CBUF	1100	511	355	127
BR4	918	499	344	131
Average	1061	494	354	128

More recently, a study was conducted in Canada on blocks of polyurethane foam (Ezinwa, Rigg, Torvi and Weckman, 2009). They conducted furniture calorimeter tests of polyurethane foam specimens in order to compare flame spread and HRRs in tests that used center and edge ignition locations. They found that flame spread rates and HRRs were similar during the early portions of tests of specimens of equal width, but that later flame spread and HRRs increased more rapidly in the center ignition tests. For the same size foam specimens, peak flame areas were approximately 10% larger in center ignition tests and PHRRs were approximately 20% higher in center ignition tests.

In summary, the following conclusions can be drawn from the literature:

- The intensity of the ignition source will markedly affect whether an item of upholstered furniture, or a mockup, will or will not ignite.
- If the same ignition source is used, its location on the item of upholstered furniture will have a significant effect both on whether an item of upholstered furniture, or a mockup, will ignite and on the times to ignition (or sustained flaming), to a self-propagating fire and to PHRR.
- Thus, the use of the same ignition source in a different location on the item of upholstered furniture is equivalent to the use of a different ignition source.
- It is possible to define high intensity ignition sources as those with a heat input of 2 MJ, although this number may be arbitrary.

- If high intensity ignition sources are used, it appears clear that, for such ignition sources, there is little, if any, effect of the ignition source on the PHRR.
- It is not yet clear whether the use of low intensity ignition sources results in the same PHRR for the upholstered furniture item. The amount of information available to date is insufficient and somewhat contradictory.

2.2.2 Enclosure Effects

The HRR of an item of upholstered furniture is typically determined in an open calorimeter (see Appendix B for a brief description of open calorimeters used for this purpose). The test specimen is usually placed directly under the exhaust hood of the calorimeter in an open environment with plenty of air supply. In an actual structure fire, the sofa or chair is located in an enclosure and air supply may be restricted. Researchers in Finland and Sweden have shown that both doorway size and room geometry affect fire growth (Kokkala, Goransson and Söderbom, 1991). Radiation from the hot gas layer, heated walls, and ceiling surfaces and from flames of other burning items could accelerate the burning rate of an upholstered furniture item compared to that measured in an open calorimeter. Reduced air supply could have the opposite effect. This section summarizes the results of studies of the effect of an enclosure on the burning rate of upholstered furniture.

In the early 1980s, Babrauskas and co-workers developed the furniture calorimeter at NIST (Babrauskas, Lawson, Walton and Twilley, 1982, Babrauskas, 1983). In subsequent years, the NIST furniture calorimeter was used in a number of studies of enclosure effects. The first comparative study was reported in 1984 (Babrauskas, 1984b). The items tested in this study were an upholstered armchair and a love seat. Both items were tested in the furniture calorimeter with a gas burner ignition (simulating a wastebasket) and in a room with the actual wastebasket. The room walls were made of gypsum wallboard but the paper was burnt off before the tests. The room was slightly different than the standard room developed later ($3.94 \times 2.26 \times 2.31$ m high) and the ventilation opening dimensions (width and height) were varied (see Table 11, rooms 1–4). Both the opening dimensions and the actual presence of walls had significant effects on the PHRR, which the author assigned to measurement variability. Interestingly the room caused a delay in time to flashover, but that may be partially due to the slower rate of rise of heat release by the ignition source (wastebasket) in the room. When a time shift was made to accommodate for this, the time effects were

virtually eliminated. The largest effect in increasing PHRR was found when the opening height was increased with a standard 2.0-m opening width. Unfortunately the results are somewhat inconclusive; see the key results in Table 11.

Table 11. Results from Study by Babrauskas et al.

	Loveseat		Chair	
	PHRR (kW)	Time to PHRR ^b or Flashover ^c (s)	PHRR (kW)	Time to PHRR ^b or Flashover ^c (s)
Furniture calorimeter	2890	230	1970	280
Room 1 (2.0 × 1.13 m)^a	2490	373	N/A	N/A
Room 2 (2.0 × 1.50 m)^a	3550	377	N/A	N/A
Room 3 (1.29 × 2.0 m)^a	2660	410	N/A	N/A
Room 4 (1.29 × 2.0m)^a	N/A	N/A	2260	302

^a Room dimensions refer to opening width and opening height

^b In furniture calorimeter, time to PHRR is reported

^c Flashover time assessed as 20-kW/m² heat flux on floor

The study by Lee involved mattresses in a “standard” room (2.4 × 3.7 × 2.4 m high) that contained some additional furnishings (bedding, box spring, headboard, and night table) and was lined with paper-covered gypsum wallboard on the walls. In this case, the results were much more conclusive: the furniture calorimeter caused PHRRs to occur significantly earlier but the room caused a 15%–30% increase in PHRR.

Key work by Parker et al. in 1990 found that room size (if the floor area lies between 8.7 and 11.4 m² and one of the room floor dimensions is between 2.4 and 3.7 m) has little effect on HRR below 600 kW (Parker, Tu, Nurbakhsh and Damant, 1990). In this work, 10 sets of chairs were obtained. One exemplar of each set was burnt in the standard 2.4 × 3.7 × 2.4-m ASTM room at NIST using the CA TB 133 burner and two exemplars of each set were burnt in a furniture calorimeter (one with the CA TB 133 burner and one with the CA TB 133 paper ignition source). Moreover, four exemplars of several of the chairs were burnt at the California Bureau of Home Furnishings in a slightly larger room (3.0 × 3.7 × 2.4 m high) with a door in one corner and not in the middle (referred to as the CA TB 133 room). Duplicate tests were performed with each ignition source. Results can be seen in Table 12. This study involved relatively few actual comparisons between room and furniture calorimeter. The two key concerns of the authors were: (a) to determine whether tests could be conducted in both rooms with equal results, particularly since the regulatory office in California had a room of a slightly different size than the standard room in fire test

labs, and (b) whether the same results were obtained in terms of pass or fail (with an 80-kW PHRR or 111 °C ceiling temperature rise criterion). The differences between the results obtained in the two rooms were found to be insignificant, but the exact effect of the enclosure on HRR was not clear.

Table 12. Results from Study by Parker et al.

Chair	PHRR CA TB 133 Room (kW)	PHRR ASTM Room (kW)	Peak ΔT CA TB 133 Room (°C)	PHRR Open Calorimeter (kW)
B	31	25	48	N/A
D	70	64	109	N/A
E	> 1700 ^a	2760	994	N/A
F	N/A	~1000 ^b	N/A	~400 ^b
G	N/A	~850 ^b	N/A	~700 ^b
H	130	80	141	N/A
I	393 ^c	502	356 ^c	~450 ^b

^a Measured when instrumentation failed

^b Estimated from published graph

^c Measured at extinguishment

Enclosure effects on heat release have not been extensively studied after that time, except within the CBUF project (Sundström, 1996). In that project, PHRR in a standard room was plotted against PHRR in the furniture calorimeter for 27 furniture items. Four of the items tested exhibited PHRR values lower than 100 kW; for those there did not seem to be any significant difference between the two scenarios. In fact the heat release values were negligible for those chairs. In 22 of the other 23 tests conducted in both scenarios, the PHRR data ranged from 414–2363 kW in the room. There was one furniture item that showed a 297-kW PHRR in the furniture calorimeter and 1599 kW in the room. In fact, out of the 27 items only 3 showed a higher PHRR in the furniture calorimeter, and those had values of 662, 1959, and 2107 kW in the room.

On average, the room calorimeter seemed to give a somewhat higher result, by a factor of about 1.25 as shown in Figure 1. Four outlying data points were removed in the trendline analysis (filled symbols in Figure 1). The R² value for the trendline is approximately 0.94.

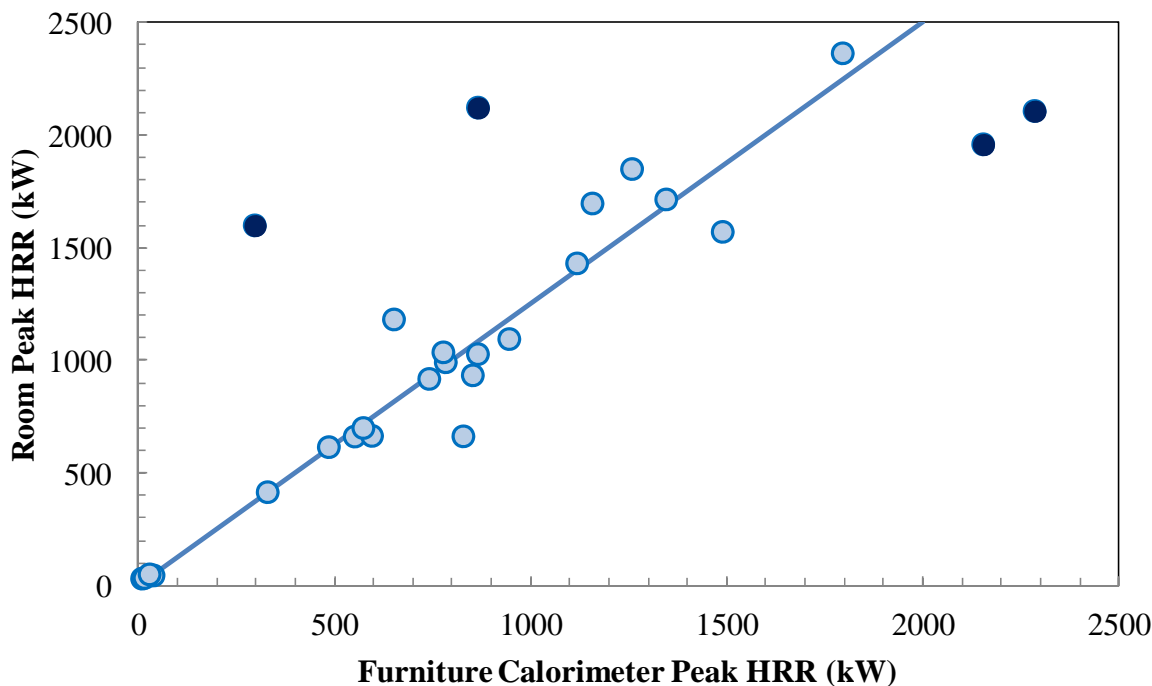


Figure 1. Enclosure Effects in CBUF Study.

For mattresses, the “augmentation effect of the room can be much greater”. The CBUF study found that mattresses can be divided into two classes, generally: very high heat release (>500 kW) and very low heat release (<100 kW). It needs to be pointed out; however, that the CBUF study did not investigate mattresses (or upholstered furniture for that matter) with barriers. Mattresses which exhibit a PHRR over 100 kW experience major radiative augmentation effects from the room and lead rapidly to the development of untenable conditions. The rationale given in the CBUF report is that chairs (upholstered furniture) create an “internal flame volume” which is largely confined by the seat, side arms, and back of the chair. Thus, the irradiance from the upper gas layer and hot wall and ceiling surfaces constitutes a relatively small fraction of the heat flux to the burning surfaces of the chair. Therefore, the enclosure has a limited effect on a burning chair prior to flashover. Mattresses do not have these internal surfaces and behave more like pool fires with very significant room enclosure effects. Mattresses are also almost invariably found in small rooms and enclosure effects are; therefore, expected to be relatively more important. Enclosure effects would be somewhat smaller for upholstered furniture in the same size room but much smaller on average because such items are more often used in larger rooms.

The CBUF study also evaluated the effect of going from the standard room to a much larger room ($7.37 \times 5.70 \times 4$ m high), with the same door opening as the standard room. It was found that such a large room caused a decrease in the HRR. This indicates, not surprisingly, that the radiative effects are reduced considerably when the walls are further away from the item on fire.

Another interesting part of the CBUF study looked at the effect of ventilation in a room with the standard dimensions. Table 13 shows these effects. The tests involved having the door fully open (1/1) and gradually closing it, reducing the ventilation (opening width) to one quarter (1/4), one eighth (1/8), and one sixteenth (1/16). As the door opening is smaller, the PHRR decreases considerably but the effect on time to PHRR is probably not significant.

Table 13. Results from CBUF Ventilation Effect Study.

Chair	Opening	PHRR (kW)	Time to PHRR (s)
4:1	1/1	684	310
4:1	1/1	864	285
4:1	¼	567	310
4:1	1/8	341	250
4:1	1/16	191	350
4:2	1/1	626	205
4:2	1/8	207	265
4:3	1/1	760	430
4:3	1/8	319	450
4:4	1/1	60	125
4:4	1/8	29	125
4:5	1/1	129	1455
4:5	1/8	28	125

In conclusion, based on CBUF data it can be stated that enclosures do have a significant effect on HRR, with HRRs in the standard room approximately 25% higher than in the furniture calorimeter. Thus, in a standard room it is likely that the effects increase in ways similar to the trendline shown in Figure 1. It is also important to note that this indicates that studies in a standard room, with a standard ventilation opening, are probably the most valuable ones from the point of view of fire hazard assessment because they represent a severe fire scenario (the standard room is at the low end of the range of residential sizes).

2.3 RATIONALE FOR THE RESEARCH

When estimating the HRR versus time curve of upholstered furniture that was involved in a fire, the investigator may encounter one of the following four distinct situations:

1. An identical (or very similar) chair or sofa as that involved in the fire is available for testing in a Furniture Calorimeter.
2. A sufficient quantity of the furniture component materials can be recovered from the fire scene to perform Cone Calorimeter tests. A single Cone Calorimeter test specimen requires approximately 0.2×0.2 m of fabric and a $0.1 \times 0.1 \times 0.05$ -m block of padding.
3. A sufficient quantity of the furniture component materials can be recovered to conduct Microscale Combustion Calorimeter tests. A single Microscale Combustion Calorimeter test requires less than 10 mg of material. Furniture component materials are tested in the Microscale Combustion Calorimeter separately and not in the form of a mixture representative of the end-use application as in the Cone Calorimeter.
4. No material is available for testing and the HRR has to be estimated on the basis of literature data.

The rationale for the research is different depending on the situation. A hotel room fire involving an upholstered furniture item is a typical example of the first situation. In this case, identical items are usually present in adjacent rooms and can be tested in a Furniture Calorimeter². However, even in this ideal situation the data obtained in the laboratory are subject to uncertainty. A distinction is made between two types of uncertainty: aleatory and epistemic. The former is uncertainty due to random variation while the latter is uncertainty due to lack of (complete) knowledge. Uncertainty due to random measurement errors is usually a significant part of the aleatory uncertainty. Methods to estimate measurement uncertainty are discussed in Appendix B. Other sources of aleatory uncertainty, such as effects of random variations in the environmental conditions in the laboratory (temperature, pressure, relative humidity, drafts, etc.) and composition of the constituent materials of the test specimen (including moisture content) are more difficult to account for.

² The Furniture Calorimeter and other test methods used to measure the heat release rate of upholstered furniture and its components are briefly described in Appendix B.

A number of correlations and engineering models have been developed to estimate the HRR of an upholstered chair or sofa based on small-scale fire test data for the component materials and some generic characteristics of the furniture item. An overview of these correlations and models is provided in Appendix C. The fire investigator can use these statistical and engineering models if a sufficient amount of the component materials is available for testing in a small-scale calorimeter, e.g., the Cone Calorimeter (second situation) or the Microscale Combustion Calorimeter (third situation). However, most existing furniture models were developed to screen materials in the design of furniture that needs to meet a flammability safety standard. These models may not be applicable to residential furniture that does not meet any fire performance requirements and typically have a much higher HRR. In addition, these models may not account for variations of the ignition scenario and for the effect of an enclosure.

Finally, quite often no additional items or components are available for testing in the laboratory (situation four). In this case, the best that the investigator can do is to determine the general characteristics of the furniture item(s) that was (were) involved in the fire based on a detailed survey of the fire scene and interviews with people who have some intimate knowledge about the furniture and to estimate the HRR based on literature data for items that are similar. Furniture flammability studies such as those described in the previous section and the “Heat Release Rates” chapter in the Society of Fire Protection Engineers (SFPE) handbook (Babrauskas, 2008a) are good sources of information. However, if the test specimen was ignited in a manner that is inconsistent with the ignition scenario postulated for the fire under investigation, the use of literature data may not be justified without some adjustments. In addition, there are virtually no HRR data in the literature for upholstered furniture ignited with an accelerant.

3 METHODS

3.1 OVERVIEW

The goal of the project was to develop guidelines for the fire investigator on how to best estimate the burning rate of upholstered furniture and quantify/optimize the uncertainty of the predictions. To accomplish this goal the project involved the following tasks:

- A parametric study was conducted involving 79 full-scale fire tests on upholstered furniture mockups. The primary objective of these tests was to quantify ignition

scenario (including incendiary) and enclosure effects on the burning behavior of upholstered furniture.

- Small-scale tests were performed to obtain fire properties of the two fabrics and six padding materials and specific fabric-padding combinations used in the construction of the mockups. Tests were conducted in the Cone Calorimeter (ASTM E 1354) and the Microscale Combustion Calorimeter (ASTM D 7309). In addition, specimens of the six padding materials were tested to verify their compliance (or non-compliance) with CA TB 117.
- The predictive capability of three upholstered furniture burning rate models was determined based on the results of the parametric study and the small-scale tests. One of the three models was slightly modified to improve agreement between calculated and measured PHRRs. In addition, an attempt was made to use the field fire model FDS to better account for the effect of the exact location of the ignition source on flame spread over the seating surface.
- Twenty-two sets of used upholstered furniture were obtained. Twenty-seven full-scale room fire tests were conducted on at least one item on each set. A reduced number of Cone Calorimeter and Microscale Combustion Calorimeter tests were performed on the soft component materials. Specimens of the padding materials were tested to verify their non-compliance with CA TB 117.
- The small- and full-scale test data on the used furniture (components) were used to assess the predictive capability of the aforementioned upholstered furniture burning rate models. In addition, the zone fire model CFAST and field fire model FDS were used to determine how the use of the upholstered furniture burning rate models (compared to the use of measured HRR data for the item) affect the accuracy of temperature and heat flux estimates in the room.
- Finally, guidelines were developed for fire investigators on how to best estimate the heat release versus time curve of upholstered furniture that was involved in a fire.

Additional details on the methods that were used are provided below.

3.2 FULL-SCALE EXPERIMENTAL SETUP

3.2.1 Calorimeters

The peak heat release for the various items that were tested in full-scale was expected to vary from a few hundred kW to several MW. To optimize the accuracy of the measurements, two full-scale calorimeters of different capacity were used. The two calorimeters were calibrated with propane burners and heptane pan fires. The uncertainty of the calibration constant for the smaller calorimeter was determined to be 3.1% based on a propane burner calibration with a PHRR of 193 kW. The uncertainty for the larger hood was determined to be 2.1% based on a heptane pan fire with a PHRR of 1.7 MW.

The first calorimeter hood is best suited for measuring HRRs up to 1 MW. The second is designed for fires up to 10-MW fires. Figure 2 shows the location of the two hoods in the calorimetry building at Southwest Research Institute (SwRI). The test room was located between the two hoods and an open doorway was provided in the end wall that connects to the hood of the calorimeter used in the test. Figure 2 also shows a large conditioning room to the North of the calorimetry building. The mockup cushions and used furniture were conditioned in this room at constant temperature of $23\text{ }^{\circ}\text{C} \pm 3\text{ }^{\circ}\text{C}$ and relative humidity of $50\% \pm 5\%$ prior to testing.

The gas sampling train for both full-scale calorimeters was configured as shown in Figure B-2. The gas analysis system comprised a Servomex 4100 series paramagnetic O₂ analyzer with integrated CO₂ and CO cells obtained from Fire Testing Technology (FTT). The FTT analyzer is optimized for oxygen consumption calorimetry. A Yokogawa DA 100 data acquisition system was used to collect data at one second intervals.

3.2.2 Test Room

The test room consisted of a light wood frame covered with two layers of ½-in. type X gypsum board. A plan view of the room is shown in Figure 3. The room interior measured $4.65 \times 3.43 \times 2.43\text{ m}$ (L × W × H). The furniture item was placed on a scale in a corner opposite the open doorway. The 0.74 m wide and 2.0 m high doorway was located in the center of one of the short walls. The interior layer of gypsum board was replaced between tests as needed. The room was rotated 180° to move from the small to the large calorimeter (the small calorimeter tests were conducted first).

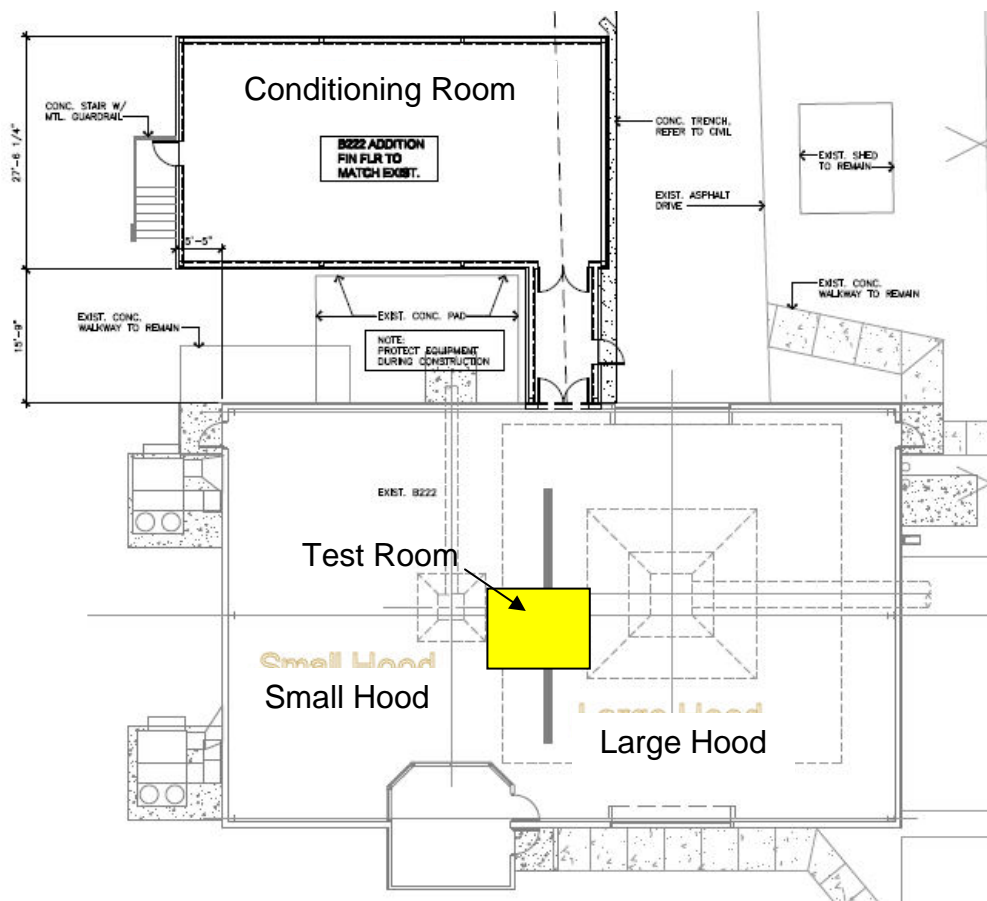


Figure 2. Plan View of SwRI Calorimeter Building and Conditioning Room.

Digital cameras were used to obtain video from three angles: through the doorway (HD), from the short wall next to the doorway, and from the long wall opposite the specimen.

Several (partial height) TC trees and heat flux meters were installed to characterize the thermal environment inside the room. The TCs located 0.1 m below the ceiling at the four quadrants and the center of the room (TCs #16–#20) were 1.6-mm diameter, stainless steel sheathed, grounded junction type K probes. Glass-insulated 24-AWG type K TCs were used to measure gas temperatures above the specimen (TCs #1–#4). All remaining TCs were 1.6-mm diameter, stainless steel, exposed junction type K probes. The location of the TCs is shown in Figure 3 and Table 14.

The heat flux meters were of the Schmidt-Boelter type with a sensing surface of 25 mm in diameter. One heat flux meter was located on the floor in the center of the room. The remaining two heat flux meters were located as shown in Figure 3, 1.68 m from the floor.

The location of the room instrumentation can also be seen in Figures 4–9. The general features and instrumentation of the calorimeter are described in Section B.1.2.

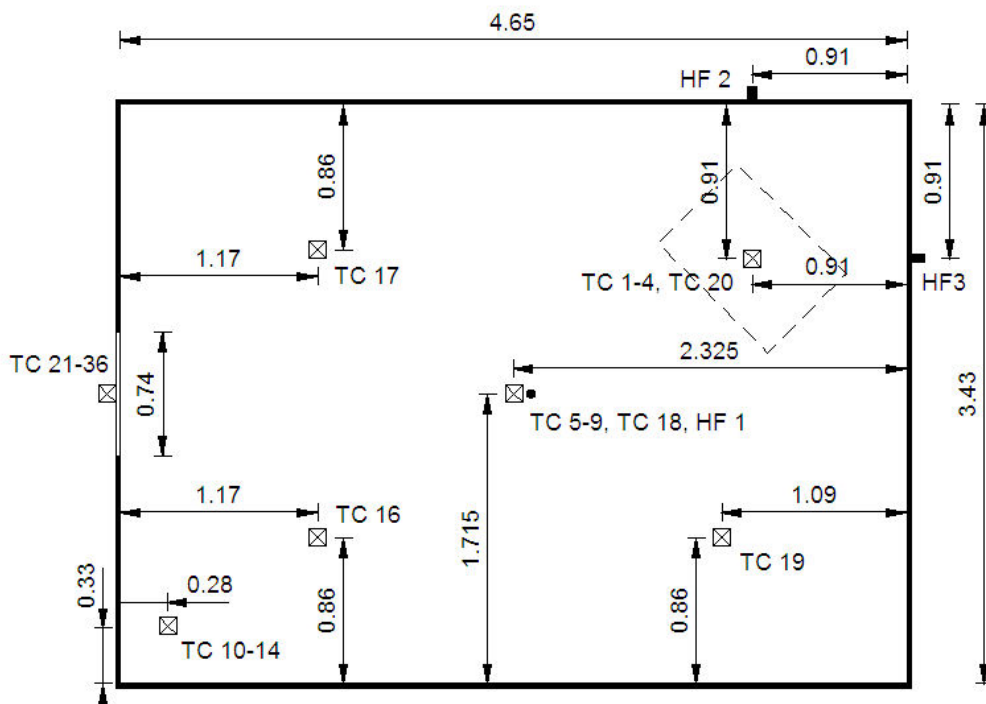


Figure 3. Plan View of Test Room.

Table 14. Distance of Tree TCs above the Floor or below the Door Header.

Specimen Tree			Doorway Tree		
TC #	Height (m)	Height (ft)	TC #	Distance from Header (m)	Distance from Header (in.)
1	1.22	4	21	0.10	4
2	1.52	5	22	0.20	8
3	1.83	6	23	0.30	12
4	2.13	7	24	0.41	16
Center Tree			25	0.51	20
TC #	Height (m)	Height (ft)	26	0.61	24
5	0.61	2	27	0.71	28
6	1.22	4	28	0.81	32
7	1.52	5	29	0.91	36
8	1.83	6	30	1.02	40
9	2.13	7	31	1.12	44
Corner Tree			32	1.27	50
TC #	Height (m)	Height (ft)	33	1.42	56
10	0.61	2	34	1.57	62
11	1.22	4	35	1.73	68
12	1.52	5	36	1.88	74
13	1.83	6			
14	2.13	7			



Figure 4. 1-Seat Sofa Mockup Placed on Scale prior to Testing.

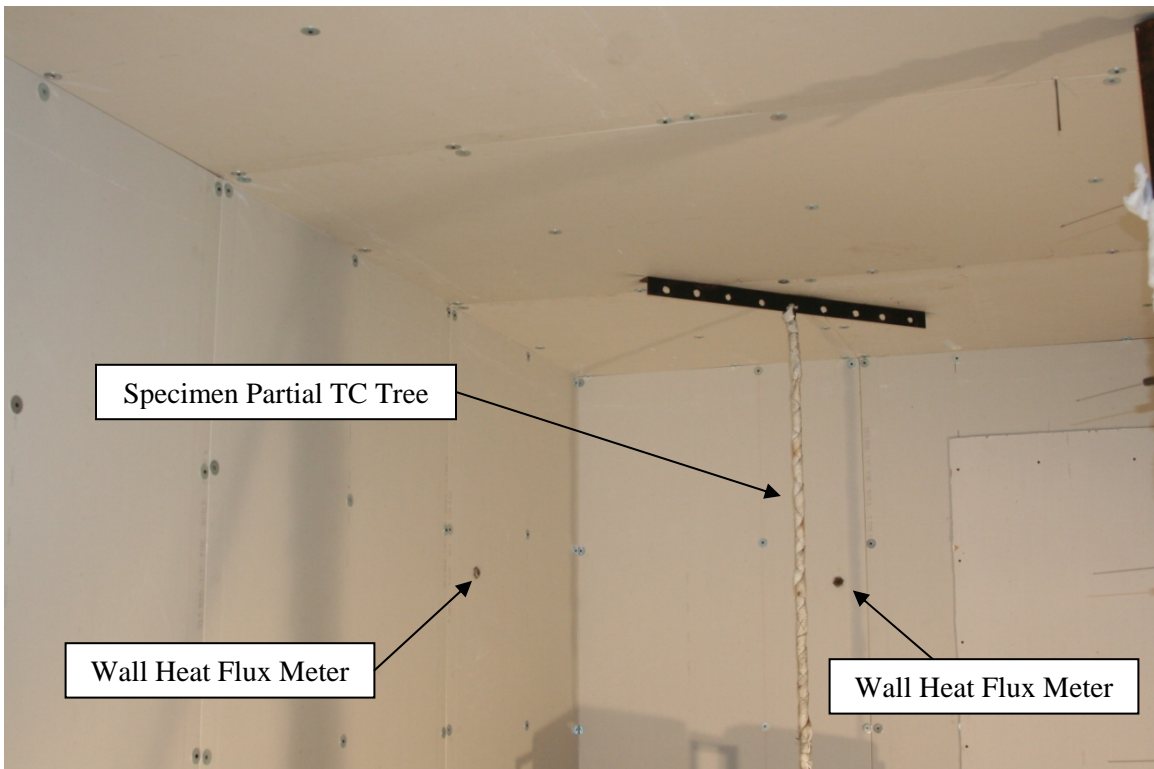


Figure 5. TC Tree above Specimen and Wall Heat Flux Meters.

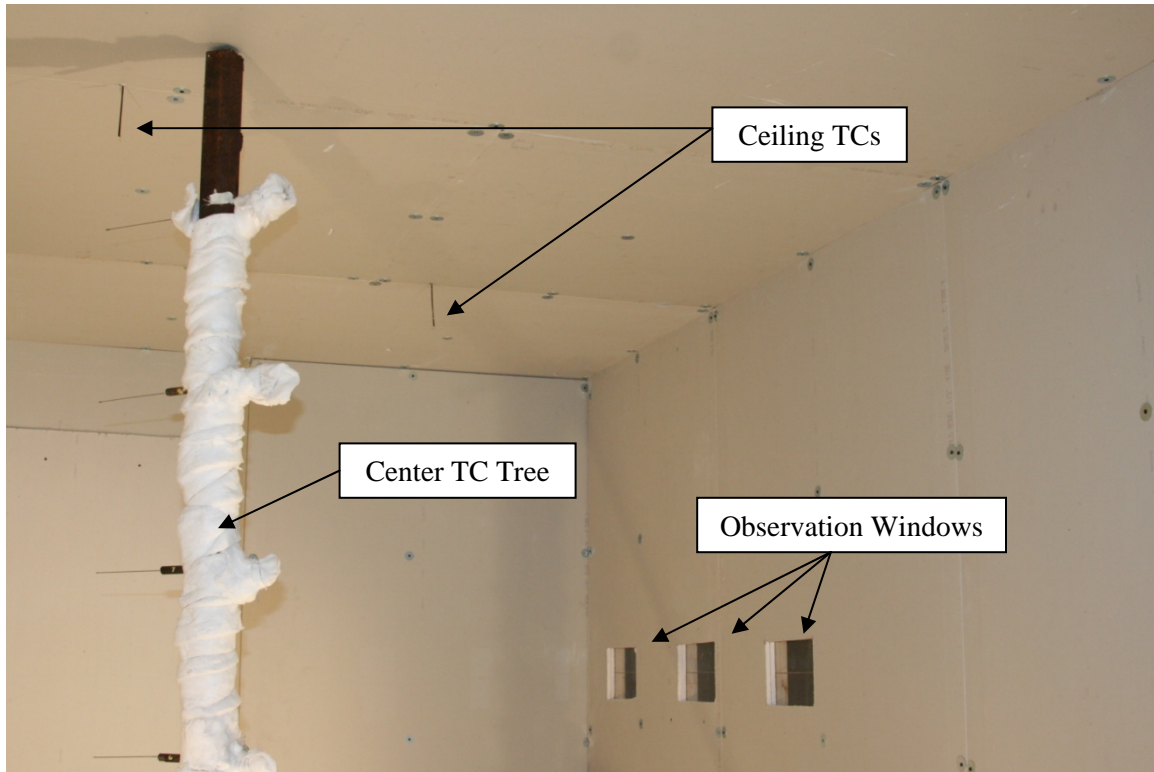


Figure 6. Back Corner in Test Room Opposite Specimen.



Figure 7. Doorway TC Tree Moved to the Side for Easy Room Access.



Figure 8. Test Shortly after Ignition with Small Flame.



Figure 9. Test on 1-Seat Sofa near Peak Burning.

3.3 FULL-SCALE FURNITURE MOCKUP TESTS

3.3.1 Overview

The primary objective of the tests on upholstered furniture mockups was to evaluate the effect of ignition source strength and location on HRR. Three types of ignition sources were used: a small tubular burner; a large gas burner; and a small liquid pool fire simulating the use of an accelerant. Three ignition source locations were evaluated: exposing the seat from the top, exposing the furniture from the front bottom, and exposing the back.

The mockup cushions were constructed with fabrics and padding materials that are common in furniture items that are currently on the market. Six different padding materials and two fabrics were selected. Chairs (without armrests) and 1-, 2-, and 3-seat sofas were included in the test matrix. The effect of a gap in the back of a chair was evaluated as well.

It is cost-prohibitive to include all combinations in the test matrix (5 types of chairs or sofas \times 3 sources \times 3 locations \times 6 padding materials \times 2 fabrics = 540 combinations). To reduce the number of tests to a manageable level, the focus was on 1- and 3-seat sofa mockups constructed with one of the two fabrics and one of the three most common padding materials. To further optimize the experimental effort, the effect of the ignition source, its location and the type of padding on the burning rate were determined on the basis of fractional factorial designs, comprising 18 tests for each type of sofa (Mason, Gunst and Hess, 2003). These 36 tests were supplemented with 25 full-scale mockup tests to obtain data for component combinations and ignition scenarios not included in the fractional factorial designs. Prior to the 61 room tests, 18 full-scale mockup tests were conducted with the item placed directly under the calorimeter hood. The primary purpose of the open calorimeter tests was to gain a better understanding of the response of the selected fabric-padding combinations to different ignition sources and refine the experimental design of the room tests.

3.3.2 Material Selection

The test matrix for the mockup tests was completed with the assistance of Dr. Mason (SwRI statistics expert on experimental design) and Dr. Hirschler (expert on upholstered furniture flammability). It was decided to use two types of fabrics, an untreated non-polyolefin fabric (polyolefin fabrics tend to result in high HRRs irrespective of the padding material and ignition scenario) and a FR treated fabric that meets the requirements of NFPA

701. Only two fabrics were considered because the type of fabric primarily affects the time to ignition and has a relatively small effect on the heat release of the chair or sofa. It was also decided to consider, at least initially, six different padding materials: a low and a high density untreated polyurethane foam, a CA TB 117 compliant polyurethane foam, a polychloroprene latex foam (meets more stringent fire performance requirements than CA TB 117 foam), a polyester fiberfill, and a densified polyester fiberfill. Table 15 provides some information about the fabrics and padding materials used in the construction of the mockup cushions.

Table 15. Fabrics and Padding Materials for Mockup Cushions.

Fabric	ID	Color	Supplier	Weight (g/m ²)
(Non-FR) Cotton	Eco Linen	Khaki	San Antonio Upholstery Fabrics	355
FR Cotton	Milano	Black	Dazian, N. Hollywood, CA	415
Padding	ID	CA TB 117	Supplier	Density (kg/m ³)
LD Polyurethane Foam	1030		San Antonio Upholstery Supply	17
HD Polyurethane Foam	25110		San Antonio Upholstery Supply	45
CA TB 117 PU Foam	FR1534	✓	San Antonio Upholstery Supply	23
Polychloroprene Latex	CR SAFGUARD XL	✓	Chestnut Ridge, Latrobe, PA	103
Polyester Wrap	Dacron	✓	San Antonio Upholstery Supply	16
Densified Polyester	FlameChek (Core)	✓	Bob Barker, Fuquay-Varina, NC	23

It was very difficult to find an FR fabric that meets NFPA 701 requirements. Swatches were obtained from three vendors. Verification tests in the laboratory showed that the fabrics did not meet NFPA 701 requirements, contrary to the claims on the vendor’s web site. On the fourth try, a fabric with the desired fire performance was finally found.

CA TB 117 tests were performed on specimens of the six padding materials to verify compliance (or non-compliance) with the standard.

3.3.3 Ignition Scenarios

Three types of ignition sources were used: a small match-like flame, a large gas burner, and a small liquid pool fire simulating the use of an accelerant. Three ignition source locations were evaluated: exposing the seat from the top, exposing the furniture from the front bottom, and exposing the back.

In most cases, the small flame ignition source was BS 5852 Source #1. In a few tests, the item could not be ignited with this source and BS 5852 Source # 2 was then tried. Both BS 5852 sources involve a diffusion burner consisting of a steel tube, with 8.0-mm outside

diameter, 6.5-mm internal diameter, and 200 mm in length, connected by a flexible tube via a rotoameter, fine control valve, an optional on-off valve, and a regulator to a cylinder containing butane.

For Source #1, a flow rate of 45 ml/min at 25 °C is used, corresponding to a HRR of ca. 83 W and a flame height of 35 mm, measured from the top of the burner tube, when held vertically upwards. For Source #2, a flow rate of 160 ml/min at 25 °C is used, corresponding to a HRR of ca. 295 W and a flame height of 145 mm, measured from the top of the burner tube, when held vertically upwards. Butane gas is used as the fuel. The burner flame is applied for 20 s for Source #1, or 40 s for Source #2. Source #1 has been shown to have an intensity equivalent to a small match.

The propane burner described in CA TB 133 and ASTM E 1537 was chosen as the large flame ignition source exposing the seat from the top. This 250 × 250-mm square burner consists of 13-mm outside diameter stainless steel tubing with holes pointing straight out, straight down and inward at a 45° angle at various locations. Propane gas with a net heat of combustion of 46.5 ± 0.5 MJ/kg is supplied at a rate of 13 l/min for a total of 80 s. The burner has an approximate intensity of 19 kW.

The 0.3 × 0.3-m sandbox burner described in NFPA 286 was chosen as the large flame ignition source for front bottom and back exposure. The burner was supplied with propane at the same rate (19 kW) and for the same duration (80 s) as the CA TB 133 burner.

Finally, the liquid pool fire ignition source consisted of 59 ml (2 oz) of gasoline distributed over a seat cushion (top exposure) or 118 ml (4 oz) of gasoline distributed over 25-mm thick ceramic fiber blanket placed inside a 0.28 × 0.43-m metal cookie sheet (front bottom and back exposure). The ceramic fiber blanket made it easier to uniformly distribute the gasoline and to obtain uniform burning over the area of the sheet. The HRR of the incendiary ignition sources was measured in the Furniture Calorimeter and the results of duplicate measurements are shown in Figure 10.

Figures 11–23 provide details on the exact location of the different ignition sources.

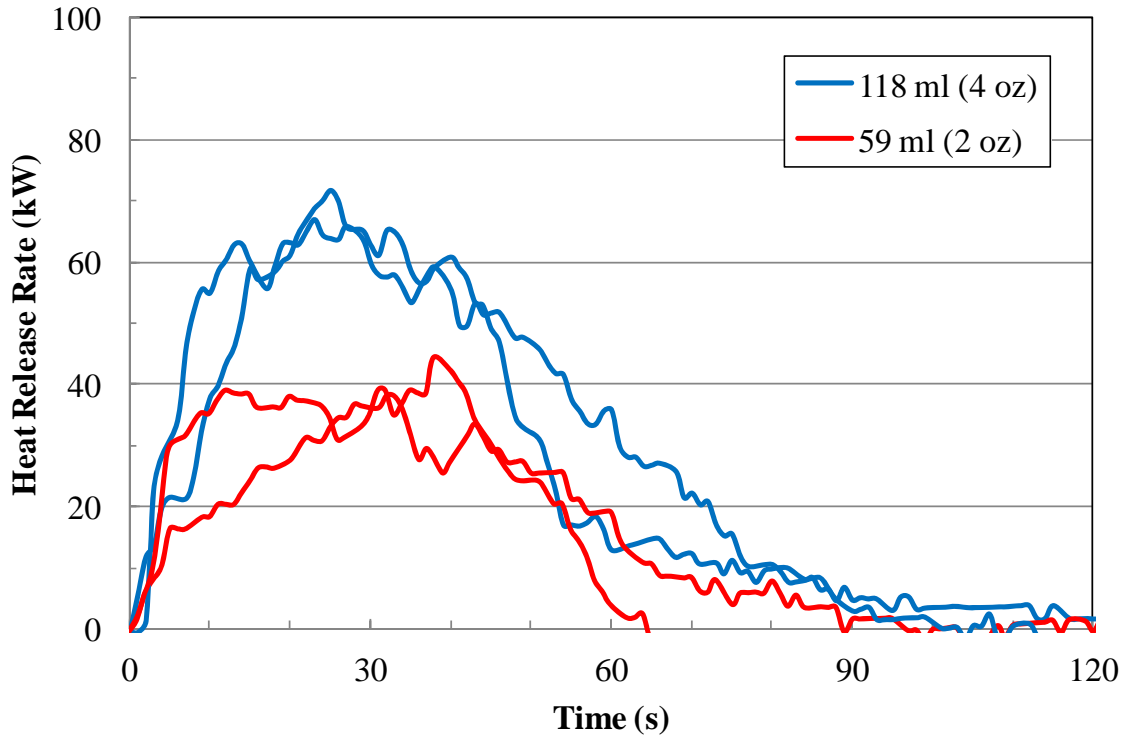


Figure 10. HRR of Liquid Pool Fire Ignition Sources.

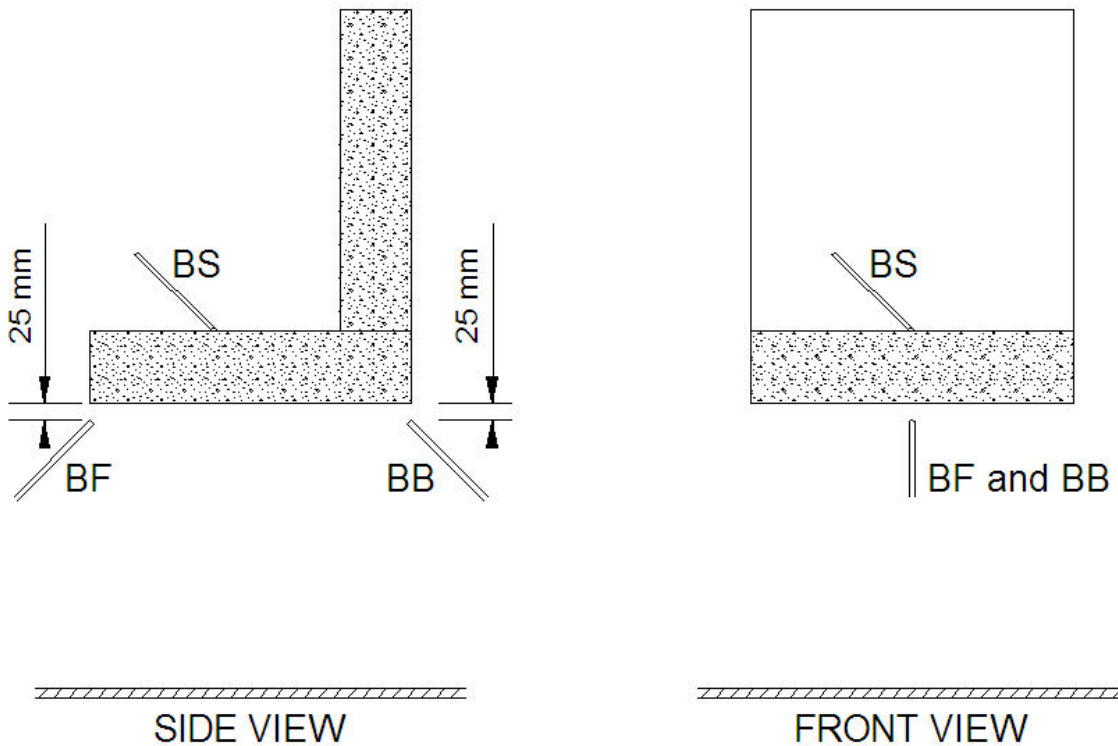


Figure 11. Locations of Small Burner Flame (B), S = Top, F = Front, B= Back.

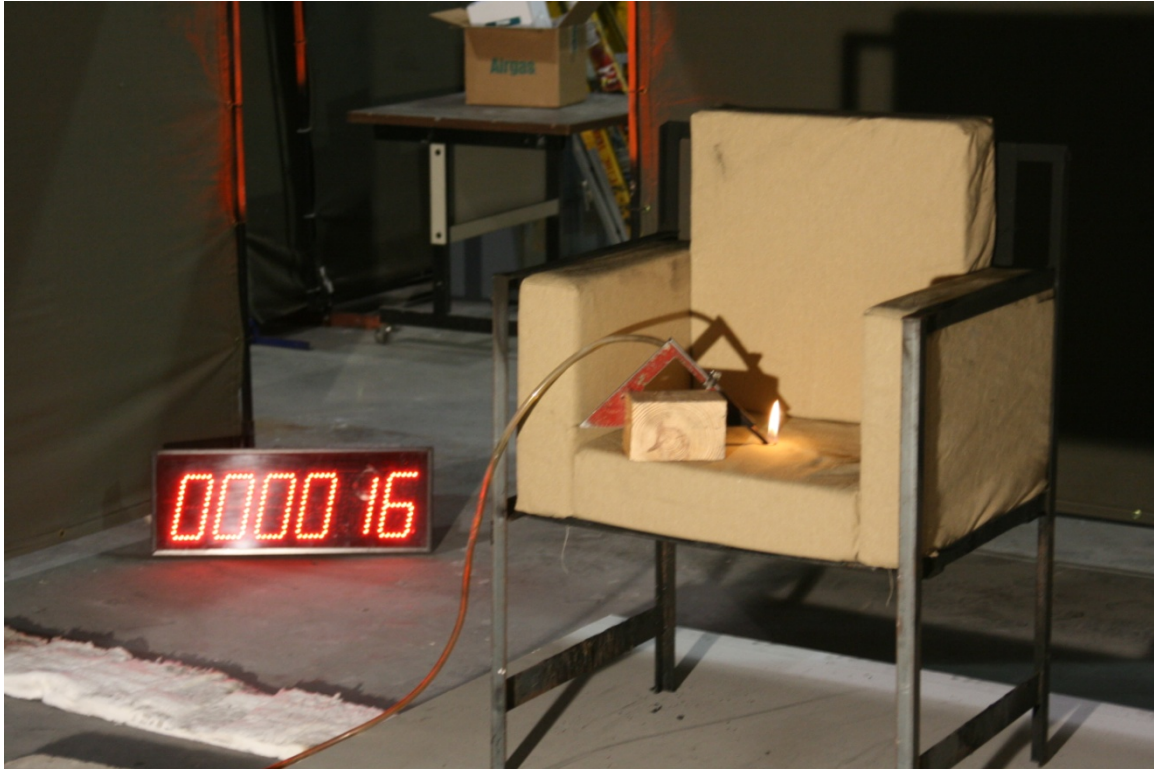


Figure 12. Small Flame Ignition Source Applied to Top (BS).

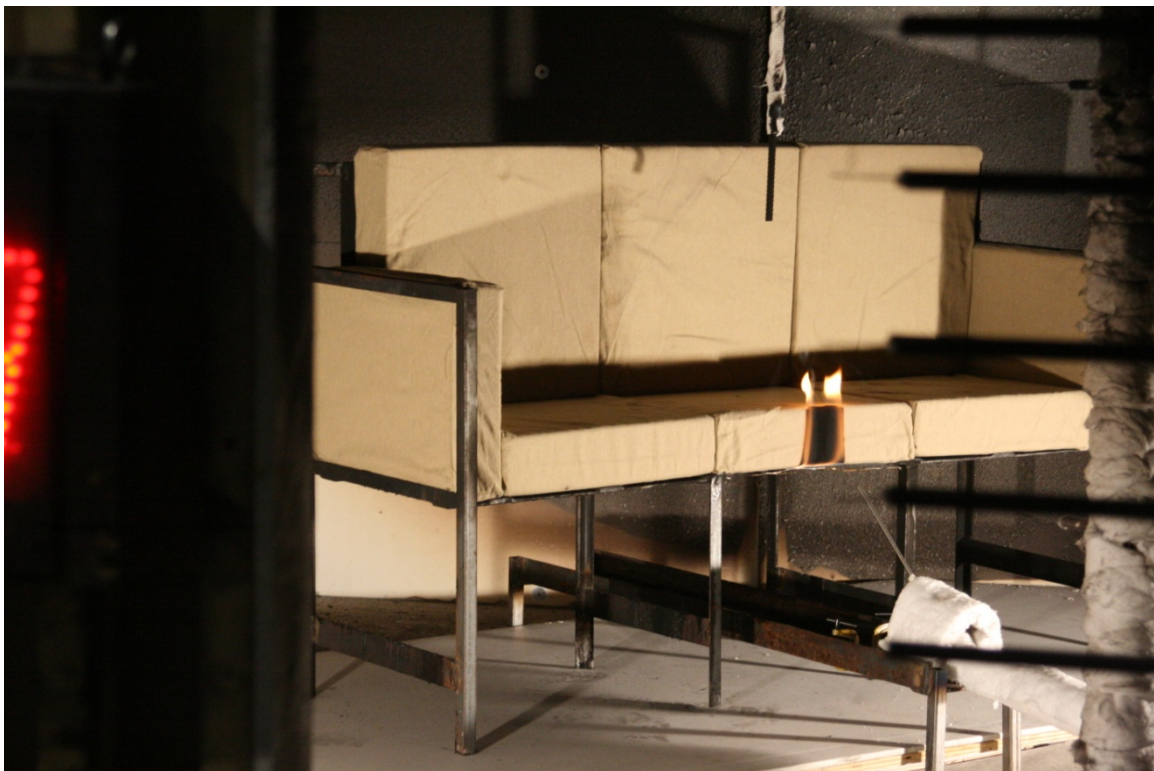


Figure 13. Small Flame Ignition Source Applied to Front Bottom (BF).



Figure 14. Small Flame Ignition Source Applied to Back (BB)

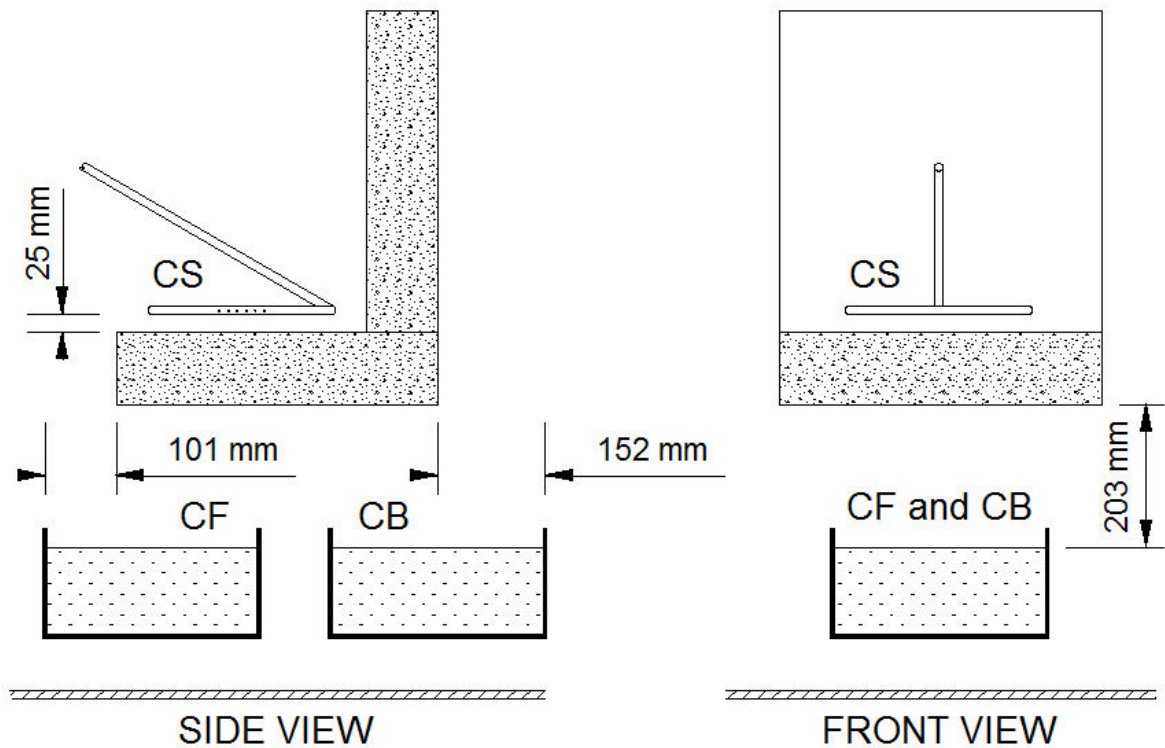


Figure 15. Locations of Large Burner Flame (C), S = Top, F = Front, B= Back.



Figure 16. Large Flame Ignition Source Applied to Top (CS).



Figure 17. Front Bottom Large Flame Ignition Source prior to Ignition (CF).



Figure 18. Large Flame Ignition Source Applied to Front Bottom (CF)

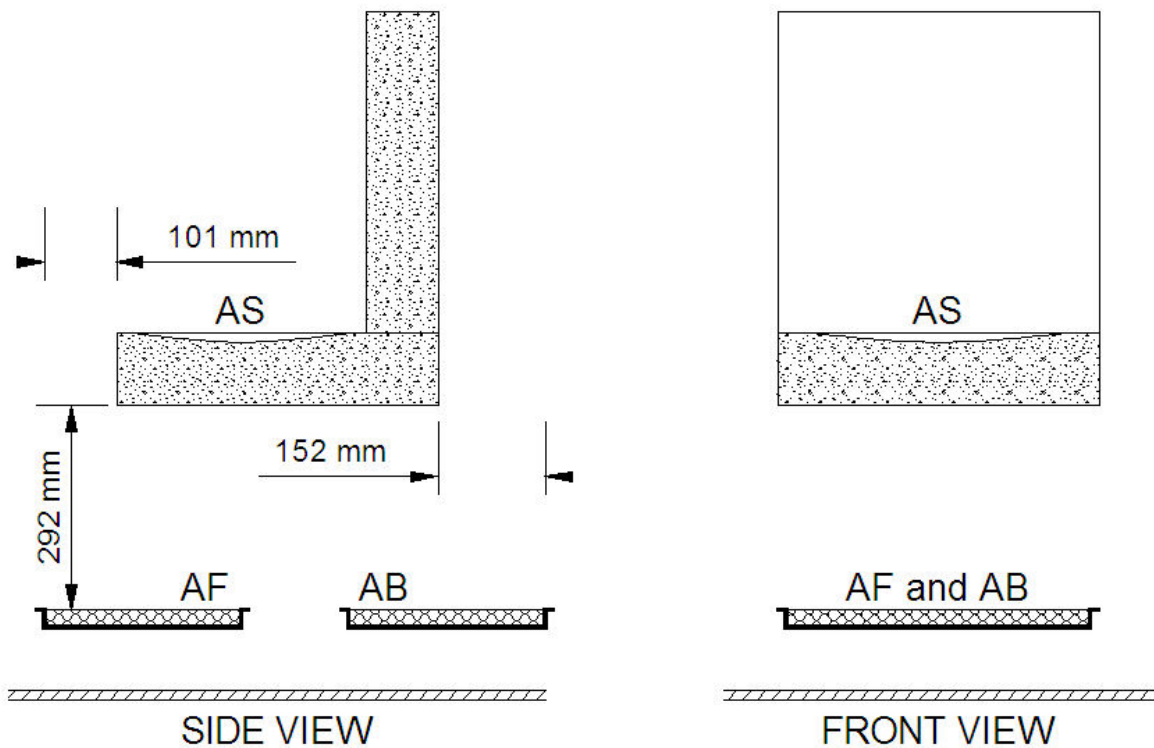


Figure 19. Locations of Liquid Pool Fire (A), S = Top, F = Front, B= Back.

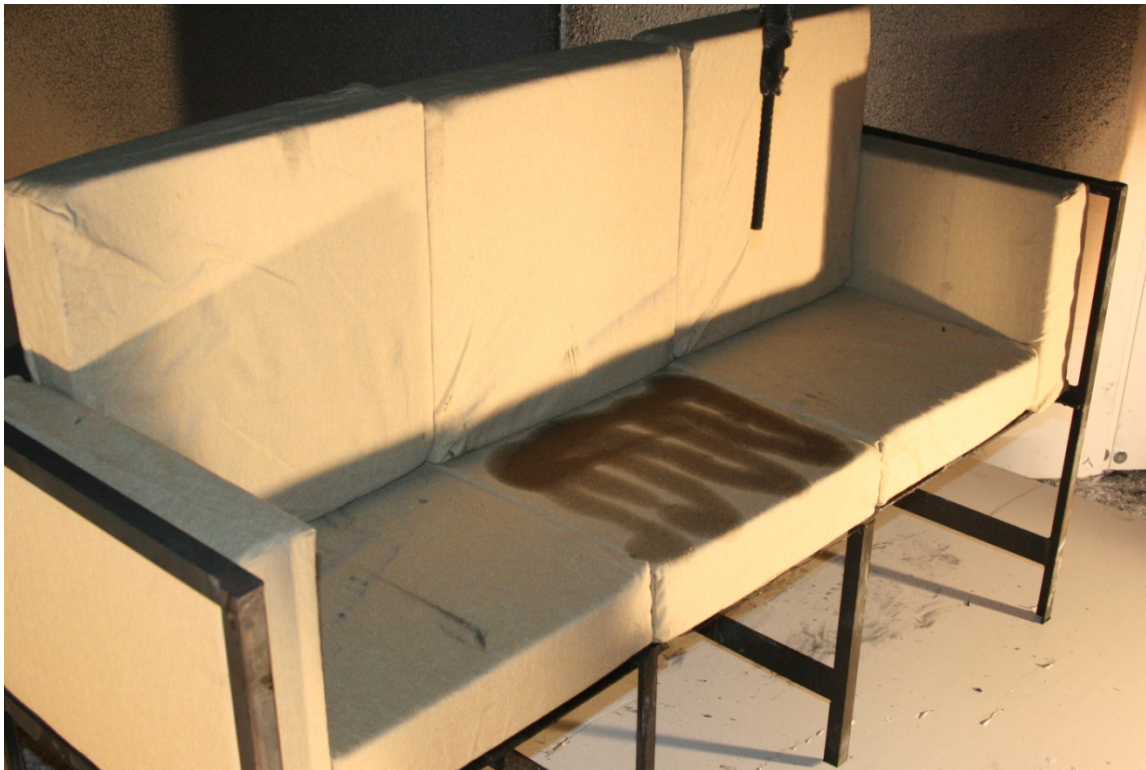


Figure 20. Gasoline Distributed over Seat Cushion (AS).



Figure 21. Liquid Pool Fire Applied to Top (AS).



Figure 22. Gasoline Distributed over Ceramic Fiber Blanket (AF)



Figure 23. Liquid Pool Fire Applied to Front Bottom (AS).

3.3.4 Open Calorimeter Tests

Before performing the statistically designed test matrix it was decided to first run 18 full-scale mockup tests outside the room, directly under the hood. The primary reasons for conducting these preliminary tests were as follows:

- Gain a basic understanding of how the different mockup components and combinations behave when exposed to a small or large flame ignition source and minimize unexpected behavior in the room tests;
- Eliminate component combinations from the test matrix that do not lead to propagating fires (i.e. will not produce any useful data);
- Obtain some information on the repeatability of the tests for small and large ignition sources; and
- Obtain some burning rate data for items tested in the room to gage enclosure effects.

The tests were conducted in general accordance³ with ASTM E 1537. Table 16 provides details about the materials and ignition sources that were used. BS 5852 Source #1 was used in three replicate tests on a 1-seat sofa mockup while the CA TB 133 burner was used in the remaining 15 tests. The two 3-seat sofa tests were actually not true duplicates. In the first test the burner flame was applied to the seat cushion on the right. In the second test the flame was applied to the center cushion.

Table 16. Open Calorimeter Mockup Tests.

Number of Seats	1	1	1	2	3	1	1	1	1	1	1
(Non-FR) Cotton	✓	✓	✓	✓	✓	✓	✓	✓			
FR Cotton									✓	✓	✓
LD Polyurethane Foam	✓	✓									
HD Polyurethane Foam			✓	✓	✓				✓		
CA TB 117 PU Foam						✓				✓	
Polychloroprene Latex											✓
Polyester Wrap							✓				
Densified Polyester								✓			
BS 5852 Source #1	✓										
CA TB 133 Burner		✓	✓	✓	✓	✓	✓	✓	✓	✓	✓
Number of Replicates	3	1	4	1	2	1	2	1	1	1	1

³ The primary deviation was the use of a different ignition source from the ASTM E 1537 standard gas burner ignition source in 3 of the 18 tests.

The furniture mockups were constructed according to the guidelines in CA TB 133. Figures 12–14, 16–18, and 20–23 illustrate how the mockups were built. The dimensions of the seat and back cushions were $0.46 \times 0.46 \times 0.10$ m ($18 \times 18 \times 4$ in.). The dimensions of the armrest cushions were $0.46 \times 0.36 \times 0.10$ m ($18 \times 14 \times 4$ in.). The padding materials were completely encapsulated in fabric cases made by a local upholstery repair shop.

The cushions were arranged in a steel frame as shown in the aforementioned figures. The bottom of the seat cushions was 0.41 m (16 in.) above the floor. After the first few tests, metal support wires were added to prevent cushion pieces from falling to the floor during a test; two to support the seat cushion(s) and two to support the back cushion(s). Room Calorimeter Tests

Sixty-one room calorimeter mockup tests were conducted in general accordance⁴ with ASTM E 1537. Thirty-six tests, eighteen on 1-seat sofas and eighteen on 3-seat sofas, were part of a one-third fraction of a 3^3 factorial experiment to systematically investigate the effect of the type (small gas burner flame, large gas burner flame and accelerant) and location (seat cushion, front bottom and back) of the ignition source. For each experiment there were 9 unique test combinations of the three factors, as well as 9 repeat runs, one for each factor-level combination. The three possible one-third fractions of the full 3^3 factorial experiment are shown in Table 17. Fraction A was used for the 1-seat sofa experiment and Fraction B was chosen for the 3-seat sofa experiment (see Table 18 for details).

The aforementioned 36 tests were supplemented with 25 full-scale mockup tests to obtain data for configurations (chairs with and without a gap in the back and 2-seat sofas), components (FR fabric and densified polyester) and ignition scenarios (small flame applied in a corner) not included in the fractional factorial experiments (see Table 19 for details).

Chairs without a gap were identical to 1-seat sofas, except that they did not have any armrests. Some chairs were tested with a gap, which was created by replacing the back cushion with an armrest cushion suspended from the top of the frame, leaving a 0.1-m (4-in.) gap between the seat cushion and the back cushion.

⁴ The primary deviations were the use of a different ignition source (the standard gas burner ignition source was used in 35 of the 79 test) and a slight larger room than the optional room described in the standard.

Table 17. Possible One-Third Fractions of a 3³ Factorial Experiment.

Fraction A			Fraction B			Fraction C		
Factor 1	Factor 2	Factor 3	Factor 1	Factor 2	Factor 3	Factor 1	Factor 2	Factor 3
0	0	0	0	0	2	0	0	1
0	1	2	0	1	1	0	1	0
0	2	1	0	2	0	0	2	2
1	0	1	1	0	0	1	0	2
1	1	0	1	1	2	1	1	1
1	2	2	1	2	1	1	2	0
2	0	2	2	0	1	2	0	0
2	1	1	2	1	0	2	1	2
2	2	0	2	2	2	2	2	1

Factor 1 = Padding	Factor 2 = Ignition Source	Factor 3 = Source Location
0-Untreated LD Polyurethane Foam	0-Small Flame (BS 5852 #1)	0-Top
1-Untreated HD Polyurethane Foam	1-Large Gas Burner	1-Front Bottom
2-CA TB 117 Polyurethane Foam	2-Liquid Pool Fire	2-Back

Table 18. Details of the Fractional Factorial Experiments.

	1-Seat Sofa (Fraction A)						3-Seat Sofa (Fraction B)								
LD Polyurethane Padding	✓	✓	✓				✓	✓	✓						
HD Polyurethane Padding				✓	✓	✓			✓	✓	✓				
CA TB 117 Foam PU Padding						✓	✓	✓					✓	✓	✓
Small Flame	✓			✓		✓		✓		✓		✓			
Large Gas Burner		✓			✓		✓		✓		✓		✓		
Liquid Pool Fire			✓		✓		✓		✓		✓		✓	✓	
Top	✓			✓		✓		✓	✓				✓		
Front Bottom			✓	✓		✓		✓			✓	✓			
Back		✓			✓	✓		✓			✓			✓	

3.4 SMALL-SCALE FURNITURE MOCKUP TESTS

Cone Calorimeter tests were performed on eight combinations of the mockup components: cotton fabric in combination with LD polyurethane foam, HD polyurethane foam, CA TB 117 compliant polyurethane foam, polyester wrap or densified polyester, and FR-treated NFPA 701 compliant cotton fabric with HD polyurethane foam, CA TB 117 compliant polyurethane foam or polychloroprene latex foam. These tests were performed in triplicate at 25, 35, and 50 kW/m² on specimens prepared according to ASTM E 1474. Selected Cone Calorimeter results obtained at 35 kW/m² are presented in Table 20. Complete results can be found on an accompanying DVD.

Table 19. Additional Room Calorimeter Tests on Mockups.

	Chairs						1-Seat Sofas						2-Seat Sofas			3-Seat Sofas							
(Non-FR) Cotton	✓	✓	✓	✓	✓	✓	✓	✓	✓	✓	✓					✓	✓	✓	✓	✓			
FR Cotton												✓	✓	✓	✓						✓	✓	✓
LD Polyurethane Foam							✓																
HD Polyurethane Foam	✓			✓								✓	✓			✓					✓	✓	✓
CA TB 117 PU Foam		✓			✓			✓	✓					✓	✓		✓						✓
Polychloroprene Latex																							
Polyester Wrap																							
Densified Polyester			✓			✓				✓	✓							✓			✓		
Small Flame							✓	✓													✓		
Large Gas Burner	✓	✓	✓	✓	✓	✓				✓		✓		✓		✓	✓	✓			✓	✓	✓
Liquid Pool Fire									✓		✓		✓	✓									✓
Top Center	✓	✓	✓	✓	✓	✓				✓	✓	✓	✓	✓	✓	✓	✓				✓	✓	✓
Top Corner							✓														✓		
Front Bottom								✓	✓														
No Gap (Chairs Only)	✓	✓	✓																				
Gap (Chairs Only)				✓	✓	✓																	
Number of Replicates	1	1	1	1	1	1	1	2	1	2	1	1	1	1	1	1	1	1	1	1	1	1	1

Table 20. Selected Cone Calorimeter Test Data for Mockup Specimens.

Fabric	Padding	t _{ig} (s)	HRR _{peak} (kW/m ²)	HRR ₁₈₀ (kW/m ²)	Δh _{c, eff} (MJ/kg)
Standard	LD Polyurethane Foam	14	532	180	21.0
Standard	HD Polyurethane Foam	17	452	243	24.3
Standard	CA TB 117 Foam	14	524	174	19.9
Standard	Polyester Wrap	14	454	173	15.5
Standard	Densified Polyester	15	400	146	17.3
FR	HD Polyurethane Foam	17	230	130	20.5
FR	CA TB 117 Foam	17	181	99	15.5
FR	Chloroprene Foam	18	62	--*	1.8

* Flaming combustion ceased before 180 s had elapsed.

The eight component materials were also tested in the Microscale Combustion Calorimeter in duplicate according to the two methods (A and B) described in ASTM D 7309. The results of these tests can be found on the accompanying DVD as well.

3.5 MODELING OF MOCKUP FURNITURE TESTS

Three models to estimate the HRR of upholstered furniture on the basis of measured (or estimated) small-scale data were initially considered. These three models are described in Appendix C.

The simplest model was developed by Babrauskas et al. (Babrauskas and Walton, 1986) and requires the heat of combustion (which can be measured in the Microscale Combustion Calorimeter) of the soft combustible materials (fabric and padding) and the total combustible mass. The padding factor in this model was adjusted to improve the agreement between PHRR estimates and those measured in the fractional factorial experiments.

The second model is described in the same paper and is slightly more complicated as it requires the 3-min average HRR measured in the Cone Calorimeter at 25 kW/m^2 . Since no tests were conducted at this heat flux, the second model was adjusted so that the HRR obtained at 35 kW/m^2 can be used.

The third model is the first model described in the CBUF report (Sundström, 1996). This model requires a complete HRR curve measured in the Cone Calorimeter at 35 kW/m^2 .

An attempt was made to use the field fire model FDS to better account for the effect of the exact location of the ignition source on flame spread over the seating surface. Version 5.5.3 of FDS was used. A detailed discussion of this approach can be found in Appendix C.

Finally, the zone fire model CFAST, version 6.1.1, was used to determine how the use of the upholstered furniture burning rate models (compared to the use of measured HRR data) for the mockups affects the accuracy of temperature and heat flux estimates in the room. A brief discussion of zone and field fire models can be found in Appendix A.

3.6 FULL-SCALE USED FURNITURE TESTS

3.6.1 Material Selection

A request was sent via SwRI's global e-mail system to determine whether any employees wanted to make a set of used sofas and/or chairs available for the study. The minimum requirement was that the set had to include at least two items of identical composition, so that one item could be tested in the room calorimeter and specimens for small-scale testing could be obtained from another item. The response was very positive and within a few weeks 22 sets were found that met the criteria. Details are provided in Table 21. The yellow-shaded cells identify the items that were tested in full-scale. Pictures can be found in Appendix D.

Table 21. Details of the Used Furniture Sets Obtained for Testing.

Set #	3-Seat	2-Seat	1-Seat	Chair	Ottoman	Notes	Test #
1	1		1		1		U16
2				2		Test one of the two chairs	U04
3	1	1					U26
4	1	1					U27
5	2					Test one 3-seat sofa	U24
6		2				Test one 2-seat sofa	U12
7	1	1					U23
8	1	1					U22
9	1	1					U20
10	1	1					U21
11	1	1	1		1	Test 1-seat and 3-seat sofa	U05 & U15
12	1	1					U19
13	1	1				3-seat sofa is sleeper	U13
14	1		1				U06
15				6		Test three chairs of six	U01-U03
16	1		2			Test both 1-seat sofas	U07 & U08
17	1	1					U18
18	1	1					U25
19	1	1					U17
20		1	1				U09
21	1	1	1		1	Test 1-seat and 3-seat sofa	U10 & U14
22	1		1			3-seat sofa is sleeper	U11

3.6.2 Room Calorimeter Tests

Twenty-seven room calorimeter tests were conducted on used furniture items: four tests on chairs, seven tests on 1-seat sofas, two tests on 2-seat sofas, and fourteen tests on 3-seat sofas. Approximately one third of the tests were conducted with a small gas burner flame (BS 5852 Source #1 or, in a few cases, BS 5852 Source #2) applied to the center of the (center) seat cushion. The same ignition source was located in a back corner in about another third of the tests. An accelerant (59 ml of gasoline) was applied to the (center) seat cushion in the remaining tests.

3.7 SMALL-SCALE USED FURNITURE TESTS

A full series of Microflow Combustion Calorimeter tests (Method A) and a reduced number of Cone Calorimeter tests (35 kW/m² in triplicate, with one exception) were performed on the upholstery materials of the used furniture items. Selected Cone Calorimeter

results obtained for used furniture fabric-padding combinations are given in Table 22. In addition, the padding materials of the used furniture were tested according to CA TB 117 to determine whether any padding materials were treated with fire retardants.

Table 22. Selected Cone Calorimeter Test Data for Used Furniture Specimens.

Set #	t_{ig} (s)	HRR_{peak} (kW/m ²)	HRR_{180} (kW/m ²)	$\Delta h_{c, eff}$ (MJ/kg)
1	16	557	154	17.6
2	7	305	188	20.9
3	39	325	219	17.9
4	21	448	288	25.1
5	7	481	--*	20.8
6	17	616	187	23.7
7	18	545	224	17.3
8	13	530	316	30.1
9	13	473	323	27.1
10	11	370	202	19.7
11	25	326	165	16.1
12	12	448	325	26.6
13	16	515	226	22.2
14	6	624	330	29.7
15	10	554	295	25.3
16	11	767	398	30.3
17	9	436	219	24.7
18	15	426	257	23.9
19	17	524	262	26.0
20	15	414	241	21.7
21	9	388	270	23.6
24	10	406	296	22.0

* Flaming combustion ceased before 180 s had elapsed

3.8 MODELING OF USED FURNITURE TESTS

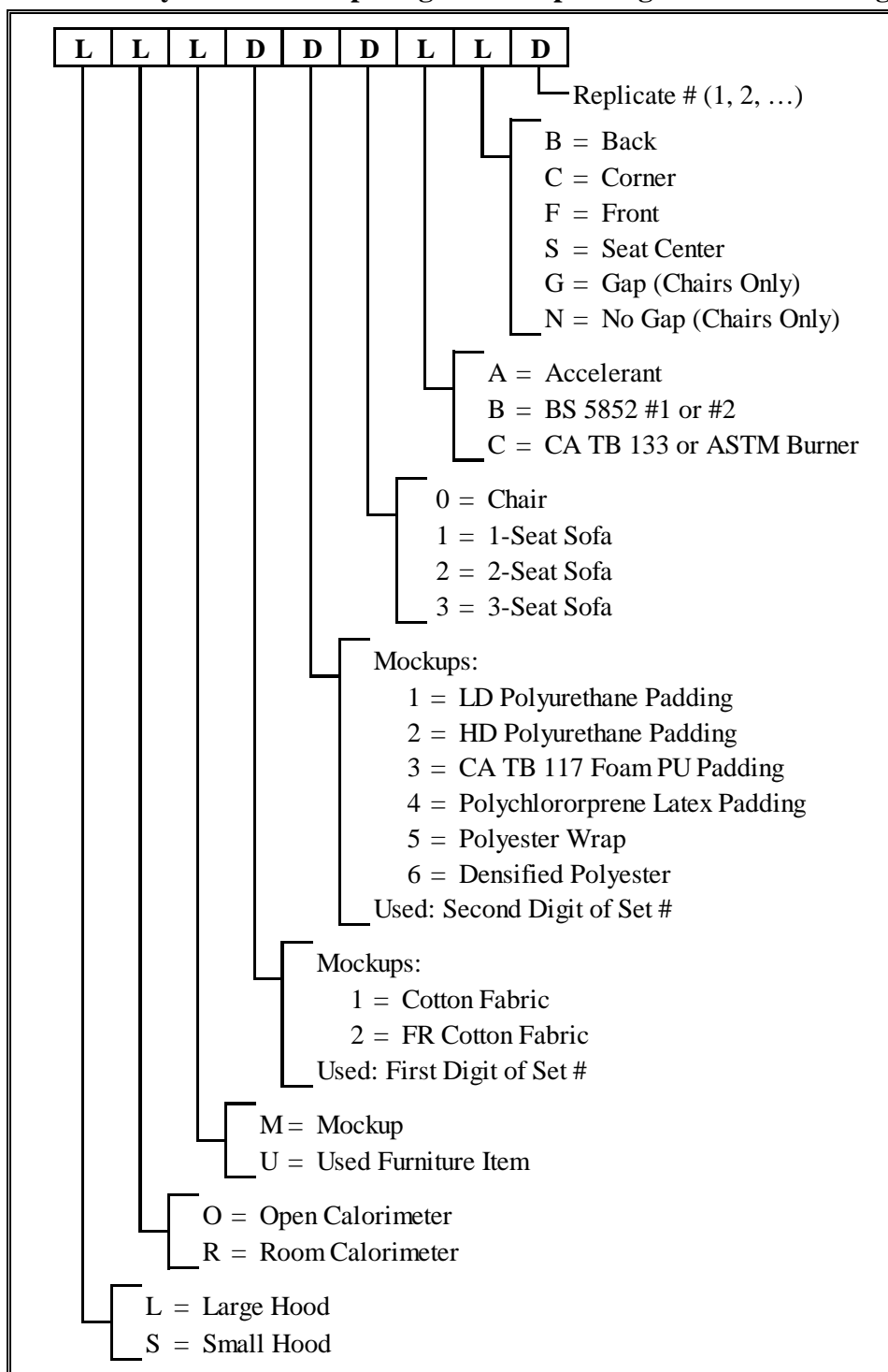
The small- and full-scale test data on the used furniture (components) were used to assess the predictive capability of the aforementioned upholstered furniture burning rate models. In addition, the zone fire model CFAST was used to determine how the use of the upholstered furniture burning rate models (compared to the use of measured HRR data for the item) affect the accuracy of temperature and heat flux estimates in the room.

4 RESULTS

4.1 TEST ID STRING

A system was developed to identify each test with a unique string of nine characters; three letters followed by three digits, two additional letters and a final digit (see Table 23).

Table 23. System for Composing and Deciphering the Test ID String.



For example SOM121CS3 refers to the third test on a 1-seat sofa mockup with cotton fabric and HD polyurethane foam padding conducted in the open under the small hood with a CA TB 133 burner flame ignition source applied to the top. LRU211BC1 refers to the first test on a 1-seat sofa mockup in used set #21 conducted in the room connected to the large hood with a small flame ignition source applied in the corner of the seat cushion.

4.2 FURNITURE MOCKUP TESTS

4.2.1 Open Calorimeter Tests

Table 24 provides a list of the open calorimeter mockup tests in chronological order and in alphabetical order by Test ID.

Table 24. List of Open Calorimeter Mockup Tests.

Test #	Test ID	Date	Data File Name	Test #	Test ID	Date	Data File Name
1	SOM121CS1	01/05/11	11-005NIJ004-1	12	SOM111BS1	01/12/11	11-012NIJ004-1
2	SOM121CS2	01/07/11	11-007NIJ004-2	16	SOM111BS2	01/20/11	11-020NIJ004-1
3	SOM121CS3	01/07/11	11-007NIJ004-3	17	SOM111BS3	01/20/11	11-020NIJ004-2
4	SOM151CS1	01/07/11	11-007NIJ004-4	8	SOM111CS1	01/10/11	11-010NIJ004-2
5	SOM161CS1	01/07/11	11-007NIJ004-5	1	SOM121CS1	01/05/11	11-005NIJ004-1
6	SOM151CS2	01/07/11	11-007NIJ004-6	2	SOM121CS2	01/07/11	11-007NIJ004-2
7	SOM131CS1	01/10/11	11-010NIJ004-1	3	SOM121CS3	01/07/11	11-007NIJ004-3
8	SOM111CS1	01/10/11	11-010NIJ004-2	18	SOM121CS4	02/17/11	11-048NIJ004-1
9	SOM122CS1	01/10/11	11-010NIJ004-3	9	SOM122CS1	01/10/11	11-010NIJ004-3
10	SOM123CS1	01/11/11	11-011NIJ004-1	10	SOM123CS1	01/11/11	11-011NIJ004-1
11	SOM123CS2	01/11/11	11-011NIJ004-2	11	SOM123CS2	01/11/11	11-011NIJ004-2
12	SOM111BS1	01/12/11	11-012NIJ004-1	7	SOM131CS1	01/10/11	11-010NIJ004-1
13	SOM241CS1	01/14/11	11-014NIJ004-1	4	SOM151CS1	01/07/11	11-007NIJ004-4
14	SOM231CS1	01/14/11	11-014NIJ004-2	6	SOM151CS2	01/07/11	11-007NIJ004-6
15	SOM221CS1	01/14/11	11-014NIJ004-3	5	SOM161CS1	01/07/11	11-007NIJ004-5
16	SOM111BS2	01/20/11	11-020NIJ004-1	15	SOM221CS1	01/14/11	11-014NIJ004-3
17	SOM111BS3	01/20/11	11-020NIJ004-2	14	SOM231CS1	01/14/11	11-014NIJ004-2
18	SOM121CS4	02/17/11	11-048NIJ004-1	13	SOM241CS1	01/14/11	11-014NIJ004-1

4.2.1.1 Measurement Uncertainty

The method that was used to quantify the uncertainty of the heat release rate measurements is discussed in Appendix B, Section B.2. Figure 24 shows the results of measurement uncertainty calculations based on Equation B-5 for test SOM121CS3. The thick line is the HRR measured with the oxygen consumption techniques. The two thin lines correspond to the HRR \pm the expanded uncertainty (coverage factor of 2). The uncertainty at

the PHRR is $\pm 8.6\%$. This is typical as for PHRRs between 170 kW and 2.5 MW the uncertainty varies between 7.8%–9.6%.

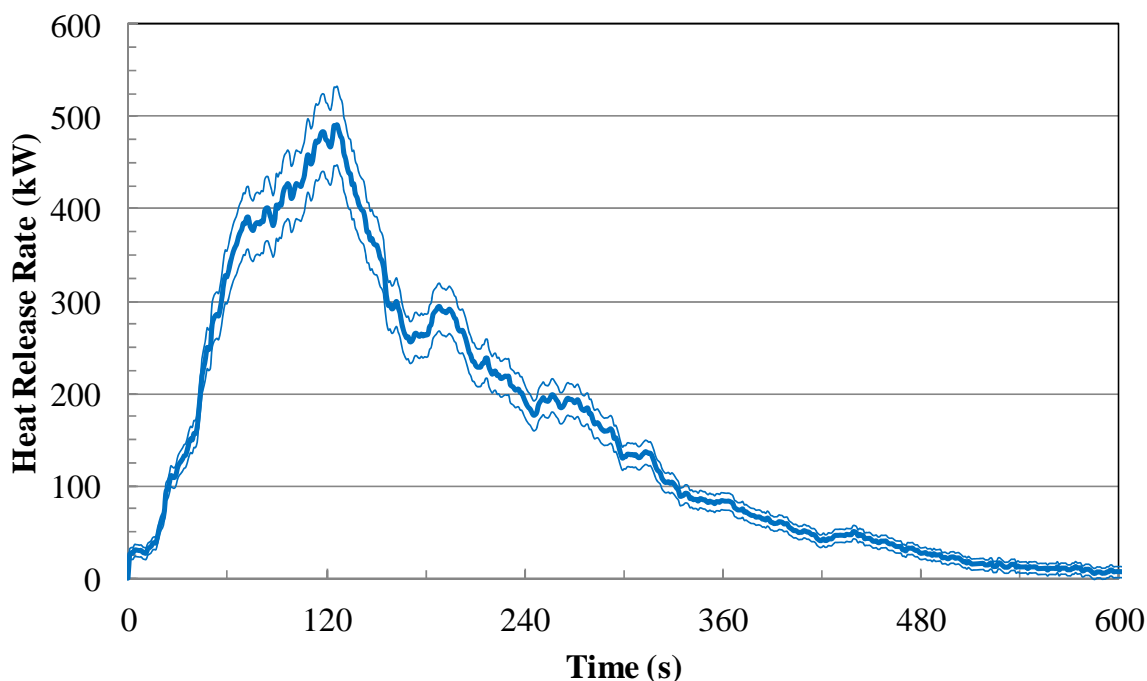


Figure 24. Measurement Uncertainty of 1-Seat Sofa Mockup HRR.

Table 24 shows that four replicate tests were conducted on the same 1-seat sofa mockup. The HRRs measured in the four tests are shown in Figure 25. The coefficient of variance at the 95% confidence level based on these four tests is 7.9%. This is slightly higher than the expanded uncertainty of the PHRR without accounting for the uncertainties of E and α , which is equal to $6.2\%^5$. The difference, $\sqrt{7.9^2 - 6.2^2} = 4.9\%$, is the uncertainty from sources that are not accounted for by Equation B-5.

4.2.1.2 Repeatability

The repeatability of tests on untreated component mockups with a large flame ignition source (CA TB 133 burner) is very good as shown in Figure 25. The repeatability of tests with a small flame ignition source is not so good as shown in Figure 26. This is due to the variability of flame propagation from the central point where the seat is ignited to the armrests and/or back cushion. This results in significant variation of the time to the onset of a self-propagating fire, but it also seems to affect the PHRR.

⁵ Identical values for E and α were used in calculating the heat release rate for the four replicate tests. The uncertainty of these two parameters should therefore not be considered when calculating the expanded combined uncertainty of \dot{Q} .

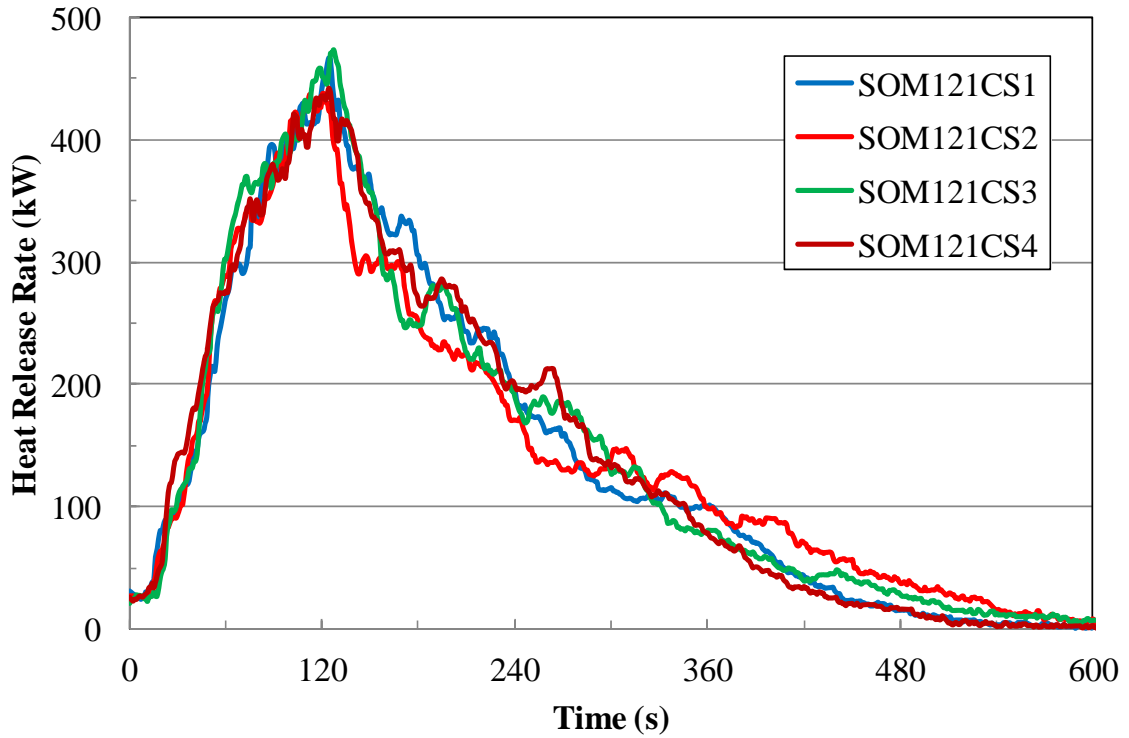


Figure 25. HRR Repeatability for a 1-Seat Sofa Ignited by a Large Flame.

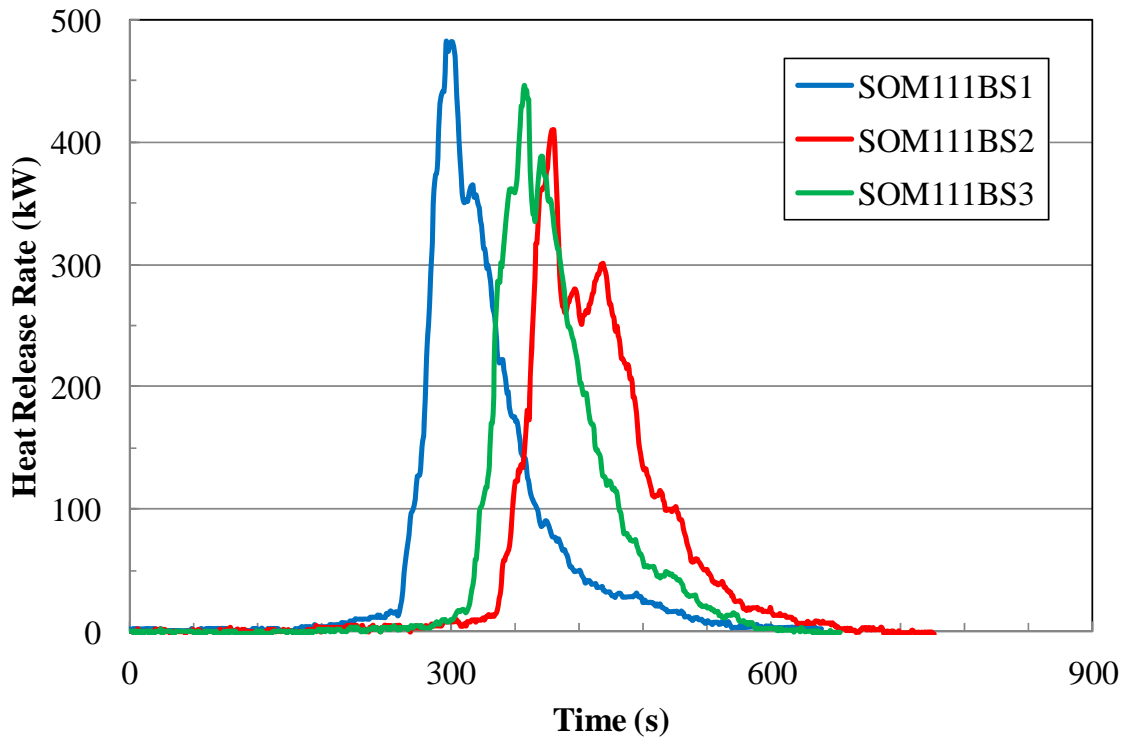


Figure 26. HRR Repeatability for a 1-Seat Sofa Ignited by a Small Flame.

4.2.1.3 *Effect of Ignition Source Location*

Two tests were performed on a 3-seat sofa with cotton fabric and HD polyurethane foam. In the first test, SOM123CS1, the CA TB 133 burner flame was applied to the seat cushion on the right (see Figure 27). In the second test, SOM123CS2, the burner flame was applied to the center seat cushion (see Figure 16). In the first test, the flames spread from the right side to the left side (see Figure 28). When the flames reached the armrest on the left side, part of the material on the right side had already been consumed. This resulted in a relatively steady HRR that peaked slightly above 400 kW (see Figure 29). In the second test, the flames spread in two directions (see Figure 30). As a result the HRR continuously increased until the two armrests ignited and a PHRR of close to 1 MW was reached (see Figure 29). Note that during the first few minutes the rate of fire growth is comparable in both tests, but the HRR vs. time curves start to deviate when flame spread becomes a factor. This example illustrates that a seemingly small difference of one parameter in the ignition scenario can have a surprisingly dramatic effect on fire growth.



Figure 27. SOM123CS1 during Large Burner Flame Exposure.



Figure 28. SOM123CS1: Flames Spread from Ignited Side to the Other Side.

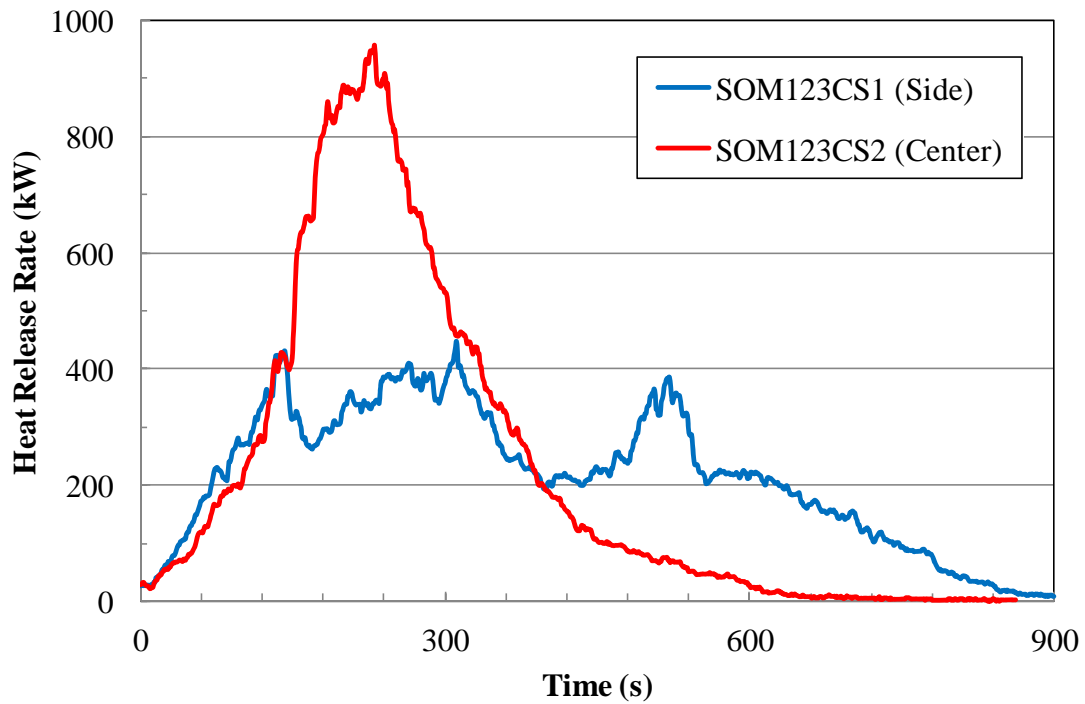


Figure 29. Effect of Ignition Source Location on HRR of a 3-Seat Sofa.



Figure 30. SOM123CS2: Flames Spread from Center to Both Sides.

4.2.1.1 Other Observations

The FR fabric in combination with the polychloroprene foam hardly ignited, even when exposed to the CA TB 133 burner flame. Combustion ceases shortly after the burner is turned off.

The lower density polyester wrap actually performed a little better (slightly lower HRR) than the densified CA TB 117 compliant polyester. Both types of padding materials seem to have very similar composition, but the densified version performs worse because there simply is more material to burn.

4.2.1.2 Conclusions

The main conclusions from the open calorimeter tests were as follows:

- The repeatability of the HRR of upholstered furniture mockups with non-FR treated components exposed to a large burner flame ignition source is very good.
- There is significant variation in the time to the onset of a self-propagating fire, and to a lesser extent the PHRR, of upholstered furniture mockups with non-FR treated components exposed to a small flame ignition source.

- Based on the significant effect on the HRR of a 3-seat sofa of side versus center ignition, it was decided in future tests on 3-seat sofas to apply the burner flame to the center seat cushion.
- There is very little information to be obtained from tests on mockups with the FR fabric and/or chloroprene latex foam.
- Room tests involving polyester padding will use the densified material because it is easier to handle and performs slightly worse than the polyester wrap.

4.2.2 Room Calorimeter Tests

4.2.2.1 Fractional Factorial Design Tests

Table 25 provides a list of the fractional factorial design tests in chronological order and in alphabetical order by Test ID.

To analyze the results from fractional factorial experiments, the heat release curve from the tests were approximated by a triangle as shown in Figure 31. The procedure was as follows:

1. Determine t_1 as the time in s when the HRR first reaches 100 kW.
2. Determine t_p as the time in s for the HRR to reach its peak. Also determine the PHRR in kW.
3. Determine t_2 as the time in s when the HRR first decreases to 100 kW after reaching the PHRR.
4. Determine t_0 by extrapolating a straight line passing through (t_p, PHRR) and $(t_1, 100)$ to the abscissa.
5. Determine t_3 by extrapolating a straight line passing through (t_p, PHRR) and $(t_2, 100)$ to the abscissa.

Charts comparing the triangular approximation to the measured HRRs for the 36 tests can be found in Appendix E. Each triangle is uniquely defined by four variables: t_0 , $t_p - t_0$, PHRR and $t_3 - t_0$. The first variable, t_0 , is a measure of the time from the start of the test (application of the ignition source) to the onset of a self-propagating fire. The second variable, $t_p - t_0$, is a measure of the growth rate of the fire, i.e., how fast the HRR rises to its peak. The third variable, PHRR, is a measure of the severity of the fire. The fourth variable,

$t_3 - t_0$, is a measure of how long the item burns. The response variables are given in Tables 26 and 27 for the 1-seat and 3-seat sofas, respectively.

Table 25. List of Fractional Factorial Design Tests.

Test #	Test ID	Date	File Name	Test #	Test ID	Date	File Name
1	SRM111BS1	01/27/11	11-027NIJ004-1	47	LRM113AS1	04/13/11	11-103NIJ004-59
2	SRM111BS2	01/27/11	11-027NIJ004-2	48	LRM113AS2	04/13/11	11-103NIJ004-60
5	SRM121BF1	01/28/11	11-028NIJ004-5	45	LRM113BB1	04/12/11	11-102NIJ004-57
6	SRM121CS1	02/21/11	11-052NIJ004-6	46	LRM113BB2	04/12/11	11-102NIJ004-58
7	SRM121CS2	02/21/11	11-052NIJ004-7	55	LRM113CF1	04/15/11	11-105NIJ004-67
12	SRM133CS1	02/23/11	11-054NIJ004-12	56	LRM113CF2	04/18/11	11-108NIJ004-68
14	SRM133CS2	02/23/11	11-054NIJ004-14	49	LRM123AF1	04/13/11	11-103NIJ004-61
24	SRM121BF2	03/09/11	11-068NIJ004-24	50	LRM123AF2	04/14/11	11-104NIJ004-62
25	SRM111CB1	03/15/11	11-074NIJ004-25	41	LRM123BS1	04/11/11	11-101NIJ004-53
26	SRM111CB2	03/15/11	11-074NIJ004-26	42	LRM123BS2	04/11/11	11-101NIJ004-54
27	SRM131CF1	03/15/11	11-074NIJ004-27	53	LRM123CB1	04/15/11	11-105NIJ004-65
28	SRM131CF2	03/16/11	11-075NIJ004-28	54	LRM123CB2	04/15/11	11-105NIJ004-66
29	SRM131BB1	03/16/11	11-075NIJ004-29	51	LRM133AB1	04/14/11	11-104NIJ004-63
30	SRM131BB2	03/16/11	11-075NIJ004-30	52	LRM133AB2	04/14/11	11-104NIJ004-64
32	SRM111AF1	03/23/11	11-082NIJ004-37	43	LRM133BF1	04/11/11	11-101NIJ004-55
33	SRM111AF2	03/23/11	11-082NIJ004-38	44	LRM133BF2	04/12/11	11-102NIJ004-56
34	SRM121AB1	03/24/11	11-083NIJ004-39	32	SRM111AF1	03/23/11	11-082NIJ004-37
35	SRM121AB2	03/24/11	11-083NIJ004-40	33	SRM111AF2	03/23/11	11-082NIJ004-38
36	SRM131AS1	03/24/11	11-083NIJ004-41	1	SRM111BS1	01/27/11	11-027NIJ004-1
37	SRM131AS2	03/24/11	11-083NIJ004-42	2	SRM111BS2	01/27/11	11-027NIJ004-2
41	LRM123BS1	04/11/11	11-101NIJ004-53	25	SRM111CB1	03/15/11	11-074NIJ004-25
42	LRM123BS2	04/11/11	11-101NIJ004-54	26	SRM111CB2	03/15/11	11-074NIJ004-26
43	LRM133BF1	04/11/11	11-101NIJ004-55	34	SRM121AB1	03/24/11	11-083NIJ004-39
44	LRM133BF2	04/12/11	11-102NIJ004-56	35	SRM121AB2	03/24/11	11-083NIJ004-40
45	LRM113BB1	04/12/11	11-102NIJ004-57	5	SRM121BF1	01/28/11	11-028NIJ004-5
46	LRM113BB2	04/12/11	11-102NIJ004-58	24	SRM121BF2	03/09/11	11-068NIJ004-24
47	LRM113AS1	04/13/11	11-103NIJ004-59	6	SRM121CS1	02/21/11	11-052NIJ004-6
48	LRM113AS2	04/13/11	11-103NIJ004-60	7	SRM121CS2	02/21/11	11-052NIJ004-7
49	LRM123AF1	04/13/11	11-103NIJ004-61	36	SRM131AS1	03/24/11	11-083NIJ004-41
50	LRM123AF2	04/14/11	11-104NIJ004-62	37	SRM131AS2	03/24/11	11-083NIJ004-42
51	LRM133AB1	04/14/11	11-104NIJ004-63	29	SRM131BB1	03/16/11	11-075NIJ004-29
52	LRM133AB2	04/14/11	11-104NIJ004-64	30	SRM131BB2	03/16/11	11-075NIJ004-30
53	LRM123CB1	04/15/11	11-105NIJ004-65	27	SRM131CF1	03/15/11	11-074NIJ004-27
54	LRM123CB2	04/15/11	11-105NIJ004-66	28	SRM131CF2	03/16/11	11-075NIJ004-28
55	LRM113CF1	04/15/11	11-105NIJ004-67	12	SRM133CS1	02/23/11	11-054NIJ004-12
56	LRM113CF2	04/18/11	11-108NIJ004-68	14	SRM133CS2	02/23/11	11-054NIJ004-14

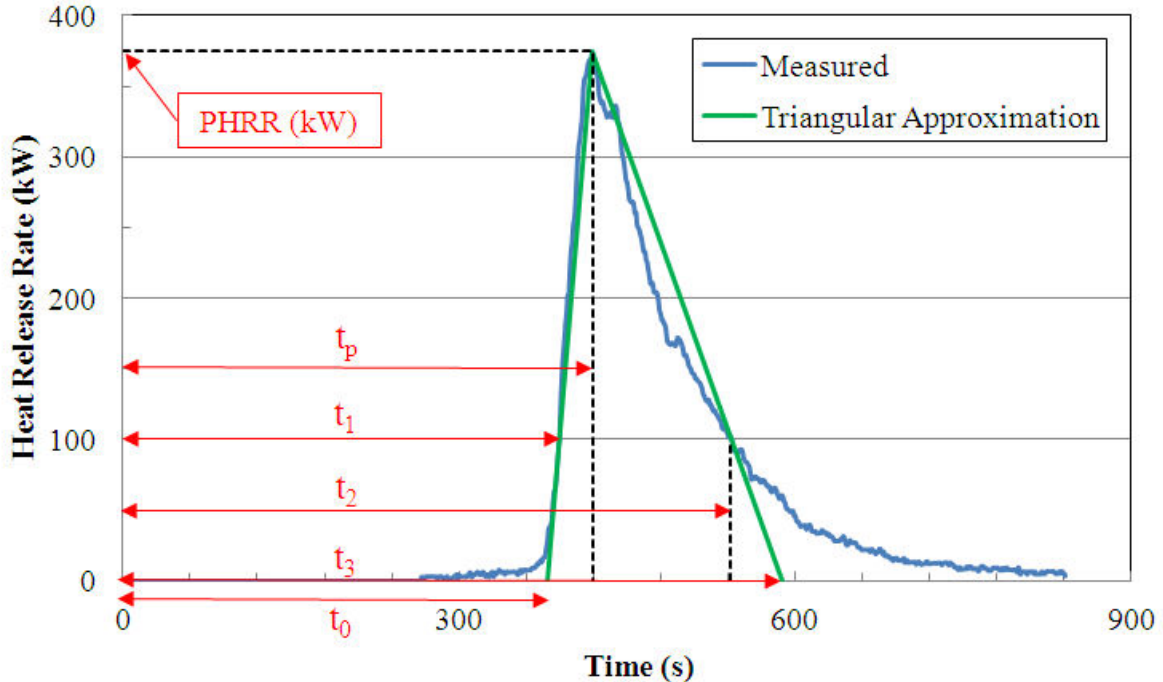


Figure 31. Triangular Approximation of HRR Curve.

Table 26. Response Variables for 1-Seat Sofa Triangular HRR Approximations.

Test ID	Date	CM (kg)	Padding	Source	Location	t_0 (s)	PHRR (kW)	Δt_{0-p} (s)	Δt_{0-3} (s)
SRM111BS1	27-Jan	1.95	0	0	0	379	375	40	209
SRM111BS2	27-Jan	1.94	0	0	0	351	376	52	195
SRM111CB1	15-Mar	1.93	0	1	2	83	390	65	192
SRM111CB2	15-Mar	1.92	0	1	2	139	341	74	201
SRM111AF1	23-Mar	1.94	0	2	1	29	457	33	205
SRM111AF2	23-Mar	1.89	0	2	1	25	433	42	199
SRM121BF1	28-Jan	3.99	1	0	1	437	830	98	323
SRM121BF2	9-Mar	3.97	1	0	1	453	492	85	370
SRM121CS1	21-Feb	3.98	1	1	0	20	442	114	442
SRM121CS2	21-Feb	3.99	1	1	0	19	428	108	438
SRM121AB1	24-Mar	3.95	1	2	2	100	322	270	564
SRM121AB2	24-Mar	4.00	1	2	2	155	329	322	530
SRM131BB1	16-Mar	2.40	2	0	2	510	167	169	385
SRM131BB2	16-Mar	2.40	2	0	2	879	183	134	343
SRM131CF1	15-Mar	2.39	2	1	1	22	245	173	296
SRM131CF2	16-Mar	2.40	2	1	1	52	322	104	239
SRM131AS1	24-Mar	2.40	2	2	0	-15	263	113	294
SRM131AS2	24-Mar	2.40	2	2	0	5	252	65	341

A statistical analysis was performed to determine if and up to what extent the three factors (Padding, Ignition Source and Source Location) have an effect on each of the aforementioned (response) variables. The procedure used in the analysis is briefly described below. A more detailed discussion can be found in the literature on statistical design and analysis of experiments, e.g., (Mason, et al., 2003).

Table 27. Response Variables for 3-Seat Sofa Triangular HRR Approximations.

Test ID	Date	CM (kg)	Padding	Source	Location	t ₀ (s)	PHRR (kW)	Δt _{0-p} (s)	Δt ₀₋₃ (s)
LRM113BB1	12-Apr	4.09	0	0	2	537	453	160	307
LRM113BB2	12-Apr	4.07	0	0	2	275	445	184	375
LRM113CF1	15-Apr	4.08	0	1	1	157	590	108	258
LRM113CF2	18-Apr	4.06	0	1	1	374	525	127	288
LRM113AS1	13-Apr	4.08	0	2	0	49	649	125	297
LRM113AS2	13-Apr	4.09	0	2	0	45	629	121	268
LRM123BS1	11-Apr	8.43	1	0	0	613	1307	149	331
LRM123BS2	11-Apr	8.33	1	0	0	537	1977	128	298
LRM123CB1	15-Apr	8.43	1	1	2	291	824	257	455
LRM123CB2	15-Apr	8.25	1	1	2	315	1118	316	437
LRM123AF1	13-Apr	8.44	1	2	1	121	1230	147	334
LRM123AF2	14-Apr	8.33	1	2	1	113	996	103	391
LRM133BF1	11-Apr	5.07	2	0	1	940	491	65	241
LRM133BF2	12-Apr	5.10	2	0	1	855	504	95	291
SRM133CS1	23-Feb	5.13	2	1	0	272	451	166	419
SRM133CS2	23-Feb	5.11	2	1	0	54	441	194	446
LRM133AB1	14-Apr	5.16	2	2	2	245	369	215	364
LRM133AB2	14-Apr	5.10	2	2	2	385	451	117	301

First, dot plots of the data for each response variable were constructed for each set of sofa data. Initial reviews indicated that 2–3 observations were very extreme and appeared to be outliers. Rather than eliminate these values, analyses were made with and without the data so that the effects of the outliers could be measured.

An analysis-of-variance (ANOVA) approach for unbalanced data was taken and the general linear model program in Statistical Analysis System (SAS®) was then used to analyze the data from each experiment. For each response variable and sofa type, an analysis of variance table was obtained and the p-value of the each of the three factors was compared to a 0.05 significance level to determine which factors had a significant effect on the corresponding response variable. The results are summarized in Table 28.

Multiple comparisons of the least square means corresponding to the three levels of each factor were made using the fitted linear model to a given response variable. A Tukey multiple comparison procedure was used and 95% confidence intervals were constructed about each mean. The results for each factor and response variable combination can be found in Appendix F. In these plots, intervals that do not overlap indicate a significant difference in the two means that are being compared at a 0.05 significance level. Intervals that overlap indicate no significant difference exists between the two means being compared.

Table 28. ANOVA Results.

	1-Seat Sofas			3-Seat Sofas		
	Padding	Source	Location	Padding	Source	Location
t_0 (s)*	0.0979	0.0000	0.0000	0.0612	0.0003	0.1751
PHRR (kW)**	0.0000	0.5097	0.0005	0.0000	0.3958	0.0427
$t_p - t_0$ (s)	0.0050	0.2830	0.0133	0.0521	0.0085	0.0006
$t_3 - t_0$ (s)	0.0000	0.0514	0.0034	0.0562	0.0443	0.0667

* t_0 for SRM131BB2 removed from analysis

**PHRR for SRM121BF1 and LRM123BS2 removed from analysis

Note: Numbers in bold print are p-values < 0.05 (effect is significant at the 5% significance level)

An ANOVA model requires the assumptions of normality for the response variable data as well as the assumption of a constant standard deviation. The Shapiro-Wilks test for normality was used to test the residuals of the model, and plots of the residuals versus the predicted response from the model were used to check for a non-constant spread in the residuals (indicating a non-constant standard deviation). The test confirmed that the observations identified as extreme in the dot plots indeed seemed to be outliers. These observations were removed from the analysis (see notes under Table 26).

Table 28 identifies the type of ignition source as a significant factor affecting the ignition delay (t_0) for the single and 3-seat sofas. Figures F-2 and F-14 further show that in terms of the effect on t_0 there is no significant difference between the large burner flame and the liquid pool fire. The same figures also show that the small flame ignition source results in a significant increase of t_0 , i.e., from an average of 53 s (large sources) to 439 s (small flame) for the 1-seat sofas, and from 202 s (large sources) to 626 s (small flame) for the 3-seat sofas. Table 28 and Figure F-3 also show that ignition source location has a significant effect on t_0 for 1-seat sofas: the time to the onset of a self-propagating fire significantly increases from top to front to back ignition. For 3-seat sofas location does not have a significant effect as evidenced by Figure F-15.

Table 28 suggests that the PHRR is strongly affected by the padding material (the average peak for CA TB 117 foam is significantly lower than that for the HD foam, see Figures F-4 and F-16) and up to a lesser extent by the location of the ignition source (back ignition results in a lower peak for 1-seat sofas, the same trend is observed for 3-seat sofas but the differences are not statistically significant, see Figures F-6 and F-18).

Table 28 also indicates that t_p-t_0 and t_3-t_0 are affected primarily by the location of the ignition source for 1-seat sofas (back ignition results in slower fire growth as shown in Figures F-9 and F-12) and by the type of ignition source for 3-seat sofas (the large flame ignition source results in slower fire growth as shown in Figures F-20 and F-23). Since the mockups were completely consumed, the remaining variables are not completely independent from the PHRR.

4.2.2.2 Other Room Calorimeter Mockup Tests

Table 29 lists all room calorimeter tests on furniture mockups in chronological order and in alphabetical order by Test ID.

Table 29. List of Open Calorimeter Mockup Tests.

Test #	Test ID	Date	File Name	Test #	Test ID	Date	File Name
3	SRM131BF1	01/28/11	11-028NIJ004-3	61	LRM111BC1	04/19/11	11-109NIJ004-73
4	SRM131BF2	01/28/11	11-028NIJ004-4	60	LRM123BC1	04/19/11	11-109NIJ004-72
8	SRM221CS1	02/21/11	11-052NIJ004-8	59	LRM163CS1	04/18/11	11-108NIJ004-71
9	SRM231CS1	02/22/11	11-053NIJ004-9	58	LRM223AS1	04/18/11	11-108NIJ004-70
10	SRM161CS1	02/22/11	11-053NIJ004-10	57	LRM223CS1	04/18/11	11-108NIJ004-69
11	SRM161CS2	02/22/11	11-053NIJ004-11	18	SRM120CG1	02/24/11	11-055NIJ004-18
13	SRM233CS1	02/23/11	11-054NIJ004-13	15	SRM120CN1	02/24/11	11-055NIJ004-15
15	SRM120CN1	02/24/11	11-055NIJ004-15	21	SRM122CS1	02/28/11	11-059NIJ004-21
16	SRM130CN1	02/24/11	11-055NIJ004-16	19	SRM130CG1	02/24/11	11-055NIJ004-19
17	SRM160CN1	02/24/11	11-055NIJ004-17	16	SRM130CN1	02/24/11	11-055NIJ004-16
18	SRM120CG1	02/24/11	11-055NIJ004-18	31	SRM131AF1	03/23/11	11-082NIJ004-36
19	SRM130CG1	02/24/11	11-055NIJ004-19	3	SRM131BF1	01/28/11	11-028NIJ004-3
20	SRM160CG1	02/24/11	11-055NIJ004-20	4	SRM131BF2	01/28/11	11-028NIJ004-4
21	SRM122CS1	02/28/11	11-059NIJ004-21	22	SRM132CS1	02/28/11	11-059NIJ004-22
22	SRM132CS1	02/28/11	11-059NIJ004-22	20	SRM160CG1	02/24/11	11-055NIJ004-20
23	SRM162CS1	03/09/11	11-068NIJ004-23	17	SRM160CN1	02/24/11	11-055NIJ004-17
31	SRM131AF1	03/23/11	11-082NIJ004-36	40	SRM161AS1	03/24/11	11-083NIJ004-45
38	SRM221AS1	03/24/11	11-083NIJ004-43	10	SRM161CS1	02/22/11	11-053NIJ004-10
39	SRM231AS1	03/24/11	11-083NIJ004-44	11	SRM161CS2	02/22/11	11-053NIJ004-11
40	SRM161AS1	03/24/11	11-083NIJ004-45	23	SRM162CS1	03/09/11	11-068NIJ004-23
57	LRM223CS1	04/18/11	11-108NIJ004-69	38	SRM221AS1	03/24/11	11-083NIJ004-43
58	LRM223AS1	04/18/11	11-108NIJ004-70	8	SRM221CS1	02/21/11	11-052NIJ004-8
59	LRM163CS1	04/18/11	11-108NIJ004-71	39	SRM231AS1	03/24/11	11-083NIJ004-44
60	LRM123BC1	04/19/11	11-109NIJ004-72	9	SRM231CS1	02/22/11	11-053NIJ004-9
61	LRM111BC1	04/19/11	11-109NIJ004-73	13	SRM233CS1	02/23/11	11-054NIJ004-13

4.2.2.3 Enclosure Effects

Figure 32 compares the HRR from an open calorimeter test (SOM161CS1) with the HRR from two room calorimeter tests (SRM161CS1-2) on the same mockup ignited with the same large flame ignition source. Figure 33 compares the HRR from three open calorimeter tests (SOM111BS1-3) with the HRR from two room calorimeter tests (SRM111BS1-2) on the same mockup ignited with the same small flame ignition source. The data do not show a systematic increase of the HRR due to enclosure effects, but the fires are too small (<500 kW PHRR) to substantiate drawing general conclusions concerning enclosure effects.

4.2.2.4 Corner versus Center Seat Small Flame Ignition

Figures 34 and 35 show the effect of the location (corner vs. center of seat) of a small flame ignition source on the HRR of a single and a 3-seat sofa, respectively. Placing the ignition source in the corner appears to accelerate the onset of a self-propagating fire, but seems to result in a lower PHRR.

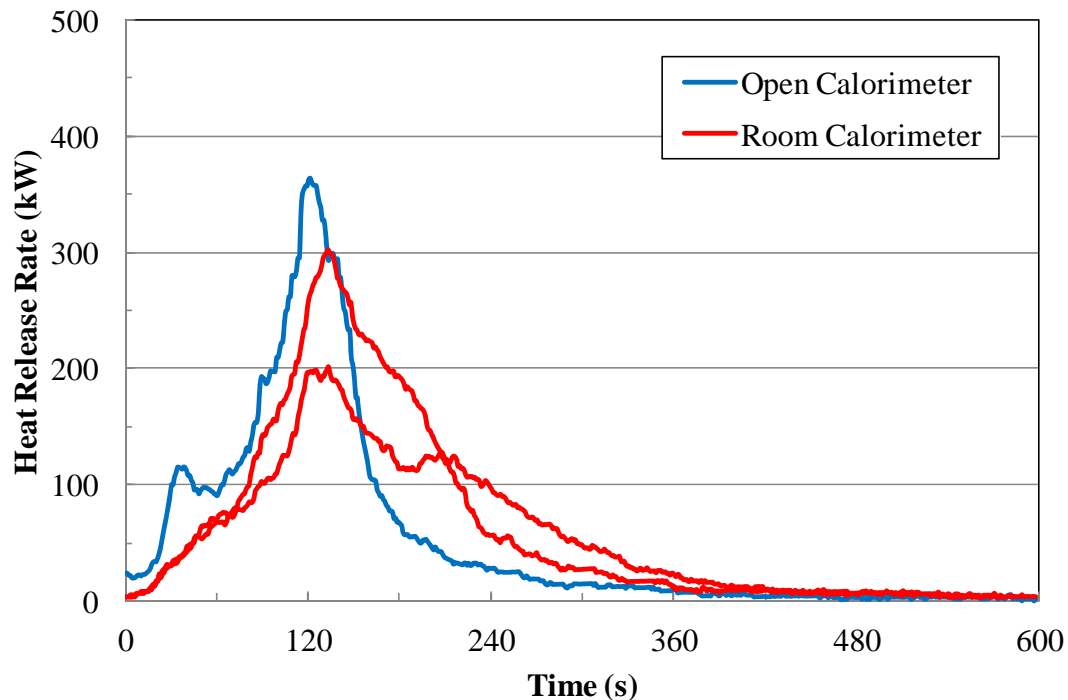


Figure 32. Enclosure Effect on HRR for Large Flame Ignition Source.

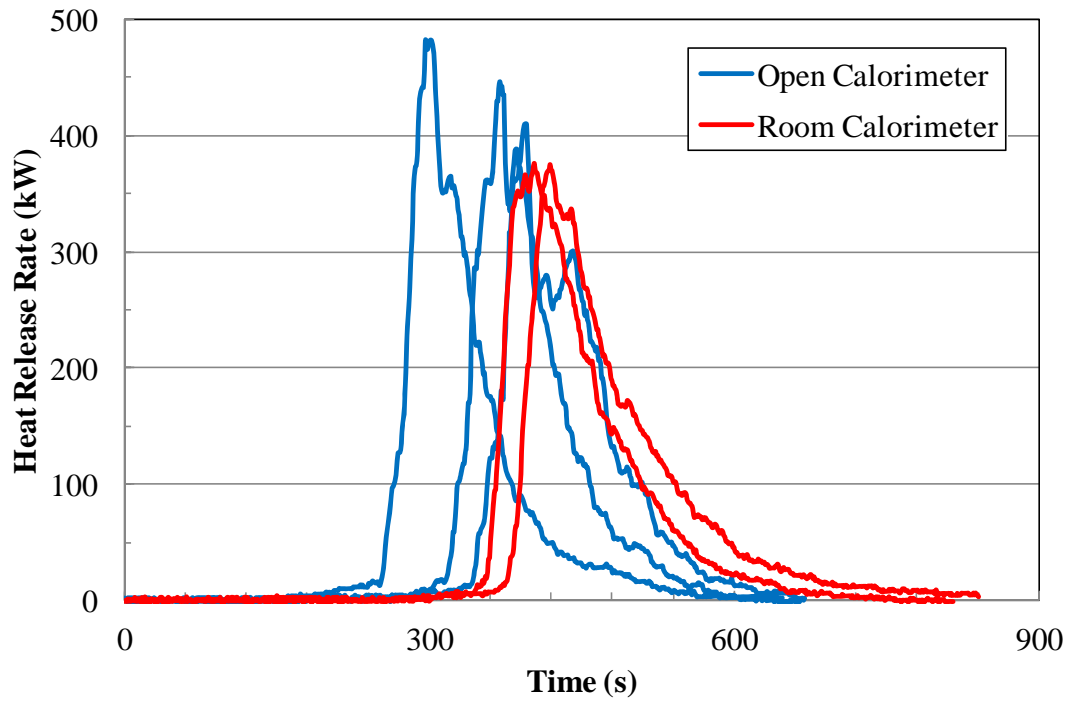


Figure 33. Enclosure Effect on HRR for Small Flame Ignition Source.

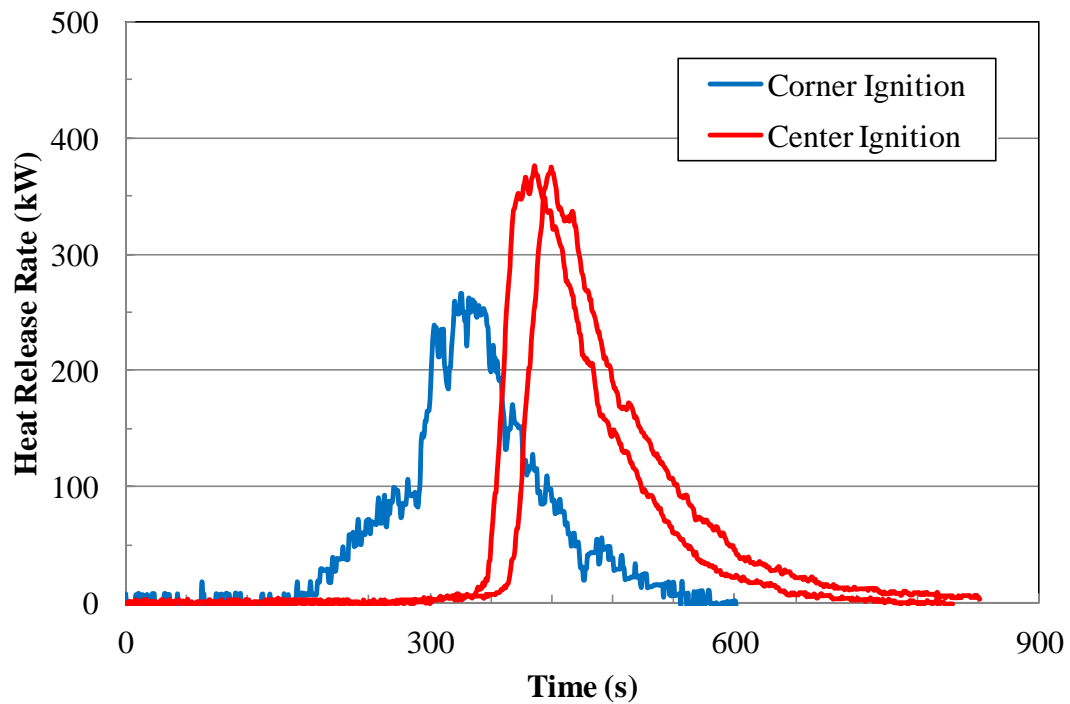


Figure 34. Effect of Small Flame Location on HRR of 1-Seat Sofa.

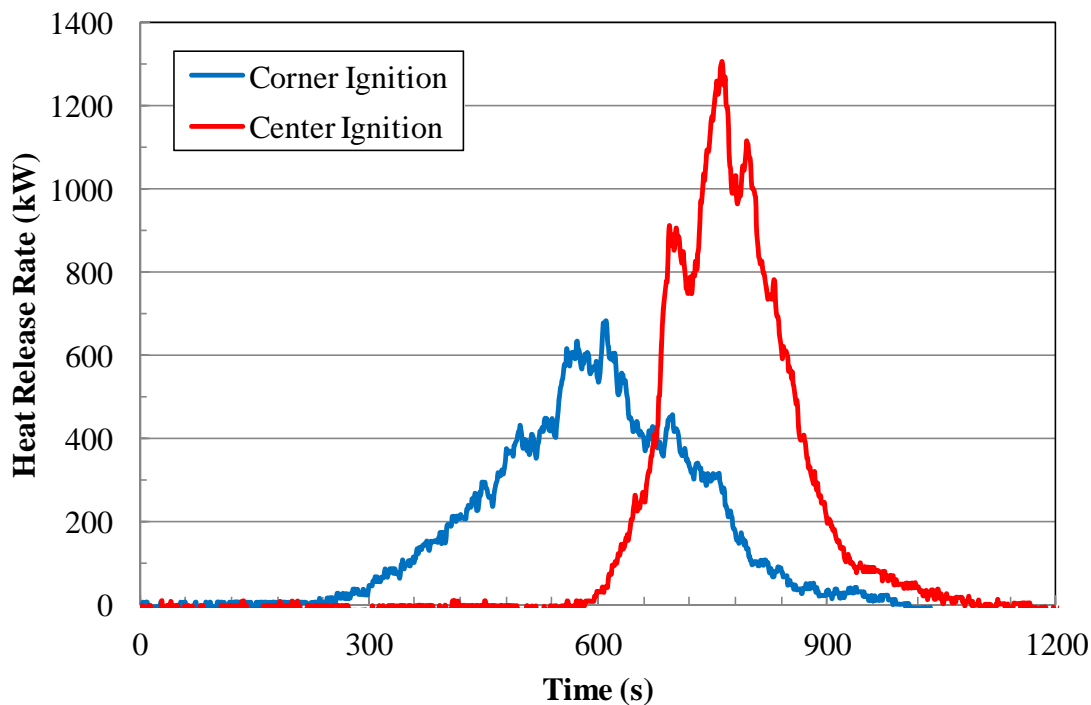


Figure 35. Effect of Small Flame Location on HRR of 1-Seat Sofa.

4.3 MODELING OF MOCKUP FURNITURE TESTS

Figure 36 compares the predicted and measured PHRRs for all mockup tests that were conducted. The solid line corresponds to perfect agreement. The dashed lines bound the (average) experimental uncertainty at the 95% confidence level ($\pm 8.7\%$). The agreement seems to be rather poor for the majority of the tests. This is primarily because the three models do not explicitly account for variations in the ignition source and the location where it is applied. For example, the row of green triangles toward the top of Figure 36 indicates that the Babrauskas 2 model predicts a PHRR of approximately 1100 kW for a 3-seat mockup with HD polyurethane foam padding and untreated cotton fabric. The measured PHRR, however, varied between 400 and 1300 kW (test LRM123BS2 had a PHRR of nearly 2 MW, but was identified in the statistical analysis as an outlier and was therefore removed) depending on the ignition source that was used and the location where it was applied. It should also be mentioned that the burning rate models are not valid for furniture with flame resistant fabric and/or padding materials, e.g., most of the data points with a measured HRR of approximately 50 kW or less.

Figures 37–39 present the same comparison for the Babrauskas, Babrauskas 2 and CBUF models individually. Based on these figures it could be concluded that the Babrauskas model overall does the best job in predicting PHRR. However, since the paper describing this model (Babrauskas, et al., 1986) does not make a distinction between low density, high density, and CA TB 117 compliant foam, Padding Factor values were determined to optimize agreement between measured and predicted PHRRs (maximum R^2) for each type of padding material individually. These values were as follows:

- LD Polyurethane Foam: 1.1
- HD Polyurethane Foam: 0.8
- CA TB 117 Foam: 0.7
- Polychloroprene Foam: 0.1
- Polyester Wrap: 0.5.
- Densified Polyester: 0.6.

Figures 37–39 also display the bias and standard error for each of the three triangular models individually. The bias and standard error were determined as described in NUREG-1824 (Hamins and McGrattan, 2007). To understand what these values mean consider, for example, Figure 36 for the Babrauskas model. A bias of 0.84 means that, on average, the model under-predicts the measured PHRR by 16% ($1 - 0.84$). The standard error is a measure of the uncertainty of the model predictions and corresponds to one standard deviation. The standard error is the lowest for the Babrauskas model, which implies that it is the most accurate of the three triangular models (provided the bias can be removed). The bias in the Babrauskas model can be eliminated by adjusting one or several of the aforementioned factors and/or constants in the equations. Adjusting the bias to 1.0 increases the standard error to $156/0.83 = 173$ kW.

Figure 36 may paint an overly pessimistic picture. Charts comparing the calculated HRR curves to the measured curves for the open calorimeter tests, fractional factorial design tests and remaining room calorimeter mockup tests are presented in Appendices G, H, and I, respectively. Qualitatively these charts suggest that the agreement is better than what Figure 36 seems to convey.

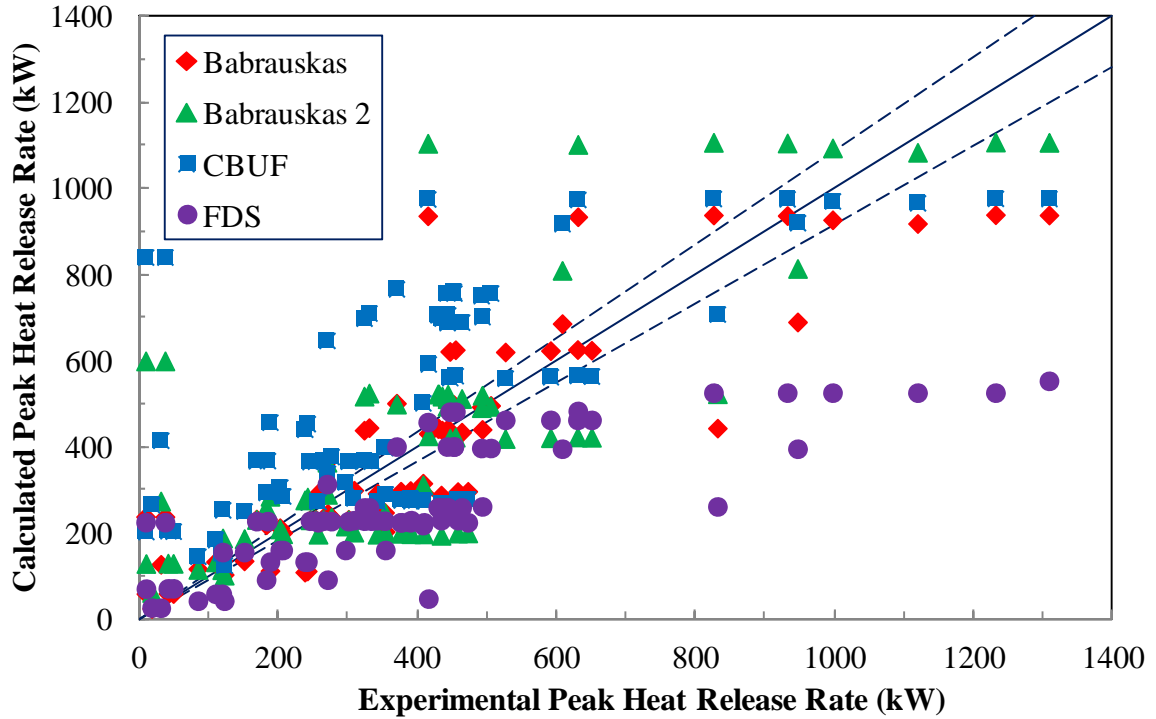


Figure 36. Calculated vs. Measured PHRR for All Mockup Tests (All Models).

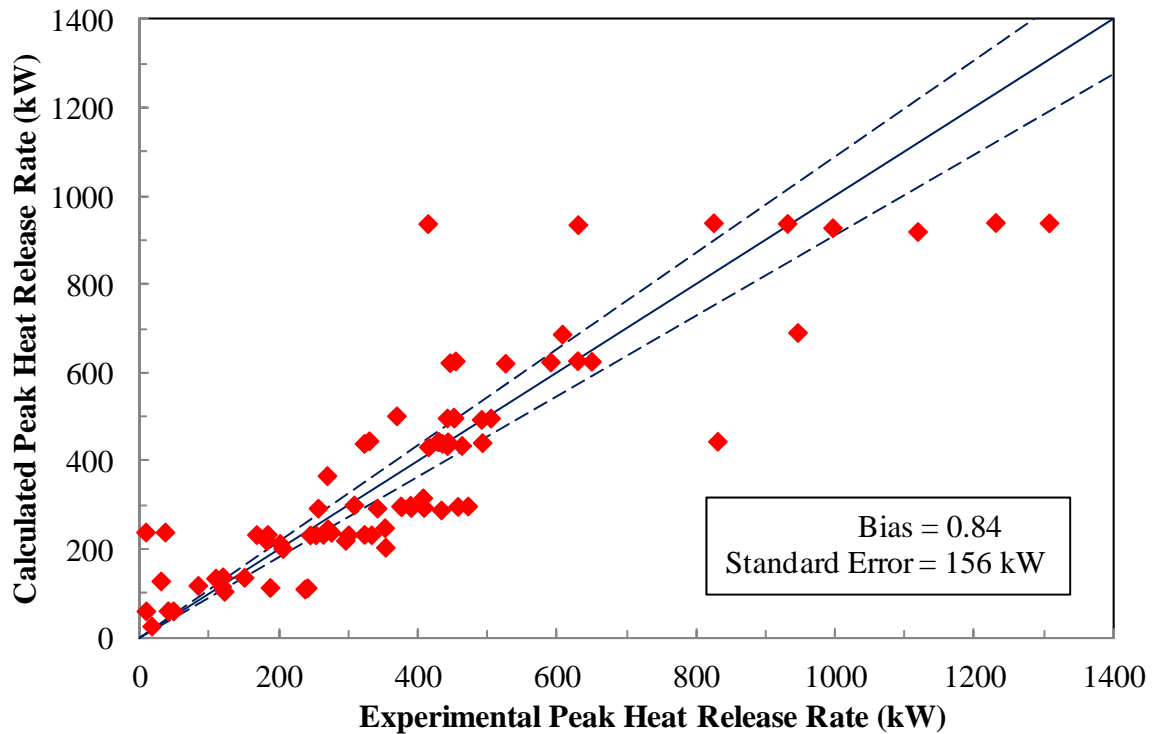


Figure 37. Calculated vs. Measured PHRR for All Mockup Tests (Babrauskas).

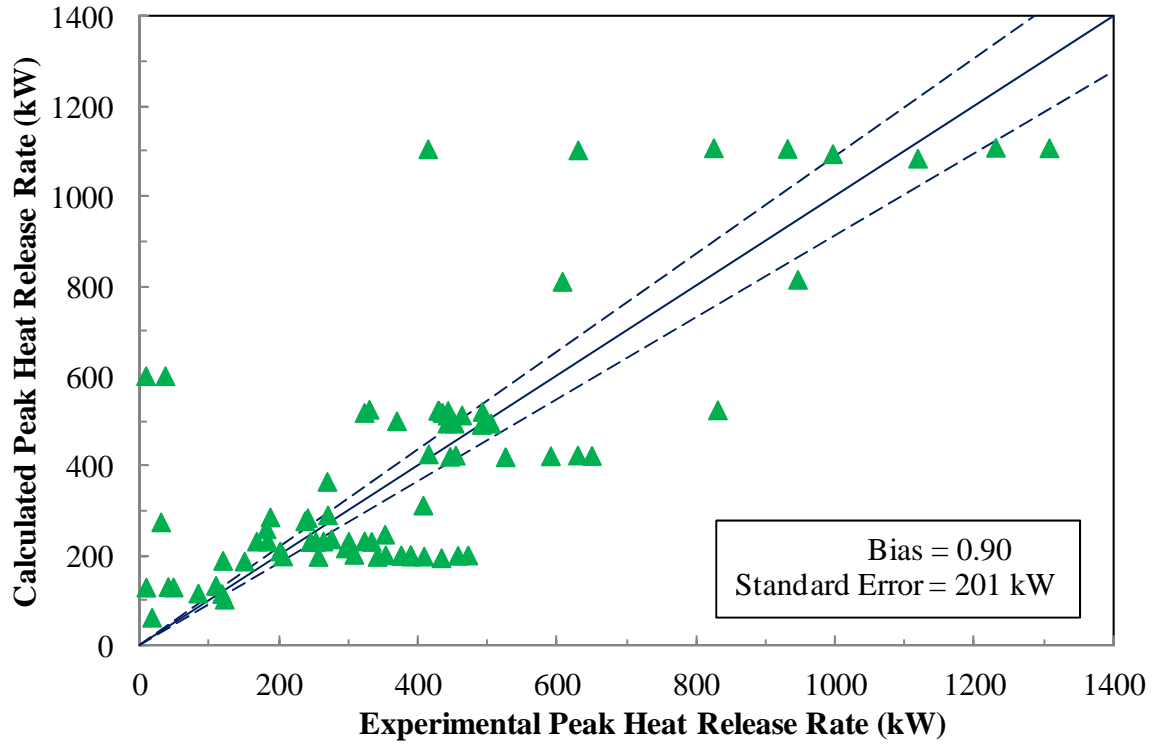


Figure 38. Calculated vs. Measured PHRR for All Mockup Tests (Babrauskas 2).

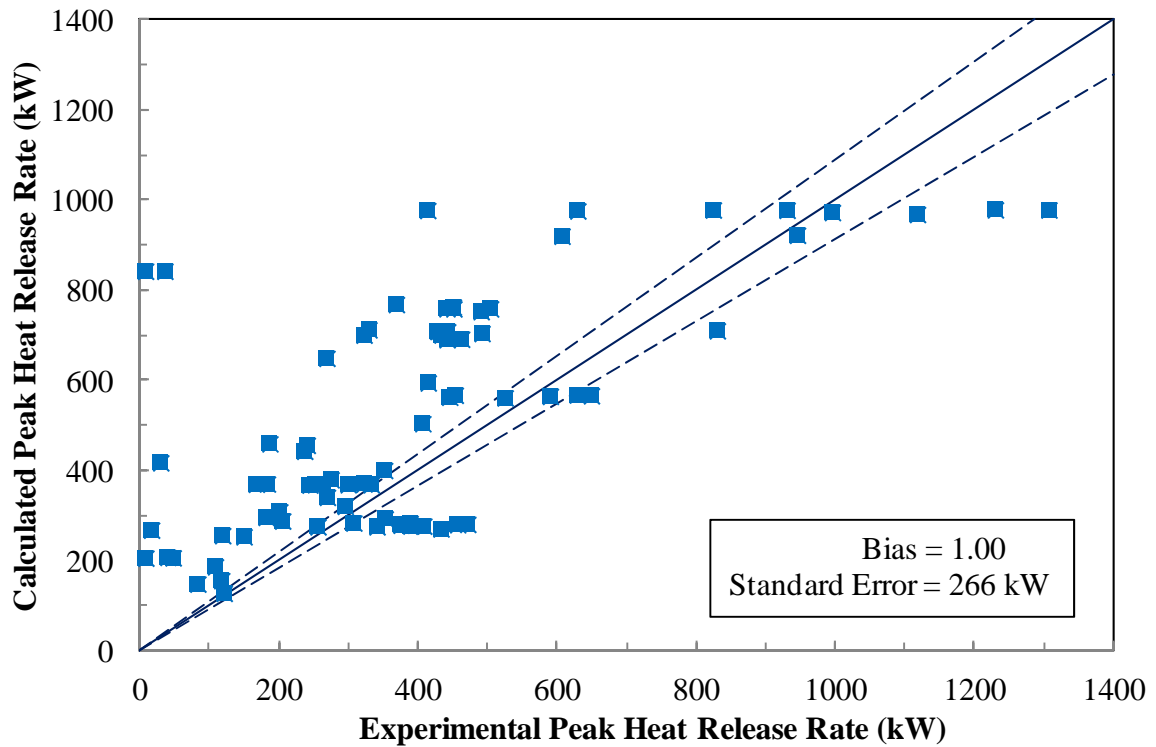


Figure 39. Calculated vs. Measured PHRR for All Mockup Tests (CBUF).

In many cases HRR predictions are actually reasonably accurate. For example, Figure 40 shows a comparison between the four models and the measured HRR for a 3-seat sofa mockup ignited with an accelerant (118 ml of gasoline in a pan beneath the front of the center seat cushion). Figure 41 compares CFAST hot gas layer (HGL) calculations in the room based on the measured HRR and that predicted with the three models. Although the calculated PHRR is lower than the measured PHRR, agreement with the measured HGL temperatures is reasonably good for the triangular models, in particular the Babrauskas model. However, the HRR predictions and corresponding CFAST results are rather poor for the same 3-seat sofa ignited with a small flame (see Figures 42 and 43).

This confirms that to improve the predictions it is necessary to include additional factors in the burning rate models to account for the type and location of the ignition source. Instead of refining the Babrauskas and CBUF models; however, it was decided to explore the use of NIST FDS model to compose a heat release curve for a sofa based on Cone Calorimeter data. A more detailed discussion of this approach and some of its challenges are discussed in Section C.4.

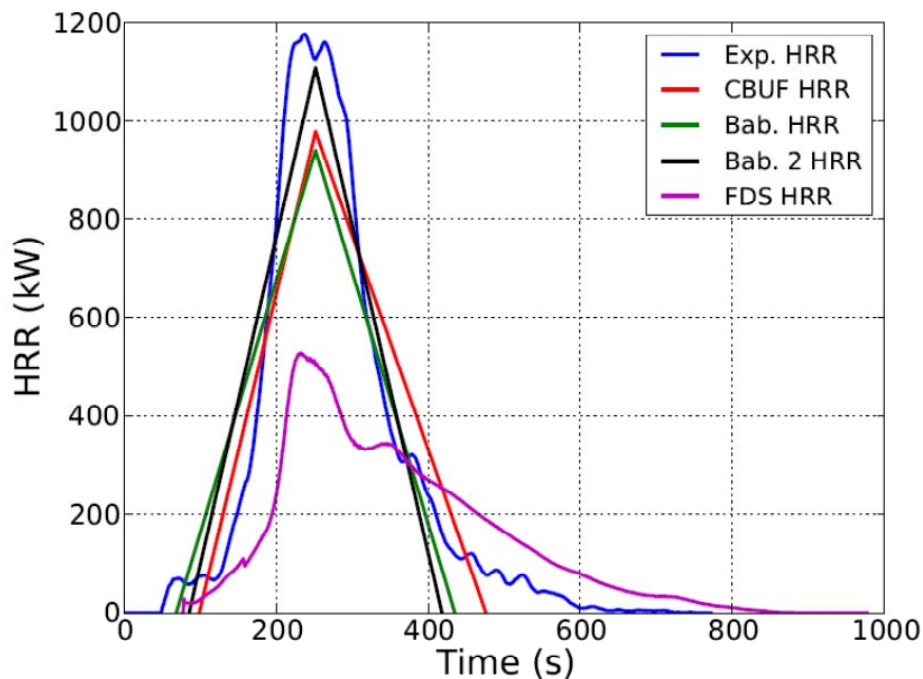


Figure 40. Measured vs. Calculated HRR (LRM123AF1).

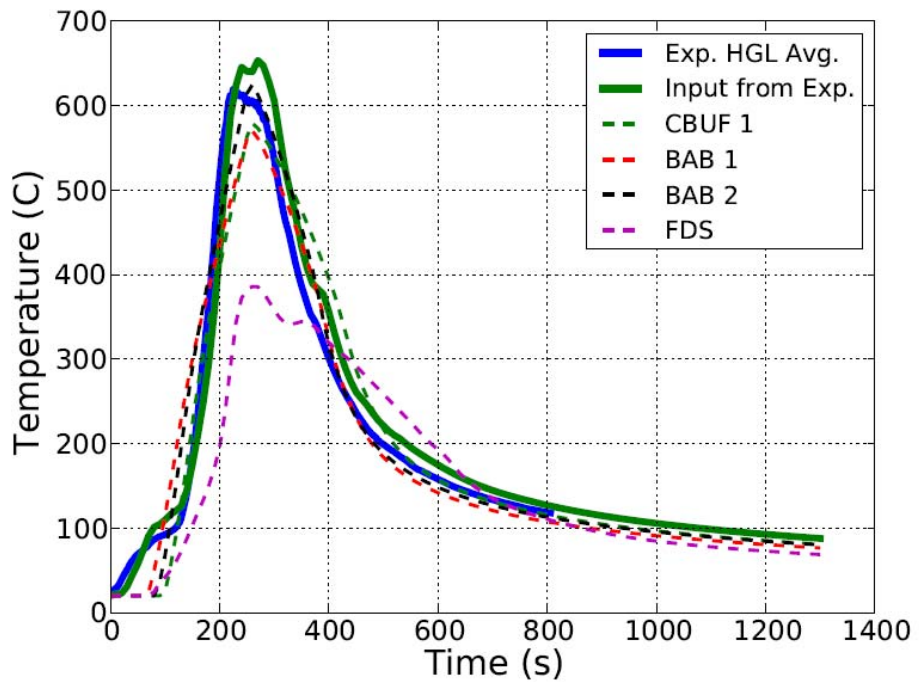


Figure 41. CFAST HGL Temperature Predictions (LRM123AF1).

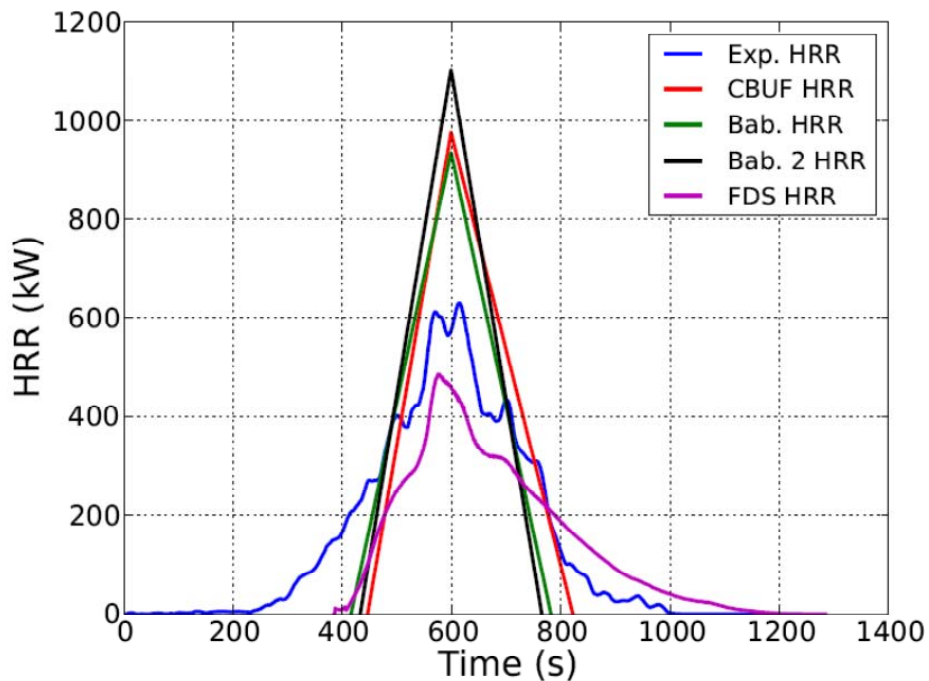


Figure 42. Measured vs. Calculated HRR (LRM123BC1).

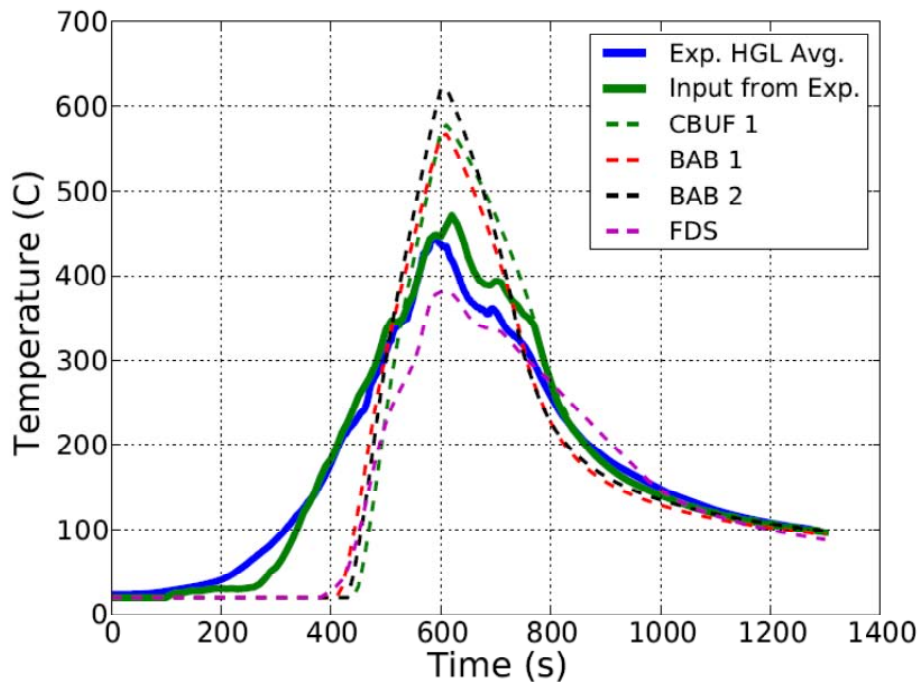


Figure 43. CFAST HGL Temperature Predictions (Small Flame Ignition).

It is apparent from Figure 36 and from scanning the charts in Appendices G–I that the FDS model in its current form significantly under-predicts the HRR. Although the FDS model is the most detailed in terms of underlying physics, additional work is needed before it can be used. The bias and standard error are not presented for the FDS model. Since this model is physics-based, it would be misleading to apply a correction factor to remove the bias.

4.4 USED FURNITURE TESTS

Table 30 lists the used furniture tests in chronological order and alphabetically by Test ID. Based on the fractional factorial experiments it was decided to focus on three ignition scenarios:

1. Accelerant (59 ml of gasoline) distributed over the (center) seat cushion;
2. A small flame ignition source applied to the center of the center seat cushion; and
3. A small flame ignition source applied in one of the corners.

The third ignition scenario was included because it is as likely as or even more likely than the second scenario. Contrary to what the mockup test results showed, there is some evidence from prior proprietary tests at SwRI that corner ignition actually leads to a more severe fire.

Table 30. Complete List of Used Furniture Tests.

Test #	Test ID	Date	File Name	Test #	Test ID	Date	File Name
U01	SRU150BS1	03/17/11	11-076NIJ004-31	U16	LRU013AS1	05/24/11	11-144NIJ004-87
U02	SRU150BS2	03/17/11	11-076NIJ004-32	U26	LRU033BS1	06/06/11	11-157NIJ004-109
U03	SRU150BS3	03/17/11	11-076NIJ004-33	U27	LRU043AS1	06/06/11	11-157NIJ004-110
U04	SRU020CS1	03/18/11	11-077NIJ004-35	U24	LRU053BS1	06/02/11	11-153NIJ004-105
U05	LRU111BS1	04/22/11	11-112NIJ004-75	U12	LRU062BS1	04/26/11	11-116NIJ004-82
U06	LRU141BS1	04/22/11	11-112NIJ004-76	U23	LRU073BS1	06/02/11	11-153NIJ004-104
U07	LRU161BS1	04/25/11	11-115NIJ004-77	U22	LRU083BC1	06/01/11	11-152NIJ004-103
U08	LRU211BC1	04/25/11	11-115NIJ004-78	U20	LRU093BC1	05/31/11	11-151NIJ004-97
U09	LRU221BC1	04/25/11	11-115NIJ004-79	U21	LRU103BC1	05/31/11	11-151NIJ004-100
U10	LRU161AS1	04/25/11	11-115NIJ004-80	U05	LRU111BS1	04/22/11	11-112NIJ004-75
U11	LRU201AS1	04/25/11	11-115NIJ004-81	U15	LRU113BS1	05/23/11	11-143NIJ004-86
U12	LRU062BS1	04/26/11	11-116NIJ004-82	U19	LRU123BS1	05/25/11	11-145NIJ004-90
U13	LRU132AS1	04/26/11	11-116NIJ004-83	U13	LRU132AS1	04/26/11	11-116NIJ004-83
U14	LRU213BC1	05/23/11	11-143NIJ004-85	U06	LRU141BS1	04/22/11	11-112NIJ004-76
U15	LRU113BS1	05/23/11	11-143NIJ004-86	U10	LRU161AS1	04/25/11	11-115NIJ004-80
U16	LRU013AS1	05/24/11	11-144NIJ004-87	U07	LRU161BS1	04/25/11	11-115NIJ004-77
U17	LRU193AS1	05/24/11	11-144NIJ004-88	U18	LRU173AS1	05/25/11	11-145NIJ004-89
U18	LRU173AS1	05/25/11	11-145NIJ004-89	U25	LRU183BC1	06/03/11	11-154NIJ004-107
U19	LRU123BS1	05/25/11	11-145NIJ004-90	U17	LRU193AS1	05/24/11	11-144NIJ004-88
U20	LRU093BC1	05/31/11	11-151NIJ004-97	U11	LRU201AS1	04/25/11	11-115NIJ004-81
U21	LRU103BC1	05/31/11	11-151NIJ004-100	U08	LRU211BC1	04/25/11	11-115NIJ004-78
U22	LRU083BC1	06/01/11	11-152NIJ004-103	U14	LRU213BC1	05/23/11	11-143NIJ004-85
U23	LRU073BS1	06/02/11	11-153NIJ004-104	U09	LRU221BC1	04/25/11	11-115NIJ004-79
U24	LRU053BS1	06/02/11	11-153NIJ004-105	U04	SRU020CS1	03/18/11	11-077NIJ004-35
U25	LRU183BC1	06/03/11	11-154NIJ004-107	U01	SRU150BS1	03/17/11	11-076NIJ004-31
U26	LRU033BS1	06/06/11	11-157NIJ004-109	U02	SRU150BS2	03/17/11	11-076NIJ004-32
U27	LRU043AS1	06/06/11	11-157NIJ004-110	U03	SRU150BS3	03/17/11	11-076NIJ004-33

The 2-seat sofas were ignited with the small flame ignition source applied in the corner. Initially the small flame ignition source was applied to the seat center of the chairs. Since it was not possible to ignite the vinyl chair in set #2 with a small flame, a large burner flame was used to force ignition. The ignition scenario for the remaining 21 items was chosen randomly: an accelerant was used in seven tests, a small center flame in nine tests, and a small corner flame in the remaining five tests.

4.4.1 Small versus Large Ignition Source

Set #16 included two identical 1-seat sofas (see Figure D-16b). In the first test (LRU161BS1), the sofa was ignited with BS 5852 Source #1 applied to the center of the seat cushion. In the second test (LRU161AS1), 59 ml of gasoline was poured on the seat cushion to simulate an incendiary fire. The resulting HRR measurements are shown in Figure 44. In

this case the use of the weaker ignition source delays the propagation to full involvement by approximately 170 s as illustrated in Figure 45.

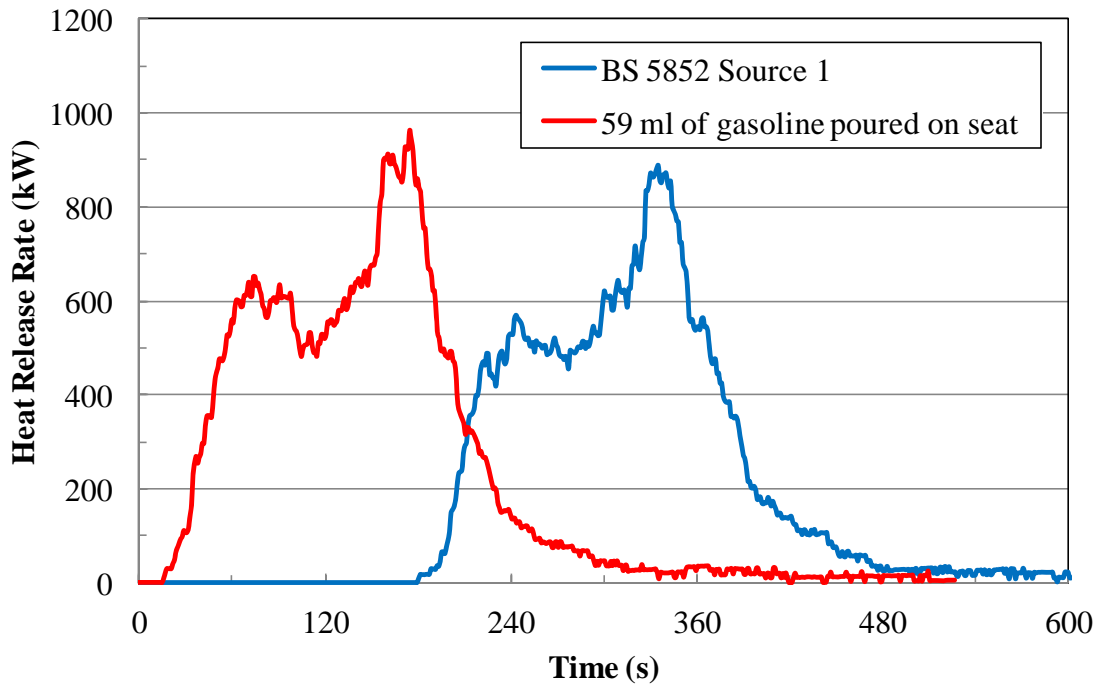


Figure 44. HRR of a Used 1-Seat Sofa for Different Ignition Sources.

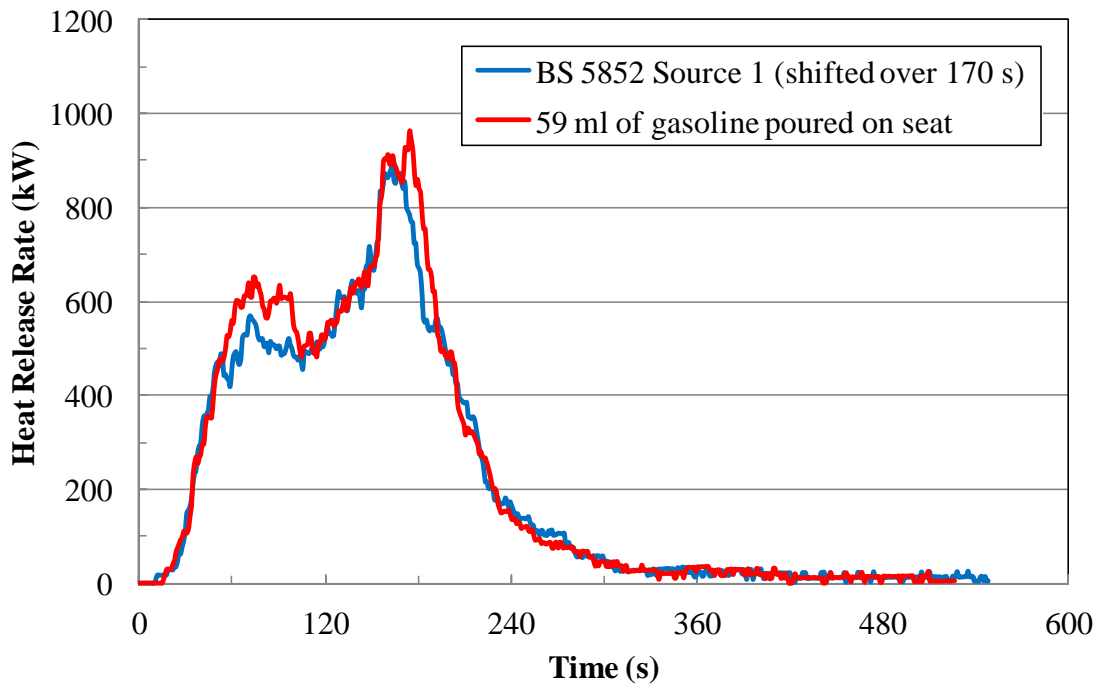


Figure 45. Effect of Ignition Source Strength on HRR of a 1-Seat Sofa.

4.4.2 Measurement Uncertainty

Figure 46 shows the results of measurement uncertainty calculations based on Equation B-5 for test LRU161BS1. The uncertainty at the PHRR is $\pm 8.3\%$.

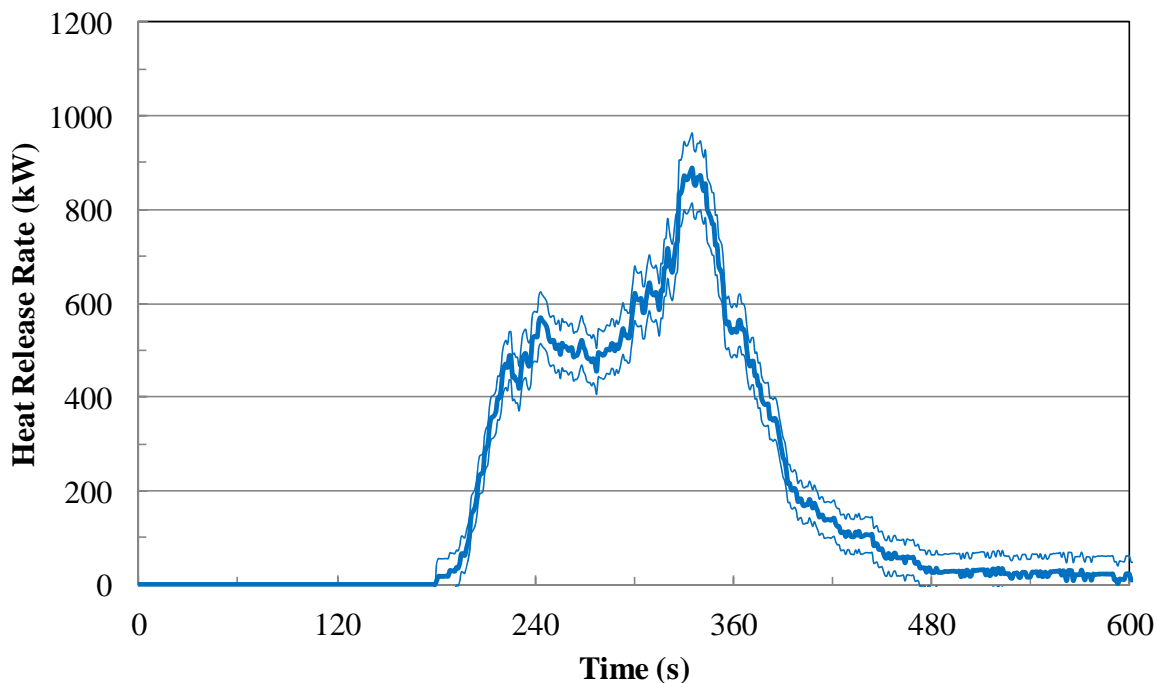


Figure 46. Measurement Uncertainty of the HRR of a Used 1-Seat Sofa.

4.5 MODELING OF USED FURNITURE TESTS

Charts comparing the calculated HRR curves to the measured curves for the used furniture room calorimeter tests are presented in Appendix J. Qualitatively these charts suggest that in most cases the PHRR is significantly under-predicted and that, consequently, the burning time is generally too long. The former is also illustrated in Figure 47, which shows a comparison between the predicted and measured PHRRs for all used furniture tests and burning rate models. The solid line corresponds to perfect agreement. The dashed lines bound the experimental uncertainty at the 95% confidence level ($\pm 8.7\%$). Figures 48–50 present the same comparison for the Babrauskas, Babrauskas 2, and CBUF models individually. Based on these figures it appears that the Babrauskas model overall does the better job in predicting PHRR (standard error of 315 kW versus 494 kW and 435 kW for the Babrauskas 2 and CBUF models, respectively), provided the bias can be removed. The comparison between the adjusted predictions with the Babrauskas model and the measurements is shown in Figure 51. The Babrauskas model predictions were obtained with

a fabric factor of 0.4 (for cotton) and a padding factor of 0.8 (for HD polyurethane foam, based on the mockup tests). The bias suggests that one or both of these factors are too low.

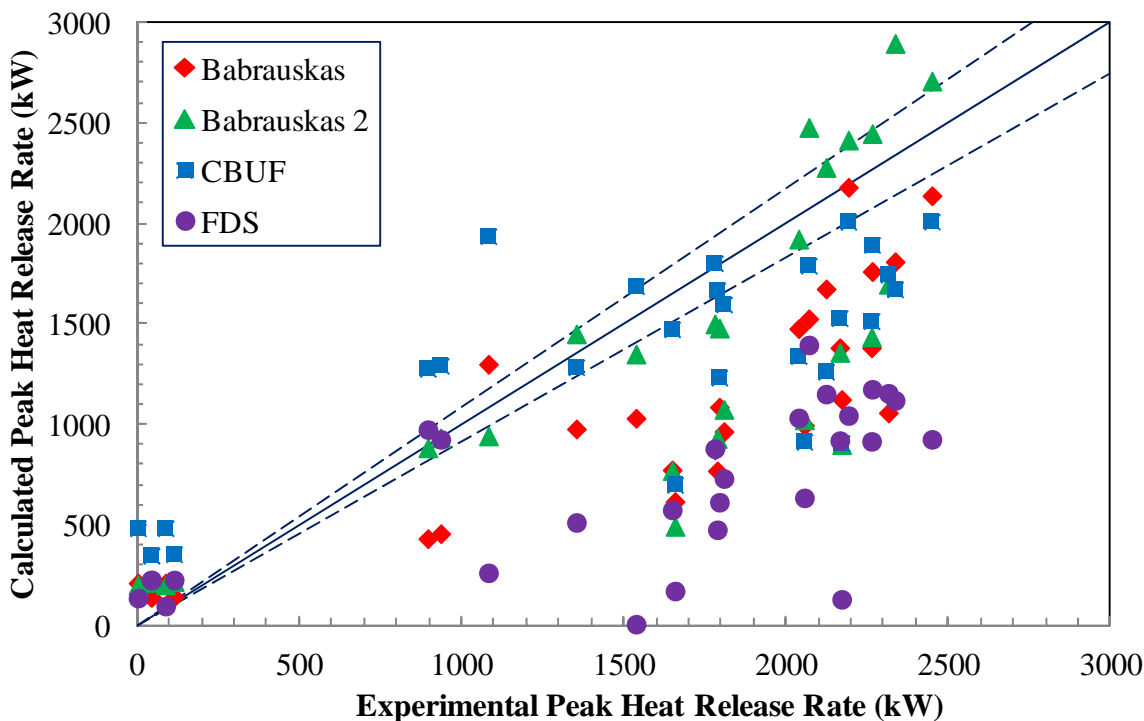


Figure 47. Calculated vs. Measured PHRR for Used Furniture (All Models).

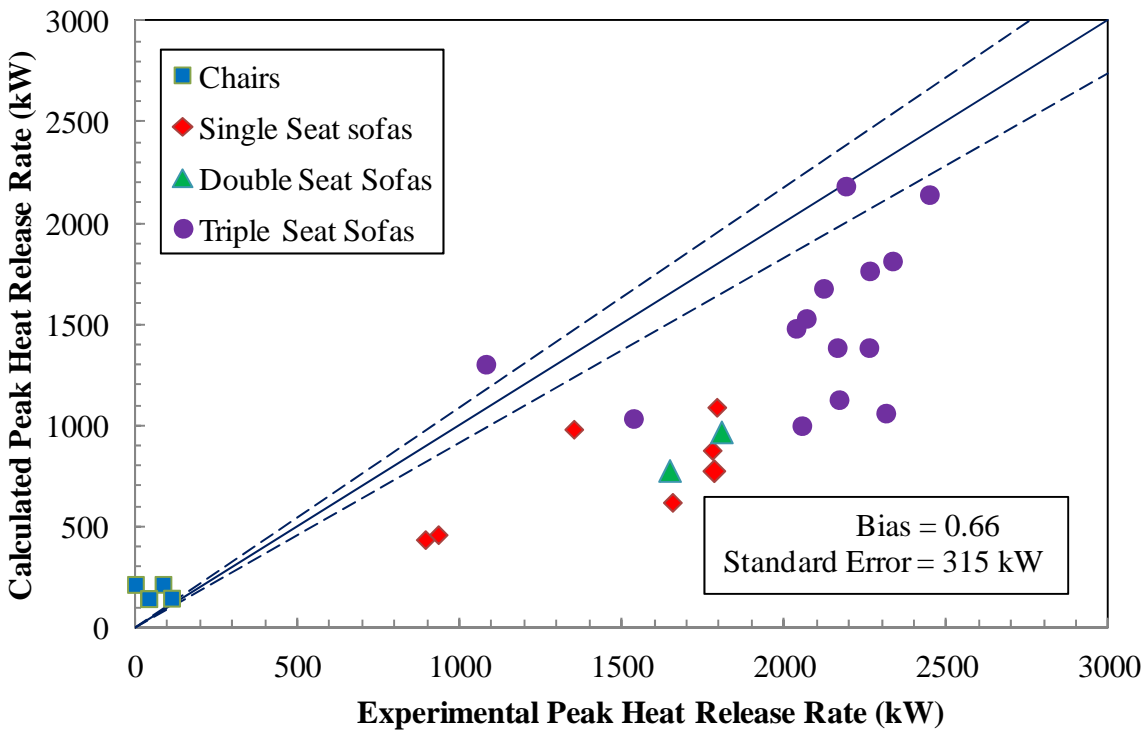


Figure 48. Calculated vs. Measured PHRR for Used Furniture (Babrauskas).

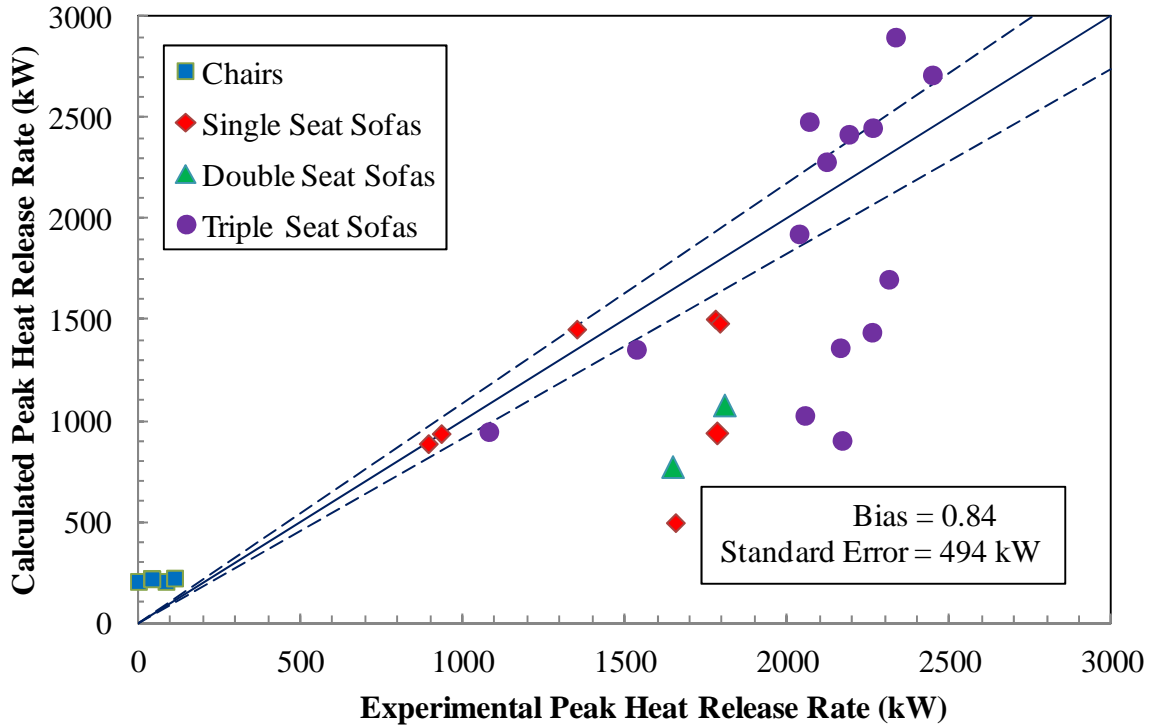


Figure 49. Calculated vs. Measured PHRR for Used Furniture (Babrauskas 2).

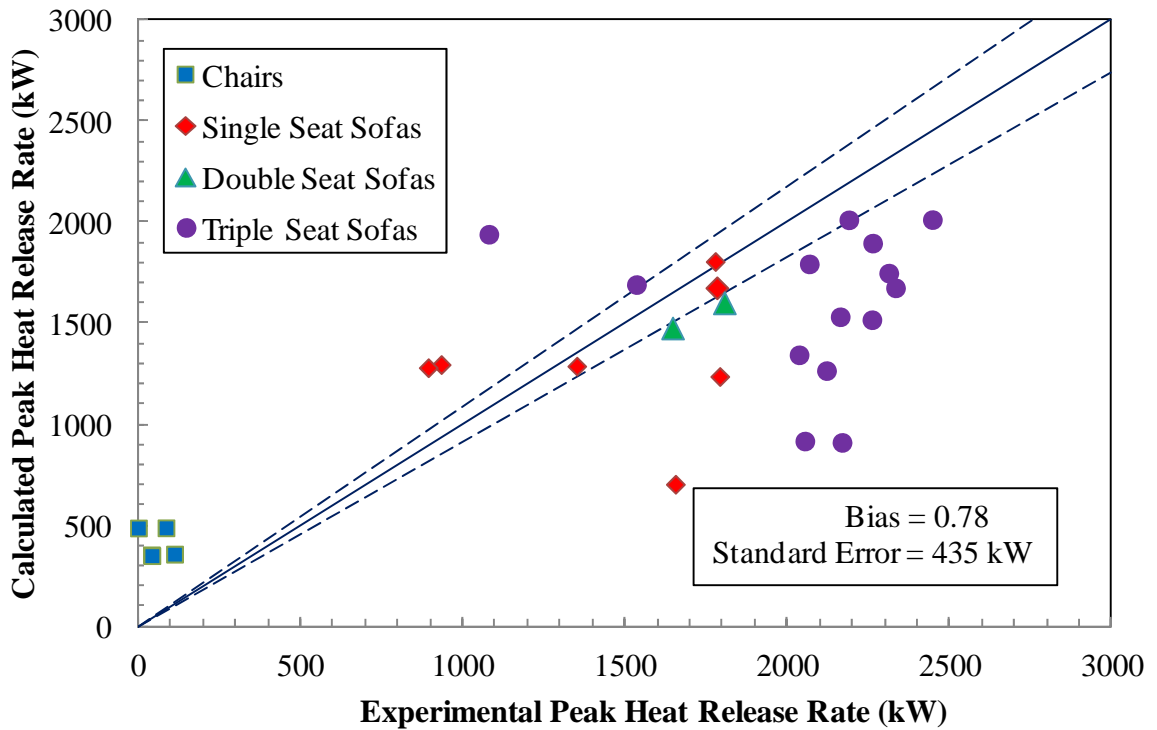


Figure 50. Calculated vs. Measured PHRR for Used Furniture (CBUF).

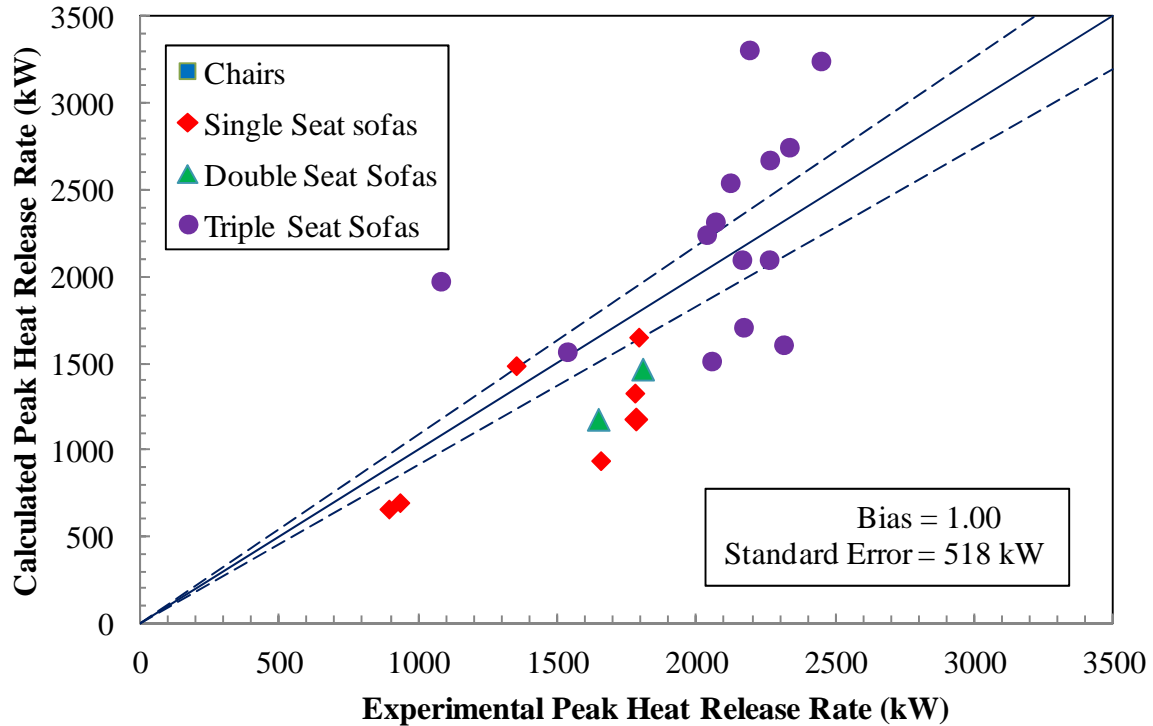


Figure 51. Calculated vs. Measured PHRR (Babrauskas Adjusted).

5 CONCLUSIONS

5.1 DISCUSSION OF FINDINGS

The goal of this project is to develop guidelines for each of these situations on how to best estimate the burning rate of upholstered furniture and quantify/optimize the uncertainty of the predictions. This uncertainty consists of an aleatory and an epistemic component. The first component is uncertainty due to random variation while the second is uncertainty due to lack of (complete) knowledge. Aleatory uncertainty can be estimated using standard mathematical techniques. Quantifying epistemic uncertainty, which is often (by far) the larger of the two uncertainty components, is much more difficult. Primary sources of epistemic uncertainty of the HRR of upholstered furniture include the lack of knowledge of the ignition scenario and limited understanding of enclosure effects. The focus of this study is on these two sources of uncertainty.

Two series of full-scale tests were conducted in this project. The first series consisted of 79 tests on CA TB 133 upholstered furniture mockups. Although most of the tests were performed on 1- and 3-seat sofa mockups, a limited number of tests were also performed on chair and 2-seat sofa mockups. The tests on the 1- and 3-seat mockups included

two fractional factorial designs to assess the effect of the padding material (LD polyurethane foam, HD polyurethane foam, and CA TB 117 compliant foam), ignition source (small flame, large gas burner flame, and liquid pool fire) and ignition source location (seat top, front bottom, and back). The main conclusions of the mockup tests are as follows:

- The repeatability of furniture calorimeter tests with a large flame ignition source is very good. For example, based on four repeat tests the coefficient of variance of the PHRR at the 95% confidence level was found to be approximately 8%. This is comparable to the measurement uncertainty, which for most items that were tested was determined to be between 7.8% and 9.6%.
- The time to the onset of a self-propagating fire was found to be considerably more variable in repeat tests with a small flame ignition source. Compared to the tests with a large flame ignition source the PHRR was also found to be more variable, although the effect on PHRR was not as pronounced. This also means that model predictions of the HRR of upholstered furniture ignited with a small ignition source such as a match or lighter flame are subject to greater uncertainty than predictions for upholstered furniture ignited with a large ignition source, such as an accelerant.
- The HRR of a 3-seat sofa is very sensitive to the location on the top surface where the ignition source is applied. The PHRR for a 3-seat sofa ignited with a large flame ignition source (CA TB 133) in the center was approximately 2.5 times the peak observed for ignition of one of the side cushions (approximately 1000 kW vs. 400 kW). A similar trend was observed for the small flame applied at the center versus the corner (approximately 1300 kW vs. 600 kW).
- The fractional factorial experiments indicated that the type of ignition source is a significant factor affecting the ignition delay (t_0). In terms of the effect on t_0 , there is no significant difference between the large burner flame and the liquid pool fire, but the small flame ignition source results in a significant increase of t_0 .
- The fractional factorial experiments also showed that the peak release rate is strongly affected by the padding material (the average peak for CA TB 117 foam is significantly lower).
- Back ignition generally resulted in a shorter ignition delay, but a slower fire growth rate and lower PHRR.

- Finally, comparison of heat release data of items tested directly under the hood versus in room indicated that enclosure effects were negligible for fire below 500 kW in size. However, the PHRR in these tests was between 200–500 kW, which is well below that required for room flashover (approximately 2 MW based on used furniture tests in which flames emerged through the door).

The predictive capability of three upholstered furniture burning rate models (referred to as Babrauskas, Babrauskas 2 and CBUF) was determined based on the results of the parametric study and small-scale test data for the upholstery materials (ASTM E 1354 Cone Calorimeter and ASTM D 7309 Microscale Combustion Calorimeter). The Babrauskas model (see Section C.2), was slightly modified to improve agreement between calculated and measured PHRR. Following the adjustment, this model gave the best matching predictions of PHRR for the mockup tests. The standard error after removing bias was 173 kW.

An attempt was also made to use the field fire model FDS to better account for the effect of the exact location of the ignition source on flame spread over the seating surface and HRR of the furniture item. The FDS model is the most advanced of the four because it is based on physics rather than a correlation. However, the following challenges were encountered:

- How to account for sub-grid surface flame spread (which is not explicitly modeled in FDS)?
- How to extrapolate Cone Calorimeter data for 50-mm thick specimens to the larger padding thicknesses in the mockups and used furniture items?
- How to account for the effect of increased heat flux on the burning rate of upholstered furniture fabric and padding materials?

These challenges could not be satisfactorily addressed, and as a result, the FDS model consistently under-predicts the HRR curve.

The zone fire model CFAST and field fire model FDS were also used to determine how the use of the upholstered furniture burning rate models (compared to the use of measured HRR data for the item) affects the accuracy of Hot Gas Layer (HGL) temperature and heat flux estimates in the room. It was determined that both compartment fire models predict the HGL temperature with remarkable accuracy when the measured HRR is specified.

This implies that the accuracy of the CFAST and FDS HGL temperature predictions depends on how well the burning rate model predictions agree with the actual HRR. CFAST and FDS consistently under-predict the heat flux to the gauges in the test room, even when the specified fire is identical to the measured HRR curve.

The second series of full-scale tests involved 27 items of used upholstered furniture. Small- and full-scale test data on the used furniture (components) were used to assess the predictive capability of the aforementioned upholstered furniture burning rate models. In this case the models significantly under-predicted the PHRR. The Babrauskas model, with a fabric factor of 0.4 and a padding factor of 0.8, gave the best agreement: bias of 0.66 and a standard error of 317 kW (increases to 518 kW when the bias is removed). The accuracy of the Babrauskas model needs refinement and more work is needed to improve the predictions. That will take some time and in the meantime the alternative approach described below may be used.

Epistemic uncertainty can indirectly be accounted for by conducting a parametric analysis. Such an analysis could, for example, consist of a series of simulations to determine the effect of different ignition scenarios and furniture sizes. The averages and standard deviations from the used furniture tests in Table 31 can be used to guide such a sensitivity study. Heat release curves can be constructed based on the values in this table, assuming that the ignition delay and PHRR are only affected by the ignition scenario and the furniture size (1-, 2-, or 3-seat), respectively. With a specified PHRR, the base of the triangle can be determined using the estimated mass of the item, a soft combustible mass fraction of 27% (based on average component weights measured for the items used to prepare the specimens for small-scale testing) and a heat of combustion of the soft furnishings of approximately 23 MJ/kg.

Table 31. Used Furniture Data to Construct HRR Curves for Sensitivity Analysis.

Sofa Size	Mass (kg)	PHRR (kW)	Ignition Source	Ignition Delay (s)
1-Seat	33.7 ± 11.3	1455 ± 401	Accelerant	71 ± 55
2-Seat	39.4 ± 6.1	1726 ± 113	Small Flame Center	435 ± 214
3-Seat	67.2 ± 17.5	2073 ± 356	Small Flame Corner	171 ± 52

To further illustrate how this table could be used, assume that it has been determined from the information obtained at the scene that a 3-seat sofa was involved in a fire under investigation. The investigator could then use a fire model like CFAST in conjunction with

the information in Table 31 to estimate the time to flashover for the three ignition scenarios (accelerant, small flame at the center of a seat cushion and small flame in a corner). The best estimate for the mass of the furniture item is the mean from the used furniture experiments, i.e., 67.2 kg. The corresponding best estimate of the mass of soft furnishings is $0.27 \times 67.2 = 18.1$ kg. The corresponding total energy released is $18.1 \times 23 = 417$ MJ. Assuming the PHRR is 2073 kW (from the table), the corresponding burning time is $417000 / 2073 = 201$ s. Based on the PHRR and burning time, a triangular HRR curve can be constructed for input into CFAST. To determine the effect of the ignition scenario for this HRR curve CFAST only needs to be run once, i.e., with the sofa infighting at $t = 0$. The flashover times can then be determined for each ignition scenario by adding the applicable ignition delay from Table 31. Additional CFAST analyses could be conducted with variations (e.g. plus or minus one standard deviation) of the estimated mass and/or peak heat release rate. The results of these calculations could give the investigator some insight into what scenarios are the most consistent with the data collected at the fire scene.

5.2 IMPLICATIONS FOR POLICY AND PRACTICE

The estimation of the performance of upholstered furniture is often a critical element of a forensic fire scene reconstruction. Unfortunately, the reliability and accuracy of this estimation are usually very low due to the large variability in furniture designs, limited understanding of the effect of the ignition scenario on the burning behavior of upholstered furniture, and the lack of reliable and accurate HRR data for upholstered furniture and its components. As a result, the reconstruction of a fire that involved upholstered furniture is usually subject to large uncertainties.

This project aims at advancing the current state-of-the-art of investigating fires that involve upholstered furniture by

- Identifying relevant data pertaining to furniture flammability from previous studies through a detailed review of the literature;
- Expanding the results of the literature review with test data (including video footage) from a parametric study that systematically examined the effect of ignition source strength, location, and other factors on the fire behavior of upholstered furniture;

- Developing guidelines for fire investigators on how to best estimate the HRR versus time curve of upholstered furniture and quantify/optimize the uncertainty of the predictions depending on the extent that materials are available for testing; and
- Illustrating the use and testing the validity of the guidelines based on small- and full-scale fire test data for a set of used chairs and sofas that is representative of the range of upholstered furniture items the fire investigator is most likely to encounter in the field.

It is expected that this project will have a significant impact by substantially improving the use of scientific tools in arson investigations through the development of a framework for applying fire modeling techniques.

This project directly impacts the arson investigation discipline, but also advances the use of fire modeling in general and the use of test data in conjunction with models to support fire engineering analyses.

Fire modeling tools, such as CFAST and FDS, are now widely used in fire protection engineering, but they are not very popular in the field of fire investigation. This project is expected to have a significant contribution to the transfer of fire modeling technology to the fire and arson investigator community. However, the project also identified a number of areas where there is need for additional work, as discussed in the next Section. It is very important that investigators have a good understanding of the limitations of fire modeling and of the need to accurately determine the heat release rate. This project is expected to provide a significant contribution to advancing this understanding.

5.3 IMPLICATIONS FOR FURTHER RESEARCH

The upholstered furniture burning rate models that were explored in this study, without adjustments, appear to significantly under-predict the HRRs that were measured for used furniture. Additional research is needed to understand what the fundamental reasons are for these discrepancies and how the predictive capability of the burning rate models can be improved.

Three of the four burning rate models that were considered assume that the HRR vs. time curve of upholstered furniture is approximately triangular in shape. Some of the HRR data that was obtained for used furniture items puts the validity of this assumption in

question. It is recommended to explore other curve shapes to fit the data, for example a t^2 fire growth stage followed by a period of steady burning at PHRR and a linear decay.

The FDS furniture flame spread and burning model shows the most promise because it is based on physics and not on correlations. As such this model has the potential of being capable of accounting for ignition source strength, source location, and enclosure effects. However, more work is needed to address the challenges that were encountered in our initial attempts at using FDS to model furniture fires. More specifically a more detailed algorithm is needed to predict opposed-flow flame spread at sub-grid scale. In addition, better method need to be developed to account for thickness and heat flux effects.

6 REFERENCES

6.1 CODES AND STANDARDS

‘ASTM D 7309: Standard Test Method for Determining Flammability Characteristics of Plastics and Other Solid Materials Using Microscale Combustion.’ *Annual Book of Standards, Vol. 08.03*, ASTM International, West Conshohocken, PA, 2007.

‘ASTM E 1354: Standard Test Method for Heat and Visible Smoke Release Rates for Materials and Products Using an Oxygen Consumption Calorimeter.’ *Annual Book of Standards, Vol. 04.07*, ASTM International, West Conshohocken, PA, 2010.

‘ASTM E 1355: Standard Guide for Evaluating the Predictive Capability of Deterministic Fire Models.’ *Annual Book of Standards, Vol. 04.07*, ASTM International, West Conshohocken, PA, 2011.

‘ASTM E 1474: Standard Test Method for Determining the Heat Release Rate of Upholstered Furniture and Mattress Components or Composites Using a Bench Scale Oxygen Consumption Calorimeter.’ *Annual Book of Standards, Vol. 04.07*, ASTM International, West Conshohocken, PA, 2010.

‘ASTM E 1537: Standard Test Method for Fire Testing of Upholstered Furniture.’ *Annual Book of Standards, Vol. 04.07*, ASTM International, West Conshohocken, PA, 2007.

‘ASTM E 1590: Standard Test Method for Fire Testing of Mattresses.’ *Annual Book of Standards, Vol. 04.07*, ASTM International, West Conshohocken, PA, 2007.

‘ASTM E 1822: Standard Test Method for Fire Testing of Stacked Chairs.’ *Annual Book of Standards, Vol. 04.07*, ASTM International, West Conshohocken, PA, 2009.

- ‘ASTM E 2067: Standard Practice for Full-Scale Oxygen Consumption Calorimetry Fire Tests.’ *Annual Book of Standards, Vol. 04.07*, ASTM International, West Conshohocken, PA, 2008.
- ‘ASTM E 2536: Standard Guide for Assessment of Measurement Uncertainty in Fire Tests.’ *Annual Book of Standards, Vol. 04.07*, ASTM International, West Conshohocken, PA, 2009.
- ‘ASTM F 1085: Standard Specification for Mattress and Box Springs for Use in Berths in Marine Vessels.’ *Annual Book ASTM Standards, Vol. 01.07*, ASTM International, West Conshohocken, PA, 2010.
- ‘ASTM F 1870: Standard Guide for Selection of Fire Test Methods for the Assessment of Upholstered Furnishings in Detention and Correctional Facilities.’ *Annual Book ASTM Standards, Vol. 15.08*, ASTM International, West Conshohocken, PA, 2005.
- ‘BS 5852: Methods of test for the assessment of the ignitability of upholstered seating by smouldering and flaming ignition sources.’ British Standards Institution, London, UK, 1982.
- ‘CA TB 117: Requirements, Test Procedures and Apparatus for Testing the Flame Retardance of Resilient Filling Materials Used in Upholstered Furniture,’ California Bureau of Electronic and Appliance Repair, Home Furnishings and Thermal Insulation, North Highlands, CA, 2000.
- ‘CA TB 133: Flammability Test Procedure for Seating Furniture for Use in Public Occupancies.’ California Bureau of Electronic and Appliance Repair, Home Furnishings and Thermal Insulation, North Highlands, CA, 1999.
- ‘CA TB 603: Requirements and Test Procedure for Resistance of a Mattress/Box Spring Set to a Large Open-Flame,’ California Bureau of Electronic and Appliance Repair, Home Furnishings and Thermal Insulation, North Highlands, CA, 2004.
- ‘Consumer Products Safety Commission 16 CFR 1633: Final Rule: Standard for the Flammability (Open Flame) of Mattress Sets,’ *Federal Register*, Vol. 72, No. 50, March 15, 2006, pp. 13472-13523.

- ‘ISO 5660-1: Reaction-to-fire tests – Heat release, smoke production and mass loss rate – Part 1: Heat release rate (cone calorimeter method).’ International Organization for Standardization, Geneva, Switzerland, 2002.
- ‘ISO 5660-2: Reaction-to-fire tests – Heat release, smoke production and mass loss rate – Part 2: Smoke production rate (dynamic measurement).’ International Organization for Standardization, Geneva, Switzerland, 2002.
- ‘ISO 9705: Fire tests – Reaction-to-fire – Room fire test.’ International Organization for Standardization, Geneva, Switzerland, 1993.
- ‘ISO 24473: Fire tests – Open calorimetry – Measurement of the rate of production of heat and combustion products for fires of up to 40 MW.’ International Organization for Standardization, Geneva, Switzerland, 2008.
- ‘ISO/IEC Guide 98-3: Uncertainty of measurement – Part 3: Guide to the expression of uncertainty in measurement (GUM:1995).’ International Organization for Standardization, Geneva, Switzerland, 2008.
- ‘NFPA 265: Standard Method of Tests for Evaluating Room Fire Growth Contribution of Textile Wall Coverings.’ National Fire Protection Association, Quincy, MA, 2008.
- ‘NFPA 271: Standard Method of Test for Heat and Visible Smoke Release Rates for Materials and Products Using an Oxygen Consumption Calorimeter.’ National Fire Protection Association, Quincy, MA, 2009 (currently withdrawn).
- ‘NFPA 286: Standard Method of Tests for Evaluating Contribution of Wall and Ceiling Interior Finish to Room Fire Growth.’ National Fire Protection Association, Quincy, MA, 2008.
- ‘NFPA 701: Standard Methods of Fire Tests for Flame Propagation of Textiles and Films.’ National Fire Protection Association, Quincy, MA, 2010.
- ‘NFPA 921: Guide for Fire and Explosion Investigations.’ National Fire Protection Association, Quincy, MA, 2008.
- ‘School Bus Fire Test: National Safety Council School Bus Seat Upholstery Fire Block Test.’ National Safety Council, Chicago, IL.

6.2 CITED REFERENCES

- Ahrens, M., (2011). "Home Upholstered Furniture Fires." NFPA Fire Analysis and Research, Quincy, MA.
- Ames, S., and Rogers, S., (1990). "Large and Small Scale Fire Calorimetry Assessment of Upholstered Furniture." *5th Interflam Conference*, Canterbury, England, 221-232.
- Babrauskas, V., (1979). "Full-Scale Burning Behavior of Upholstered Chairs." Technical Note 1103, National Bureau of Standards, Gaithersburg, MD.
- Babrauskas, V., Lawson, J., Walton, W., and Twilley, W., (1982). "Upholstered Furniture Heat Release Rates Measured with a Furniture Calorimeter." NBSIR 82-2604, National Bureau of Standards, Gaithersburg, MD.
- Babrauskas, V., (1983). "Upholstered Furniture Heat Release Rates—Measurements and Estimation," *Journal of Fire Sciences*, 1, 9-32.
- Babrauskas, V., (1984a). "Development of the Cone Calorimeter - A Bench-Scale Heat Release Rate Apparatus Based on O₂ Consumption," *Fire and Materials*, 8, 81-95.
- Babrauskas, V., (1984b). "Upholstered Furniture Room Fire—Measurements, Comparison with Furniture Calorimeter Data, and Flashover Predictions," *Journal of Fire Sciences*, 2, 5-19.
- Babrauskas, V., and Walton, W., (1986). "A Simplified Characterization of Upholstered Furniture Heat Release Rates," *Fire Safety Journal*, 11, 181-192.
- Babrauskas, V., Twilley, W., Janssens, M., and Yusa, S., (1992). "A Cone Calorimeter for Controlled Atmosphere Studies," *Fire and Materials*, 16, 37-43.
- Babrauskas, V., (1996). "Fire Modeling Tools for FSE: Are They Good Enough?," *Journal of Fire Protection Engineering*, 8, 87-96.
- Babrauskas, V., (2008a). "Heat Release Rates," in *The SFPE Handbook of Fire Protection Engineering*, 4th Edition, National Fire Protection Association, Quincy, MA, Section 3, Chapter 1.
- Babrauskas, V., (2008b). *The SFPE Handbook of Fire Protection Engineering*, 4th Edition, National Fire Protection Association, Quincy, MA, Appendix C, Tables C.2-C.4.
- Benisek, L., and Phillips, W., (1978). "The Importance and Relevance of Burning Behavior, Smoke, and CO Emission from Upholstered Seating," *Journal of Consumer Product Flammability*, 5, 96-110.
- Chasteen, C., (2008). "Fire and Explosion Investigation and Forensic Analyses: Near- and Long-Term Needs Assessment for State and Local Law Enforcement." Award 2005-MU-MU-K044, Supplement No. 1, The National Institute of Justice, Washington, DC.

- Cleary, T., Ohlemiller, T., and Villa, K., (1992). "The Influence of Ignition Source on the Flaming Fire Hazard of Upholstered Furniture." NISTIR 4847, National Institute of Standards and Technology, Gaithersburg, MD.
- Cleary, T., Ohlemiller, T., and Villa, K., (1994). "The Influence of Ignition Source on the Flaming Fire Hazard of Upholstered Furniture," *Fire Safety Journal*, 23, 79-102.
- Cooper, L., (1994). "Some Factors in the Design of a Calorimeter Hood and Exhaust," *Journal of Fire Protection Engineering*, 6, 99-112.
- Dahlberg, M., (1994). "Error Analysis for Heat Release Rate Measurements with the SP Industry Calorimeter." SP Report 1994:29, National Testing Institute (SP), Borås, Sweden.
- Ezinwa, J., Rigg, J., Torvi, D., and Weckman, E., (2009). "Effects of Ignition Location on Flame Spread and Heat Release Rates in Furniture Calorimeter Tests of Polyurethane Foams." *11th International Fire and Materials Conference*, San Francisco, CA, 645-656.
- Hamins, A., and McGrattan, K., (2007). "Verification and Validation of Selected Fire Models for Nuclear Power Plant Applications - Volume 2: Experimental Uncertainty." NUREG-1824, Volume 2, U.S. Nuclear Regulatory Commission, Washington DC.
- Heskestad, G., (2008). "Fire Plumes, Flame Height and Air Entrainment," in *The SFPE Handbook of Fire Protection Engineering, 4th Edition*, National Fire Protection Association, Quincy, MA, Section 2, Chapter 1.
- Hill, K., et al., (2007a). "Verification & Validation of Selected Fire Models for Nuclear Power Plant Applications, Volume 7: Fire Dynamics Simulator." NUREG-1824, Vol. 7, U.S. Nuclear Regulatory Commission, Office of Nuclear Regulatory Research (RES), Rockville, MD.
- Hill, K., et al., (2007b). "Verification & Validation of Selected Fire Models for Nuclear Power Plant Applications, Volume 5: Consolidated Fire Growth and Smoke Transport Model (CFAST)." NUREG-1824, Vol. 5, U.S. Nuclear Regulatory Commission, Office of Nuclear Regulatory Research (RES), Rockville, MD.
- Hirschler, M., (1997). "A New Mattress Fire Test for Use In Detention Environments." *8th Annual Conference on Recent Advances in Flame Retardancy of Polymeric Materials*, Stamford, CT, 309-322.
- Hirschler, M., (2004). "Residential Upholstered Furniture in the United States and Fire Hazard." *15th Annual Conference on Recent Advances in Flame Retardancy of Polymeric Materials*, Stamford, CT, 300-315.
- Hirschler, M., (2005). "Experience in Full Scale Fire Testing of Consumer Products." *10th European Meeting on Fire Retardancy and Protection of Materials*, Berlin, Germany.
- Hshieh, F., and Buch, R., (1997). "Controlled-Atmosphere Cone Calorimeter Studies of Silicones," *Fire and Materials*, 21, 265-272.

- Huggett, C., (1980). "Estimation of the Rate of Heat Release by Means of Oxygen Consumption," *Fire and Materials*, 12, 61-65.
- Icove, D., and DeHaan, J. (2004). *Forensic Fire Scene Reconstruction*, Pearson Education, Inc., Upper Saddle River, NJ.
- Janssens, M., (1991). "Measuring Rate of Heat Release by Oxygen Consumption," *Fire Technology*, 27, 234-249.
- Janssens, M. (2000). *Introduction to Mathematical Fire Modeling (Second Edition)*, Technomic Publishing Co., Lancaster, PA.
- Janssens, M., (2008). "Calorimetry," in *SFPE Handbook of Fire Protection Engineering (4th Edition)*, National Fire Protection Association, Quincy, MA, Section 3, Chapter 2, 60-89.
- Janssens, M., and Gomez, C., (2009). "Thornton's Constant Revisited." *Fire and Materials '09, 11th International Conference*, San Francisco, CA, 91-102.
- Kokkala, M., Goransson, U., and Söderbom, J., (1991). "Experiments in a Large Room with Combustible Linings." *2nd International Heat Release and Fire Hazard Symposium*.
- Krasny, J., Parker, W., and Babrauskas, V. (2001). *Fire Behavior of Upholstered Furniture and Mattresses*, Noyes Publications, Park Ridge, NJ.
- Leonard, J., Bowditch, P., and Dowling, V., (2000). "Development of a Controlled-Atmosphere Cone Calorimeter," *Fire and Materials*, 24, 143-150.
- Lyon, R., (2000). "Heat Release Kinetics," *Fire and Materials*, 24, 179-186.
- Lyon, R., (2004). "Plastics and Rubber," in *Handbook of Building Materials for Fire Protection*, ed. C. Harper, McGraw-Hill., New York, NY, 3.1-3.51.
- Lyon, R., and Janssens, M., (2005). "Polymer Flammability." *Encyclopedia of Polymer Science & Engineering (On-line Edition)*.
- Lyon, R., Walters, R., and Stoliarov, S., (2006). "A Thermal Analysis Method for Measuring Polymer Flammability," *Journal of ASTM International*, 3, 1-18.
- Lyon, R., Walters, R., Safronava, N., and Stoliarov, S., (2009). "A Statistical Model for the Results of Flammability Tests." *11th International Fire and Materials Conference*, San Francisco, CA, 141-159.
- Mason, R., Gunst, F., and Hess, J. (2003). *Statistical Design and Analysis of Experiments, with Applications to Engineering and Science* Wiley-Interscience, Hoboken, NJ.
- McCaffrey, B., (1982). "Entrainment and Heat Flux of Buoyant Diffusion Flames." NBSIR 82-2473, National Bureau of Standards, Washington, DC.
- McGrattan, K., Hostikka, S., Floyd, J., and McDermott, R., (2010). "Fire Dynamics Simulator (Version 5) Technical Reference Guide, Volume 3: Validation." National Institute of Standards and Technology, Gaithersburg, MD.

- McGrattan, K., McDermott, R., Hostikka, S., and Floyd, J., (2010). "Fire Dynamics Simulator (Version 5), User's Guide." National Institute of Standards and Technology, Gaithersburg, MD.
- Mitler, H., and Tu, K., (1994). "Effect of Ignition Location on Heat Release Rate of Burning Upholstered Furniture." Annual Conference on Fire Research Book of Abstracts, NISTIR 5499, National Institute of Standards and Technology, Gaithersburg, MD.
- Newman, J., Wieczorek, C., and Troup, J., (2005). "Application of Building-Scale Calorimetry." *Eighth International Symposium on Fire Safety Science*, Beijing, China, 1425-1434.
- Nussbaum, R., (1987). "Oxygen Consumption Measurements in the Cone Calorimeter. A Direct Comparison Between a Paramagnetic Cell and a High-Temperature Cell," *Fire and Materials*, 11, 201-203.
- Ohlemiller, T., and Villa, K., (1990). "An Investigation of the California Technical Bulletin 133 Test, Part II: Characteristics of the Ignition Source and a Comparable Gas Burner." NBSIR 90-4348, National Bureau of Standards, Gaithersburg, MD.
- Parker, W., (1984). "Calculations of the Heat Release Rate by Oxygen Consumption for Various Applications," *Journal of Fire Sciences*, 2, 380-395.
- Parker, W., Tu, K., Nurbakhsh, S., and Damant, G., (1990). "An Investigation of the California Technical Bulletin 133 Test, Part III: Full Scale Chair Burns." NBSIR 90-4375, National Bureau of Standards, Gaithersburg, MD.
- Paul, K., and Christian, S. D., (1987). "Standard Flaming Ignition Sources for Upholstered Composites, Furniture and Bed Assembly Tests," *Journal of Fire Sciences*, 5, 178-211.
- Peacock, R., Jones, W., Reneke, P., and Forney, G., (2008a). "CFAST–Consolidated Model of Fire Growth and Smoke Transport (Version 6)– Software Development and Model Evaluation Guide." NIST Special Publication 1086, National Institute of Standards and Technology, Gaithersburg, MD.
- Peacock, R., Jones, W., Reneke, P., and Forney, G., (2008b). "CFAST–Consolidated Model of Fire Growth and Smoke Transport (Version 6)–User’s Guide." NIST Special Publication 1041, National Institute of Standards and Technology, Gaithersburg, MD.
- Sundström, B., (1987). "Full-Scale Fire Testing of Upholstered Furniture and the Use of Test Data," *Cellular Polymers*, 6, 28-38.
- Sundström, B., (1996). "CBUF: Fire Safety of Upholstered Furniture - The Final Report on the CBUF Research Programme." EUR 16477 EN, European Commission, Measurements and Testing, Brussels, Belgium.
- Tewarson, A., (2008). "Generation of Heat and Chemical Compounds in Fires," in *The SFPE Handbook of Fire Protection Engineering, 4th Edition*, National Fire Protection Association, Quincy, MA, Section 3, Chapter 4.

- Thornton, W., (1917). "The Relation of Oxygen to the Heat of Combustion of Organic Compounds," *Philosophical Magazine and Journal of Science*, 33.
- Walters, R., Hackett, S., and Lyon, R., (2000). "Heats of Combustion of High Temperature Polymers," *Fire and Materials*, 24, 245-252.
- Zukoski, E., Kubota, T., and Cetegen, H., (1980). "Entrainment in Fire Plumes," *Fire Safety Journal*, 3, 107-121.

7 DISSEMINATION OF RESEARCH FINDINGS

7.1 PUBLICATIONS AND PRESENTATIONS

- On March 9, 2011, the San Antonio-Austin Chapter of the Society of Fire Protection Engineers (SFPE) visited SwRI. Approximately 45 heard a presentation about the NIJ program and witnessed a full-scale room tests on a mockup.
- On May 25, 2011, Mr. Mitch Westin, representing the Harris County Fire Marshall's Office (Houston, TX), visited SwRI to witness a room test on a used 3-seat sofa and to discuss the project.
- Dr. Janssens gave a presentation entitled "Relevance of ASTM E 2536 in Fire Safety Engineering Analysis" at the *ASTM E05 Symposium—Uncertainty and What to Do About It* in Anaheim, CA, June 16, 2011.
- Dr. Hirschler gave a presentation entitled "Ignition Scenario and Enclosure Effects on the Burning Rate of Upholstered Furniture" at the *SFPE Engineering Technology Conference* in Portland, OR, on October 25, 2011.
- Mr. Kris Overholt gave a presentation entitled "Upholstered Furniture Fire Behavior, Experiments, Modeling, and Prediction" at the *Central Texas Fire Investigators Association Meeting* in Pflugerville, TX, on October 7, 2011.
- Drs. Janssens and Hirschler gave a three-part presentation on the NIJ project at the ASTM E05 Research Review Meeting in Tampa, FL, on December 5, 2011.
- A massive amount of information was generated in this project. It is anticipated that the results of this work will be presented at several technical conferences and published in peer-reviewed journals in the coming year(s).

7.2 DATA

The results and report of this study and any papers presented at conferences can be made available to the fire investigation community, e.g. through the T/SWGFEX web site. A database will be provided on DVD with a complete set of test data and model input and output files that resulted from this work. The database can serve as a central repository for other relevant data that are now at many places in different formats.

7.3 VIDEO

A DVD with video clips was created as training material that will give arson investigators the opportunity to witness the full-scale fire tests a posteriori. Video plots are included with information on the enclosure temperature and HRR, which will help arson investigators develop an understanding of fire dynamics in upholstered furniture fires. Figure 52 shows a screen shot of the video of Test LRM161AS1 discussed in Section 4.4.1. The production and distribution of copies of the DVDs may require additional NIJ funding.

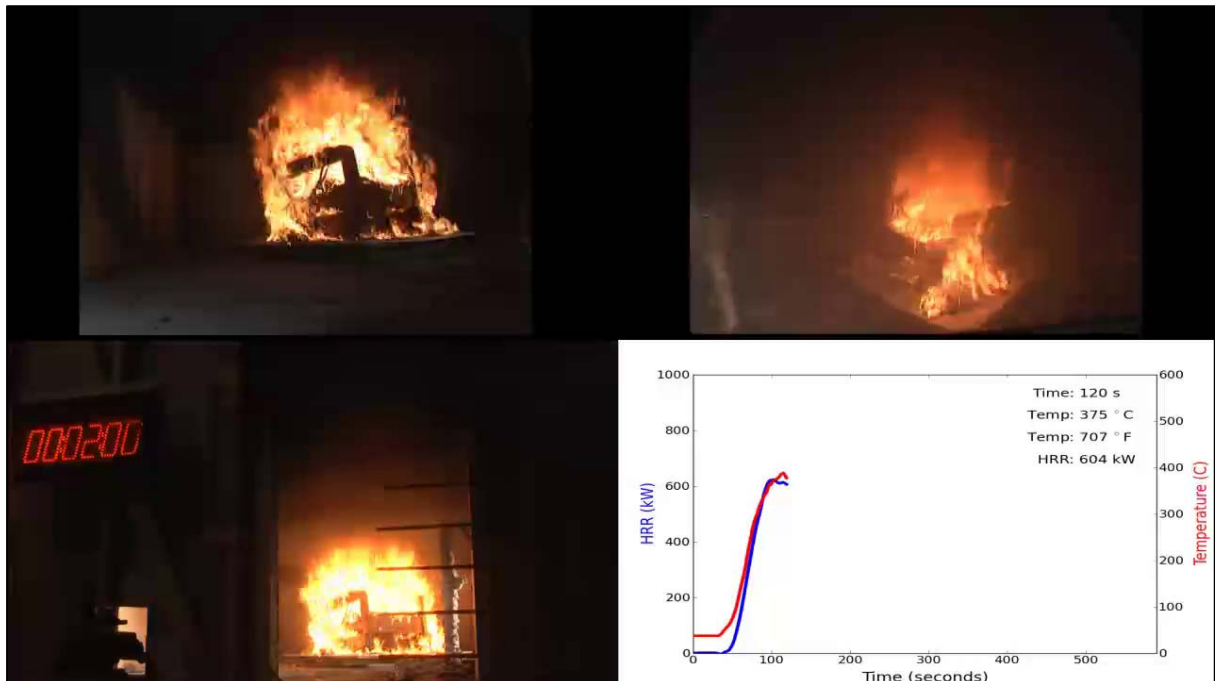


Figure 52. Snapshot of Video of Test LRU161AS1.

APPENDIX A

MATHEMATICAL MODELING OF COMPARTMENT FIRES

(CONSISTING OF 13 PAGES)

A.1 COMPARTMENT FIRE DYNAMICS

A burning object inside a compartment can be viewed as a source of fuel vapors, which mix with the surrounding air and react with its oxygen, releasing heat and forming products of combustion. The combustion reactions take place in a luminous gas volume that is referred to as the flame. The heat generated in the flame is released partly in the form of radiation, and partly by convection. The hot products of combustion rise from the flame, and form a thermal plume. Additional surrounding air is entrained in the plume, resulting in increasing plume mass flow and decreasing temperature as a function of height. The air is supplied by natural ventilation through a (partly) open door or window or by forced ventilation through an HVAC system. The rising plume gases collect below the ceiling and form a hot smoky layer. The space between the floor and the hot layer consists of cool uncontaminated air. The main elements of a compartment fire are shown in Figure A-1.

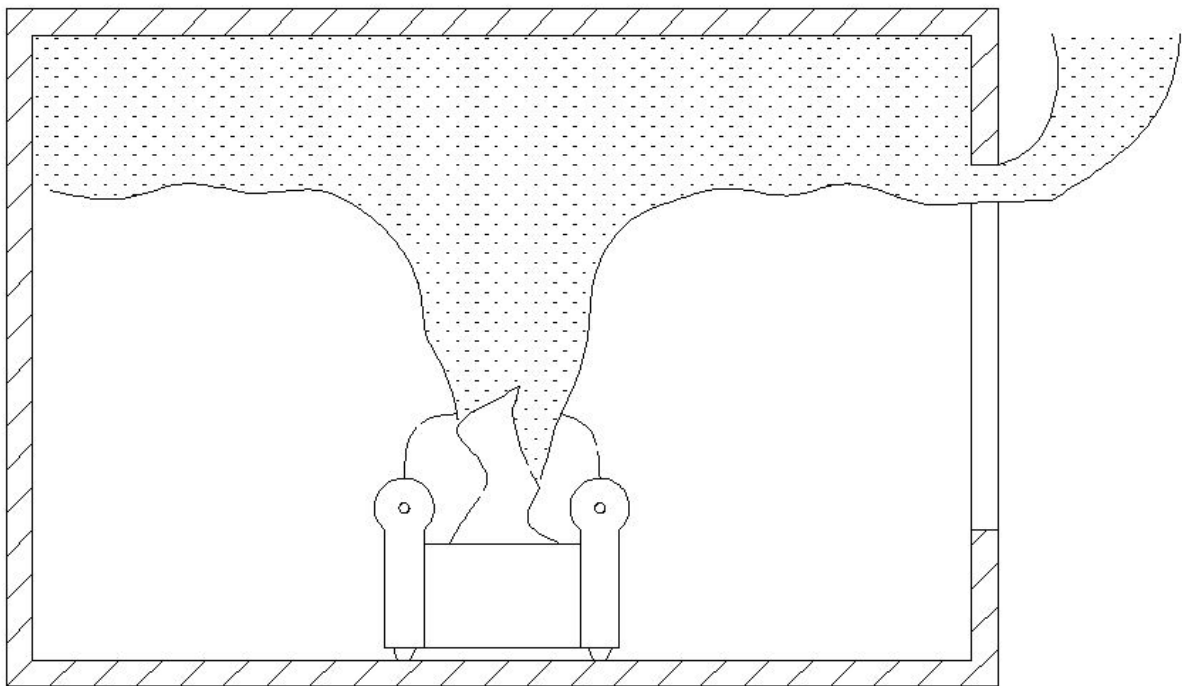


Figure A-1. Schematic of a Compartment Fire with Natural Ventilation.

The radiation from the flame is transferred to the floor, wall, and ceiling surfaces, and is partly absorbed by the upper hot layer gases. In addition, the bounding surfaces of the enclosure exchange heat internally by radiation, and with the gas layers by radiation and convection. At each surface, there is a balance between the total radiative and convective heat flux that is received, and the heat flux that is reradiated from the surface and transferred

by conduction into the solid. It is clear; therefore, that it is not trivial to calculate the heat loss or gain of the gas layers. An enclosure-wide heat balance is needed that includes the three modes of heat transfer.

A.2 MATHEMATICAL MODELING OF COMPARTMENT FIRES

Compartment fire models are used to calculate the time-varying conditions due to a fire in the compartment. It is a common misconception that compartment fire models predict fire growth. In reality, except in a few simple cases, they are only capable of determining the effects of a fire that is specified by the user. Two different types of compartment fire models have been developed: zone models and field models. These two types of models are briefly described below.

A.2.1 ZONE MODELS

Numerous pre-flashover, full-scale room fire tests have shown that the interface between both layers is relatively sharp, while the composition and temperature of the layers are reasonably uniform. Consistent with these experimental observations, zone models are based on the assumption that the room gas volume comprises two distinct and uniform layers or zones: a lower layer of cold air and an upper layer of hot gases. The resulting idealized geometry of the gas volume inside the compartment is shown in Figure A-2.

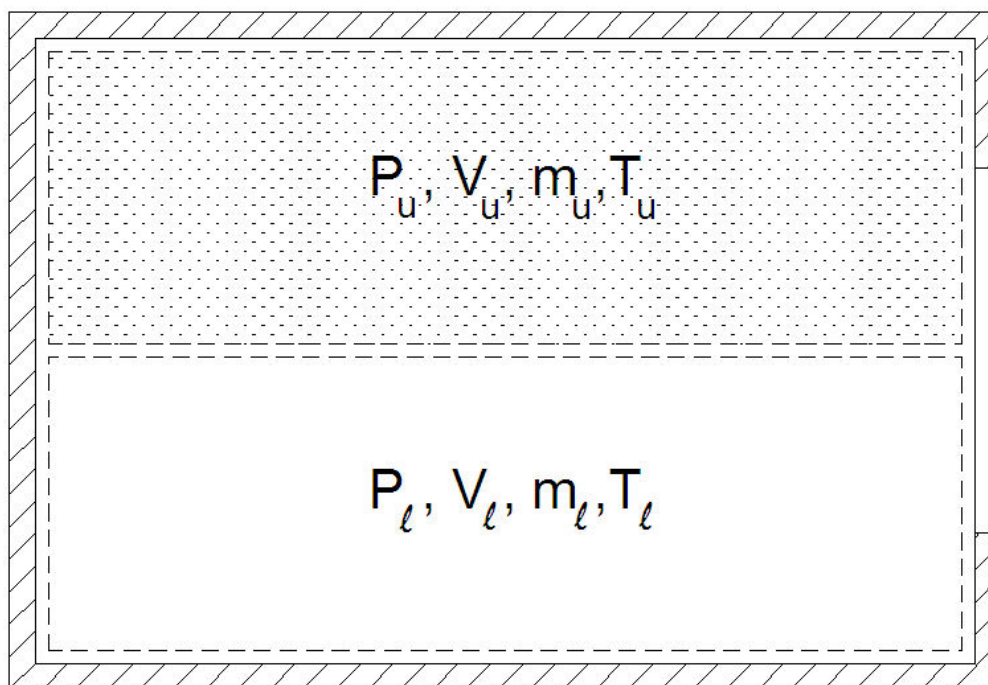


Figure A-2. Zone Model Approximation of Compartment Gas Volume.

The flame and plume are either considered part of the hot gas layer or their volume is neglected. The two layers depicted in Figure A-2 are uniquely defined by their pressure, volume, mass, and temperature. Hence, a set of eight equations are needed to determine how these properties vary as a function of time.

Because the total volume of the enclosure is fixed, the following relationship exists between the volumes of upper and lower layer:

$$V = V_{\ell} + V_u \quad [A-1]$$

where

V = Total volume of the compartment (m^3);

V_{ℓ} = Volume of the lower layer (m^3); and

V_u = Volume of the upper layer (m^3).

The static pressure difference between floor and ceiling level is equal to the hydrostatic pressure at the bottom of an air column of room height. At ambient temperature this is approximately 12 Pa per m of room height, or 35 Pa for a typical room height of 3 m. Because atmospheric pressure is close to 100,000 Pa, the pressure difference between the two layers can be neglected and it can be assumed that

$$P_{\ell} = P_u = P \quad [A-2]$$

where

P_{ℓ} = Average pressure of the lower layer (Pa);

P_u = Average pressure of the upper layer (Pa); and

P = Average pressure in the compartment (Pa).

A pressure difference of a few Pa is sufficient to cause significant air movement. Therefore, hydrostatic pressure differences need to be considered when calculating gas flows through openings.

Since mixing between the layers is usually minimal and can be ignored, the lower layer consists of clean cool air. The pressure at floor level is near ambient. Atmospheric air contains small amounts of carbondioxide and water vapor, but the radiation absorbed by these gases is negligible. The temperature of the air rises slightly due to convective heat transfer with the floor and lower wall sections, which are heated by radiation from the flame, upper

layer, upper wall sections, and ceiling. Under such conditions of pressure and temperature, the lower layer air behaves as an ideal gas for which the following equation of state is valid:

$$P_\ell V_\ell = m_\ell R_\ell T_\ell \quad [A-3]$$

where

m_ℓ = Mass accumulated in the lower layer (kg);

R_ℓ = Gas constant for the mixture in the lower layer (J/kg·K); and

T_ℓ = Temperature of the lower layer (K).

For practical purposes, moisture may be ignored and the lower layer air considered dry so that $R_\ell \approx 287$ J/kg·K.

Based on the discussion leading to Equation A-2, pressure at ceiling level is also of the order of atmospheric pressure. The upper layer temperature seldom exceeds 1500 K. Therefore, the upper layer also behaves as an ideal gas so that

$$P_u V_u = m_u R_u T_u \quad [A-4]$$

where

m_u = Mass accumulated in the upper layer (kg);

R_u = Gas constant for the mixture in the upper layer (J/kg·K); and

T_u = Temperature of the upper layer (K).

The main constituents of the upper layer are N_2 , O_2 , H_2O , CO_2 , and CO . Under some conditions appreciable amounts of other species such as HCl , HCN , and unburnt hydrocarbons may also be present. The ideal gas constant for the upper layer can be expressed as

$$R_u = \sum_{\text{all species}} Y_{u,i} R_{u,i} \quad [A-5]$$

where

$Y_{u,i}$ = Upper layer mass fraction of species i (kg/kg); and

$R_{u,i}$ = Gas constant of species i (J/kg·K).

Note that as the composition of the upper layer varies with time, the value of R_u changes also. To determine $Y_{u,i}$, it is necessary to solve additional mass conservation

equations for the species that need to be tracked. To avoid this, the following approximation can be made. Air entrained into the flame, up to the tip of the flame, is typically 10–20 times that required for complete combustion. Since the plume above the flame entrains even more air, it is clear that the plume is composed mostly of entrained air. (This is particularly true for free-burn fires, but is perhaps questionable for compartment fires that are oxygen-limited.) Therefore, it can be assumed that the smoke produced by the fire behaves like heated air.

To close the set, four additional equations are needed to supplement Equations A-1–A-4. The additional equations express the conservation of mass and energy for the two layers and are briefly discussed below.

Conservation of mass of a layer requires that at any time the rate of change of the mass accumulated in the layer is equal to the inflow rate minus the outflow rate. The mass inflow and outflow rates for the two layers are shown in Figure A-3. Mass conservation of the lower layer can be expressed mathematically as follows:

$$\frac{dm_\ell}{dt} = \dot{m}_a - \dot{m}_e \quad [A-6]$$

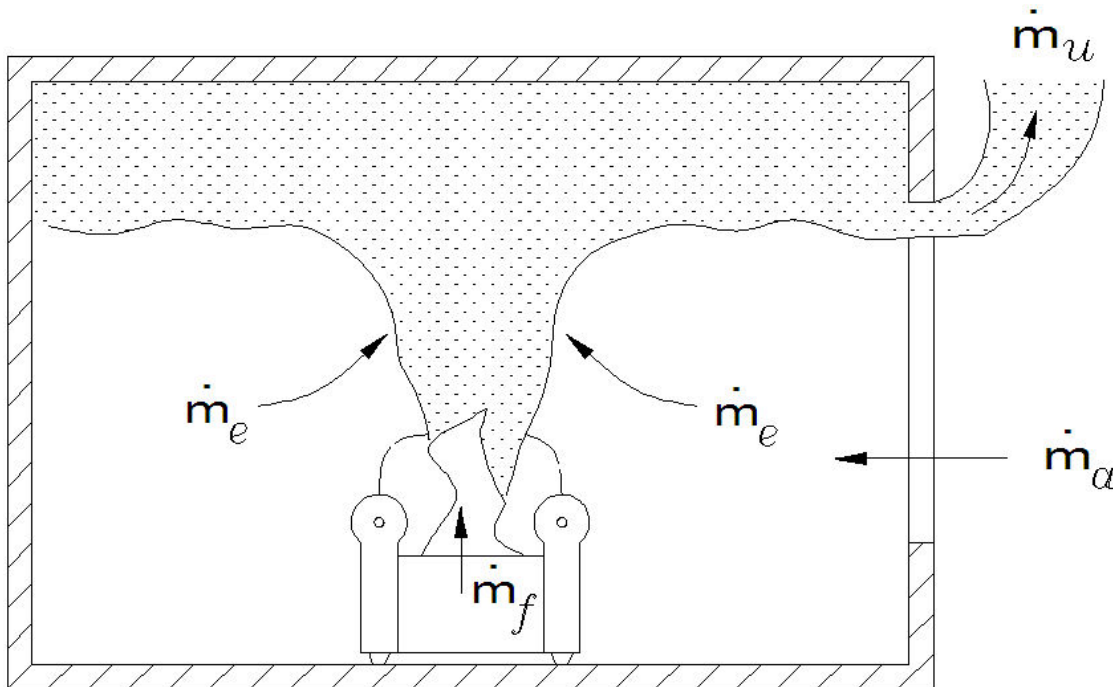


Figure A-3. Layer Mass Inflow and Outflow Rates.

where

$$t = \text{Time (s);}$$

\dot{m}_a = Inflow of air into the compartment (kg/s); and

\dot{m}_e = Mass flow rate of lower layer gas entrained in the flame and plume (kg/s).

Similarly, the mass conservation equation for the upper layer is as follows:

$$\frac{dm_u}{dt} = \dot{m}_f + \dot{m}_e - \dot{m}_e \quad [A-7]$$

where

\dot{m}_f = Mass flow rate of fuel vapors (kg/s); and

\dot{m}_u = Mass flow rate of upper layer gas exiting the compartment (kg/s).

For a naturally vented compartment, the mass flow rates of air entering (\dot{m}_a) and hot layer gas leaving (\dot{m}_u) the compartment are a function of the hydrostatic pressure difference across the ventilation opening. These flows can be calculated based on the layer temperatures, the height of the interface between the two layers, the height of the room, and the height of the top and bottom of the ventilation opening (Janssens, 2000). The rate of entrainment can be determined from correlations in the literature as a function of the dimensions and heat release rate (HRR) of the fire and the height over which the gases are entrained (Heskestad, 2008, McCaffrey, 1982, Zukoski, Kubota and Cetegen, 1980). The mass flow rate of fuel vapors, \dot{m}_f , is usually either specified directly by the user or calculated from the HRR of the fire. The fuel flow rate can usually be neglected without major loss of accuracy.

Conservation of energy of a layer requires that at any time the rate of change of the energy accumulated in the layer is equal to the net inflow rate of enthalpy, h , plus the heat transferred to the layer (by convective heat transfer from the compartment boundaries and absorption of radiation) minus the work associated with volumetric changes of the layer. This is the second law of thermodynamics. The inflow and outflow rates of enthalpy for the two layers are shown in Figure A-4. The internal energy and enthalpy of a specified gas mixture are unique functions of the temperature of the mixture. Assuming a constant specific heat capacity, energy conservation of the lower layer can be expressed mathematically as follows (Janssens, 2000):

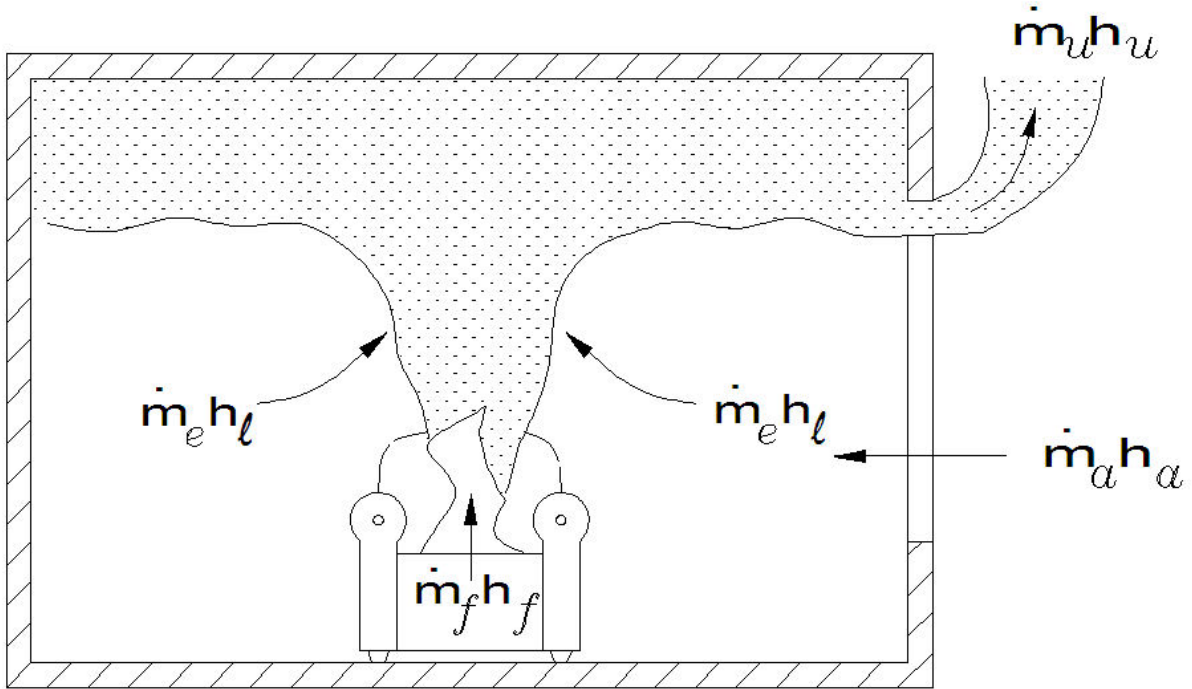


Figure A-4. Layer Enthalpy Inflow and Outflow Rates.

$$m_\ell c_p \frac{dT_\ell}{dt} = \dot{m}_a c_p (T_a - T_\ell) + \dot{Q}_\ell \quad [\text{A-8}]$$

where

c_p = Average specific heat capacity (J/kg·K);

T_a = Temperature of the air flowing into the compartment (K); and

\dot{Q}_ℓ = Total heat flow to the lower layer (W).

The derivation of the upper layer energy conservation equation is similar, but slightly more complicated (Janssens, 2000). The resulting expression, assuming the enthalpy of the fuel vapors can be neglected, is as follows:

$$m_u c_p \frac{dT_u}{dt} = \dot{m}_e c_p (T_\ell - T_u) + \dot{Q} + \dot{Q}_u \quad [\text{A-9}]$$

where

\dot{Q} = HRR of the fire (W); and

\dot{Q}_u = Total heat flow to the upper layer (W).

In summary, the simplest zone compartment fire modeling programs solve a closed set of algebraic (A-1 through A-4) and ordinary differential (A-6 through A-9) equations to obtain the pressure and upper and lower layer volume, mass and temperature as a function of time for a user-specified fire. More complex zone models include additional equations to determine the concentrations of soot and gas species of interest. In addition to the primary variables (pressure, layer volumes, etc.), zone model output typically includes other useful information such as vent flow rates, heat flux to a target, etc. Zone models have proven to provide useful engineering approximations of fire development within an enclosure. They can be a very powerful tool in the hands of a fire investigator. The Consolidated Fire and Smoke Transport (CFAST) model developed at NIST is arguably the most comprehensive and widely used zone model (Peacock, Jones, Reneke and Forney, 2008b). The latest version and supporting documentation can be freely downloaded from the following website: http://www.nist.gov/el/fire_research/cfast.cfm.

A.2.2 FIELD MODELS

Field models subdivide a compartment into a large number (typically tens or hundreds of thousands) of elemental volumes. The model then solves the fundamental equations describing the conservation of mass, momentum, and energy in these small volumes to predict the pressure, density, temperature, and velocity distribution in the compartment. Conservation of mass is also referred to as “continuity”. The equations describing the conservation of momentum are also called the Navier-Stokes equations. The five conservation equations (mass, momentum in three directions, and energy) are typically supplemented with auxiliary equations describing turbulence, combustion, conservation of species, etc. Field models are also referred to as Computational Fluid Dynamics (CFD) models, because they are extensions of computer codes that were originally developed to solve complex fluid flow problems. This type of modeling can be considered as a micro approach to the fire modeling problem.

Field models have extensive computer requirements. Also, a more detailed understanding of the fundamental physical phenomena, such as turbulence, combustion kinetics and chemistry, etc., are needed. The trade-off for these drawbacks is a much more detailed and accurate description of the environment in the fire room. The Fire Dynamics Simulator (FDS) developed at NIST is one of the most popular and powerful field models

available to the fire investigator (McGrattan, McDermott, Hostikka and Floyd, 2010). The latest version of and supporting software and documentation for FDS can be freely downloaded from <http://fire.nist.gov/fds/>.

A.3 PREDICTIVE CAPABILITY OF COMPARTMENT FIRE MODELS

Before it can be used, a compartment fire model must be rigorously tested to assure that it yields acceptable results, regardless of its simplicity or complexity. This "test" is commonly referred to as "an evaluation of the predictive capability of a model". Without this evaluation, the results of a model will be suspect.

The aforementioned evaluation is typically performed following the guidelines of ASTM E 1355. The evaluation process, according to ASTM E 1355, consists of the following four steps:

1. Define the scenarios for which the evaluation is to be conducted;
2. Validate the theoretical basis and assumptions used in the model;
3. Verify the mathematical and numerical robustness of the model; and
4. Evaluate the model, i.e., quantify its uncertainty and accuracy.

Step 4 is usually based on a comparison between model output and experimental data, and provides an indirect method for validation (step 2) and verification (step 3) of a model for the scenarios of interest (step 1). It is generally assumed that the model equations are solved correctly, and the terms validation and evaluation are therefore often used interchangeably.

Both CFAST and FDS have been verified and validated for an wide range of scenarios (Hill, et al., 2007a, b, McGrattan, Hostikka, Floyd and McDermott, 2010, Peacock, Jones, Reneke and Forney, 2008a).

A.4 SETUP OF COMPARTMENT FIRE MODELS TO SIMULATE NIJ EXPERIMENTS

A.4.1 SETUP OF CFAST

CFAST was configured to match the conditions and measurements of the NIJ experiments. A single enclosure was defined as a $4.65 \times 3.43 \times 2.4$ m room with an open doorway measuring 2×0.74 m. The simulation time was 1300 s with an ambient temperature of 20 °C and a relative humidity of 50% for all of the cases. The boundary conditions were applied as follows: the walls and ceiling were specified as 2.54-cm (1-in.)

thick type X gypsum board, and the floor was specified as 1.27-cm (½-in.) thick type X gypsum board.

A radiative fraction of 0.30 was specified and a heat of combustion of 22.7 MJ/kg or 23.8 MJ/kg, was used for the cases with polyurethane and polyester padding, respectively. Depending on the furniture item, the fire source had dimensions of 0.45 × 0.56 m (chair), 0.66 × 0.56 m (1-seat sofa), 1.12 × 0.56 m (2-seat sofa), and 1.58 × 0.56 m (3-seat sofa) and was located 0.6 m above the floor. The HRR ramp was specified depending on the type of burning rate model that was run, as explained in Appendix C. Five cases were run for each room test, i.e., one run for each of the following HRR inputs:

1. Full-scale HRR curve measured in the experiment;
2. CBUF Model I predicted curve;
3. Babrauskas Model I predicted curve;
4. Babrauskas Model II predicted curve; and
5. FDS predicted curve.

Three targets were specified to compare the predicted heat fluxes to the heat flux gauges used in the experiments. Because it is not possible to specify a fixed temperature for each target (to accurately model the measured cold wall heat flux), the CFAST source code was modified and an executable was compiled in which the targets had a fixed surface temperature of 65 °C (temperature of the cooling water in the experiments).

Figure A-5 shows a screenshot of CFAST in Smokeview that indicates the hot gas layer temperature, fire location, flame height, doorway flows, target locations, and general setup of the fire room in CFAST.

A.4.2 SETUP OF FDS

FDS was configured to match the conditions and measurements of the NIJ experiments. A single enclosure was defined as a 4.65 × 3.45 × 2.4 m room with an open doorway measuring 2.1 × 0.75 m. The simulation time was 1270 s with an ambient temperature of 20 °C and a relative humidity of 40% for all of the cases. The boundary conditions were applied as follows: the walls and ceiling were specified as 2.54-cm (1-in.) thick type X gypsum board.

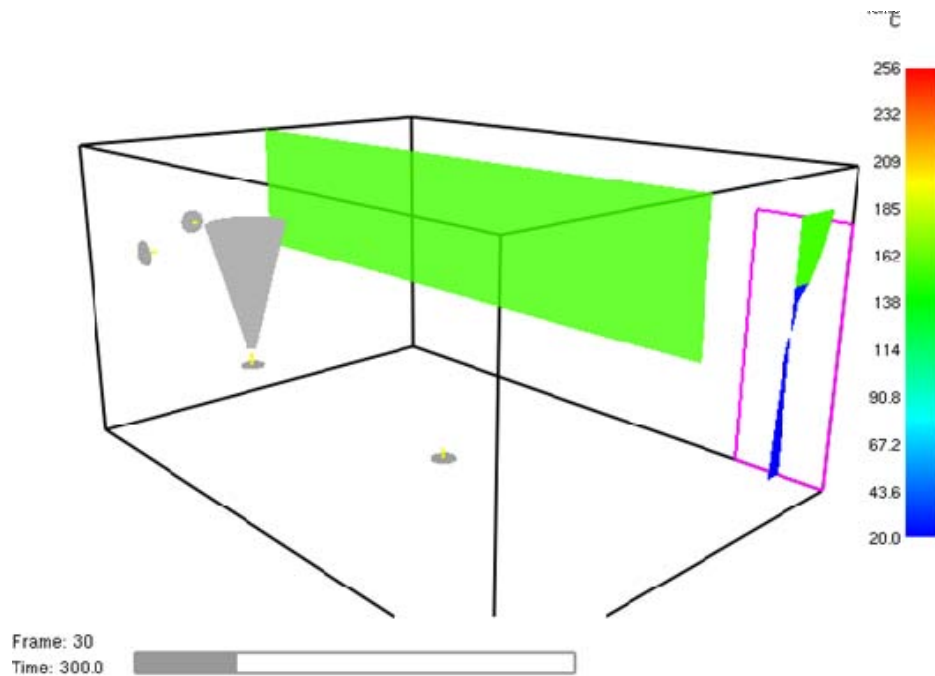


Figure A-5. Screenshot of CFAST model setup in Smokeview.

The grid cells were used as 15-cm cells on each edge, which was determined to be a reasonable grid resolution to adequately model the fire effects (temperatures, hot gas layer, heat fluxes, etc.) in the enclosure. For a 500-kW fire, the characteristic fire diameter (D^*) is 0.727, which gives a D^*/dx of 4.8. This value is within the range of D^*/dx values used in NUREG 1824 (Verification and Validation of Selected Fire Models for Nuclear Power Plant Applications), which used D^*/dx values between 4 and 16. It is good practice to conduct a grid sensitivity analysis. However, since the FDS results were consistent with CFAST and in reasonable agreement with the experiments, a 15-cm grid was deemed to be acceptable

A radiative fraction of 0.35 was specified and a heat of combustion of 22.7 MJ/kg or 23.8 MJ/kg, was used for the cases with polyurethane and polyester padding, respectively. The gas phase reaction used in the FDS models was either that for polyurethane or polyester, depending on the specimen. Polyurethane reaction parameters were used for the used furniture and mockups with polyurethane or polychloroprene foam padding, whereas the polyester reaction parameters were used for the mockups with polyester padding. The polyurethane gas phase reaction parameters were as follows:

- Soot yield: 0.10 kg/kg
- Nitrogen atoms: 1.0

- Carbon atoms: 6.3
- Hydrogen atoms: 7.1
- Oxygen atoms: 2.1
- Heat of combustion: 22,700 kJ/kg

The polyester gas phase reaction parameters were as follows:

- Soot yield: 0.09 kg/kg
- Carbon atoms: 5.77
- Hydrogen atoms: 6.25
- Oxygen atoms: 1.63
- Heat of combustion: 23,800 kJ/kg

The values were obtained from the 19th Edition of the NFPA handbook and the 4th Edition of the SFPE Handbook.

Depending on the furniture item, the burner was placed on the top surface of an obstruction located 0.6 m above the floor. Because the diagonal placement of the furniture made it difficult to accurately represent the furniture items on a coarse grid, the detailed geometry of the furniture items was not modeled. Instead, the furniture items were modeled as gas burner surface, which is justified by the fact that the purpose of these FDS simulations was to quantify the enclosure fire effects in which the HRR was specified based on predicted HRR curves. Five cases were run for each room test, i.e., one run for each of the following HRR ramp inputs:

1. Full-scale HRR curve measured in the experiment;
2. CBUF Model I predicted curve;
3. Babrauskas Model I predicted curve;
4. Babrauskas Model II predicted curve; and
5. FDS predicted curve.

The output devices in the FDS models were placed to match the instrumentation in the experiments as follows:

- Five TCs located 10 cm below the ceiling;
- Three TC trees located in the room (specimen, center, and corner);
- 16 TCs located in the doorway;
- Heat flux gauge (net and radiative) on the floor (fixed temperature of 65 °C); and
- Two heat flux gauges on the wall near the specimen (fixed temperature of 65 °C).

In addition, two temperature slice files through the enclosure and net heat flux, gauge heat flux, and wall temperature boundary files were generated.

Figure A-6 show screenshots of FDS in Smokeview from different views that indicate the fire location, instrumentation, and general setup of the fire room in FDS.

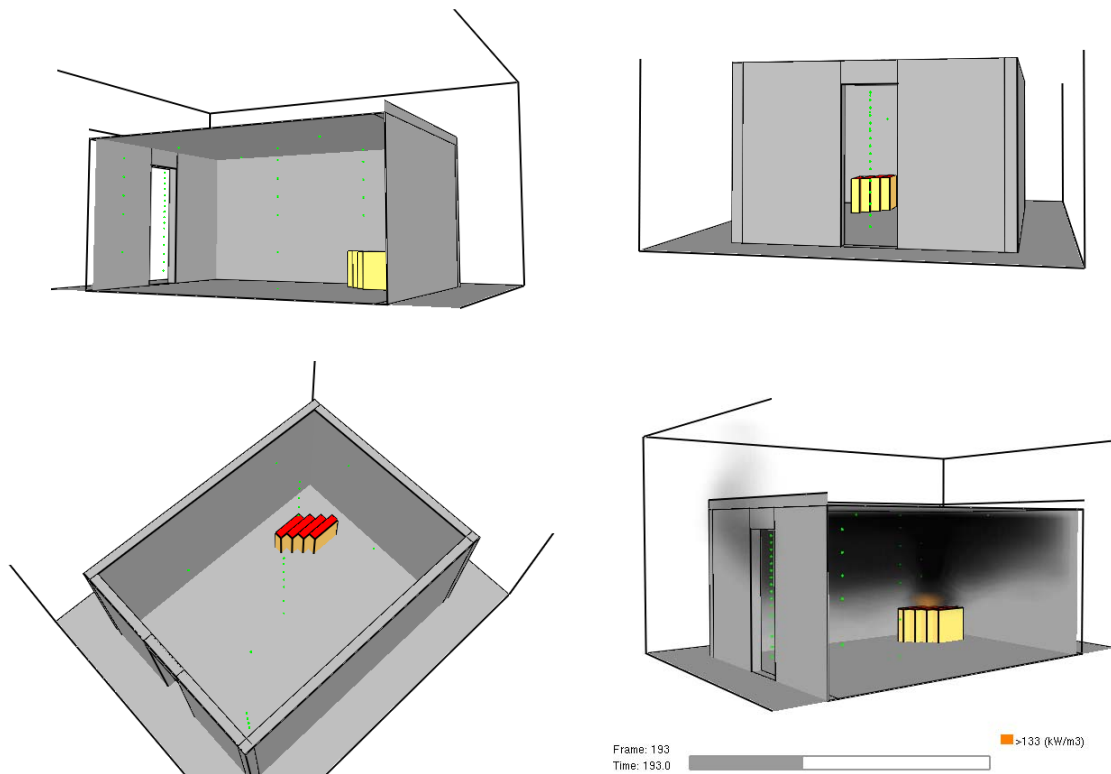


Figure A-6. Screenshots of FDS model setup in Smokeview.

APPENDIX B

EXPERIMENTAL METHODS AND MEASUREMENT UNCERTAINTY CALCULATIONS

(CONSISTING OF 12 PAGES)

B.1 EXPERIMENTAL METHODS FOR MEASURING HEAT RELEASE RATE

Various methods have been used for measuring the heat release rate (HRR) in fire tests (Janssens, 2008). However, since the early 1980s, the oxygen consumption technique has become the methods of choice. This technique is described in the next section. The oxygen consumption calorimeters that were used in this work are described in subsequent sections.

B.1.1 OXYGEN CONSUMPTION CALORIMETRY

In 1917, Thornton showed that for a large number of organic liquids and gases, a nearly constant net amount of heat, E , is released per unit mass of oxygen consumed for complete combustion (Thornton, 1917). Huggett found this also to be true for organic solids (Huggett, 1980). Based on data for 39 fuels he suggested an average value of 13.1 kJ per g of oxygen consumed and stated that for most fuels, the actual value is within $\pm 5\%$ of the average. This implies that the HRR in a fire test can be measured with reasonable accuracy based on the rate at which oxygen is consumed. The exact value of E for a specific fuel is equal to the net heat of combustion of the fuel divided by the mass of oxygen needed for complete combustion of a mass unit of fuel. Several extensive lists of E values can be found in the literature (Babrauskas, 2008b, Janssens and Gomez, 2009, Tewarson, 2008, Walters, Hackett and Lyon, 2000).

The basic requirement to use the oxygen consumption technique is that all combustion products are collected and removed through an exhaust duct. At a distance downstream sufficient for adequate mixing, both flow rate and composition of the gases are measured. A schematic of an oxygen consumption calorimeter is shown in Figure B-1. It is not necessary to measure the inflow of air, provided the flow rate is measured in the exhaust duct. Therefore, oxygen consumption calorimeters are typically open, to avoid an uncontrolled radiant heat flux to the specimen surface from the heated calorimeter walls. The practical implementation of the oxygen consumption technique is not straightforward. Application of Thornton's rule to the combustion system shown in Figure B-1 leads to the following equation for the HRR⁶:

$$\dot{Q} = E(\dot{m}_{O_2}^a - \dot{m}_{O_2}^e) = E(\dot{m}_a Y_{O_2}^a - \dot{m}_e Y_{O_2}^e) \quad [B-1]$$

⁶ Equation B-1 applies at any time during a test. The time dependency of \dot{Q} , \dot{m} and Y is not explicitly shown to simplify the equation.

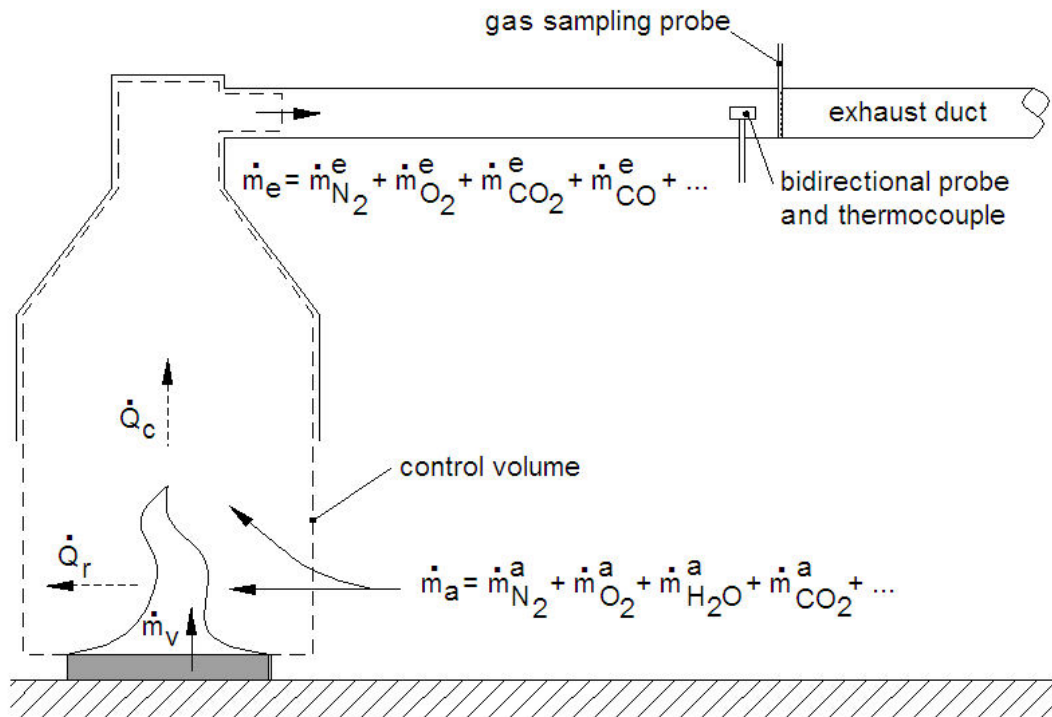


Figure B-1. Schematic of an Oxygen Consumption Calorimeter.

where

$$\dot{Q} = \text{HRR (kW);}$$

$$E = \text{Thornton's constant } (\approx 13.1 \text{ kJ/g});$$

$$\dot{m}_{O_2}^a = \text{Inflow rate of oxygen from ambient environment (g/s);}$$

$$\dot{m}_{O_2}^e = \text{Exhaust flow rate of oxygen (g/s);}$$

$$\dot{m}_a = \text{Inflow rate of ambient air (g/s);}$$

$$Y_{O_2}^a = \text{Ambient oxygen mass fraction } (\approx 0.2303 \text{ g/g in dry air});$$

$$\dot{m}_e = \text{Exhaust flow rate (g/s); and}$$

$$Y_{O_2}^e = \text{Oxygen mass fraction in the exhaust (g/g).}$$

There are several problems with the practical implementation of this equation. First, oxygen analyzers measure the mole (volume) fraction and not the mass fraction of oxygen in a gas sample. Mole fractions can be converted to mass fractions by multiplying the mole fraction with the ratio between the molecular mass of oxygen and the molecular mass of the gas sample. The latter is usually close to the molecular mass of air (≈ 29 g/mol). Second, water vapor is removed from the sample before it passes through a paramagnetic analyzer, so that the resulting mole fraction is on a dry basis. Note that paramagnetic analyzers are the only type of analyzers suitable for oxygen consumption calorimetry (Nussbaum, 1987).

Third, flow meters measure volumetric rather than mass flow rates. The volumetric flow rate in the exhaust duct, normalized to the same pressure and temperature, is usually slightly different from the inflow rate of air because of expansion due to the combustion reactions.

Parker and Janssens solved these problems and developed equations for calculating HRR by oxygen consumption for various applications (Janssens, 1991, Parker, 1984). The equations are a function of the extent of the gas analysis. Figure B-2 shows a common configuration, which includes gas analyzers to measure the concentration of O₂, CO₂, and CO. Detailed derivations of the equations are not repeated here, and can be found in the aforementioned references. However, the resulting equations are quite complicated as illustrated below for the gas analyzer configuration shown in Figure B-2.

$$\dot{Q} = \left[E\phi - (E_{CO} - E) \frac{1 - \phi X_{CO}^{Ae}}{2 X_{O_2}^{Ae}} \right] \frac{\dot{m}_e}{1 + \phi(\alpha - 1)} \frac{M_{O_2}}{M_a} (1 - X_{H_2O}^a) X_{O_2}^{Aa} \quad [B-2a]$$

with

$$\phi = \frac{X_{O_2}^{Aa} (1 - X_{CO_2}^{Ae} - X_{CO}^{Ae}) - X_{O_2}^{Ae} (1 - X_{CO_2}^{Aa})}{(1 - X_{O_2}^{Ae} - X_{CO_2}^{Ae} - X_{CO}^{Ae}) X_{O_2}^{Aa}} \quad [B-2b]$$

where

- ϕ = Oxygen depletion factor (-);
- E_{CO} = Heat released per mass unit of O₂ consumed for combustion of CO (kJ/g);
- X_{CO}^{Ae} = Measured mole fraction of carbon monoxide in the exhaust flow (-);
- $X_{O_2}^{Ae}$ = Measured mole fraction of oxygen in the exhaust flow (-);
- \dot{m}_e = Mass flow rate in the exhaust duct of the calorimeter (g/s);
- α = Volumetric expansion factor (-);
- M_{O_2} = Molecular mass of oxygen (32 g/mol);
- M_a = Molecular mass of the combustion air (29 g/mol for dry air);
- $X_{H_2O}^a$ = Actual mole fraction of water vapor in the combustion air (-);
- $X_{O_2}^{Aa}$ = Measured mole fraction of oxygen in the combustion air (-);
- $X_{CO_2}^{Ae}$ = Measured mole fraction of carbon dioxide in the exhaust flow (-); and
- $X_{CO_2}^{Aa}$ = Measured mole fraction of carbon dioxide in the combustion air (-).

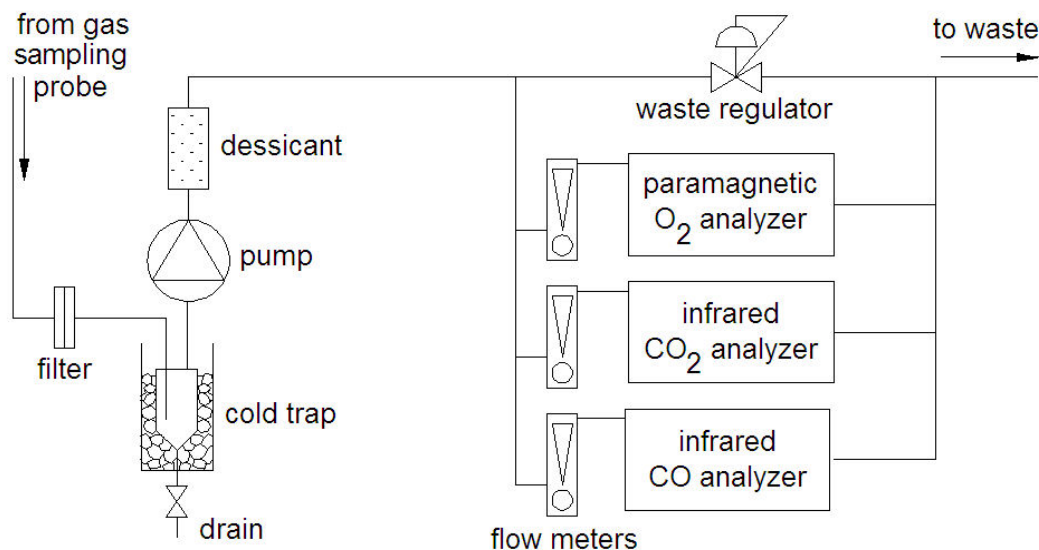


Figure B-2. Common Gas Sampling Train for Oxygen Consumption Calorimetry.

Due to the combustion chemistry, the number of moles in the fraction of the air fully depleted of its oxygen is replaced by an equal or larger number of moles of combustion products in the exhaust flow. The volumetric expansion factor, α , is equal to the ratio of these two molar quantities. If the fuel composition is unknown, as is often the case, an average value has to be used for α . Complete combustion of carbon in dry air results in $\alpha = 1$. If the fuel is pure hydrogen, α is equal to 1.21. A recommended average value for α is; therefore, 1.105. $X_{\text{H}_2\text{O}}^a$ can be calculated from the relative humidity and temperature in the laboratory. Typically it is of the order of 1% or 2% in a temperature-controlled laboratory⁷. $X_{\text{CO}_2}^A$ in dry air is approximately 390 ppm⁸. Note that the symbols for oxygen mole fraction measured in the combustion air (prior to a test) and the exhaust flow include a superscripted A. This is to make a distinction between the actual and measured mole fractions of oxygen, since the latter are for a dry gas sample.

Equation 2-4a is expected to be accurate to within $\pm 8\%$ provided all carbon is converted to CO₂ or CO. The error might be larger if soot production and/or the amount of unburnt fuel is considerable, or if a significant amount of combustion products consist of species other than CO₂ or H₂O (e.g. HCl). The error is partly due to the uncertainty of E and

7 For example, air at 20°C, 1013 mbar and a relative humidity of 50% contains 1.2 % of water vapor by volume.

8 The concentration of carbon dioxide in the atmosphere is measured at the Mauna Loa Observatory in Hawaii. The average concentration measured in 2010 was 390 ppm. The concentration varies annually by about 3-9 ppm, but the annual average has steadily increased by about 74 ppm since 1958, when the measurements were first recorded.

α . If more exact values are available, accuracy can be improved by using those instead of the generic values of 13.1 kJ/g and 1.105.

B.1.2 THE FURNITURE CALORIMETER

It is very hard to determine the burning behavior of upholstered furniture on the basis of the fire characteristics of the padding, fabric, and framing materials and to account for the geometry and configuration of the furniture and how it is ignited. It is much easier to test the entire furniture item. The calorimeter described in the section was developed for this purpose.

A furniture calorimeter consists of a weighing platform that is located on the floor of the laboratory, beneath a hood connected to an instrumented exhaust duct (see Figure B-3). The object is placed on the platform and ignited with the specified ignition source. The products of combustion are collected in the hood and extracted through the exhaust duct. Measurements of oxygen concentration, flow rate and light transmission in the exhaust duct are used to determine the HRR and smoke production rate from the object as a function of time.

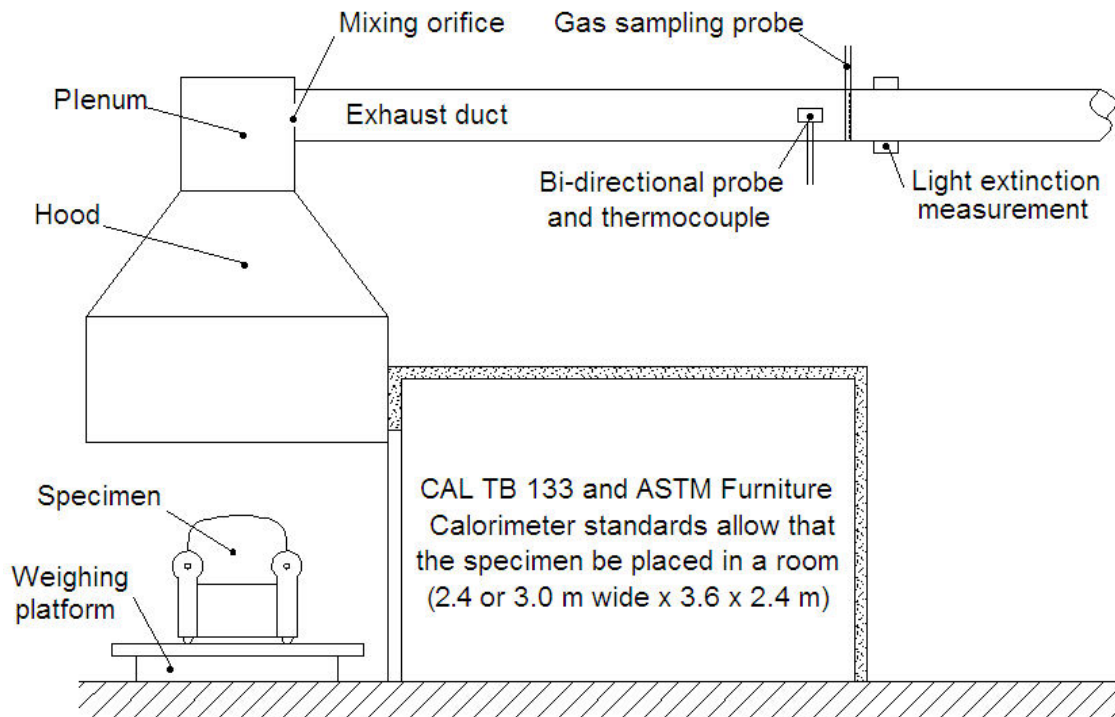


Figure B-3. Schematic of the Furniture Calorimeter.

Furniture calorimeters were developed in the 1980s in several laboratories to obtain this kind of data (Ames and Rogers, 1990, Babrauskas, et al., 1982, Sundström, 1987). The first furniture calorimeter test standard was published in 1987 in the Nordic countries as NT Fire 032. Furniture calorimeter test standards have been developed by ASTM for chairs, National Institute of Justice, OJP

mattresses, and stacked chairs. The corresponding designations are ASTM E 1537, ASTM E 1590, and ASTM E 1822, respectively. The California Bureau of Home Furnishings and Thermal Insulation developed California Technical Bulletins (CA TB) 133 and 603. These documents describe fire test procedures to qualify seating furniture and mattresses, respectively, for use in public occupancies in California. CA TB 603 has been superseded by the Federal CPSC standard 16 CFR 1633. The primary difference between the various chair and mattress tests is the ignition source. ISO 24473 is an international standard describing a large-scale open calorimeter that can be used to measure HRR from upholstered furniture.

The square opening of the hood of the furniture calorimeters listed in the previous paragraph is typically 3×3 m and the bottom of the hood is at 2.4–3 m above the floor of the laboratory. Combustion products and excess air are extracted through the 0.4-m diameter exhaust duct at a rate of up to $3.5 \text{ m}^3/\text{s}$. As a result the maximum capacity of these calorimeters is of the order of 1 MW.

The HRR of an upholstered sofa can easily exceed 1 MW. To measure HRRs of this magnitude, a scaled-up version of the hood and exhaust duct shown in Figure B-3 is needed. To handle fires up to 10 MW in size for a short duration, the hood must be at least 6×6 m in size or 6 m in diameter and is typically located at 6.5 m above the floor of the laboratory or higher. The fan must be capable of extracting combustion products through a 0.9-m diameter exhaust duct at a minimum rate of $15 \text{ m}^3/\text{s}$. A larger calorimeter and higher fan capacity are needed to handle more severe experimental fires. Measuring HRR from multi-megawatt experimental fires presents special challenges that are not observed in smaller calorimeters. Guidelines for addressing these challenges can be found in ASTM E 2067 and in the literature (Cooper, 1994, Newman, Wieczorek and Troup, 2005).

B.1.3 THE CONE CALORIMETER

The Cone Calorimeter was developed at the National Bureau of Standards (NBS), currently the National Institute of Standards and Technology (NIST) by Dr. Vytenis Babrauskas in the early 1980s (Babrauskas, 1984a). It is presently the most commonly used bench-scale calorimeter. A bibliography compiled by the inventor indicates that over 1,000 papers on Cone Calorimeter studies had been published at the end of 2002. The apparatus and test procedure are standardized in the United States as ASTM E 1354 and

NFPA 271 and internationally as ISO 5660 Parts 1 and 2. A schematic of the apparatus is shown in Figure B-4.

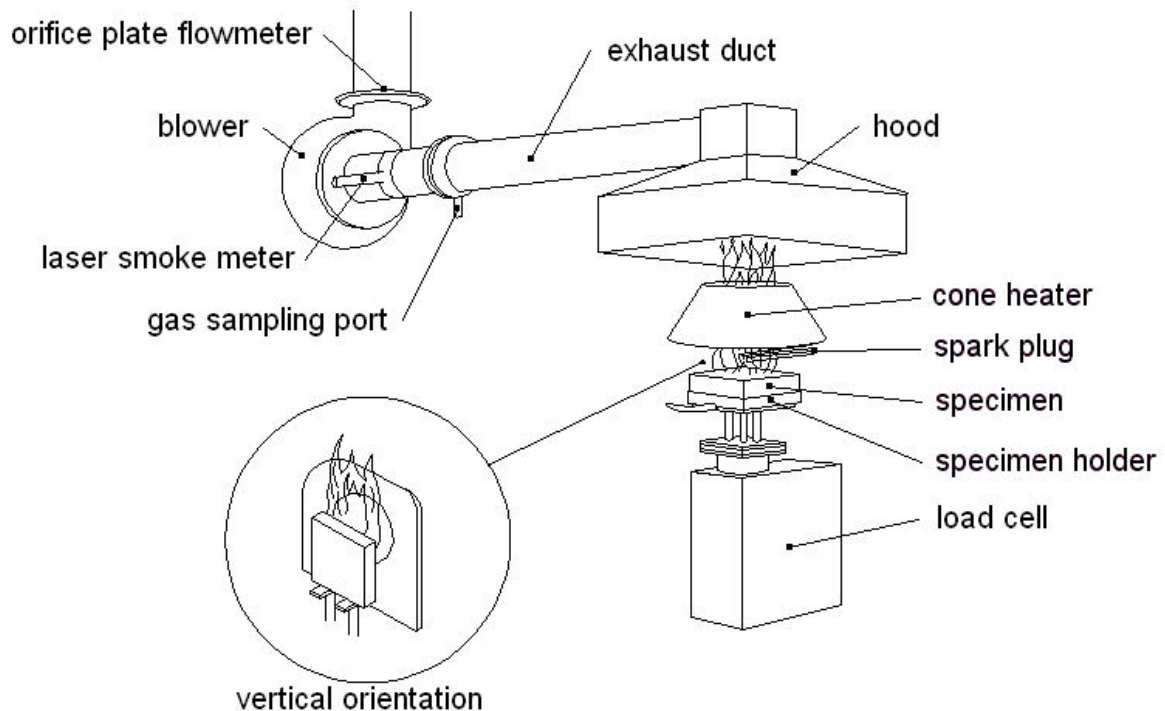


Figure B-4. Schematic of the Cone Calorimeter.

A square specimen of 100×100 mm is exposed to the radiant flux of an electric heater. The heater has the shape of a truncated cone (hence the name of the instrument) and is capable of providing heat fluxes to the specimen in the range of $10\text{--}110 \text{ kW/m}^2$. Prior to testing, the heater temperature is set at the appropriate value resulting in the desired heat flux. At the start of a test, the specimen in the appropriate holder and the retainer frame (if used) is placed on the load cell, which is located below the heater. An electric spark is used to ignite the pyrolysis products released by the specimen. As soon as sustained flaming is observed, the electric spark igniter is removed. All combustion products and entrained air are collected by an exhaust hood. At a sufficient distance downstream from a mixing orifice, a gas sample is taken and analyzed for oxygen concentration. Measurements of the gas temperature and differential pressure across the orifice plate are used for calculating the mass flow rate of the exhaust gases. The heat released rate can be determined on the basis of the oxygen depletion and the mass flow rate in the exhaust duct. The HRR is expressed per unit area initially exposed to the heater, units are kW/m^2 .

Most Cone Calorimeters include instrumentation for measuring light extinction in the exhaust duct, using a laser light source, described in ASTM E 1354 and ISO 5660-2. Instrumentation to measure concentrations of carbon dioxide and carbon monoxide are commonly added. Some laboratories have used a modified version of the standard apparatus to conduct studies in vitiated or oxygen enriched atmospheres (Babrauskas, Twilley, Janssens and Yusa, 1992, Hshieh and Buch, 1997, Leonard, Bowditch and Dowling, 2000).

Note that ASTM developed an applications standard specifically for measuring the HRR of furniture upholstery. This standard, ASTM E 1474, is based on the main Cone Calorimeter standard ASTM E 1354, but provides detailed instructions for the preparation of fabric-padding specimens and specifies that tests be conducted in triplicate at a heat flux of 35 kW/m^2 . The protocol described in ASTM E 1474 is based on that developed in the European CBUF project (Sundström, 1996).

B.1.4 THE MICROSCALE COMBUSTION CALORIMETER

The U.S. Federal Aviation Administration developed the Microscale Combustion Calorimeter to assist with the development of fire-resistant polymers for use in commercial passenger aircraft. A schematic of this micro-scale calorimeter is shown in Figure B-5. The apparatus and test procedure are described in ASTM D 7309.

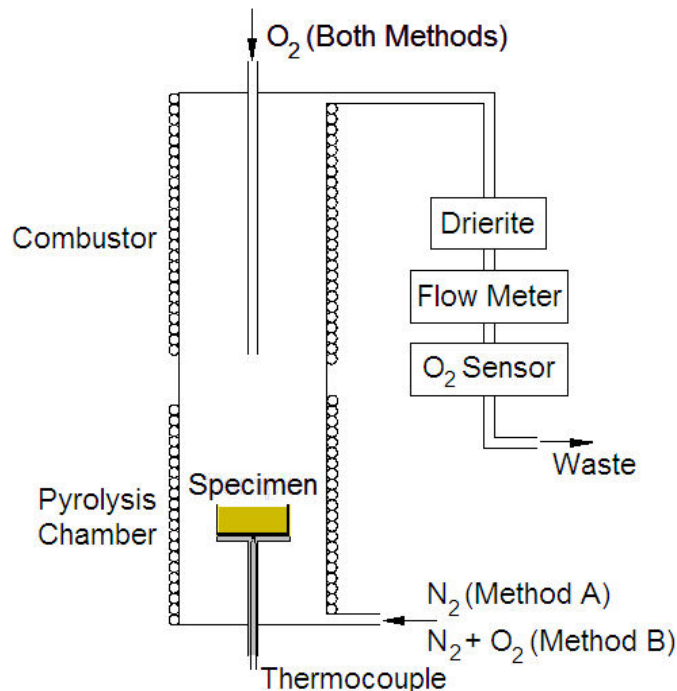


Figure B-5. Schematic of the Microscale Combustion Calorimeter.

A 1–10 mg specimen (typically between 2–5 mg) is heated at a constant rate between 0.2–2 K/s in the lower chamber. Decomposition can take place in nitrogen (Method A) or in a mixture of nitrogen and oxygen (Method B). When Method A is used, char-forming specimens do not decompose completely and leave a solid residue. In this case the volatiles are mixed with a metered supply of oxygen in the combustor to obtain the HRR of the volatiles. When Method B is used, the specimen is completely consumed with the exception of any non-combustible components. The THR in this case is comparable to that measured in an oxygen bomb calorimeter. The temperature of the combustor is set at approximately 900°C to ensure that all specimen gases are completely oxidized.

Oxygen consumption calorimetry with $E = 13.1$ kJ/g is used to measure HRR as a function of time. The specific HRR, $\dot{Q}(t)$, in W/g is equal to the HRR divided by the initial specimen mass, m_o . The following five parameters are calculated when Method A is used:

- The heat release capacity $\eta_c \equiv \dot{Q}_{\max}/\beta$ in J/g·K, where \dot{Q}_{\max} is the maximum value of $\dot{Q}(t)$ and β is the heating rate in K/s;
- The heat release temperature T_{\max} in K as the pyrolysis chamber temperature at which $\dot{Q}(t) = \dot{Q}_{\max}$;
- The specific heat release h_c in J/g as the area under the $\dot{Q}(t)$ curve;
- The pyrolysis residue $Y_p \equiv m_p/m_o$ in g/g, where m_p is the residual mass of the specimen at the end of the test; and
- The specific heat of combustion of the specimen gases $h_{c,\text{gas}} \equiv h_c/(1-Y_p)$ in J/g.

For method B only three parameters are calculated:

- The combustion temperature T_{\max} in K as the pyrolysis chamber temperature at which the specific HRR is a maximum, i.e., $\dot{Q}(t) = \dot{Q}_{\max}$;
- The combustion residue $Y_c \equiv m_c/m_o$ in g/g, where m_c is the residual mass of the specimen at the end of the test; and
- The net calorific value h_c^0 in J/g as the area under the $\dot{Q}(t)$ curve.

The thermal combustion properties measured in the test are related to flammability characteristics of the material (Lyon, 2000, 2004, Lyon and Janssens, 2005, Lyon, Walters

and Stoliarov, 2006, Lyon, Walters, Safronava and Stoliarov, 2009). For example, the heat release temperature from Method A approximates the surface temperature at ignition. The net calorific value from Method B approximates the net heat of combustion measured in an oxygen bomb calorimeter. Since the test specimens are very small, the Microscale Combustion Calorimeter is a useful device to obtain information about the ignition and HRR characteristics when the amount of available material is insufficient for Cone Calorimeter testing.

B.2 UNCERTAINTY OF HRR MEASUREMENTS

The objective of a measurement is to determine the value of the measurand, i.e. the physical quantity that needs to be measured. The value of the measurand is generally not obtained from a direct measurement, but is determined as a function (f) from N input quantities X_1, X_2, \dots, X_N :

$$Y = f(X_1, X_2, \dots, X_N) \quad [B-3]$$

where

Y = True value of the measurand;

f = Functional relationship between measurand and input quantities; and

X_i = True values of the input quantities ($i = 1 \dots N$).

The input quantities may be categorized as:

- Quantities whose values and uncertainties are directly determined from single or repeated observation; or
- Quantities whose values and uncertainties are brought into the measurement from external sources such as reference data obtained from handbooks.

An estimate of the value of the measurand, y , is obtained from Equation B-3 using input estimates x_1, x_2, \dots, x_N for the values of the N input quantities:

$$y = f(x_1, x_2, \dots, x_N) \quad [B-4]$$

The standard uncertainty of y is obtained by appropriately combining the standard uncertainties of the input estimates x_1, x_2, \dots, x_N . If all input quantities are independent, the combined standard uncertainty of y is given by:

$$u_c(y) = \sqrt{\sum_{i=1}^N \left[\left. \frac{\partial f}{\partial X_i} \right|_{x_i} \right]^2} u^2(x_i) \equiv \sqrt{\sum_{i=1}^N [c_i u(x_i)]^2} \quad [\text{B-5}]$$

where

u = Standard uncertainty;

u_c = Combined standard uncertainty; and

c_i = Sensitivity coefficients.

The standard uncertainty of an input estimate x_i is obtained from the distribution of possible values of the input quantity X_i . There are two types of evaluations depending on how the distribution of possible values is obtained.

- A type A evaluation of the standard uncertainty of x_i is based on the dispersion of its frequency distribution, which is estimated from a series of n repeated observations $x_{i,k}$ ($k = 1 \dots n$).

$$u(x_i) \approx \sqrt{s^2(\bar{x}_i)} = \sqrt{\frac{s^2(\bar{x}_i)}{n}} = \sqrt{\frac{\sum_{k=1}^n (x_{i,k} - \bar{x}_i)^2}{n(n-1)}} \quad [\text{B-6}]$$

- A type B evaluation of standard uncertainty of x_i is not based on repeated measurements but on an a priori frequency distribution. In this case the uncertainty is determined from previous measurements, experience, or general knowledge, manufacturer specifications, data provided in calibration certificates, uncertainties assigned to reference data taken from handbooks, etc.

Equation B-5 is referred to as the law of propagation of uncertainty and based on a first-order Taylor series approximation of $Y = f(X_1, X_2, \dots, X_N)$. When the nonlinearity of f is significant, higher-order terms must be included. When the input quantities are correlated, Equation B-5 must be revised to include the covariance terms. The combined standard uncertainty of y is then calculated from:

$$u_c(y) = \sqrt{\sum_{i=1}^N [c_i u(x_i)]^2 + 2 \sum_{i=1}^{N-1} \sum_{j=i+1}^N c_i c_j u(x_i) u(x_j) r(x_i, x_j)} \quad [\text{B-7}]$$

where

$r(x_i, x_j)$ = Estimated correlation coefficient between X_i and X_{ij} .

Since the values of the input quantities are not known, the correlation coefficient is estimated on the basis of the measured values of the input quantities. The combined standard uncertainty in Equations B-5 and B-7 is usually multiplied by a coverage factor to raise the confidence level, to obtain the “expanded” uncertainty. A multiplier of 2 is often used, which corresponds to a confidence level of approximately 95%.

Equations B-5 and B-7 can be used to calculate the uncertainty of HRR measurement based on oxygen consumption calorimetry. Equations B-2a and B-2b provide the functional relationship between the measurand (HRR) and the input quantities. Assuming the mass flow rate in the exhaust duct is calculated from the differential pressure and temperature at a bi-directional probe, the output and input quantities are defined as follows:

$$Y \equiv \dot{Q}, X_1 \equiv E, X_2 \equiv X_{O_2}^{Ae}, X_3 \equiv X_{CO_2}^{Ae}, X_4 \equiv X_{CO}^{Ae}, X_5 \equiv C, X_6 \equiv \Delta P, X_7 \equiv T_e, X_8 \equiv \alpha \quad [\text{B-8}]$$

C is the calibration coefficient, which relates the mass flow rate in the exhaust duct to the differential pressure and gas temperature measurements. Note that in a test \dot{Q} is calculated as a function of time based on the input quantities measured at discrete time intervals Δt . The uncertainty of \dot{Q} measured at each time interval is estimated from Equation B-5 or B-7. Dahlberg used this approach to determine the uncertainty of HRR measured in the multi-megawatt calorimeter at SP and reported values of $\pm 7\%$ and $\pm 12\%$ depending on the use of the CO correction in the HRR calculations (Dahlberg, 1994). A more detailed discussion of methods for calculating measurement uncertainty in fire tests can be found in ASTM E 2536.

APPENDIX C

UPHOLSTERED FURNITURE BURNING RATE CORRELATIONS AND MODELS

(CONSISTING OF 11 PAGES)

C.1 INTRODUCTION

A literature review was conducted to identify correlations and models to estimate the heat release rate (HRR) of upholstered furniture on the basis of small scale fire test data of the furniture components and generic characteristics of the item. Three models were found to be most promising and were selected for this work. These models are described below. The use of the field fire model Fire Dynamics Simulator (FDS) to better account for the effect of the exact location of the ignition source on flame spread over the seating surface is also discussed.

C.2 MODELS DEVELOPED BY BABRAUSKAS

Based on the results of furniture flammability studies conducted at NIST in the early 1980s, Babrauskas observed that many upholstered furniture items have HRR versus time graphs that are triangular in shape. He found that the area of the triangular part of the curve on average accounts for 63% of the total heat released (THR) by furniture items with a combustible frame. This is because the triangular part of the curve does not include the “tail”, which is primarily the HRR of the frame. Babrauskas also found that the triangular part accounted on average for 91% of the THR by furniture items with a non-combustible frame. These observations formed the basis for a simple model to predict PHRR (top of the triangle) and burning time (triangle base width) on the basis of generic characteristics of the furniture item (Babrauskas, et al., 1986). According to the model, PHRR can be estimated from

$$\dot{Q}_{\max} = 210 [\text{FF}][\text{PF}][\text{CM}][\text{FC}][\text{SF}] \quad [\text{C-1}]$$

where

$$\dot{Q}_{\max} = \text{PHRR (kW)};$$

$$\text{FF} = \text{Fabric factor};$$

1.0 for thermoplastic fabrics (e.g. polyolefin)

0.4 for cellulosic fabrics (e.g. cotton)

0.25 for PVC or polyurethane film-type coverings

PF = Padding factor;

1.0 for polyurethane foam, latex foam, or mixed materials

0.4 for cotton batting or neoprene foam

CM = Combustible mass (kg);

FC = Frame combustibility factor.

1.66 for non-combustible frames

0.58 for melting plastic

0.30 for wood

0.18 for charring plastic

SF = Style factor; and

1.5 for ornate convoluted shapes

1.2–1.3 for intermediate shapes

1.0 for plain, primarily rectilinear construction

The triangle base width (burn time) is estimated by

$$t_b = \frac{[FM][CM]\Delta h_c}{\dot{Q}_{\max}} \quad [C-2]$$

where

t_b = Burn time (s);

FM = Frame material factor; and

1.8 for metal or plastic frames

1.3 for wood frames

Δh_c = Effective heat of combustion for the fuel item (kJ/kg).

The advantage of this model is that the HRR can be estimated based on some generic characteristics, the combustible mass and the effective heat of combustion. Only a few grams of material are needed to measure the latter in an oxygen bomb calorimeter or the Microflow

Combustion Calorimeter. The heat of combustion can also be estimated with reasonable accuracy from tabulated values (Babrauskas, 2008a).

In the same paper, Babrauskas and Walton presented a second model that requires that a fabric-covered padding specimen be tested in the Cone Calorimeter at 25 kW/m². The PHRR of the furniture item is estimated from

$$\dot{Q}_{\max} = \dot{Q}_{180}'' [CM][FC][SF] \quad [C-3]$$

where

$$\dot{Q}_{180}'' = \text{3-min average HRR at 25 kW/m}^2 \text{ (kW/m}^2\text{)}.$$

The definitions of the combustible mass [CM], frame combustibility factor [FC], and style factor [SF] are identical as in Equation C-1. The burn time t_b is again calculated according to Equation C-2.

C.3 CBUF I MODEL

Perhaps the most comprehensive research program on flammability of upholstered furniture was conducted in Europe in the early to mid-1990s. The program was referred to as the CBUF program (Sundström, 1996). The CBUF program developed three models to predict the HRR versus time curve of upholstered furniture. The models were validated with an extensive database of furniture calorimeter measurements. The CBUF I model is described in the SFPE handbook “Heat Release Rates” chapter (Babrauskas, 2008a). A description of this model follows.

The CBUF I model is based on the observation from experiments that the HRR versus time curve of an upholstered chair or sofa is often approximately triangular in shape. The model predicts the PHRR, time from ignition (defined as the moment when the HRR first reaches 50 kW) to the PHRR and THR. A triangular HRR versus time curve can then be constructed on the basis of these three parameters as shown in Figure C-1. The triangle can be shifted along the time axis to account for ignition delays.

The PHRR is determined on the basis of two correlating variables, x_1 and x_2 , which are defined as follows:

$$x_1 = (m_{\text{soft}})^{1.25} (\text{style factor } A) (\dot{Q}_{\text{peak}}'' + \dot{Q}_{300}'')^{0.7} (1.5 + t_{\text{ig}})^{-0.7} \quad [C-4a]$$

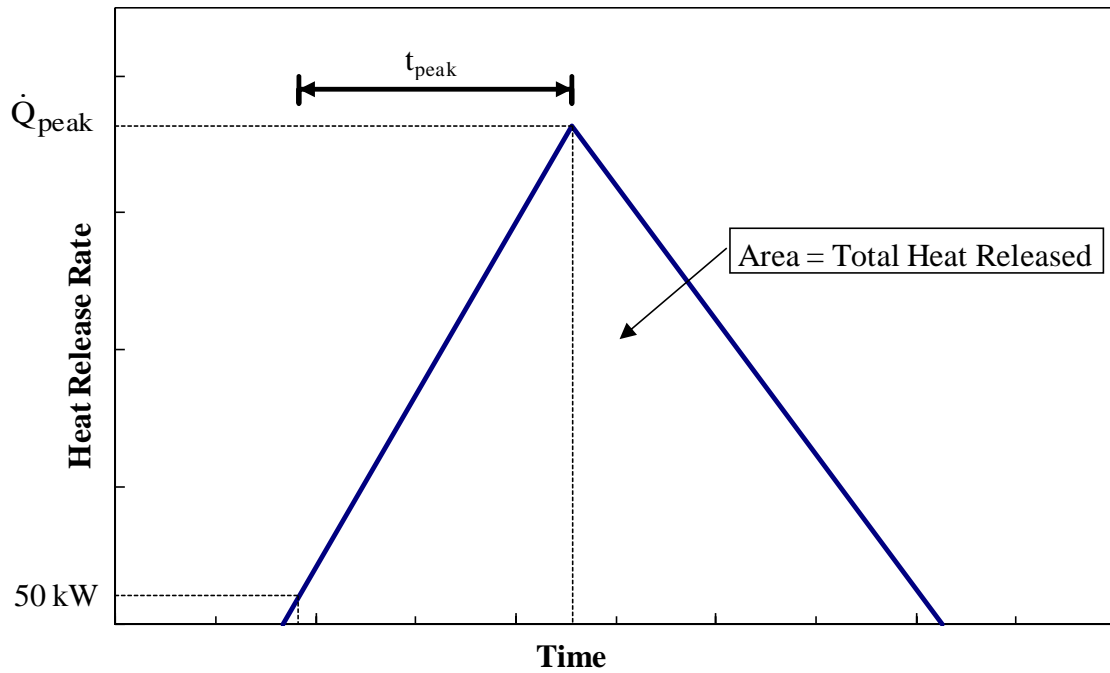


Figure C-1. CBUF I Triangular HRR versus Time Curve.

and

$$x_2 = 880 + 500(m_{\text{soft}})^{0.7}(\text{style factor A}) \left(\frac{\Delta h_{c,\text{eff}}}{Q_{\text{tot}}''} \right)^{1.4} \quad [\text{C-4b}]$$

where

m_{soft} = Total mass of combustible soft parts, i.e., padding and fabric (kg);

\dot{Q}_{peak}'' = PHRR of the padding-fabric combination measured in the Cone Calorimeter at a heat flux of 35 kW/m² (kW/m²);

\dot{Q}_{300}'' = Average HRR over the first 5 min following ignition of the padding-fabric in the Cone Calorimeter at 35 kW/m² (kW/m²);

t_{ig} = Ignition time of the padding-fabric combination measured in the Cone Calorimeter at a heat flux of 35 kW/m² (s);

$\Delta h_{c,\text{eff}}$ = Test-average effective heat of combustion of the padding-fabric combination in the Cone Calorimeter at 35 kW/m² (MJ/kg); and

Q_{tot}'' = THR by the padding-fabric combination measured in the Cone Calorimeter at a heat flux of 35 kW/m² (kW/m²);

The style factor A varies between 0.6–1.0, as shown in Table C-1.

Table C-1. Style Factors used in the CBUF I Model.

Type of Furniture	Style Factor A	Style Factor B
Armchair, fully upholstered, average amount of padding	1.0	1.0
2-Seat Sofa	1.0	0.8
3-Seat Sofa	0.8	0.8
Armchair, fully upholstered, highly padded	0.9	0.9
Armchair, small amount of padding	1.2	0.8
Wingback chair	1.0	2.5
Sofa-bed (convertible)	0.6	0.75
Armchair, fully upholstered, metal frame	1.0	0.8
Armless chair, seat and back cushions only	1.0	0.75
Two-seater, armless, seat and back cushions only	1.0	1.0

The PHRR of the furniture item, \dot{Q}_{peak}'' , in kW now follows from:

If $x_1 > 115$ or ($Q_{\text{tot}}'' > 70$ and $x_1 > 40$) then

$$\dot{Q}_{\text{peak}} = x_2 \quad [\text{C-5a}]$$

else if $x_1 < 56$ then

$$\dot{Q}_{\text{peak}} = 14.4 x_1 \quad [\text{C-5b}]$$

else

$$\dot{Q}_{\text{peak}} = 600 + 3.77 x_1 \quad [\text{C-5c}]$$

The THR, Q_{tot} , in MJ is estimated from

$$Q_{\text{tot}} = 0.9 m_{\text{soft}} \Delta h_{\text{c,eff}} + 2.1(m_{\text{comb,tot}} - m_{\text{soft}}) \quad [\text{C-6}]$$

where

$$m_{\text{comb,tot}} = \text{Total combustible mass of the item (kg).}$$

The time between ignition (defined as when the HRR first reaches 50 kW) and when the PHRR occurs, t_{peak} , in s is given by:

$$t_{\text{peak}} = 30 + 4900(\text{style factor B})(m_{\text{soft}})^{0.3}(\dot{Q}_{\text{peak \#2}}'' \cdot \dot{Q}_{\text{trough}}'')^{-0.5} (t_{\text{peak \#1}} + 200)^{0.2} \quad [\text{C-7}]$$

where

$\dot{Q}''_{\text{peak}\#2}$ = Second PHRR of the padding-fabric combination measured in the Cone Calorimeter at a heat flux of 35 kW/m^2 (kW/m^2);

$\dot{Q}''_{\text{trough}}$ = Lowest HRR of the padding-fabric combination between the two peaks measured in the Cone Calorimeter at 35 kW/m^2 (kW/m^2); and

$t_{\text{peak}\#1}$ = Time when the first PHRR is measured for the padding-fabric combination in the Cone Calorimeter at a heat flux of 35 kW/m^2 (s).

Figure C-2 shows how $\dot{Q}''_{\text{peak}\#2}$ and $\dot{Q}''_{\text{trough}}$ are determined. Style factor B varies between 0.75 and 2.5. Values for different types of furniture are given in Table C-1.

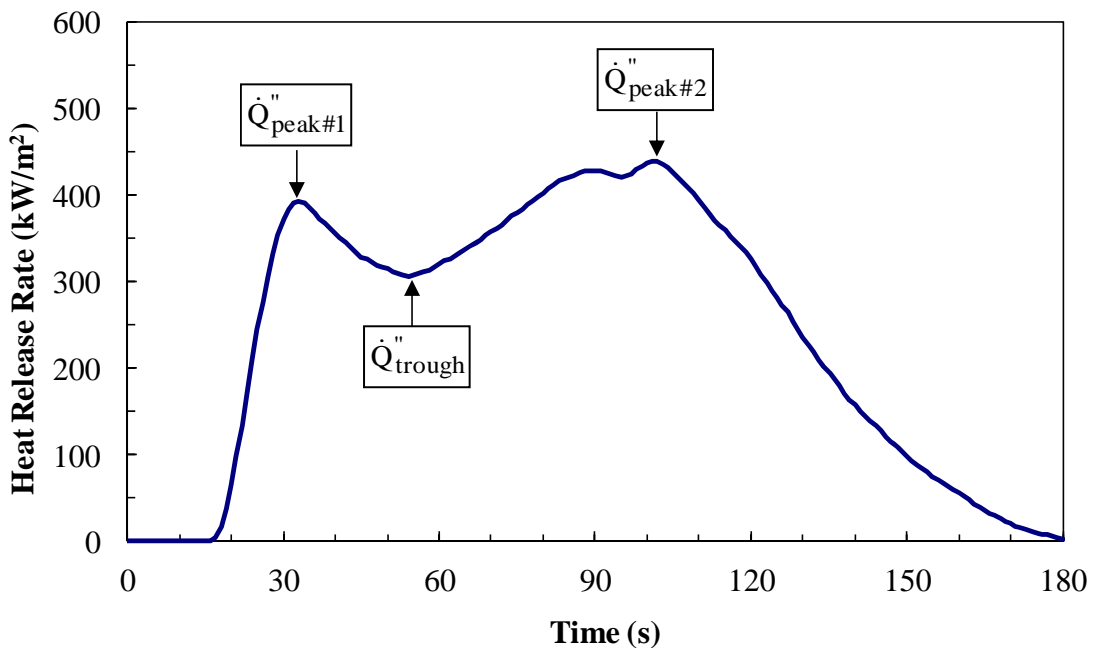


Figure C-2. Cone Calorimeter HRR of Padding-Fabric Combination.

C.4 FDS MODEL

The field fire model, FDS, was used to predict the full-scale flame spread behavior of each test based on measured cone calorimeter data. The average HRR curve from the Cone Calorimeter tests (at 35 kW/m^2) was input along with an ignition temperature that was determined from ignition data. The FDS model calculated the rate of flame spread (and resulting full-scale HRR) by activating the Cone Calorimeter HRR curve on each computational cell based on its local cell temperature, which is a function of the incident heat

flux from the flame. The resulting total HRR from FDS was compared to the full-scale HRR measurements.

The four sides of the domain and the top of the domain were specified as open boundary conditions, which allows for energy and mass to exit the domain and ambient air to enter the domain. A time of 900 s was used for each simulation case.

Figure C-3 shows a representation of the flame spread process on a furniture specimen in FDS. The surface of the furniture item is subdivided into a number of relatively small cells. FDS calculates the surface temperature of each cell and assumes that a cell starts to release combustible vapors at a user-specified rate when the surface temperature reaches the user-specified ignition temperature of the material. The cell(s) exposed to the ignition source is (are) the first to ignite. Flames spread when the surface temperature of adjacent cells reach the ignition temperature. The different colors in Figure C-3 are an indication of the mass loss rate of each cell. The red cell represents the small ignition source used in this case, the green cells indicate the cells that are injecting combustible vapors into the domain, and the blue cells have not yet reached the ignition temperature

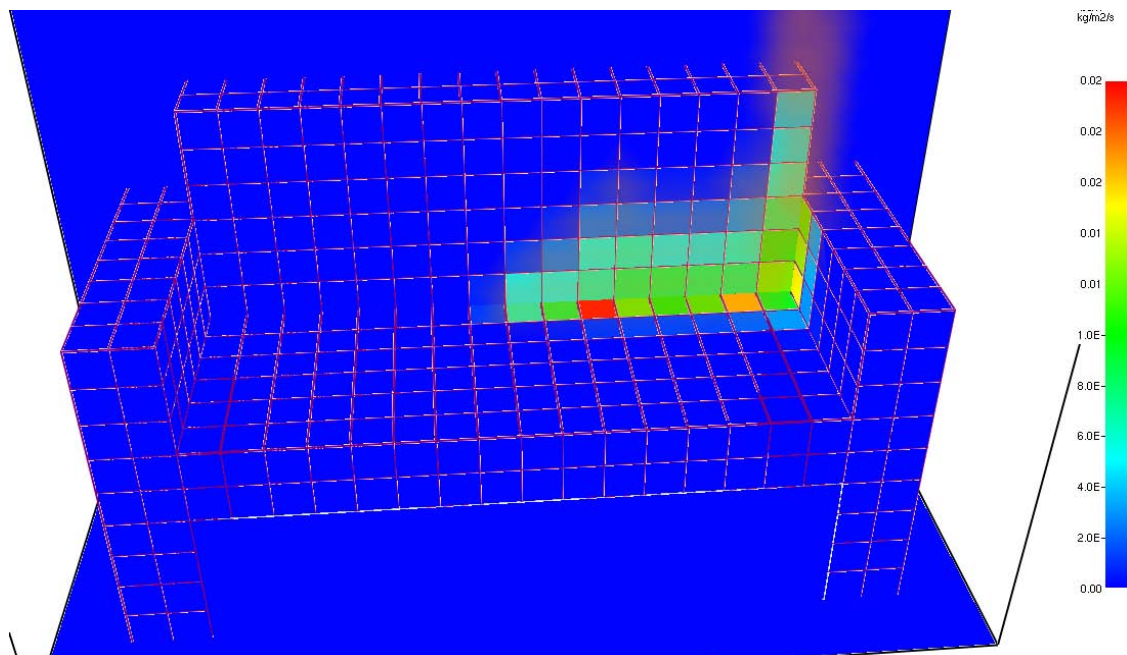


Figure C-3. Flame Spread Process in FDS using Cone Calorimeter Data.

The inputs to the FDS spread model are described in the following subsections.

C.4.1 GEOMETRY

For the mockup tests, the simplified furniture item geometry was input into the model using the measurements provided in the lab notebooks. For the used furniture tests, the measurements of the furniture specimens were estimated by using photographs of the specimens with a gridded background. Four measurements were used to characterize each specimen: the seat width, seat depth, back height, and arm height. The FDS geometry was then created for each specimen using the specified measurements. Figure C-4 shows the FDS geometry of a single furniture item (colors have been added for emphasis to indicate the different obstructions).

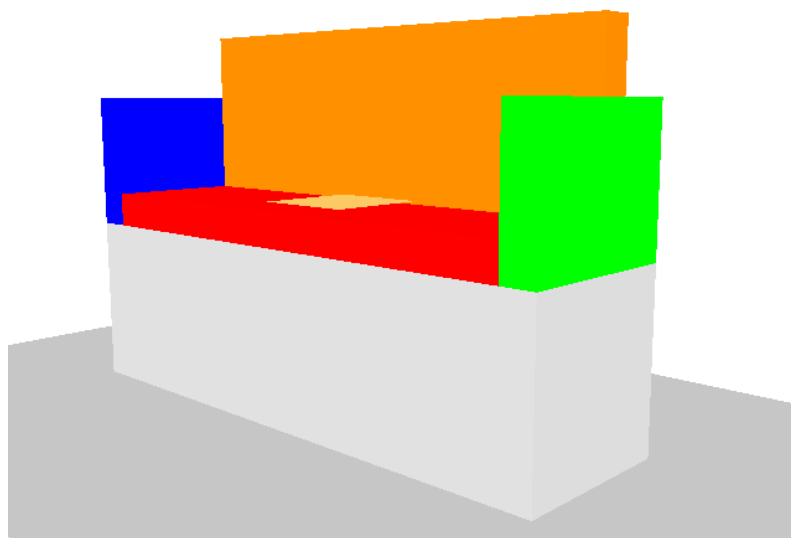


Figure C-4. FDS Geometry of a Mockup 3-Seat Sofa.

C.4.2 DOMAIN AND GRID SELECTION

For all of the cases, the size of the domain was 3 (length) \times 2 (width) \times 3 m (height). The cell size was 10 cm on each side. For a 500-kW fire, the characteristic fire diameter (D^*) is 0.727, which results in a D^*/dx ratio of 7.3. This value is within the range of D^*/dx values used in NUREG-1824 (Verification and Validation of Selected Fire Models for Nuclear Power Plant Applications), which used D^*/dx values between 4 and 16.

For fire sizes such as gas burners and small flames used as an ignition source, the amount of grid cells required to accurately resolve the flame becomes on the order of a few mm, which exponentially increases the required computational expense.

For this study, a grid cell size of 10 cm was used in all of the cases because thousands of simulations were performed. A few simulations were performed with a finer grid (5 cm) to see if this would improve the flame spread predictions. Since the predicted HRR was

essentially the same as for the coarser grid but the run time was much longer, it was decided not to use the finer grid. The gas burner and gasoline ignition source were fairly resolved for the purposes of this study, but the size of the small flame (BS 5852 Source #1 and #2) had to be increased in FDS to cause ignition because of the smearing effect of a small flame on a coarse grid. More details on ignition are described in the following subsections.

C.4.3 GAS PHASE REACTION PARAMETERS

The gas phase reaction used in the FDS models was either that for polyurethane or polyester, depending on the specimen. The gas phase reaction parameter values that were used can be found in Section A.4.2.

C.4.4 SOLID PHASE PARAMETERS

The solid phase parameters were input into each FDS simulation to correspond to the test that was being simulated. The required inputs for this ignition-temperature-driven flame spread scenario were the thermal conductivity, density, and specific heat of the fabric/padding (assumed to be one material/surface) as well as the ignition temperature and HRR per unit area (or HRRPUA in kW/m²) of the fabric/padding combination.

The specific heat was input as 1 kJ/kg·K, the density of the material was calculated from the measured mass of the Cone Calorimeter specimens, and the thermal conductivity and ignition temperature were input based on the calculations from the Cone Calorimeter tests at multiple heat fluxes. The ignition temperature was determined using the following energy balance on the surface of the sample:

$$\varepsilon \dot{q}_{cr}'' = h_c(T_{ig} - T_{\infty}) + \varepsilon \sigma(T_{ig}^4 - T_{\infty}^4) \quad [C-8]$$

The critical heat flux, \dot{q}_{cr}'' , was determined from a linear regression (assuming thermally-thick behavior) on the Cone Calorimeter ignition times at 20, 35, and 50 kW/m². The h_c value was used as 12 W/m²·K, and 20 °C was used as the ambient temperature.

The lumped $k\rho c$ value was determined from the slope of the linear regression procedure described above by using the following equation:

$$k\rho c = \frac{4 h_{ig}^2}{\pi * \text{slope}^2} \quad [C-9]$$

After the lumped $k\rho c$ value was calculated, the thermal conductivity (k) was determined using the assumed specific heat (c) and measured density (ρ) of each sample.

C.4.5 IGNITION SOURCES

Two types of ignition sources were modeled in FDS, a large ignition source (accelerant or large gas burner flame) and a small ignition source (BS 5852 Source #1 or #2).

The small ignition flame (~80 W) was not resolved on the 10-cm grid, thus a 10-kW flame was used. The effect of this larger ignition source was that the flame spread during the initial period was not modeled, but the PHRR predictions should be accurately resolved. The small ignition source (used as 10 kW) was active for 20 s at the beginning of the simulation using a burner in FDS, after which the small burner was deactivated. The small ignition source was placed in the center or corner of the furniture item, depending on the test key.

The large ignition source was modeled as a 30 × 30-cm burner in FDS in the center cushion with a HRR of 20 kW for a period of 80 s, after which the burner was deactivated. In one special case (SOM123CS1), the large burner was placed on the side cushion, which was the location of the gas burner in that particular test.

C.4.6 CONE CALORIMETER HRR RAMP

Based on the test code for each furniture item, the complete HRR vs. time curve from the Cone Calorimeter was input into FDS as a ramp function, and the HRRPUA was specified using the highest of the triplicate Cone Calorimeter HRRPUA values.

Note that the thickness value of the solid phase fabric/padding material on the SURF line in FDS was not used by FDS because each cell followed the input HRR ramp from the Cone Calorimeter.

C.4.7 ADDITIONAL OUTPUTS

In addition to the predicted HRR vs. time, there are additional output quantities available in the FDS results as follows:

- Two temperature slice files through the furniture specimen;
- Radiative heat flux boundary file;
- Convective heat flux boundary file;

- Net heat flux boundary file;
- Wall temperature boundary file; and
- Burning rate flux boundary file.

Note that the FDS HRR predictions were shifted to align the PHRR with the middle of the top 30% of the experimental HRR values.

C.4.8 MODIFICATIONS FOR INCREASED HEAT FLUXES AND THICKNESSES

There are two major challenges in using FDS to predict the burning rate of upholstered furniture based on Cone Calorimeter data:

1. Maximum specimen thickness in the Cone Calorimeter is 50 mm (2 in.) while end use thickness is usually much greater; and
2. By specifying the HRRPUA from the Cone Calorimeter at a single heat flux in FDS, the effect of heat flux variations (increases) on the burning rate is not accounted for.

In an attempt to address these challenges, three furniture flame spread cases were simulated in FDS:

1. Using Cone Calorimeter data obtained on 50 mm thick specimens;
2. A modified version of Case 1 to approximate the effects of an increased heat flux; and
3. A modified version of Case 2 to account for additional thickness (100 vs. 50 mm).

The Cone Calorimeter HRRPUA in Case 2 was modified by doubling the measured values and reducing the time scale by one half, which approximated the effects of a higher flame heat flux while preserving the amount of THR.

The Cone Calorimeter HRRPUA in Case 3 was a further modified version of Case 2 in which the time was scaled by a factor of 2 after the Cone Calorimeter HRRPUA decreased to 50% of the PHRRPUA value.

The HRRPUA vs. time for Cases 1, 2, and 3 for HDPU foam are shown in Figure C-5.

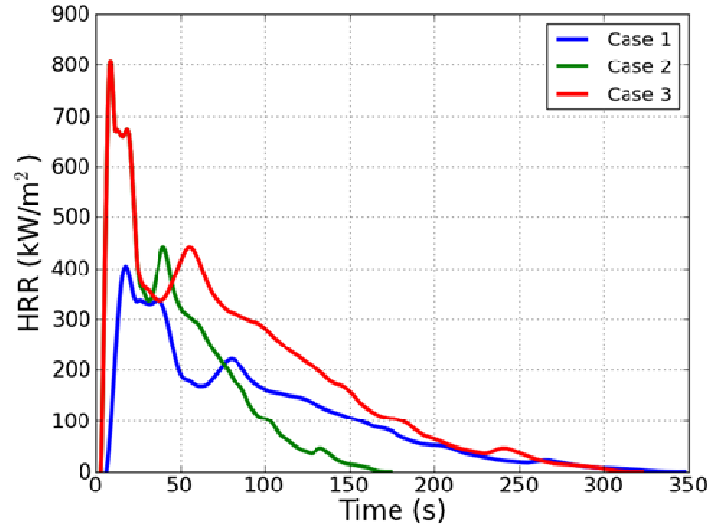


Figure C-5. Approaches to Account for Thickness and Heat Flux Effects on HRRPUA.

APPENDIX D

PICTURES OF USED FURNITURE SETS OBTAINED FOR TESTING

(CONSISTING OF 23 PAGES)



Figure D-1a. Set #1 3-Seat Sofa.



Figure D-1b. Set #1 1-Seat Sofa.



Figure D-1c. Set #1 Ottoman.



Figure D-2. Set #2 Chair.



Figure D-3a. Set #3 3-Seat Sofa.



Figure D-3b. Set #3 2-Seat Sofa.



Figure D-4a. Set #4 3-Seat Sofa.



Figure D-4b. Set #4 2-Seat Sofa.



Figure D-5. One of Two Set #5 3-Seat Sofas.



Figure D-6. Set #6 2-Seat Sofas.



Figure D-7a. Set #7 3-Seat Sofa.



Figure D-7b. Set #7 2-Seat Sofa.



Figure D-8a. Set #8 3-Seat Sofa.



Figure D-8b. Set #8 2-Seat Sofa.



Figure D-9a. Set #9 3-Seat Sofa.



Figure D-9b. Set #9 2-Seat Sofa.



Figure D-10a. Set #10 3-Seat Sofa.



Figure D-10b. Set #10 2-Seat Sofa.



Figure D-11a. Set #11 3-Seat Sofa.



Figure D-11b. Set #11 2-Seat Sofa.



Figure D-11c. Set #11 1-Seat Sofa.



Figure D-11d. Set #11 Ottoman.



Figure D-12a. Set #12 3-Seat Sofa.



Figure D-12b. Set #12 2-Seat Sofa.



Figure D-13a. Set #13 3-Seat Sofa.



Figure D-13b. Set #13 2-Seat Sofa.



Figure D-14a. Set #14 3-Seat Sofa.



Figure D-14b. Set #14 1-Seat Sofa.



Figure D-15. One of Six Set #15 Chairs.



Figure D-16a. Set #16 3-Seat Sofa.



Figure D-16b. Set #16 1-Seat Sofas.



Figure D-17a. Set #17 3-Seat Sofa.



Figure D-17b. Set #17 2-Seat Sofa.



Figure D-18a. Set #18 3-Seat Sofa.



Figure D-18b. Set #18 2-Seat Sofa.



Figure D-19a. Set #19 3-Seat Sofa.



Figure D-19b. Set #19 2-Seat Sofa.



Figure D-20a. Set #20 2-Seat Sofa.



Figure D-20b. Set #20 1-Seat Sofa.



Figure D-21a. Set #21 3-Seat Sofa.



Figure D-21b. Set #21 2-Seat Sofa.



Figure D-21c. Set #21 1-Seat Sofa.



Figure D-21d. Set #21 Ottoman.



Figure D-22a. Set #22 3-Seat Sofa.



Figure D-22b. Set #22 1-Seat Sofa.

APPENDIX E

TRIANGULAR HRR APPROXIMATIONS FOR FRACTIONAL FACTORIAL DESIGN ANALYSIS

(CONSISTING OF 9 PAGES)

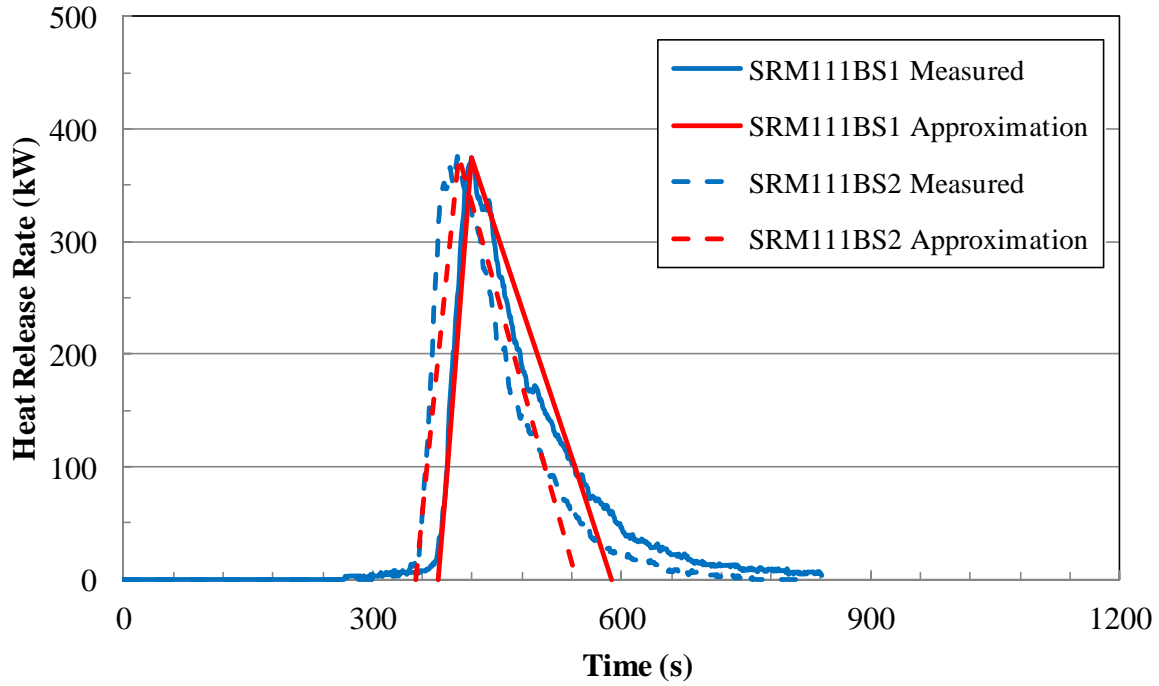


Figure E-1. Triangular HRR Approximations for SRM111BS1 and SRM111BS2.

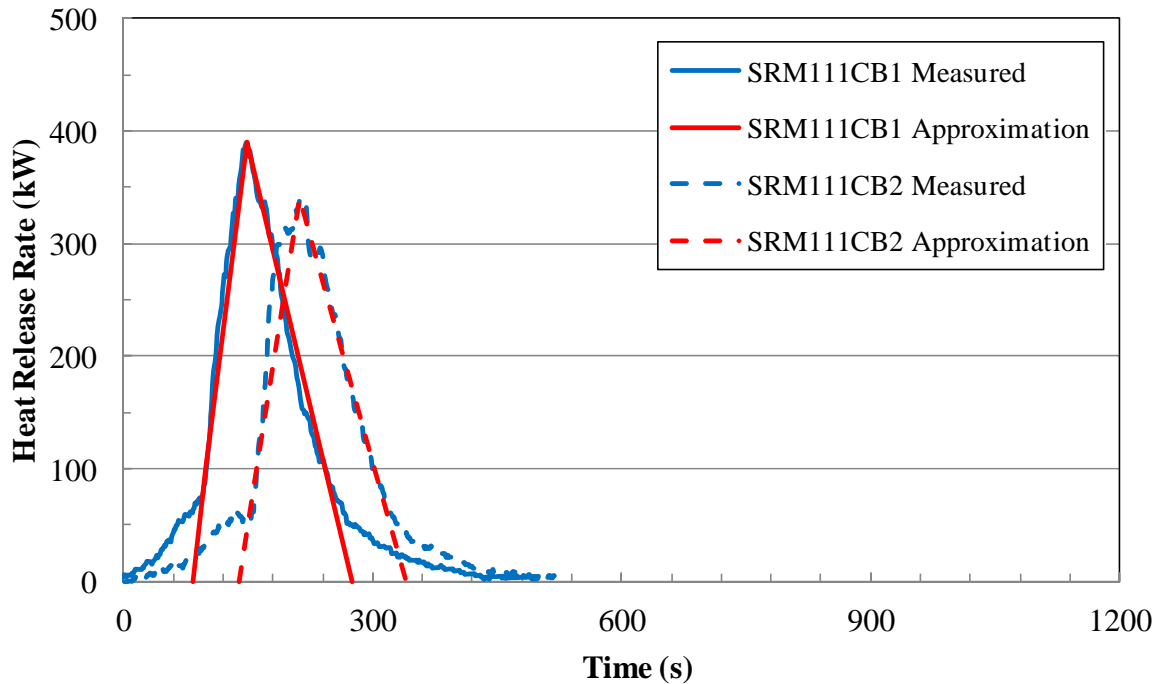


Figure E-2. Triangular HRR Approximations for SRM111CB1 and SRM111CB2.

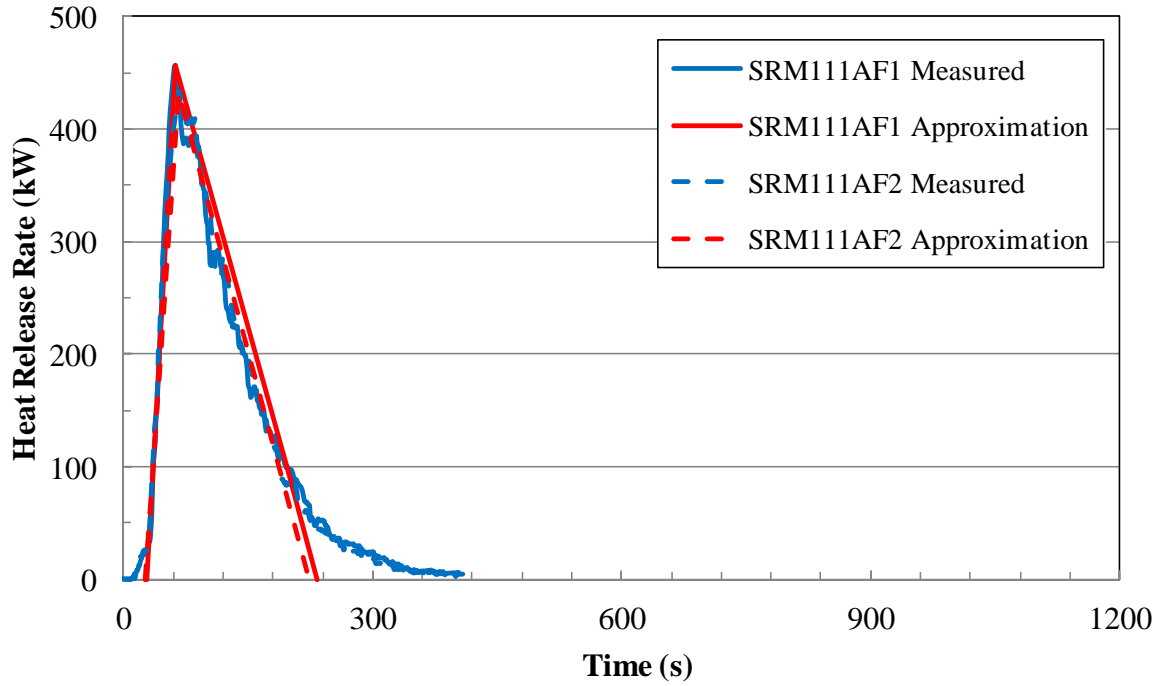


Figure E-3. Triangular HRR Approximations for SRM111AF1 and SRM111AF2.

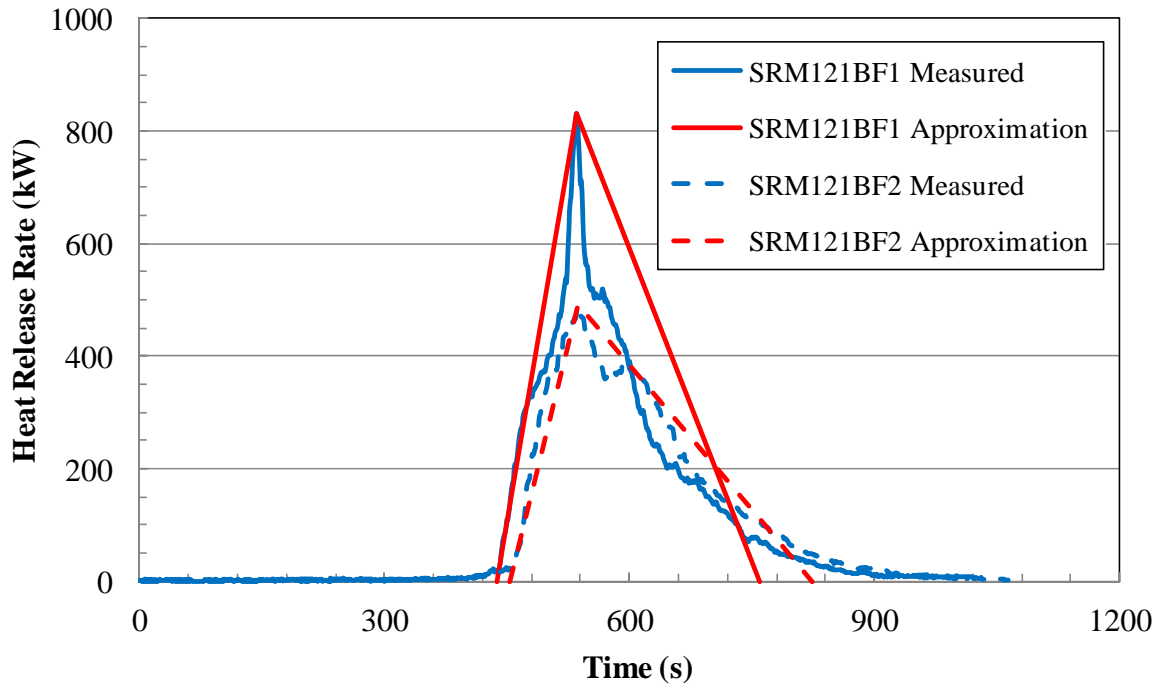


Figure E-4. Triangular HRR Approximations for SRM121BF1 and SRM121BF2.

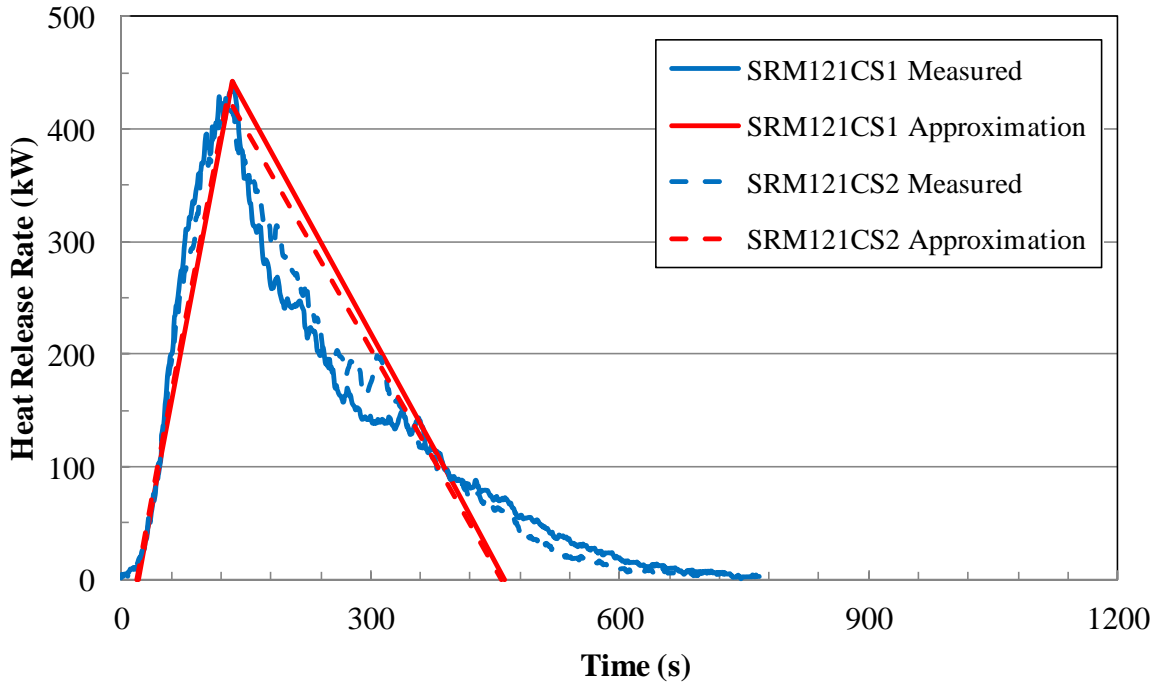


Figure E-5. Triangular HRR Approximations for SRM121CS1 and SRM121CS2.

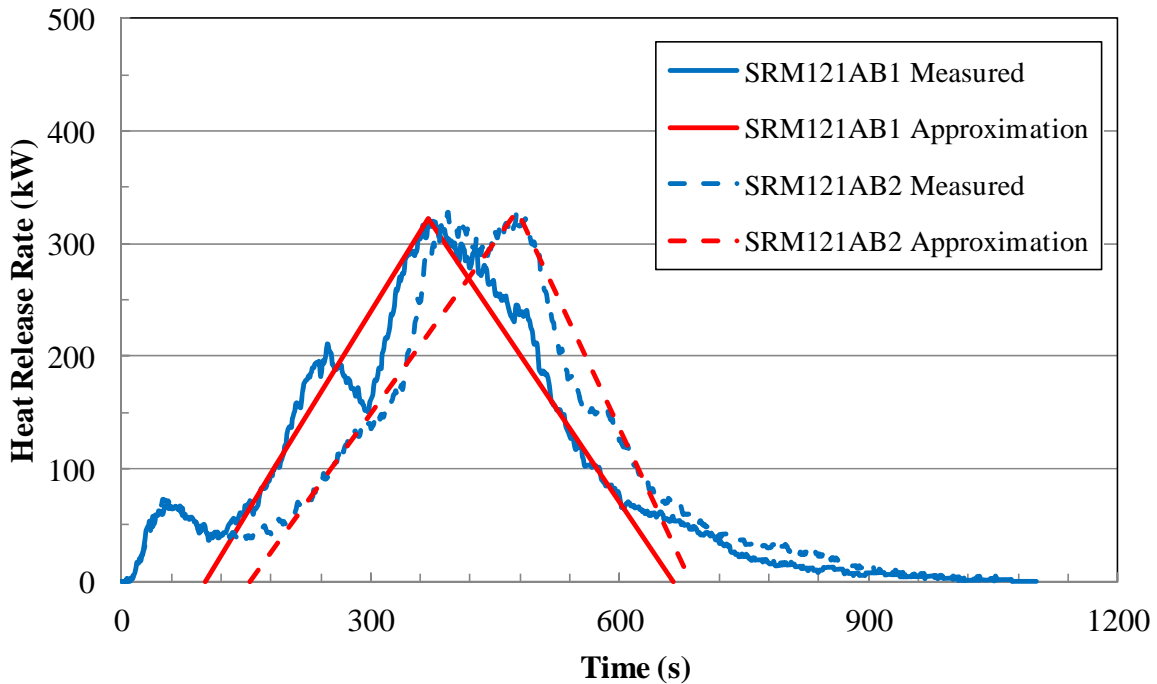


Figure E-6. Triangular HRR Approximations for SRM121AB1 and SRM121AB2.

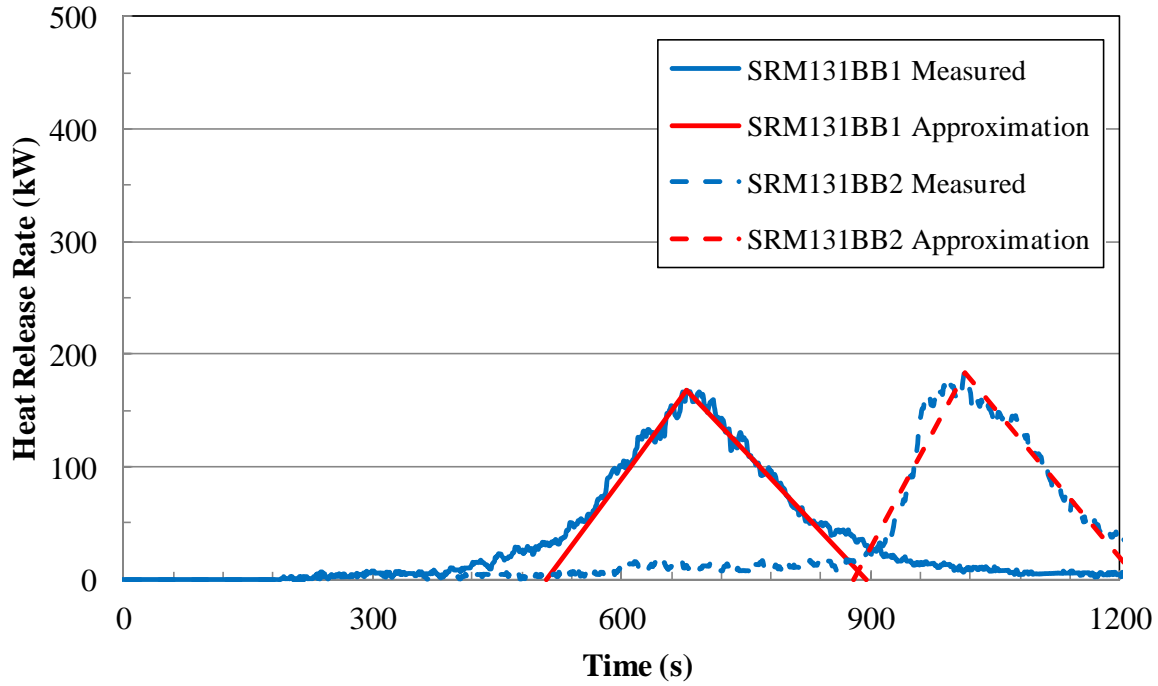


Figure E-7. Triangular HRR Approximations for SRM131BB1 and SRM131BB2

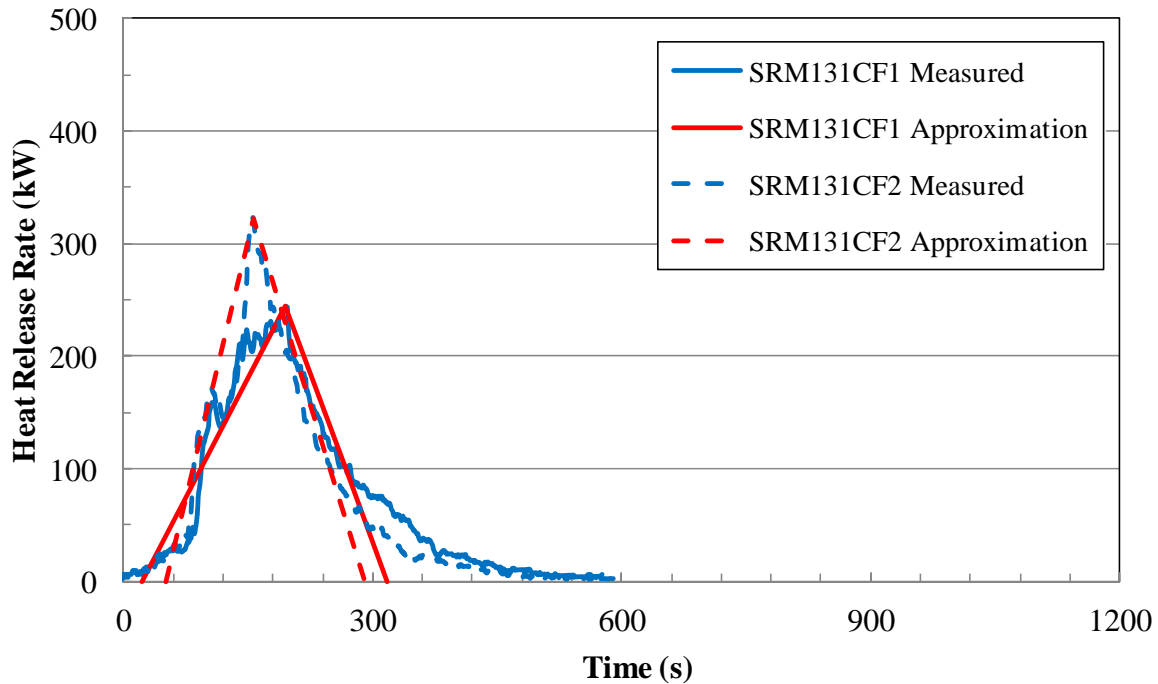


Figure E-8. Triangular HRR Approximations for SRM131CF1 and SRM131CF2.

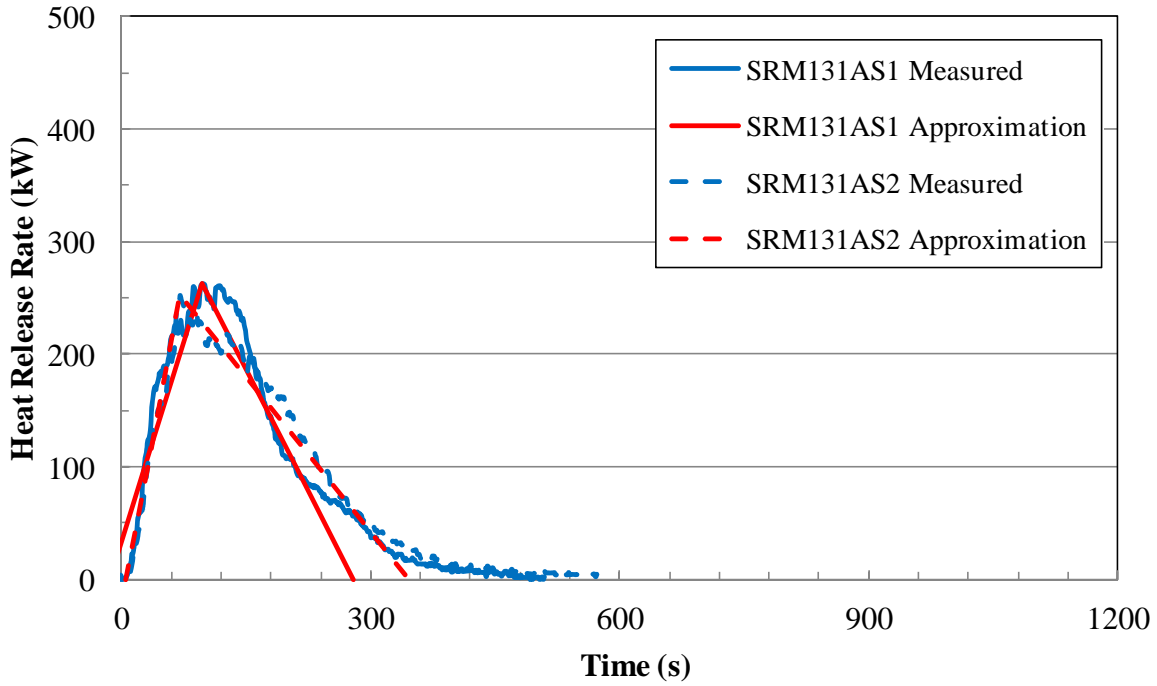


Figure E-9. Triangular HRR Approximations for SRM131AS1 and SRM131AS2.

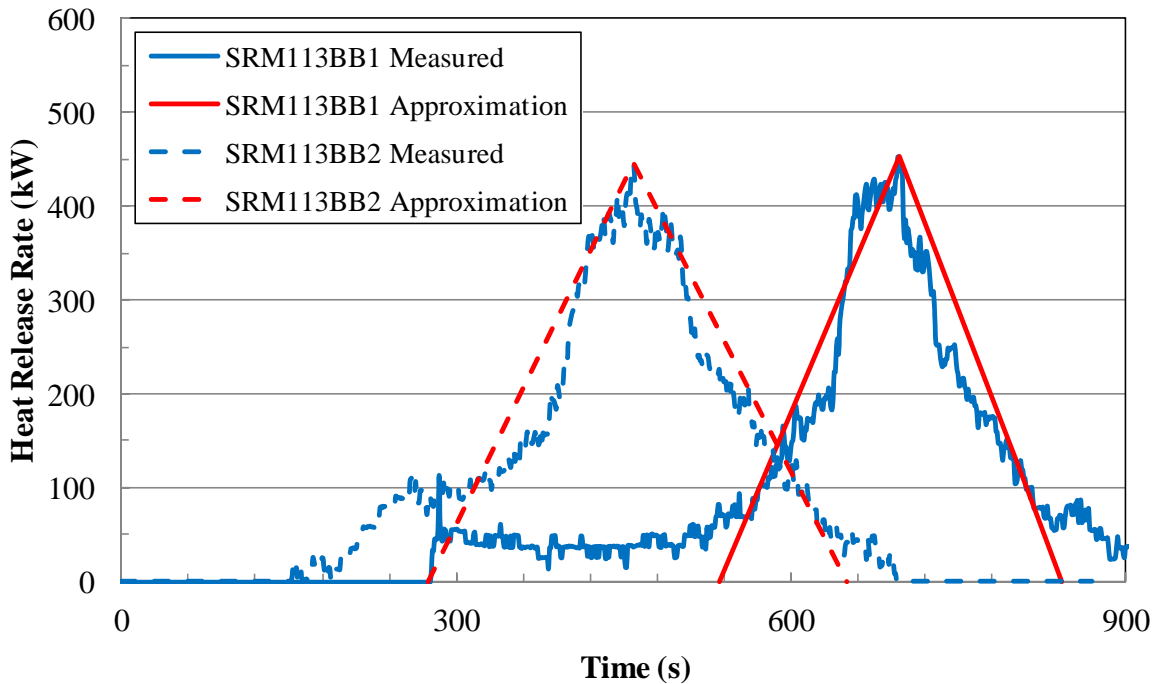


Figure E-10. Triangular HRR Approximations for SRM113BB1 and SRM113BB2.

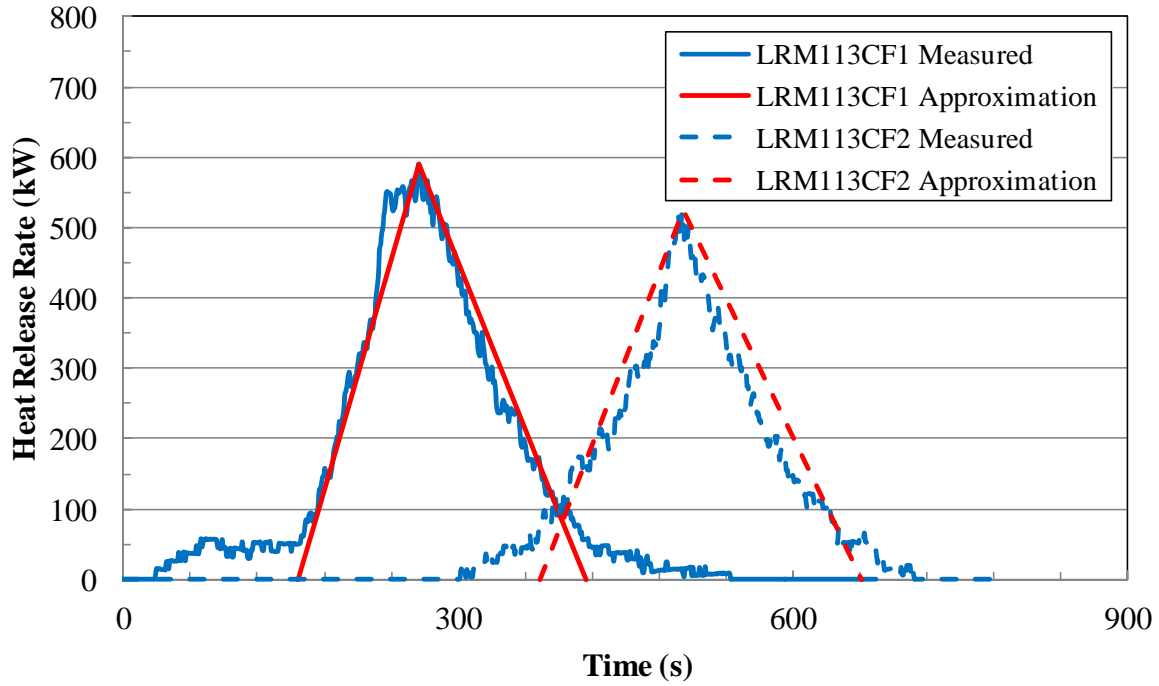


Figure E-11. Triangular HRR Approximations for LRM113CF1 and LRM113CF2.

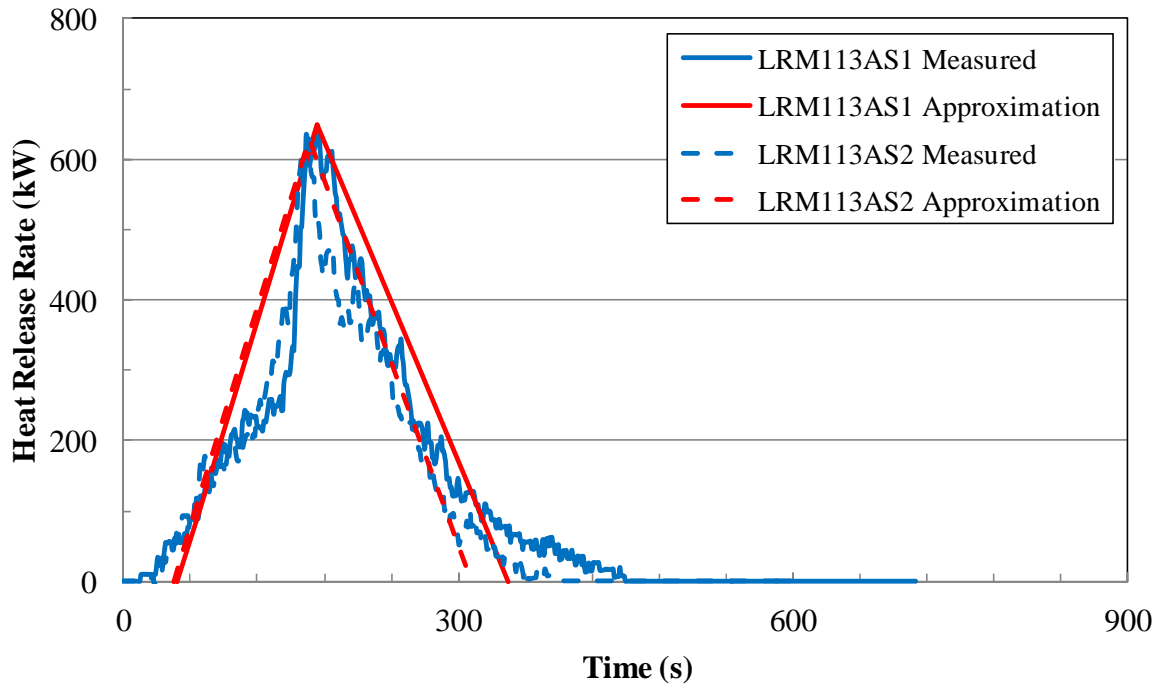


Figure E-12. Triangular HRR Approximations for LRM113AS1 and LRM113AS2.

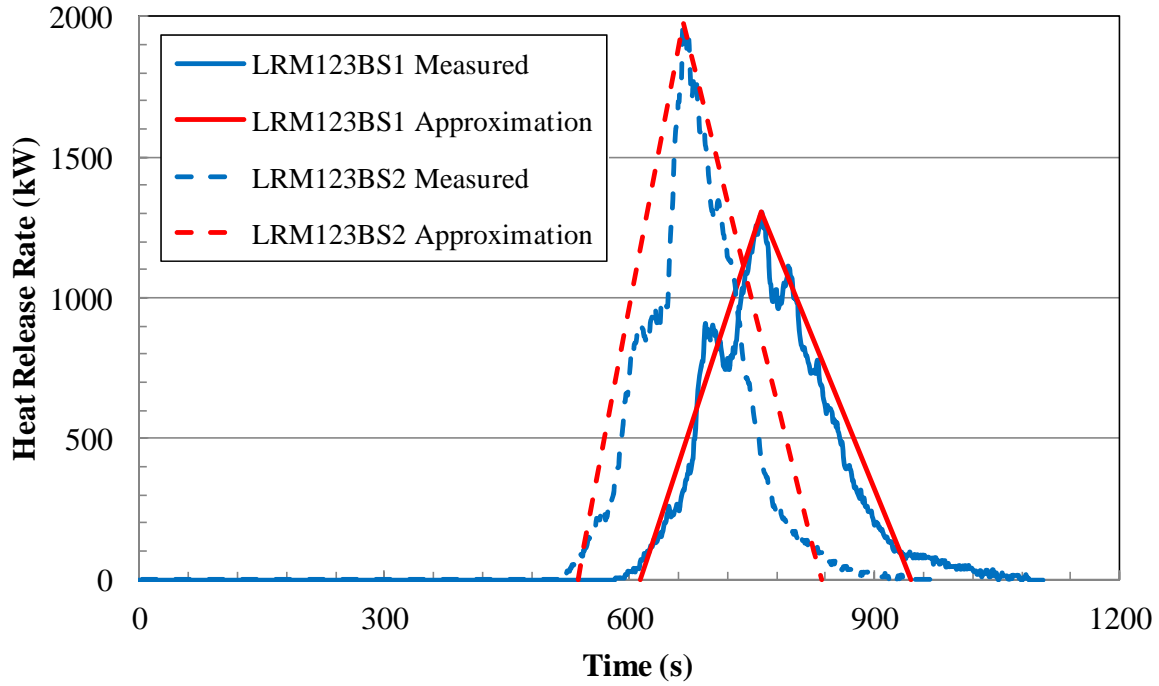


Figure E-13. Triangular HRR Approximations for LRM123BS1 and LRM123BS2.

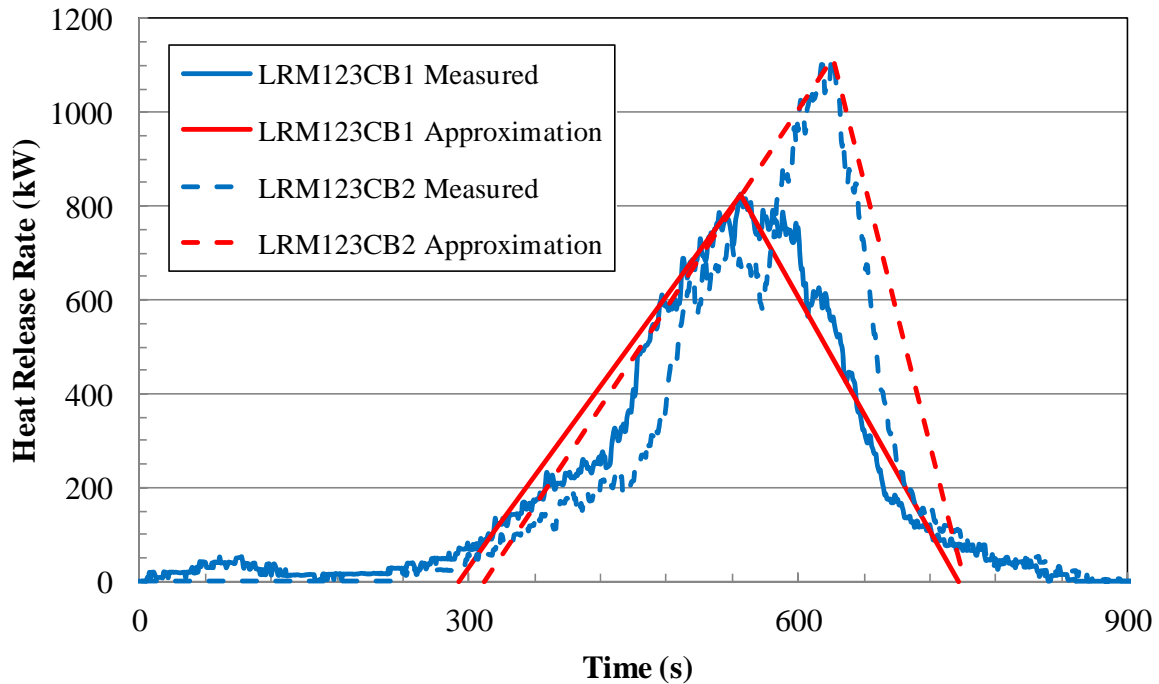


Figure E-14. Triangular HRR Approximations for LRM123CB1 and LRM123CB2.

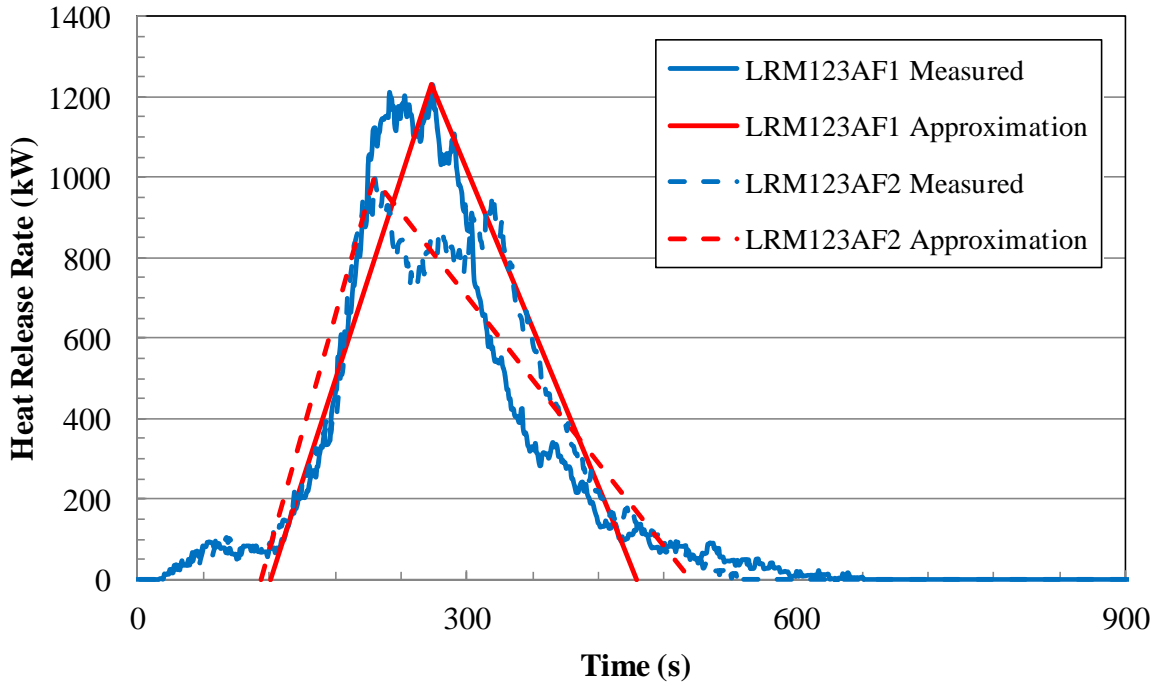


Figure E-15. Triangular HRR Approximations for LRM123AF1 and LRM123AF2.

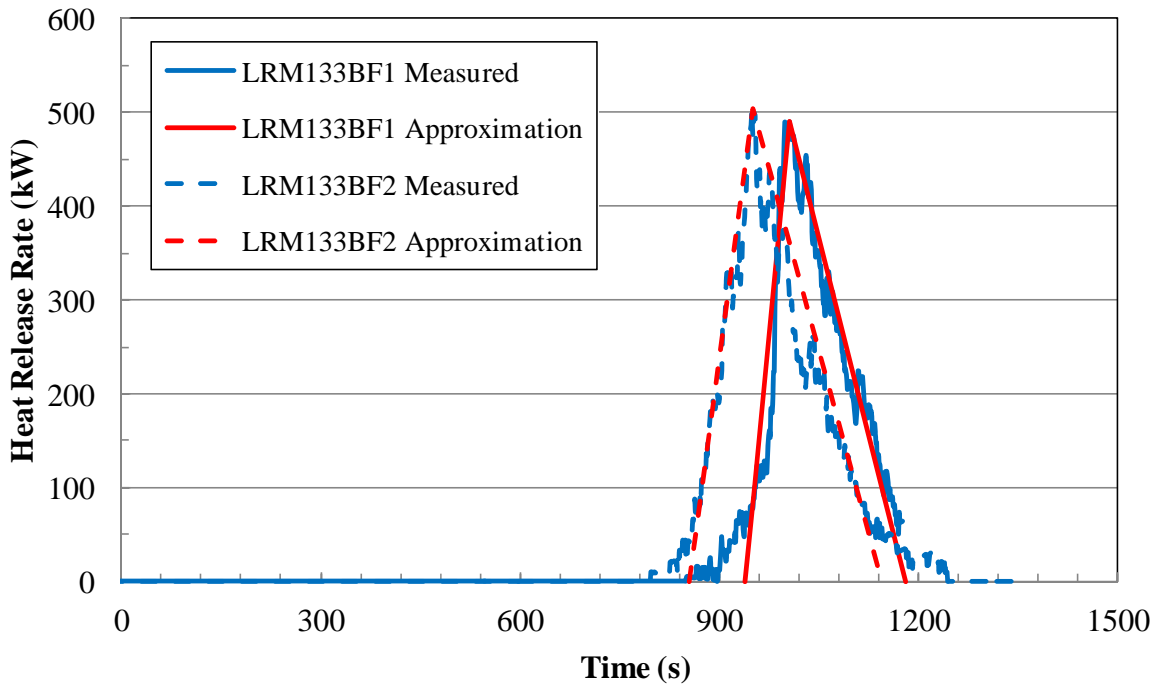


Figure E-16. Triangular HRR Approximations for LRM133BF1 and LRM133BF2.

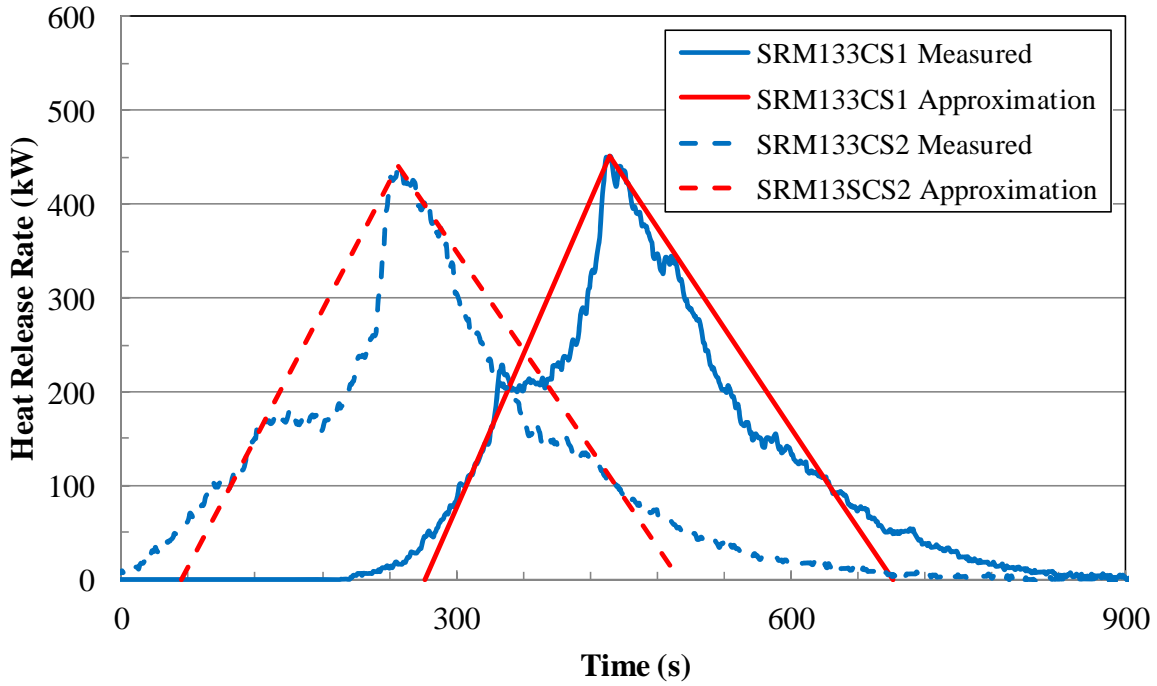


Figure E-17. Triangular HRR Approximations for LRM133CS1 and LRM133CS2.

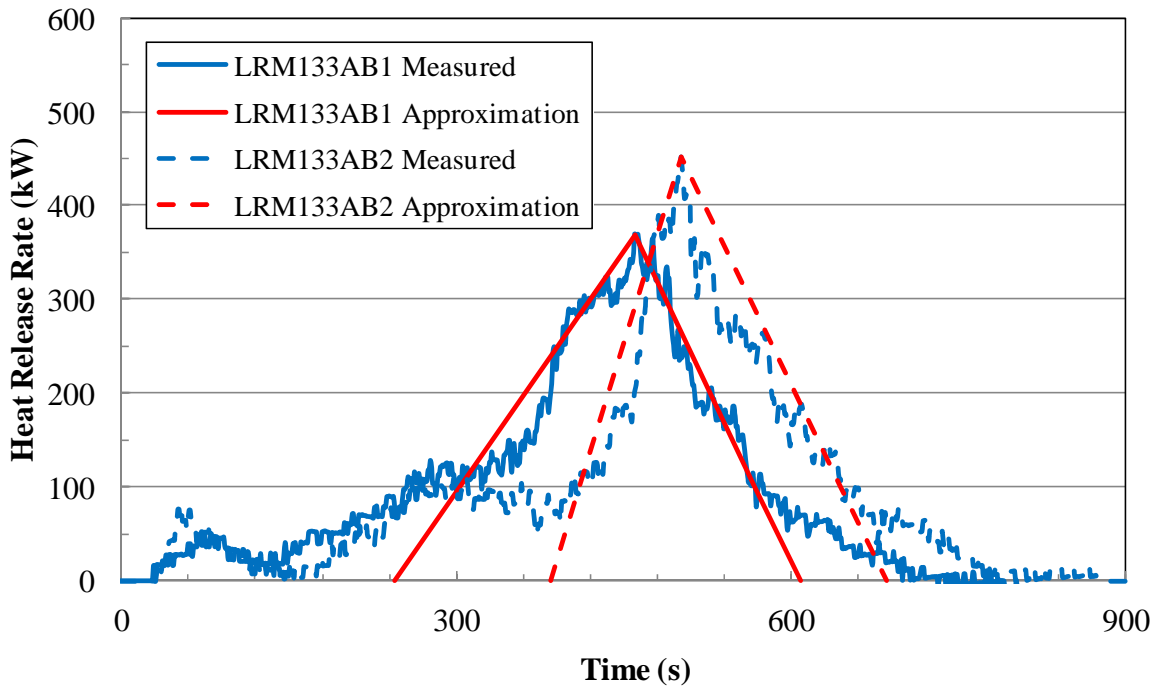


Figure E-18. Triangular HRR Approximations for LRM133AB1 and LRM133AB2.

APPENDIX F
TUKEY MULTIPLE COMPARISONS
(CONSISTING OF 12 PAGES)

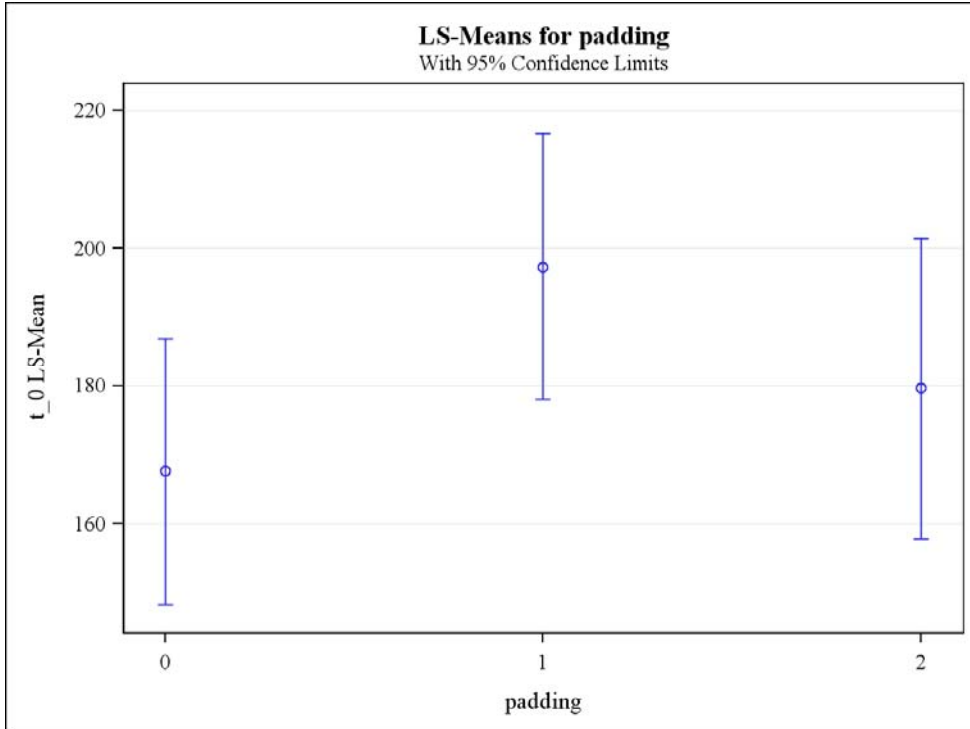


Figure F-1. 1-Seat Sofas: Effect of Padding on t₀.

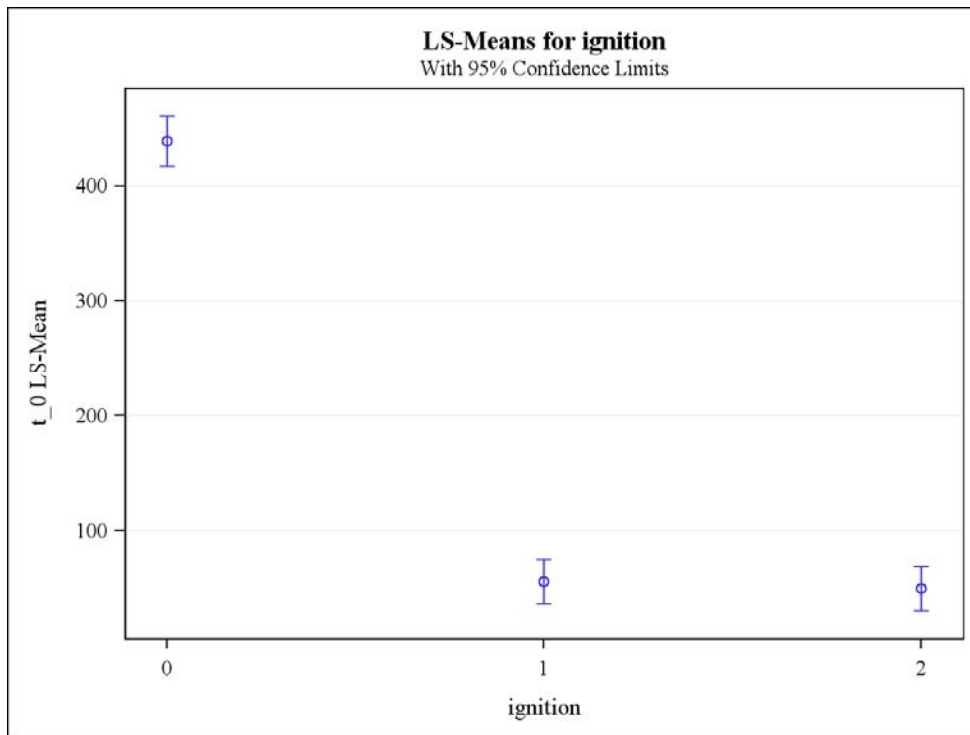


Figure F-2. 1-Seat Sofas: Effect of Ignition Source on t₀.

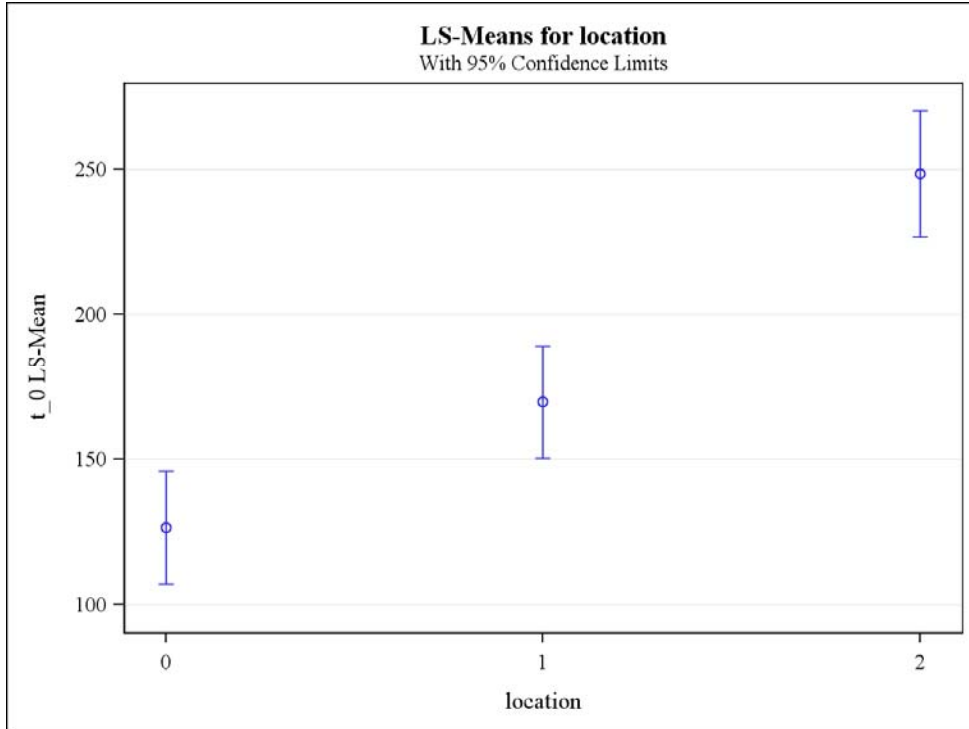


Figure F-3. 1-Seat Sofas: Effect of Source Location on t_0 .

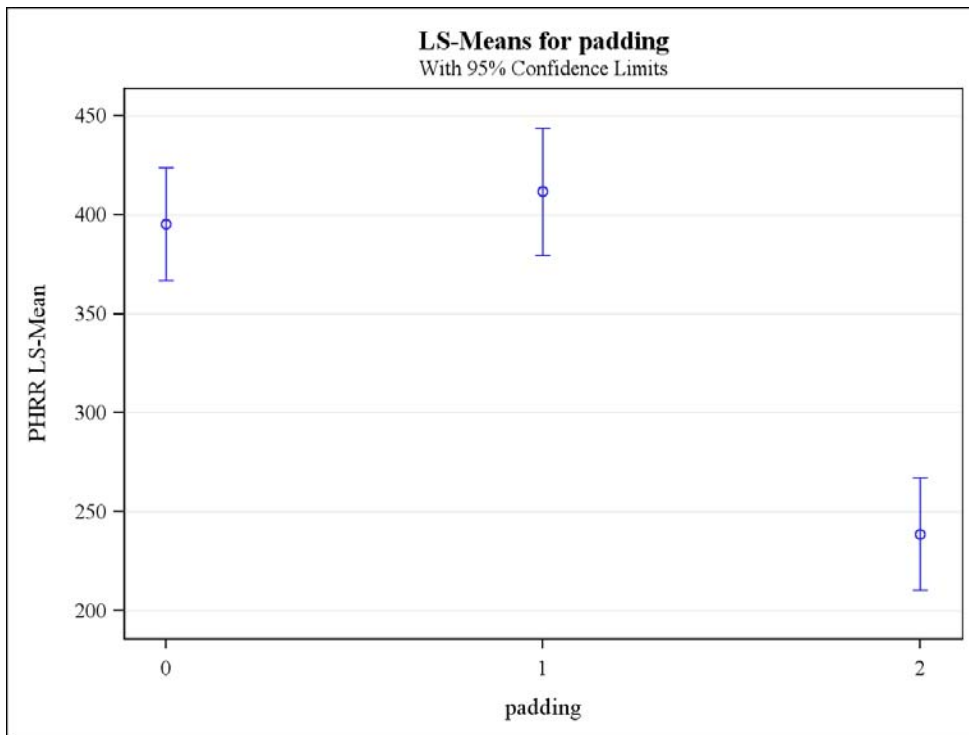


Figure F-4. 1-Seat Sofas: Effect of Padding on PHRR.

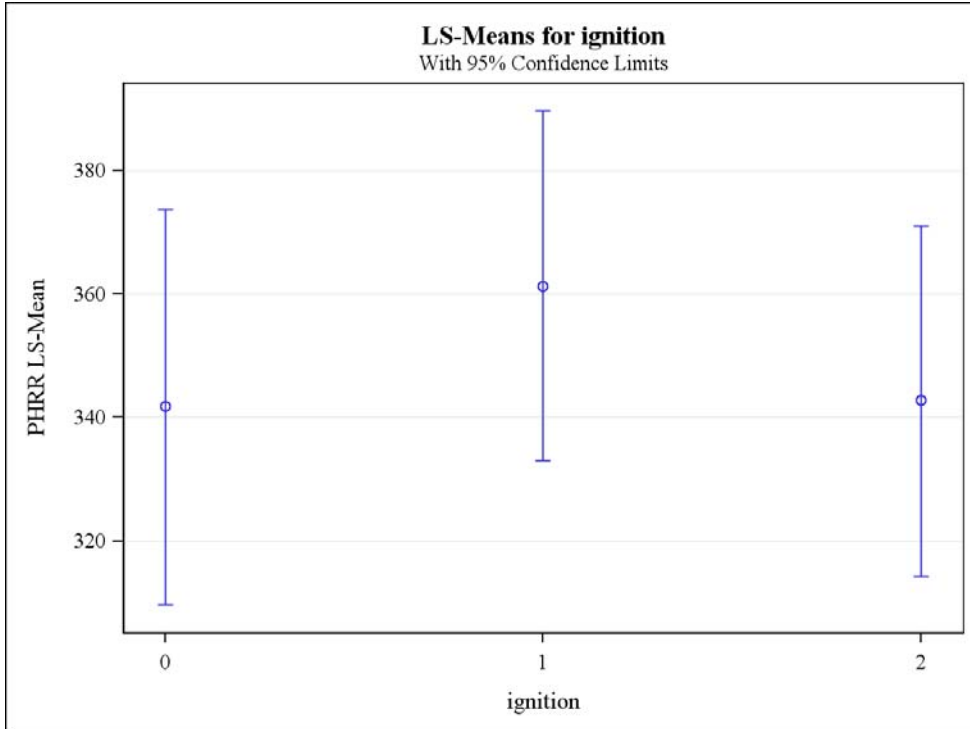


Figure F-5. 1-Seat Sofas: Effect of Ignition Source on PHRR.

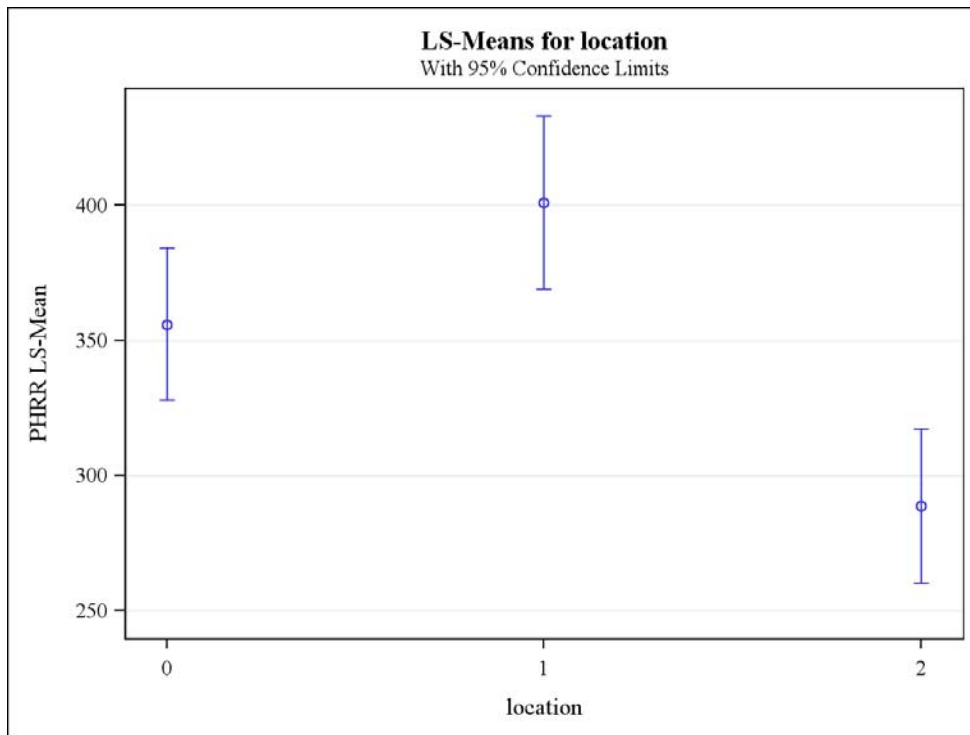


Figure F-6. 1-Seat Sofas: Effect of Source Location on PHRR.

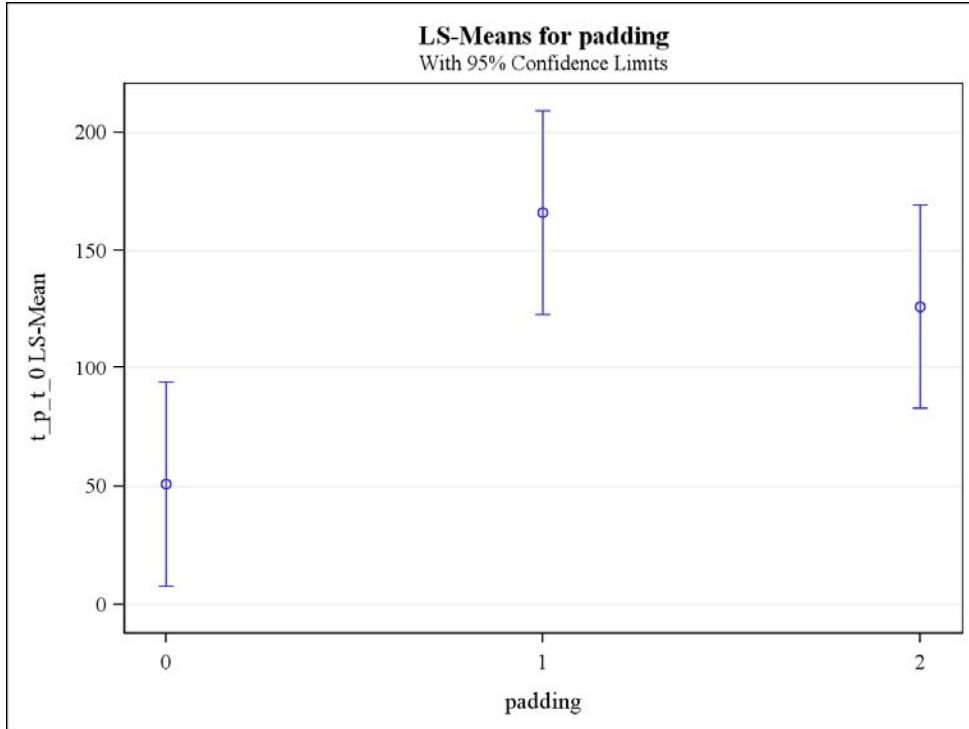


Figure F-7. 1-Seat Sofas: Effect of Padding on $t_p - t_0$.

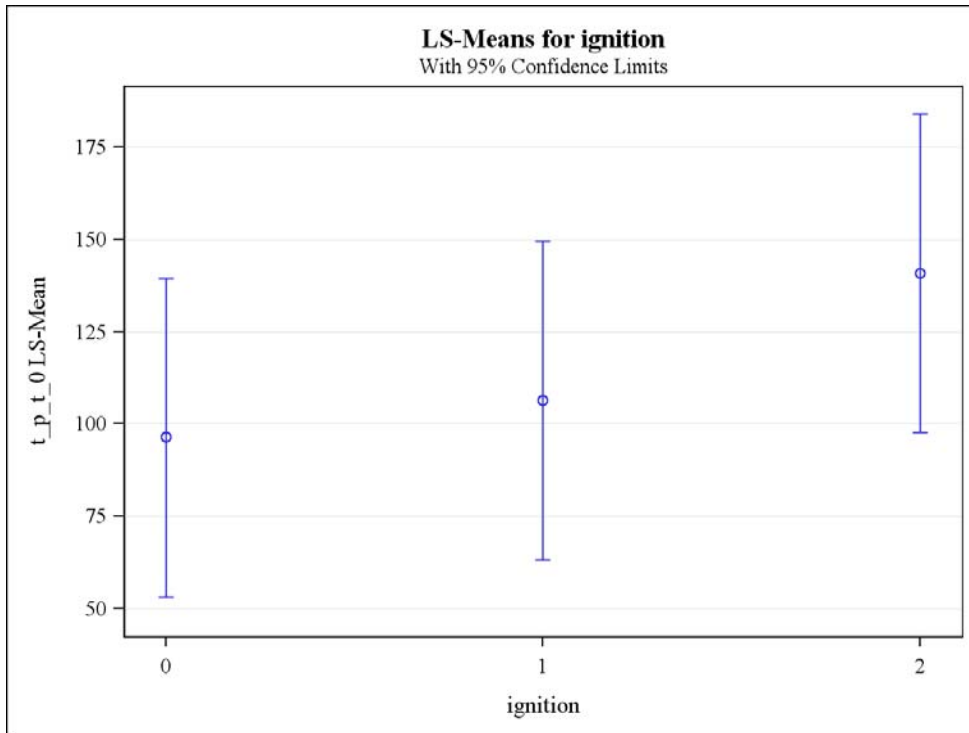


Figure F-8. 1-Seat Sofas: Effect of Ignition Source on $t_p - t_0$.

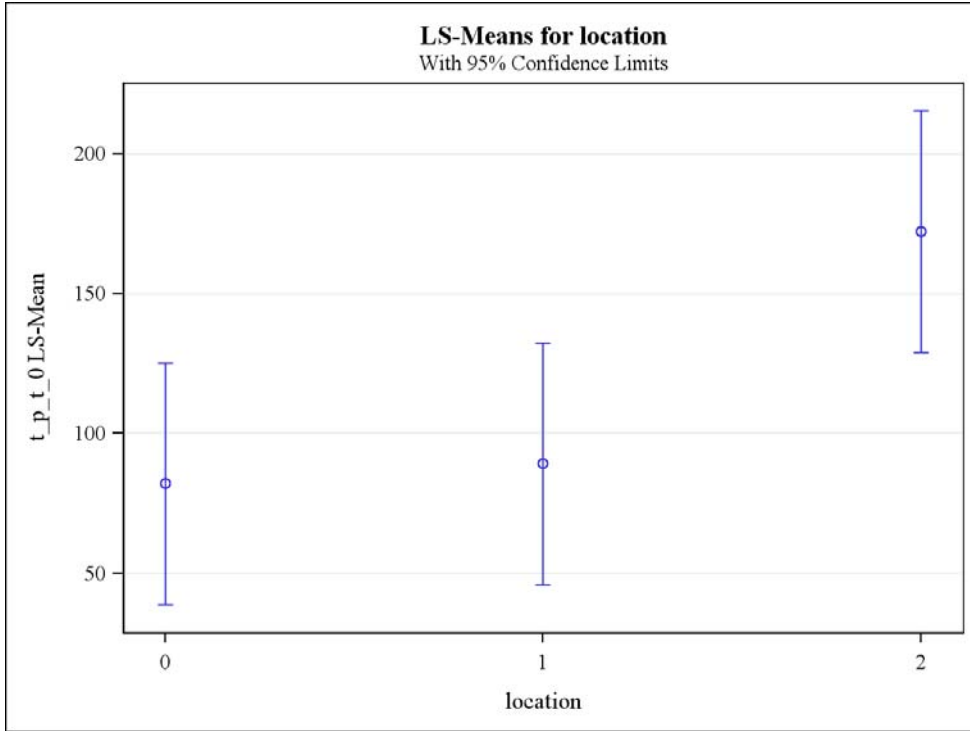


Figure F-9. 1-Seat Sofas: Effect of Source Location on $t_p - t_0$.

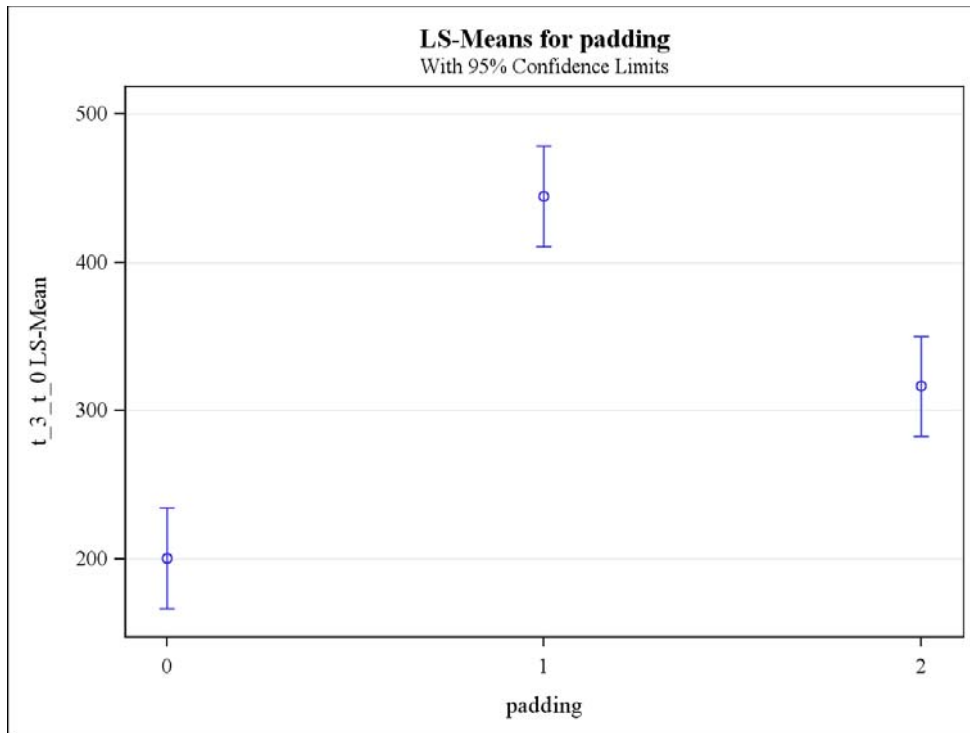


Figure F-10. 1-Seat Sofas: Effect of Padding on $t_3 - t_0$.

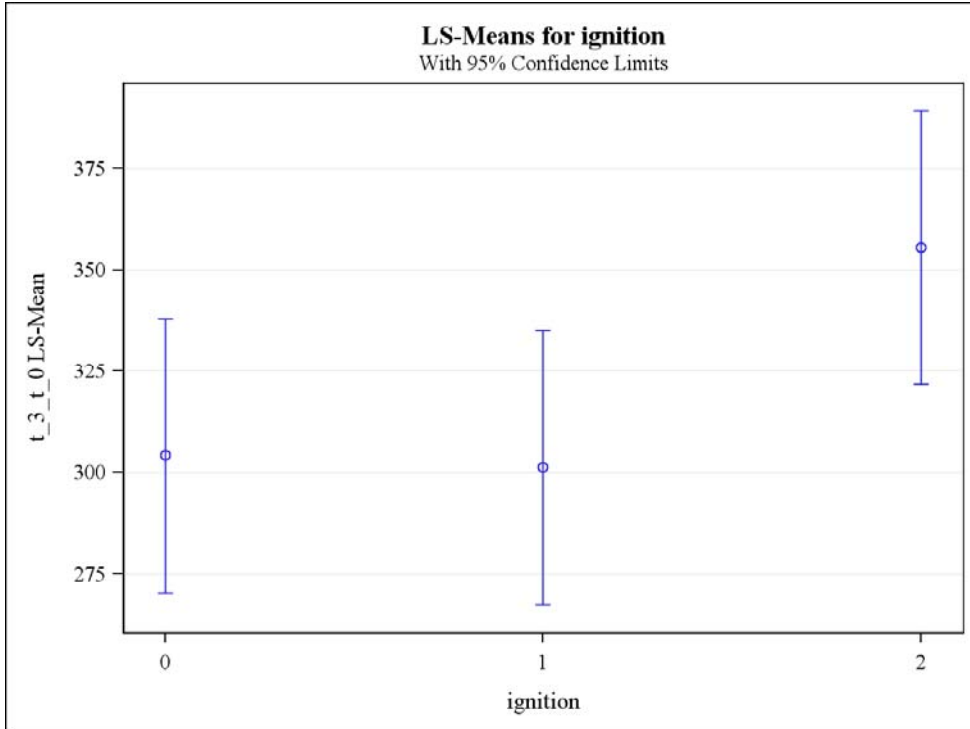


Figure F-11. 1-Seat Sofas: Effect of Ignition Source on t_3-t_0 .

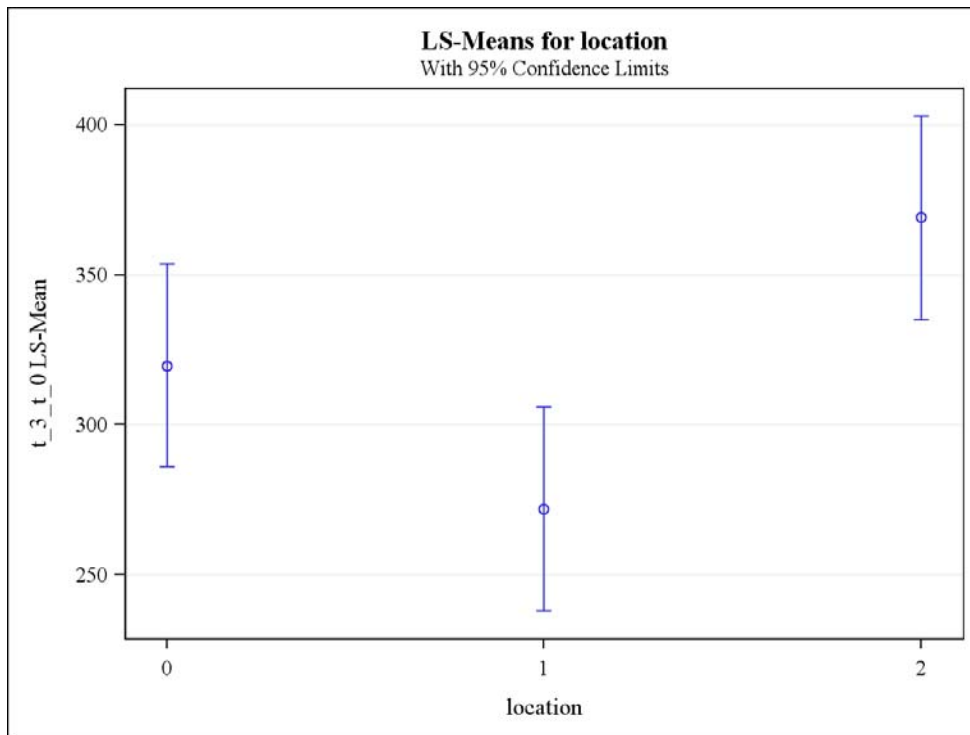


Figure F-12. 1-Seat Sofas: Effect of Source Location on t_3-t_0 .

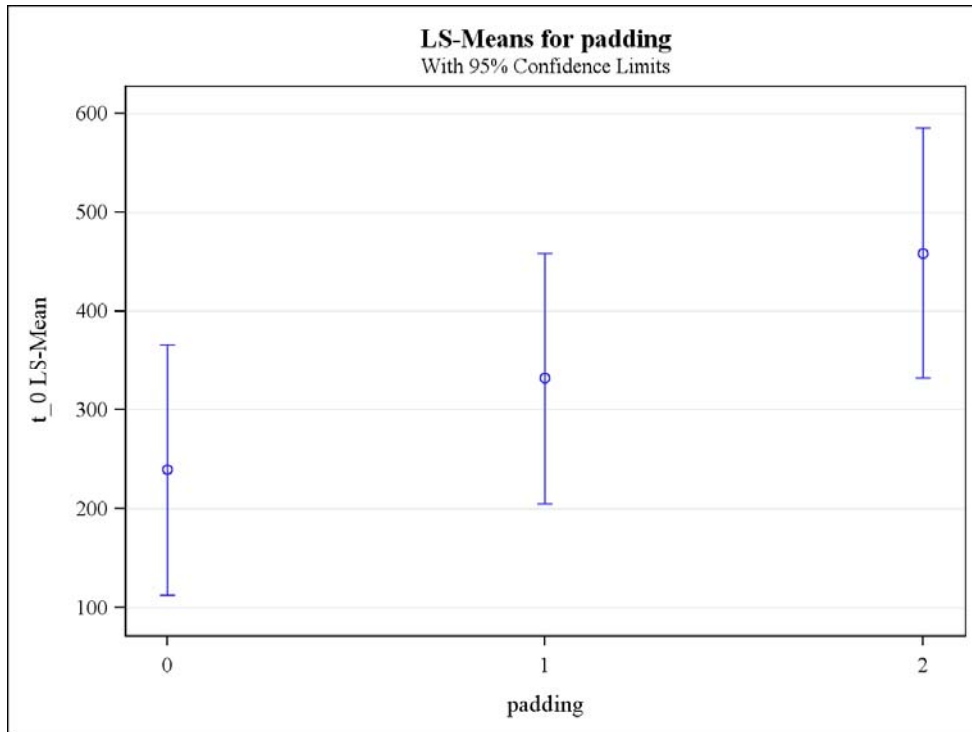


Figure F-13. 3-Seat Sofas: Effect of Padding on t₀.

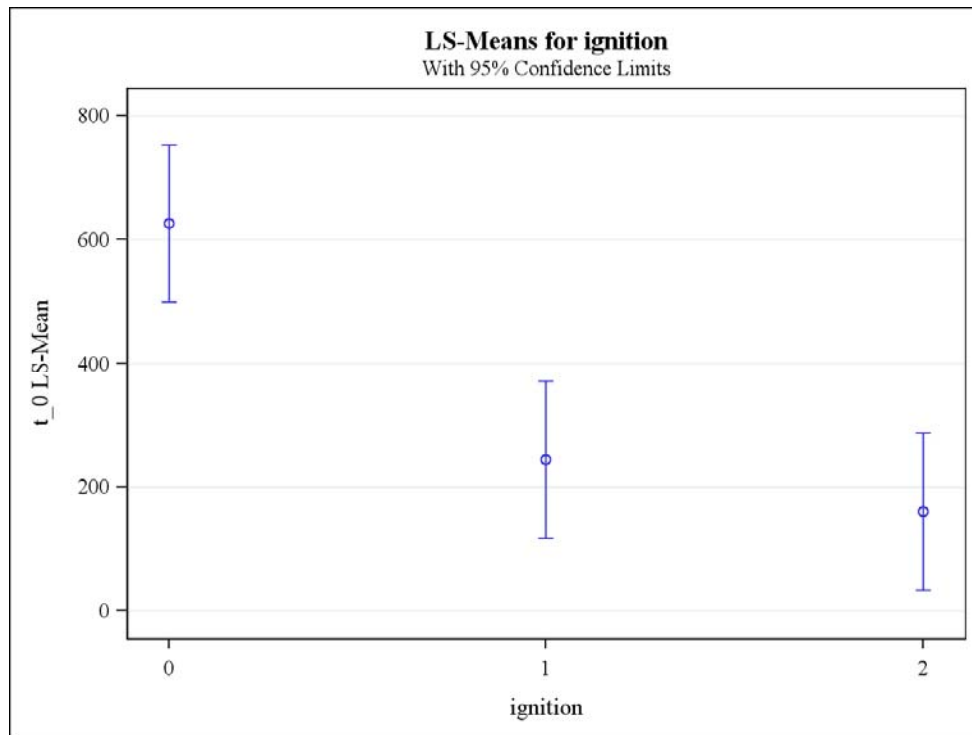


Figure F-14. 3-Seat Sofas: Effect of Ignition Source on t₀.

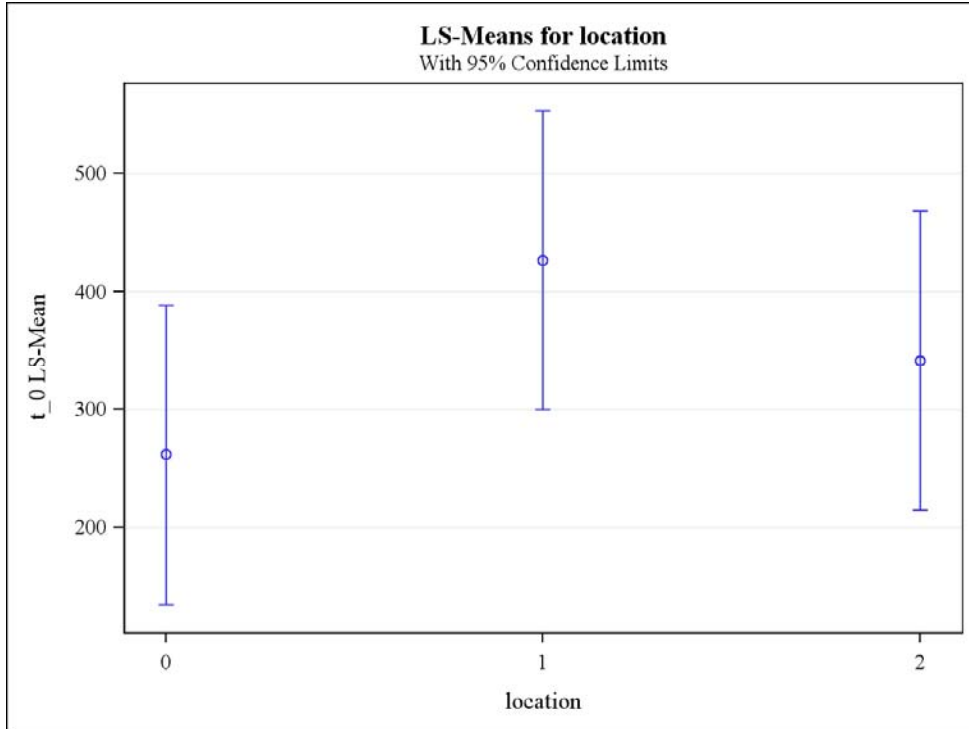


Figure F-15. 3-Seat Sofas: Effect of Source Location on t₀.

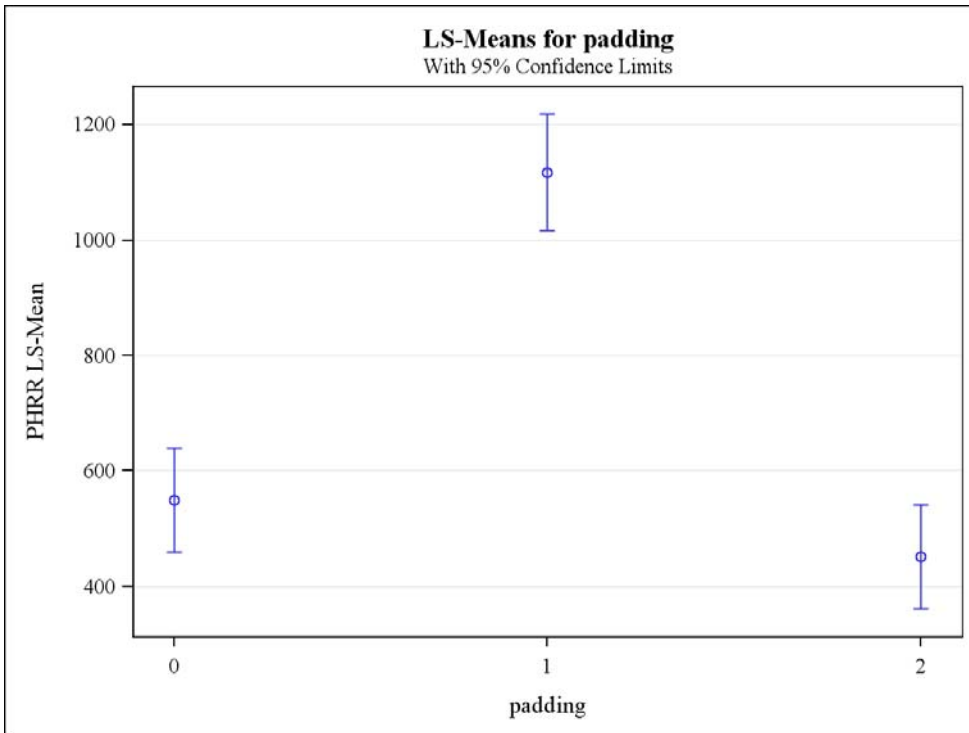


Figure F-16. 3-Seat Sofas: Effect of Padding on PHRR.

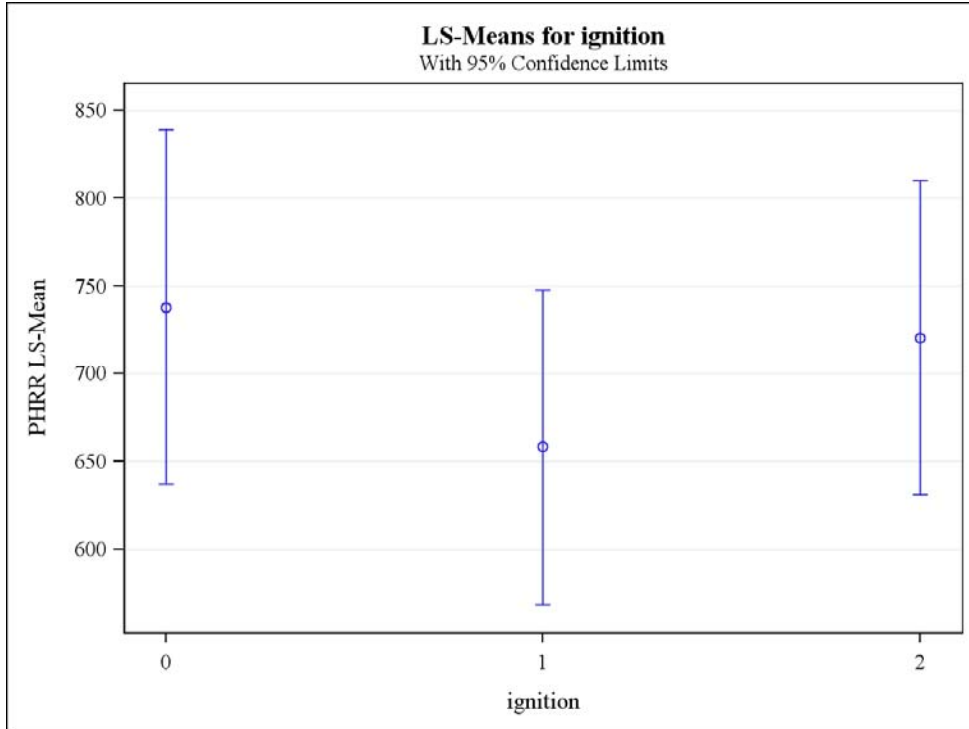


Figure F-17. 3-Seat Sofas: Effect of Ignition Source on PHRR.

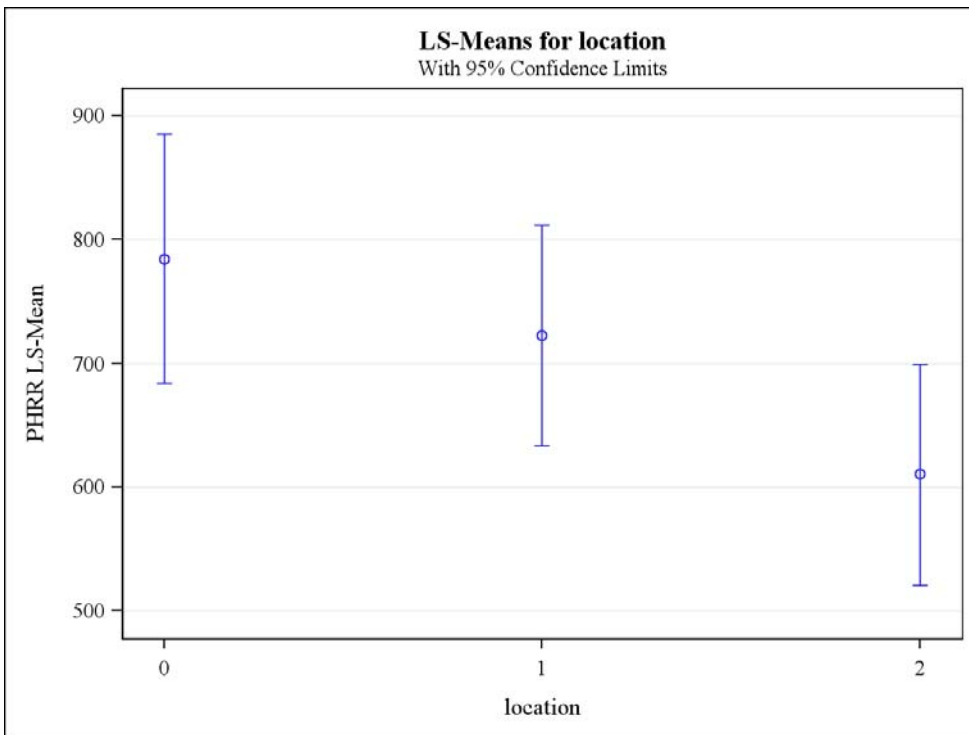


Figure F-18. 3-Seat Sofas: Effect of Source Location on PHRR.

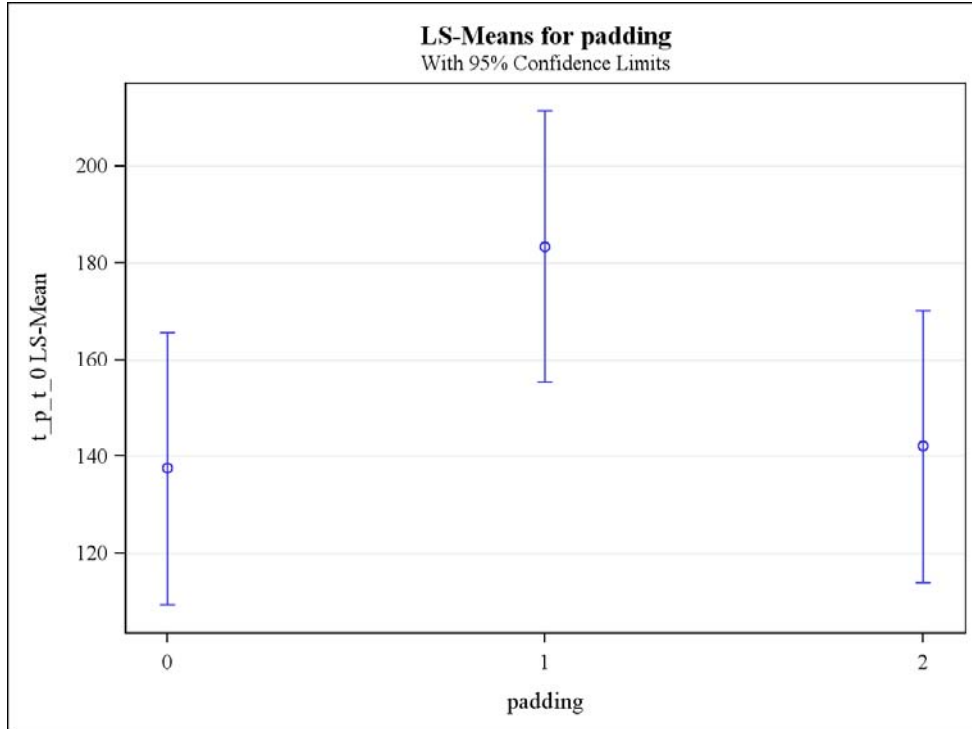


Figure F-19. 3-Seat Sofas: Effect of Padding on $t_p - t_0$.

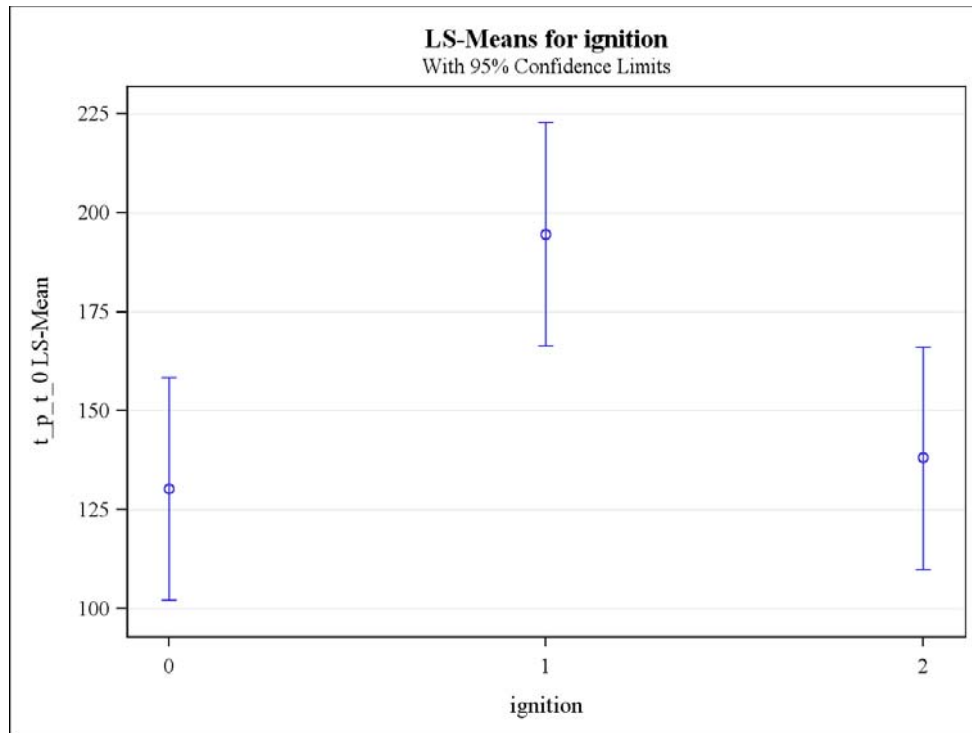


Figure F-20. 3-Seat Sofas: Effect of Ignition Source on $t_p - t_0$.

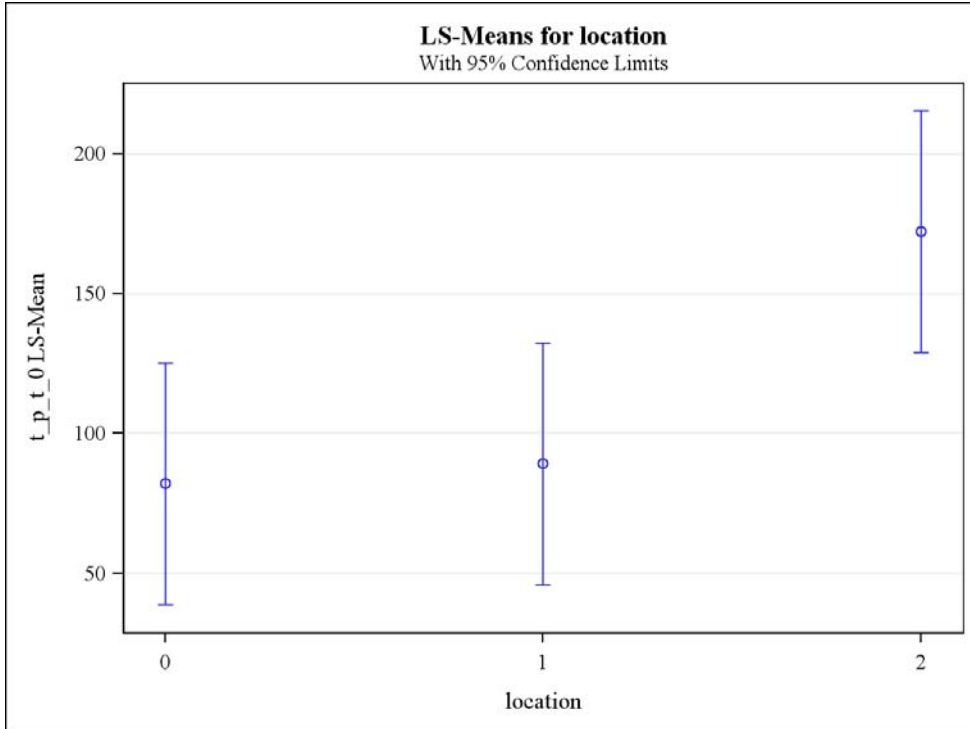


Figure F-21. 3-Seat Sofas: Effect of Source Location on $t_p - t_0$.

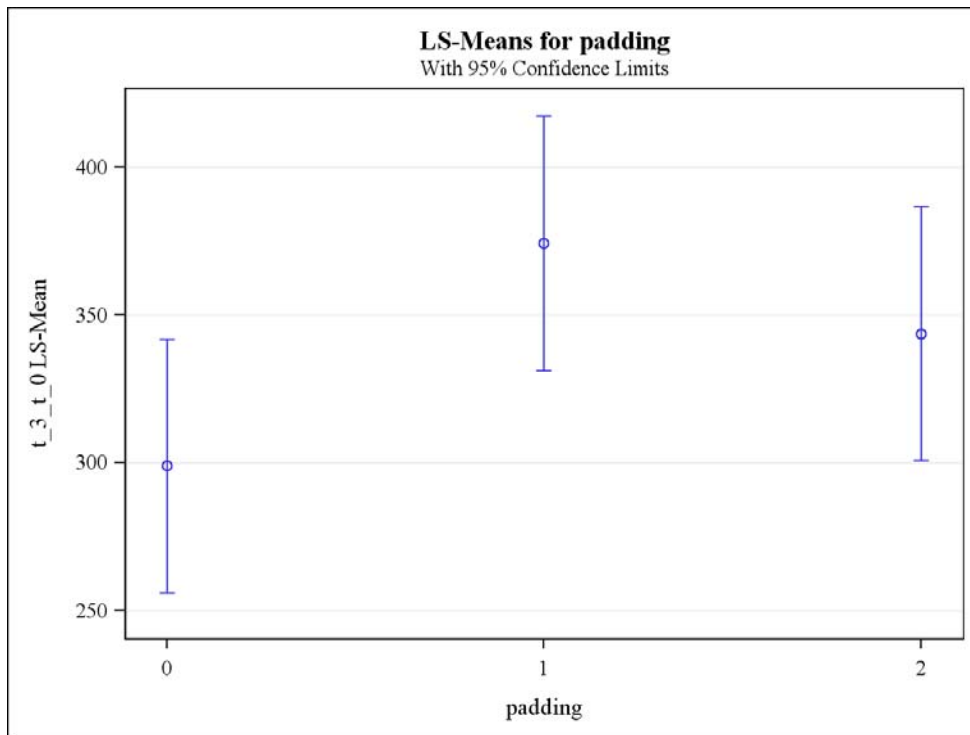


Figure F-22. 3-Seat Sofas: Effect of Padding on $t_3 - t_0$.

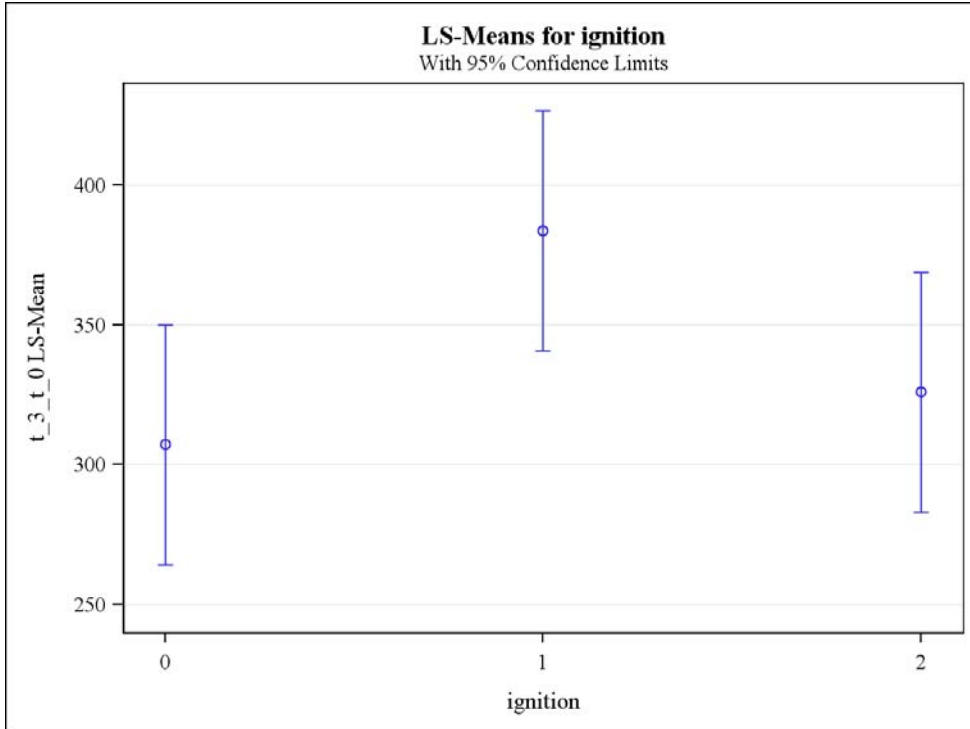


Figure F-23. 3-Seat Sofas: Effect of Ignition Source on $t_3 - t_0$.

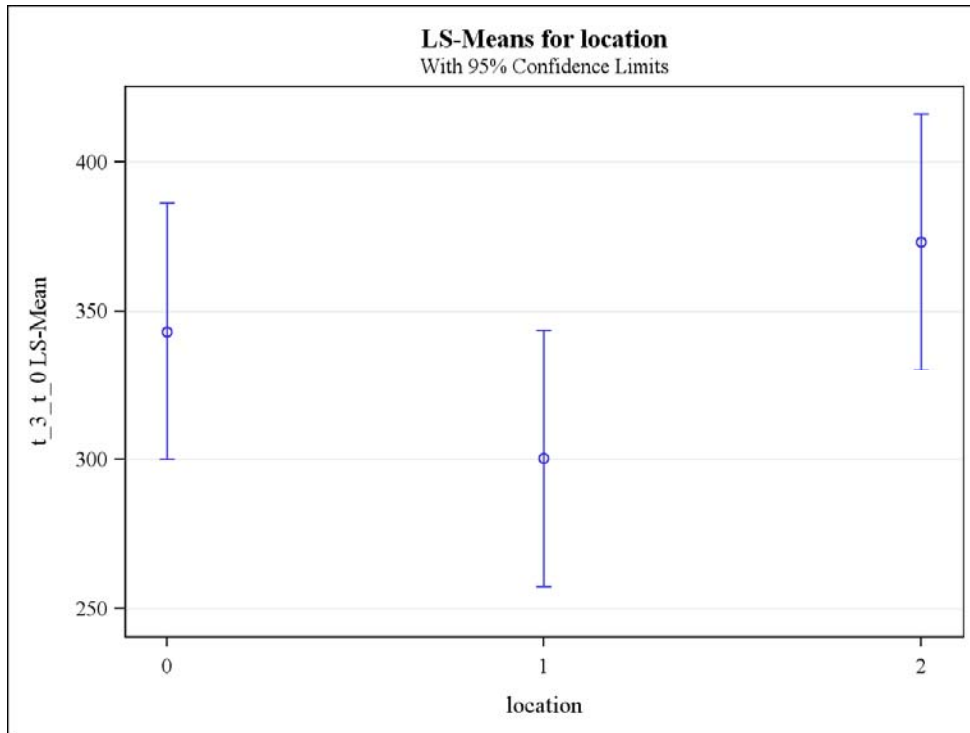


Figure F-24. 3-Seat Sofas: Effect of Source Location on $t_3 - t_0$.

APPENDIX G

BURNING RATE PREDICTIONS FOR OPEN CALORIMETER MOCKUP TESTS

(CONSISTING OF 3 PAGES)

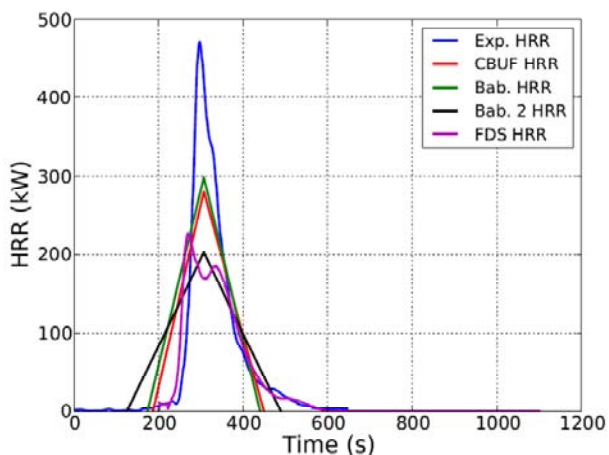


Figure G-1. SOM111BS1.

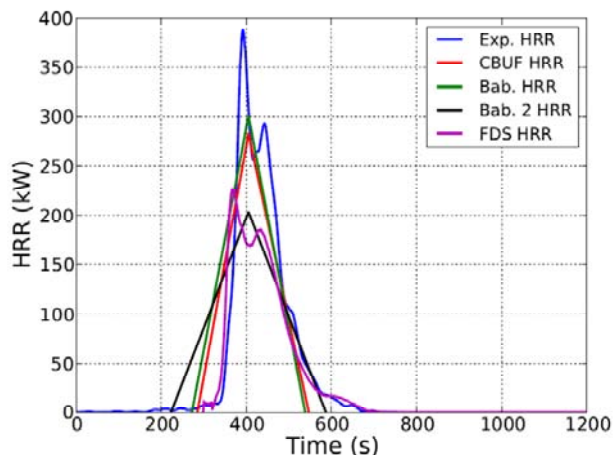


Figure G-2. SOM111BS2.

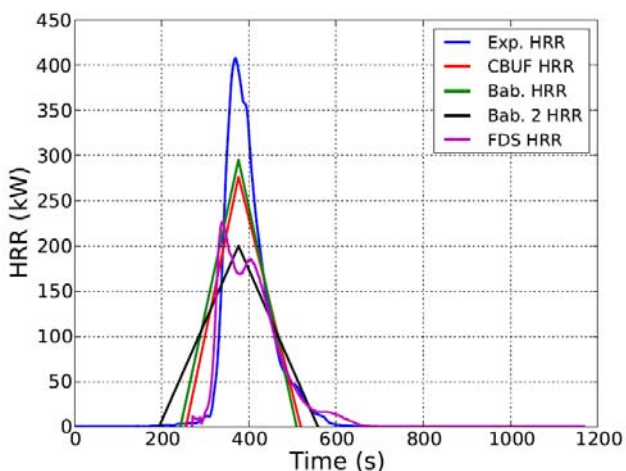


Figure G-3. SOM111BS3.

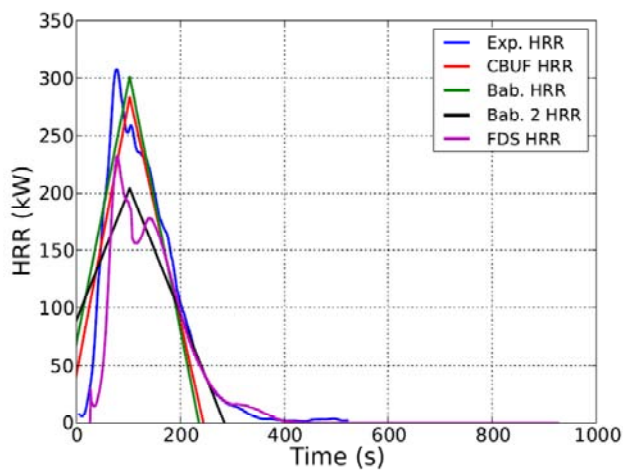


Figure G-4. SOM111CS1.

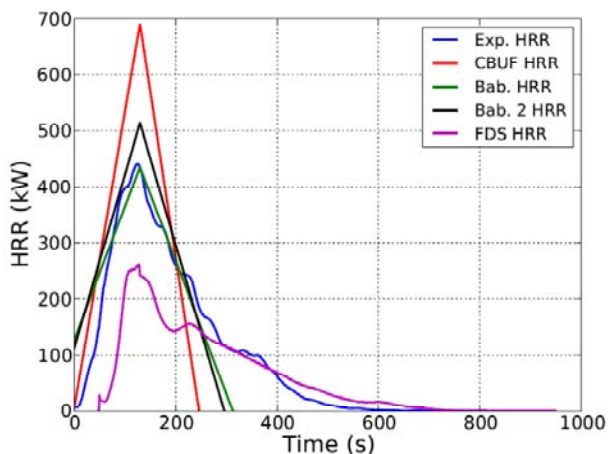


Figure G-5. SOM121CS1.

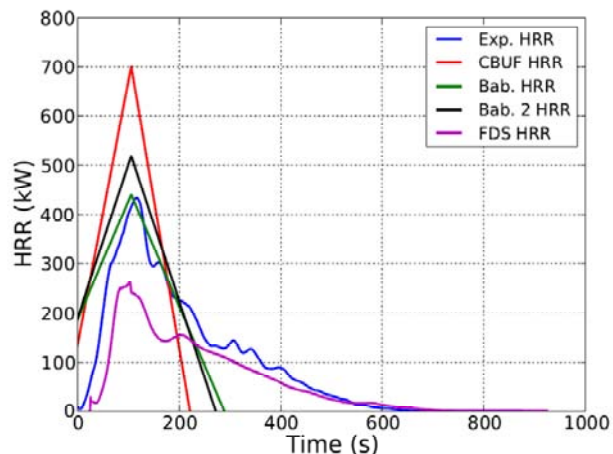


Figure G-6. SOM121CS2.

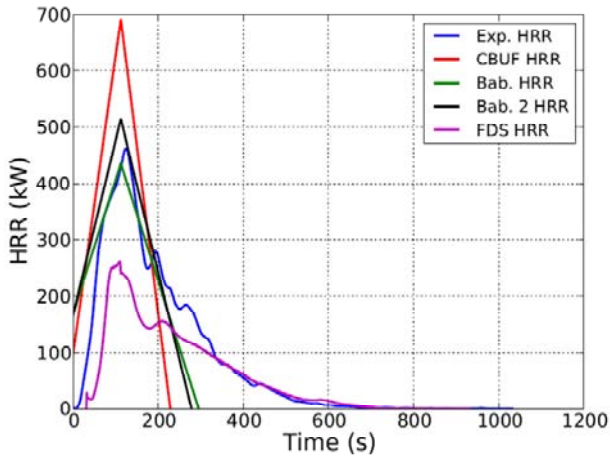


Figure G-7. SOM121CS3.

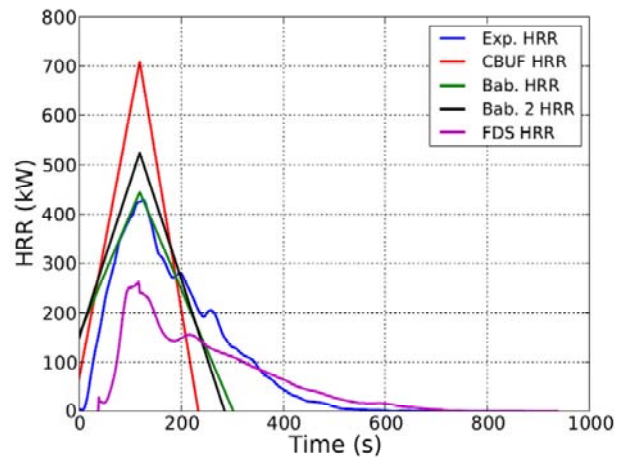


Figure G-8. SOM121CS4.

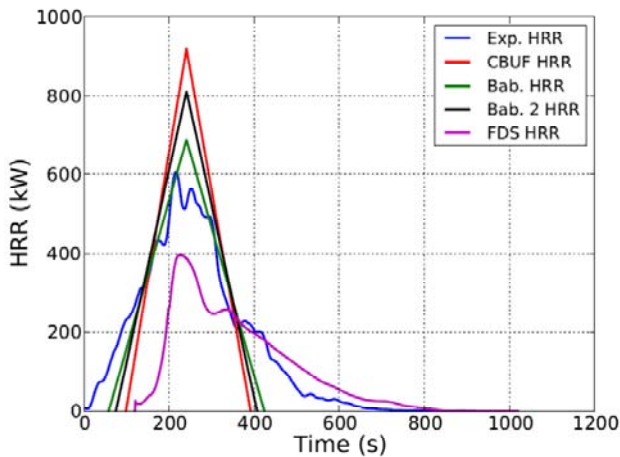


Figure G-9. SOM122CS1.

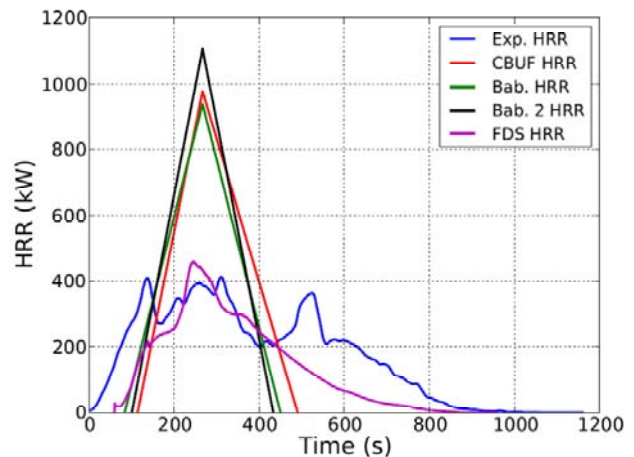


Figure G-10. SOM123CS1.

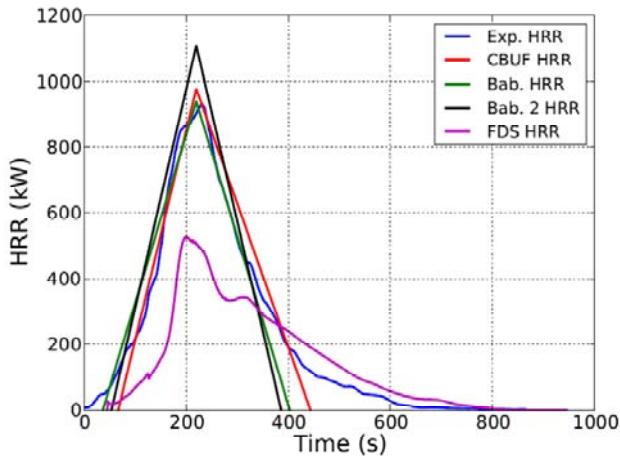


Figure G-11. SOM123CS2.

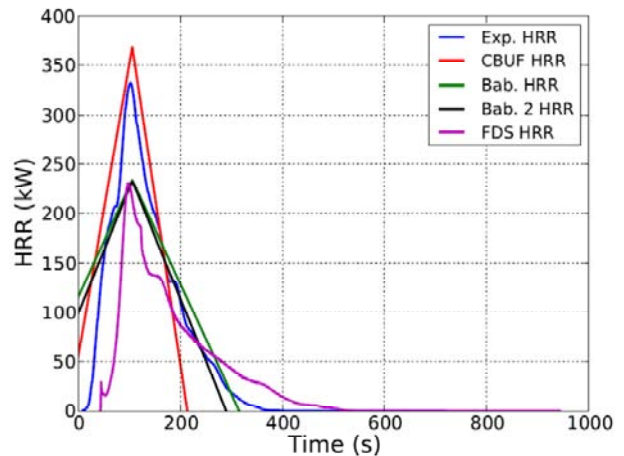


Figure G-12. SOM131CS1.

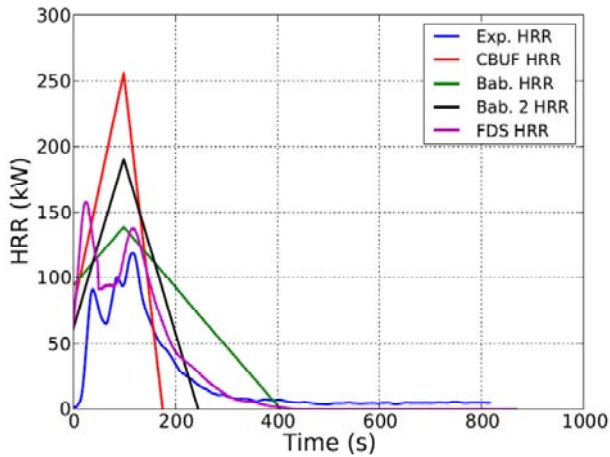


Figure G-13. SOM151CS1.

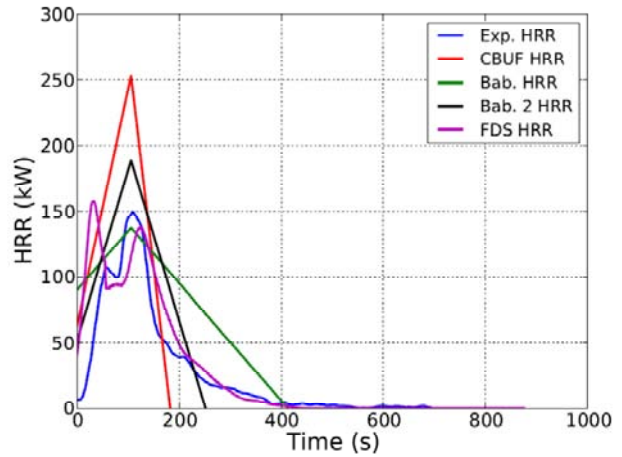


Figure G-14. SOM151CS2.

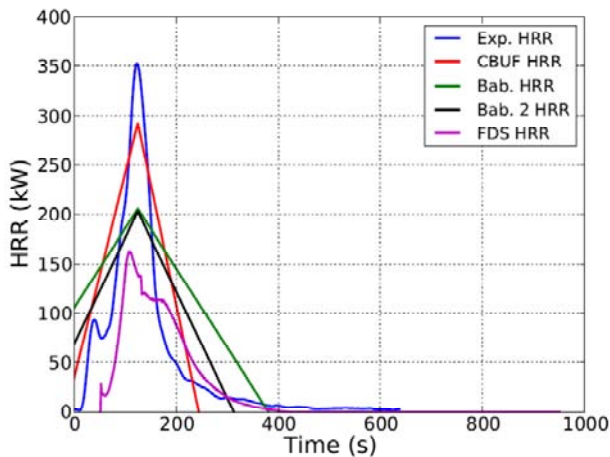


Figure G-15. SOM161CS1.

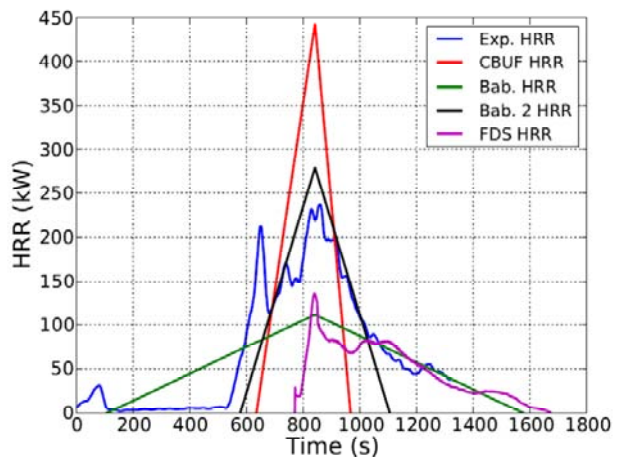


Figure G-16. SOM221CS1.

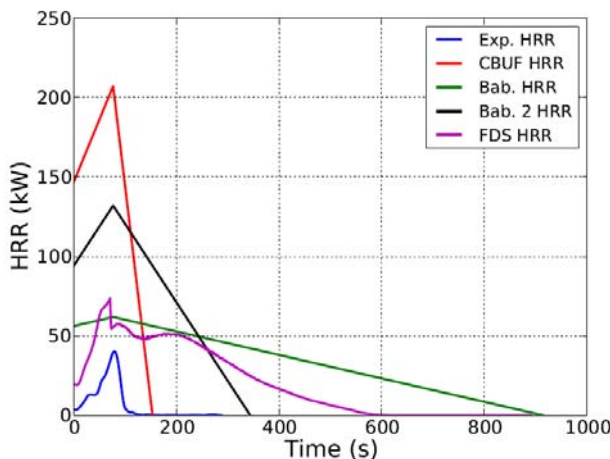


Figure G-17. SOM231CS1.

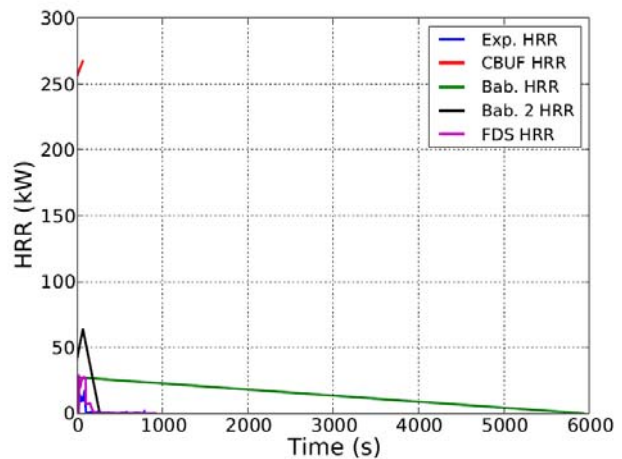


Figure G-18. SOM241CS1.

APPENDIX H

BURNING RATE PREDICTIONS FOR FRACTIONAL FACTORIAL DESIGN TESTS

(CONSISTING OF 6 PAGES)

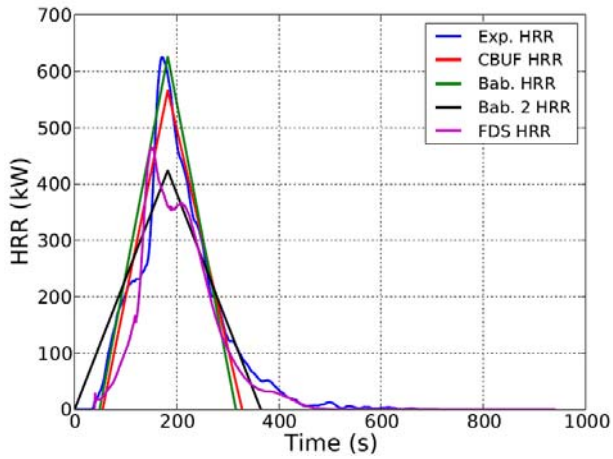


Figure H-1. LRM113AS1.

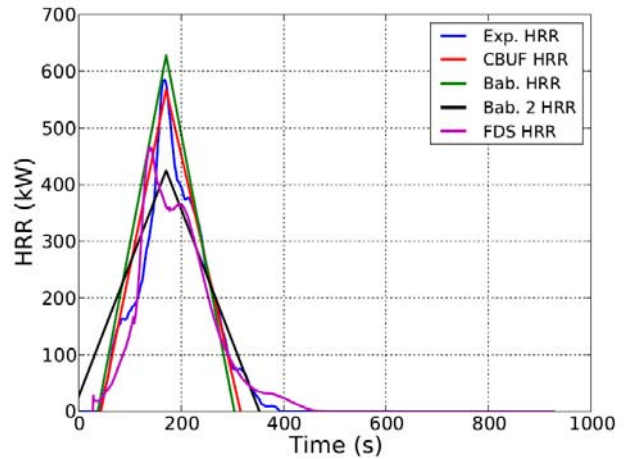


Figure H-2. LRM113AS2.

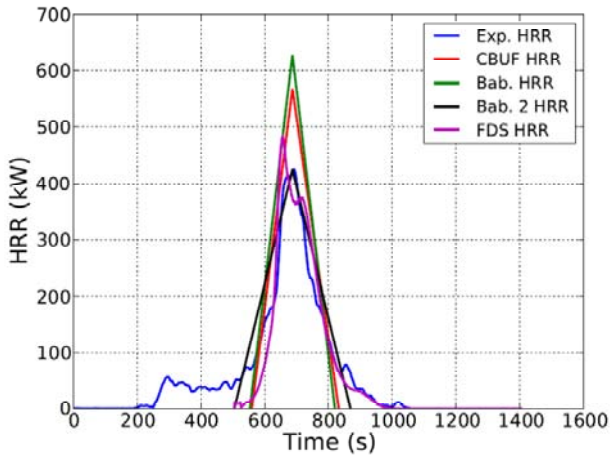


Figure H-3. LRM113BB1.

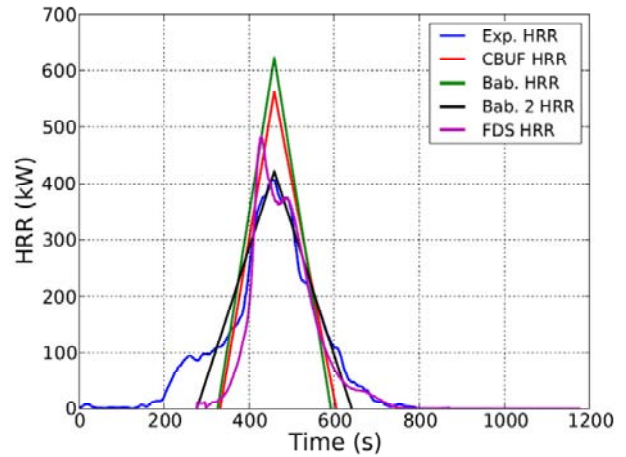


Figure H-4. LRM113BB2.

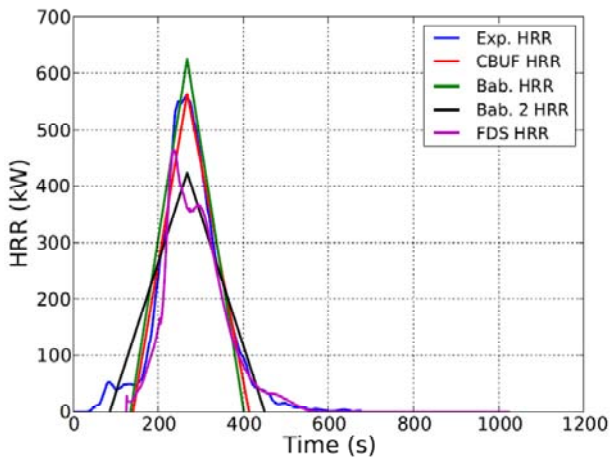


Figure H-5. LRM113CF1.

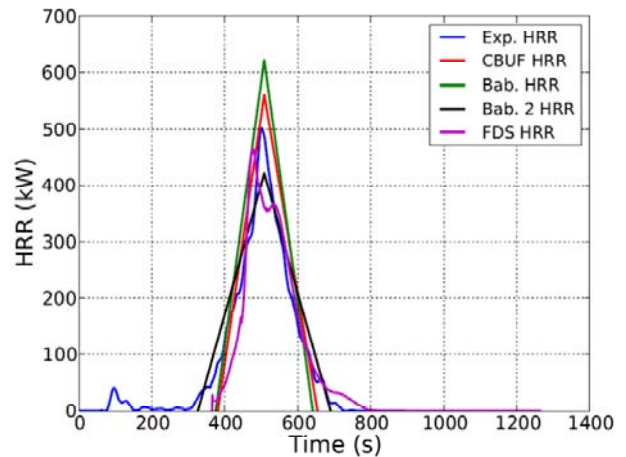


Figure H-6. LRM113CF2.

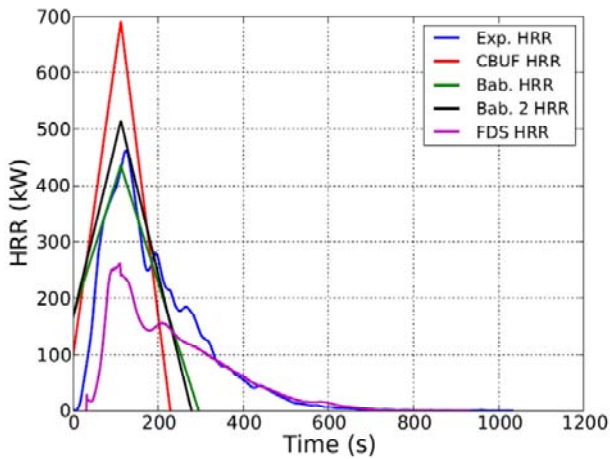


Figure H-7. LRM123AF1.

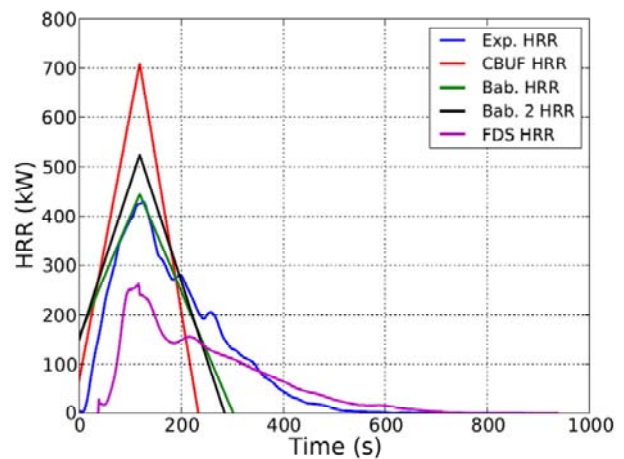


Figure H-8. LRM123AF2.

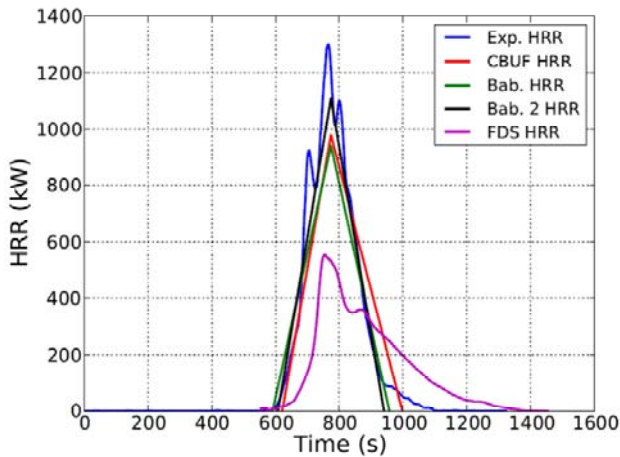


Figure H-9. LRM123BS1.

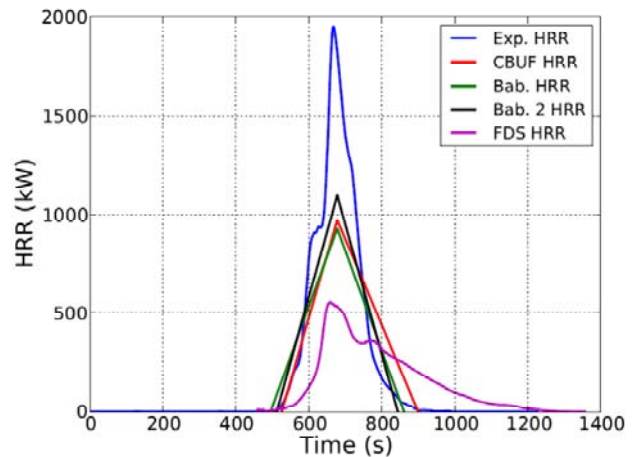


Figure H-10. LRM123BS2.

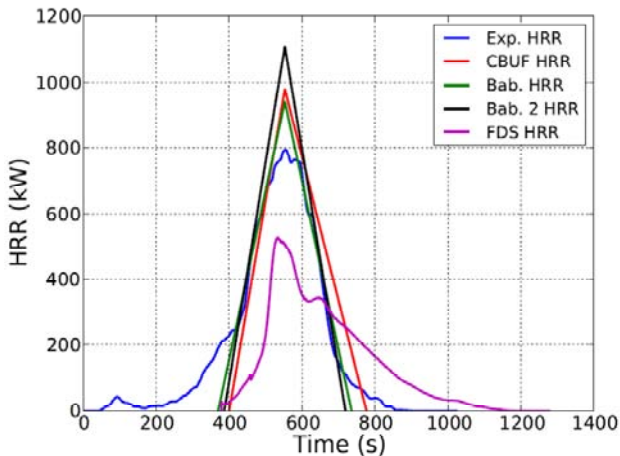


Figure H-11. LRM123CB1.

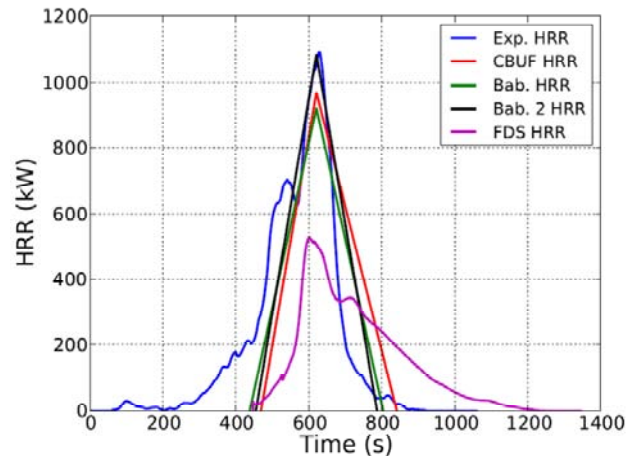


Figure H-12. LRM123CB2.

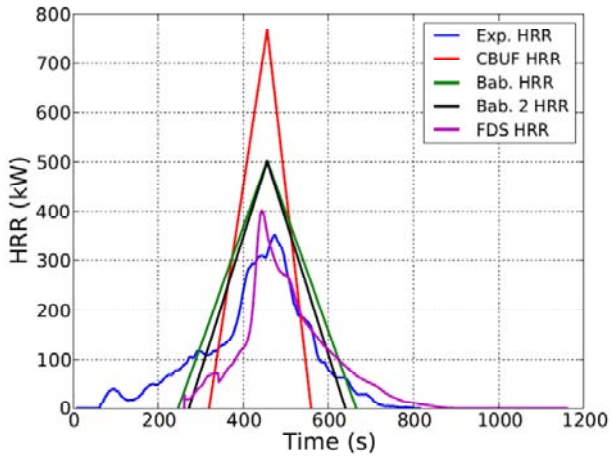


Figure H-13. LRM133AB1.

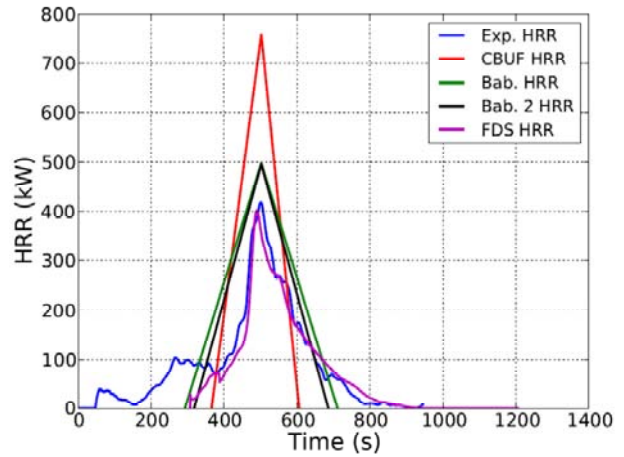


Figure H-14. LRM133AB2.

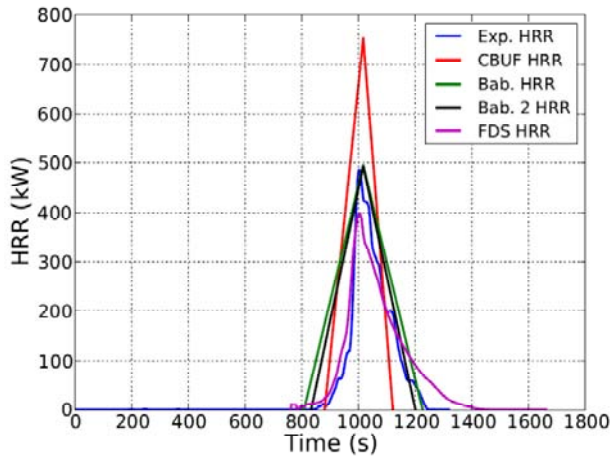


Figure H-15. LRM133BF1.

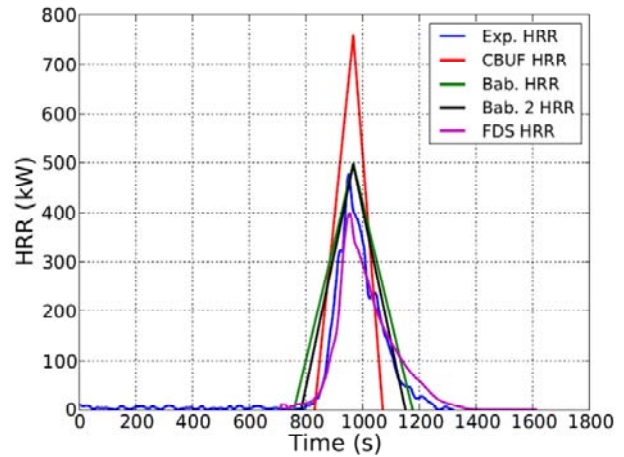


Figure H-16. LRM133BF2.

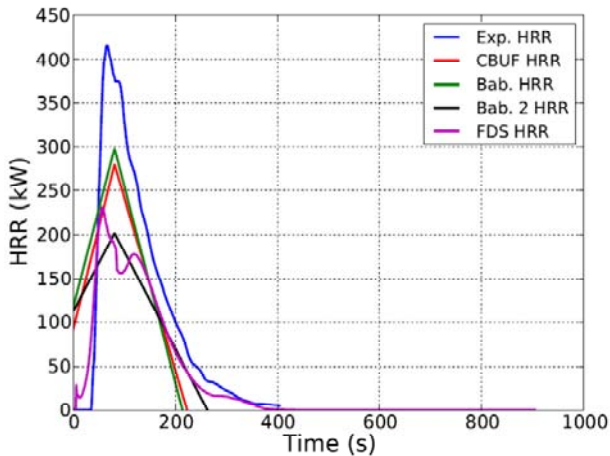


Figure H-17. SRM111AF1.

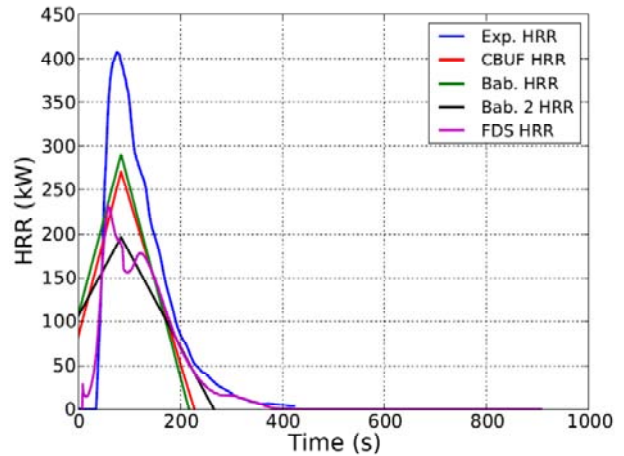


Figure H-18. SRM111AF2.

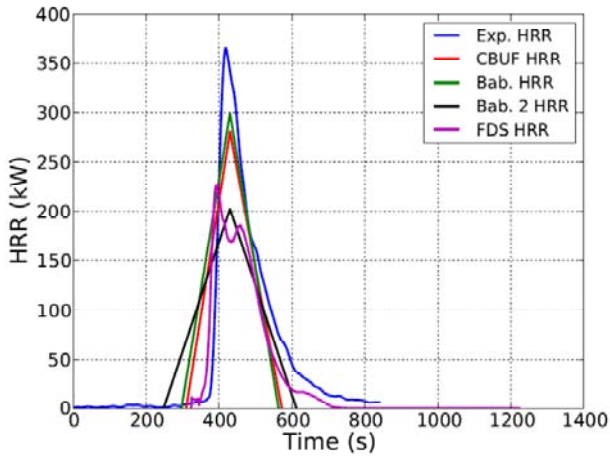


Figure H-19. SRM111BS1.

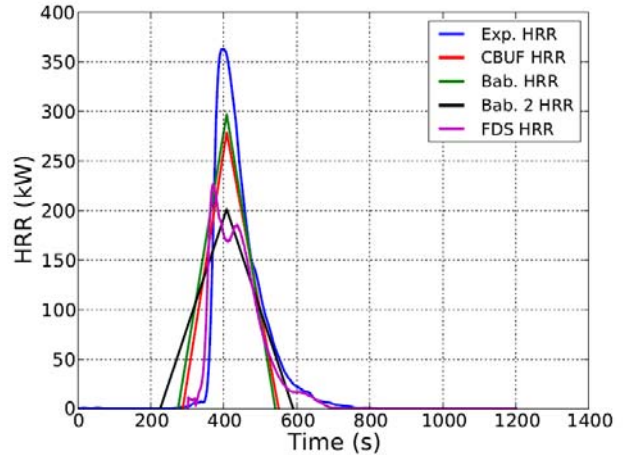


Figure H-20. SRM111BS2.

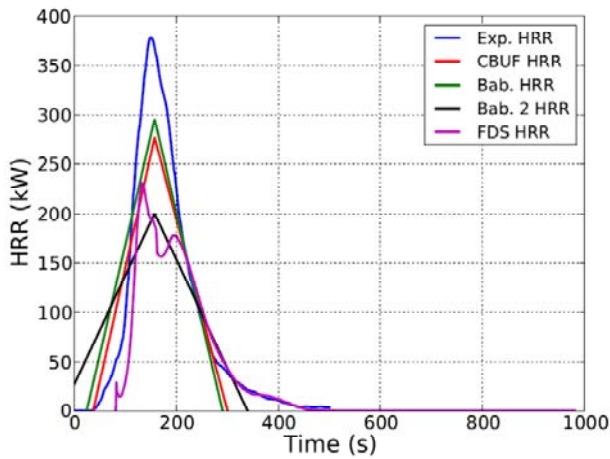


Figure H-21. SRM111CB1.

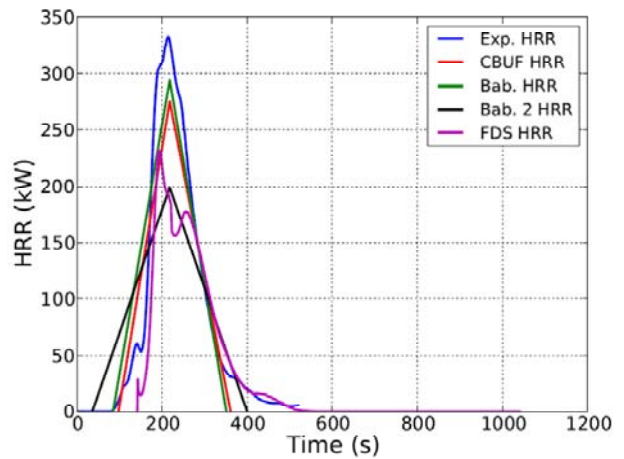


Figure H-22. SRM111CB2.

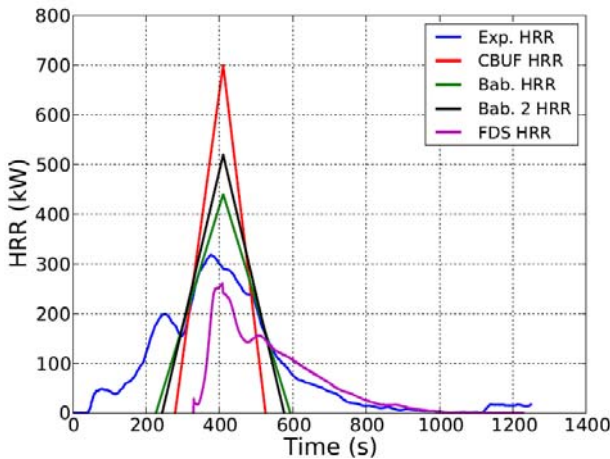


Figure H-23. SRM121AB1.

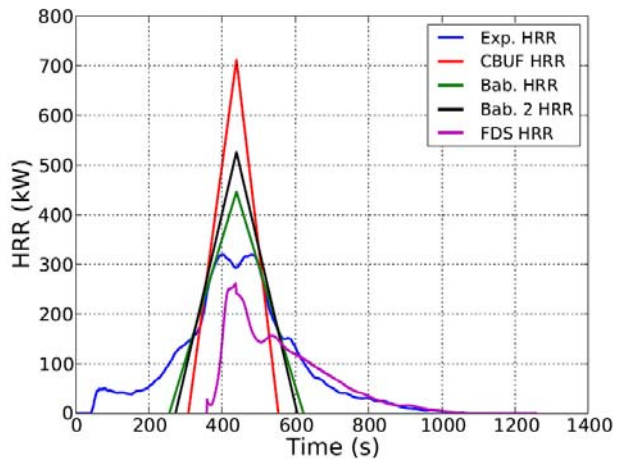


Figure H-24. SRM121AB2.

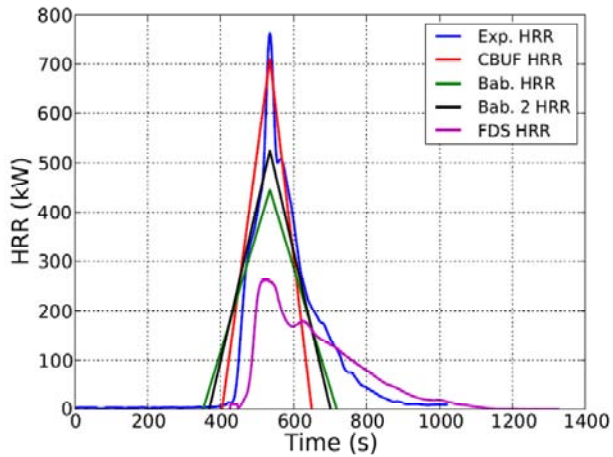


Figure H-25. SRM121BF1.

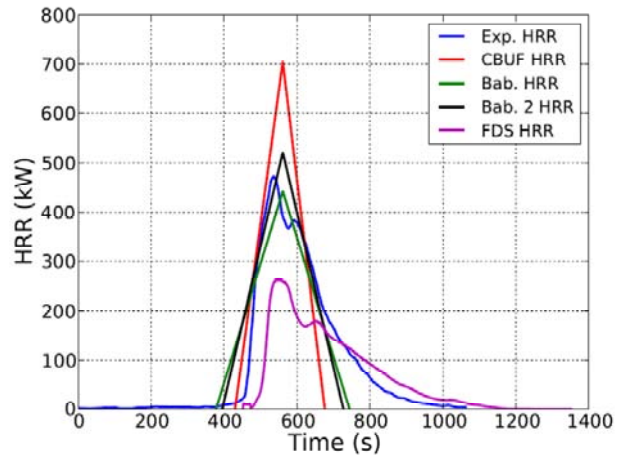


Figure H-26. SRM121BF2.

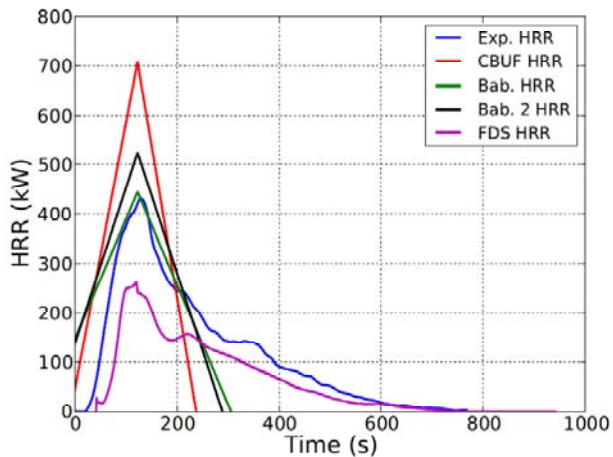


Figure H-27. SRM121CS1.

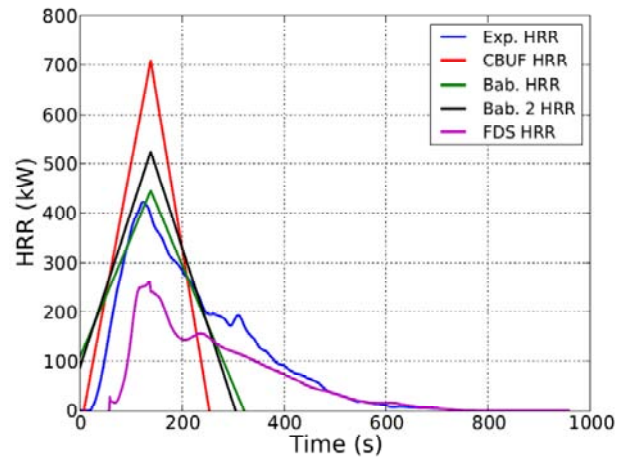


Figure H-28. SRM121CS2.

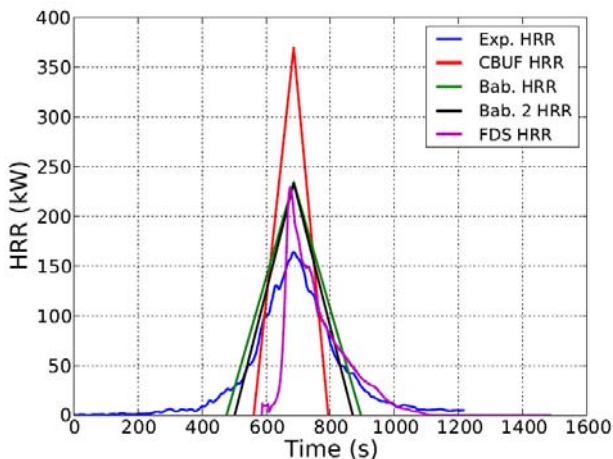


Figure H-29. SRM131BB1.

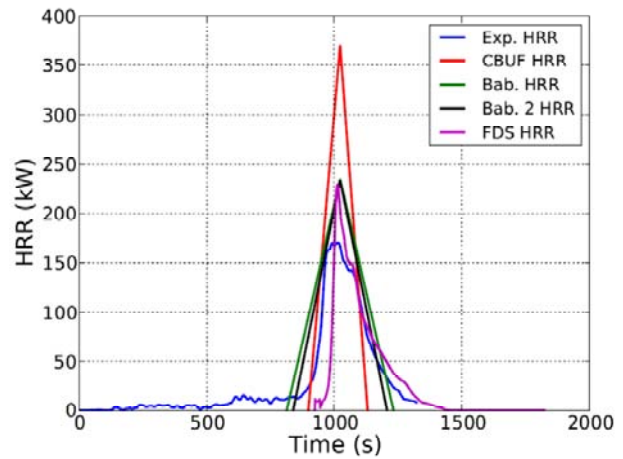


Figure H-30. SRM131BB2.

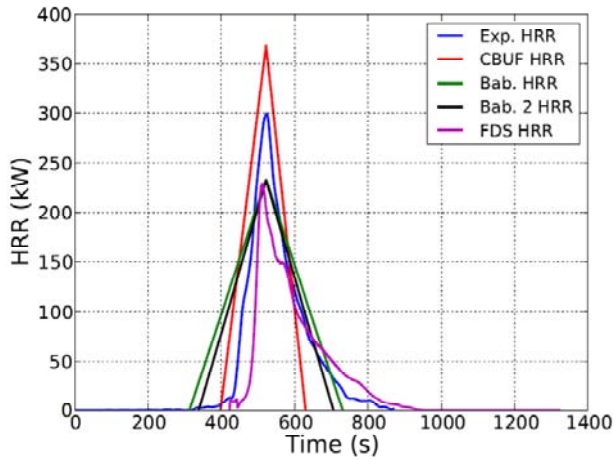


Figure H-31. SRM131BF1.

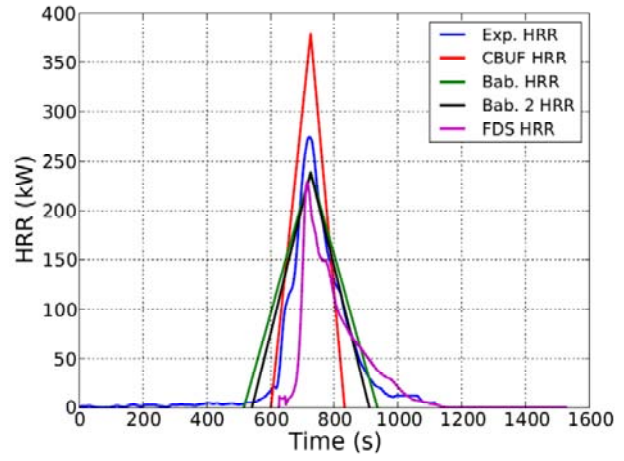


Figure H-32. SRM131BF2.

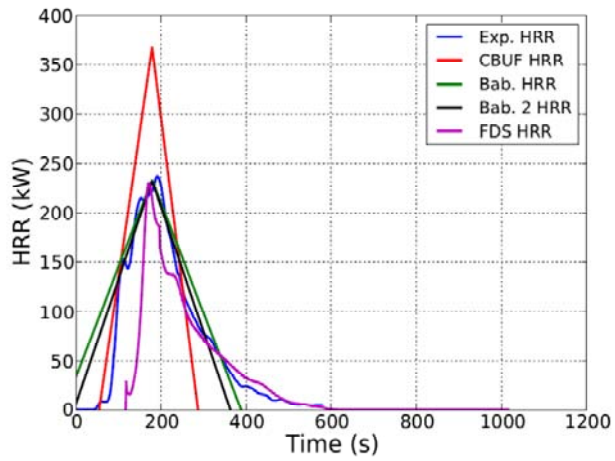


Figure H-33. SRM131CF1.

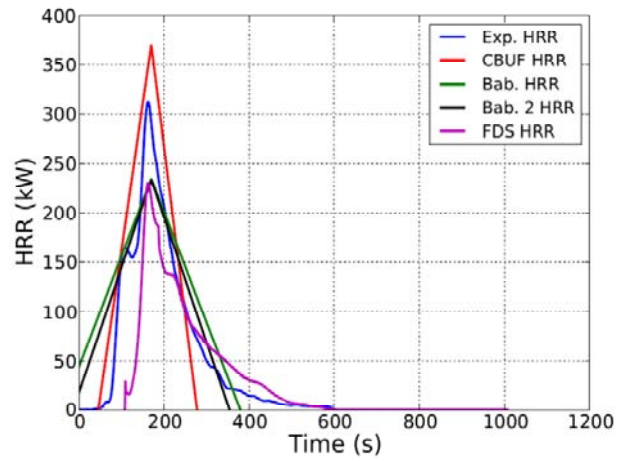


Figure H-34. SRM131CF2.

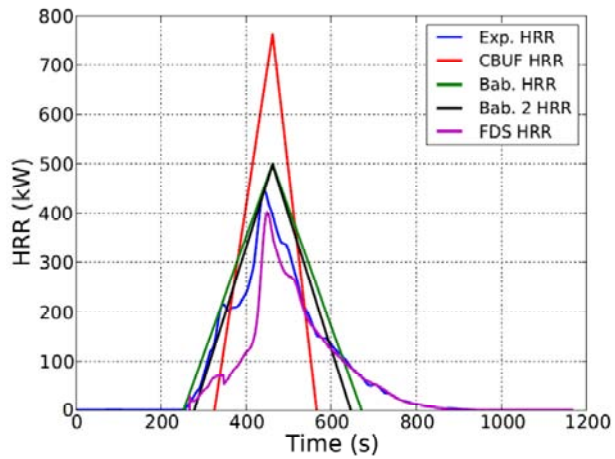


Figure H-35. SRM133CS1.

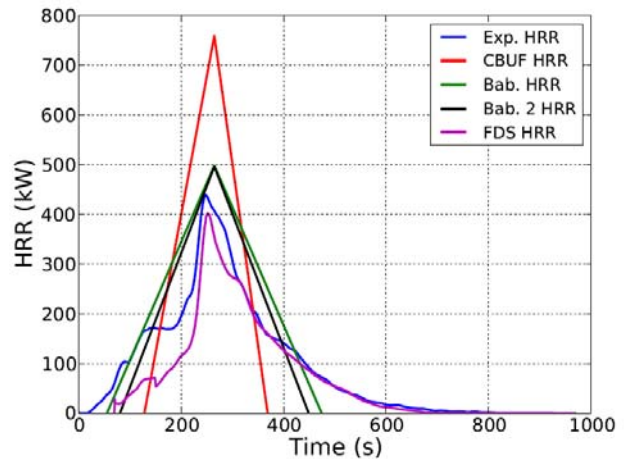


Figure H-36. SRM133CS2.

APPENDIX I

BURNING RATE PREDICTIONS FOR REMAINING ROOM CALORIMETER MOCKUP TESTS

(CONSISTING OF 5 PAGES)

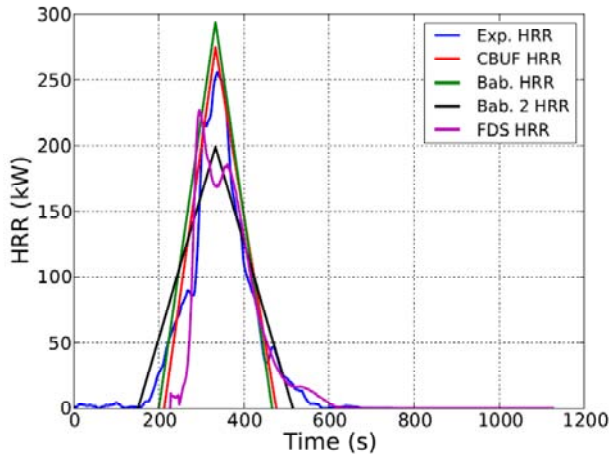


Figure I-1. LRM111BC1.

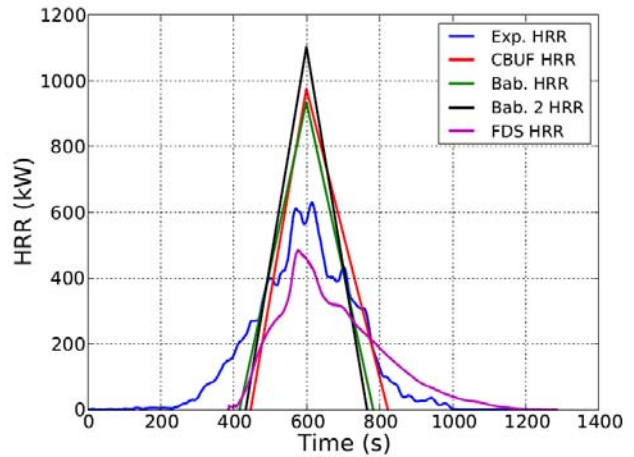


Figure I-2. LRM123BC1.

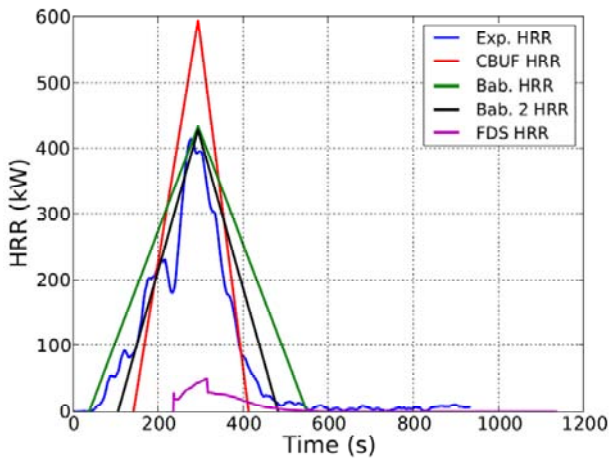


Figure I-3. LRM163CS1.

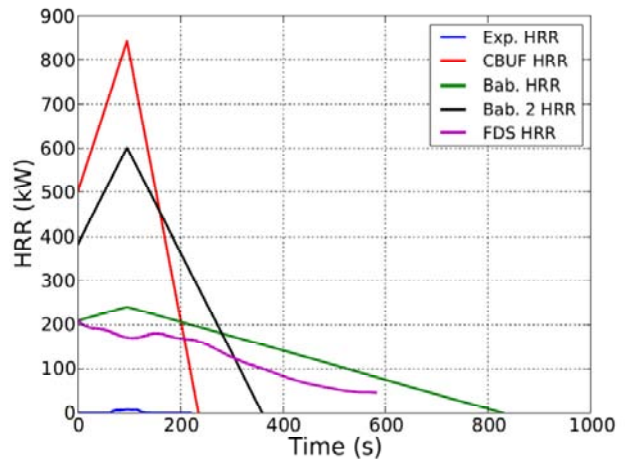


Figure I-4. LRM223AS1.

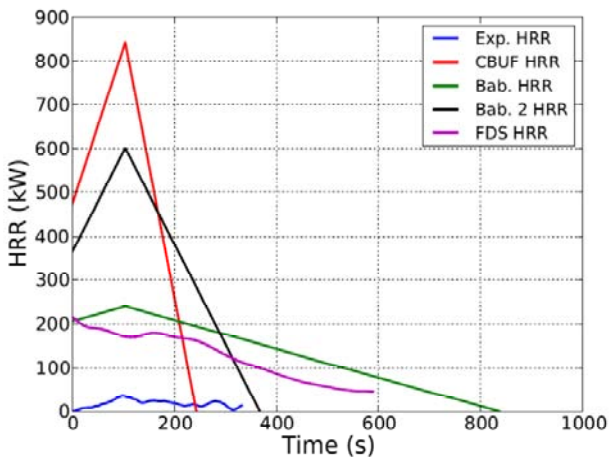


Figure I-5. LRM223CS1.

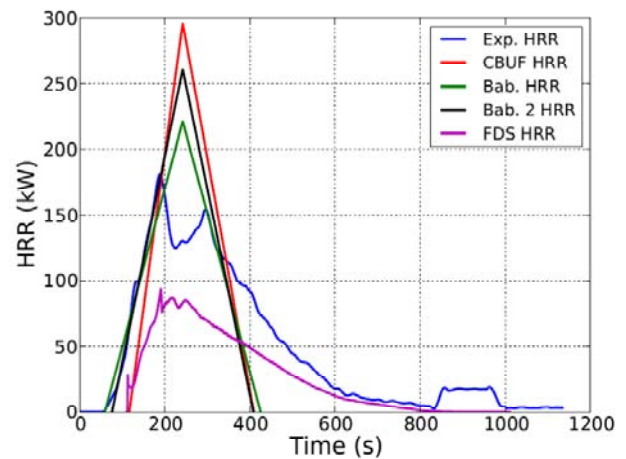


Figure I-6. SRM120CG1.

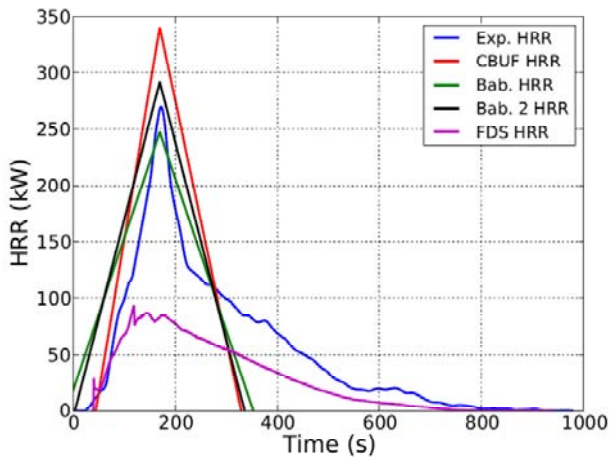


Figure I-7. SRM120CN1.

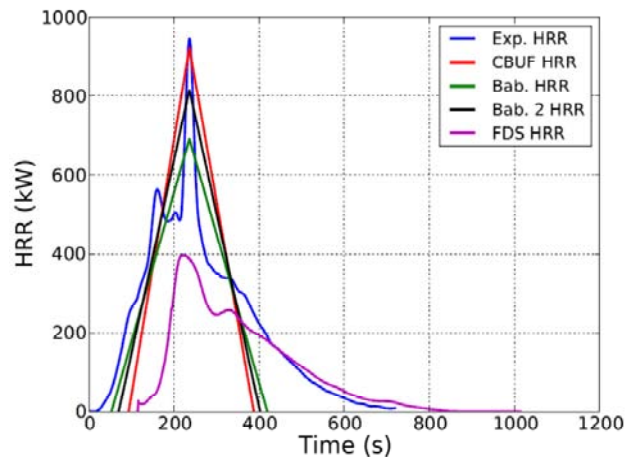


Figure I-8. SRM122CS1.

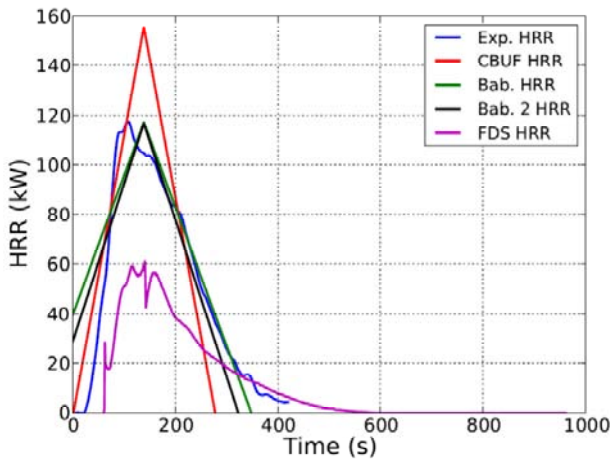


Figure I-9. SRM130CG1.

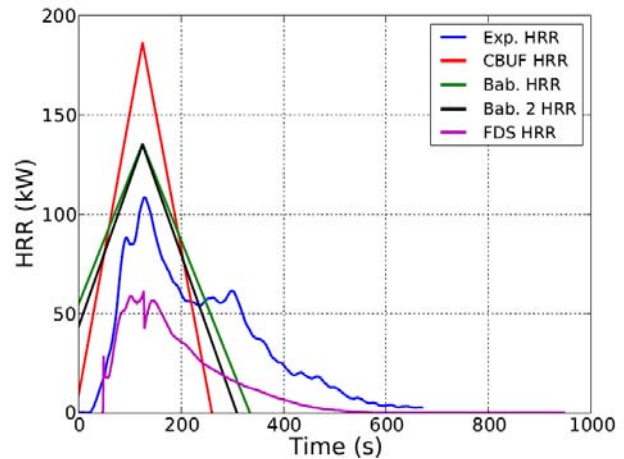


Figure I-10. SRM130CN1.

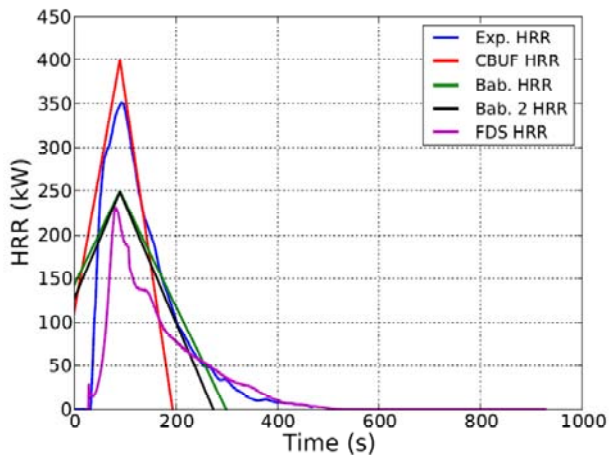


Figure I-11. SRM131AF1.

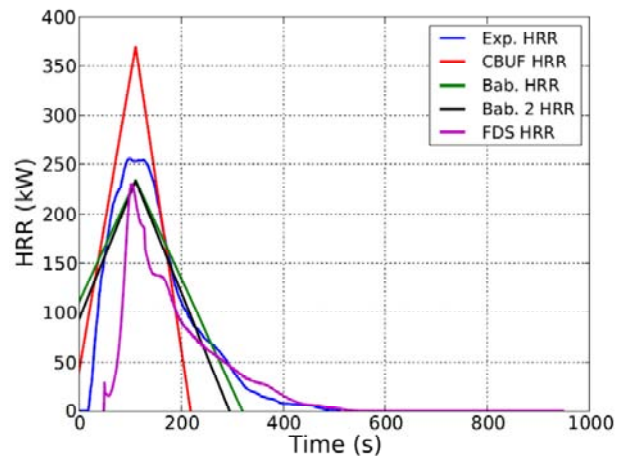


Figure I-12. SRM131AS1.

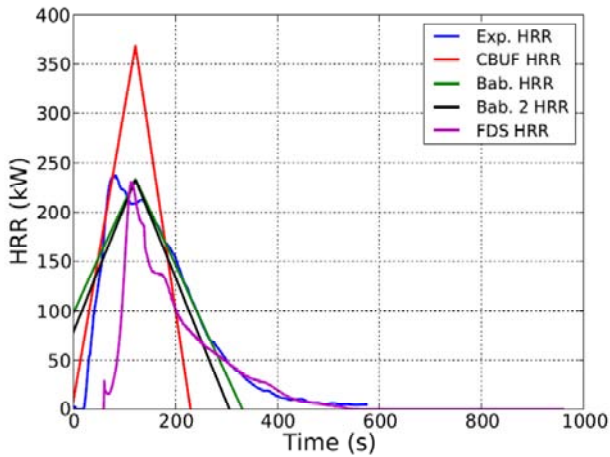


Figure I-13. SRM131AS2.

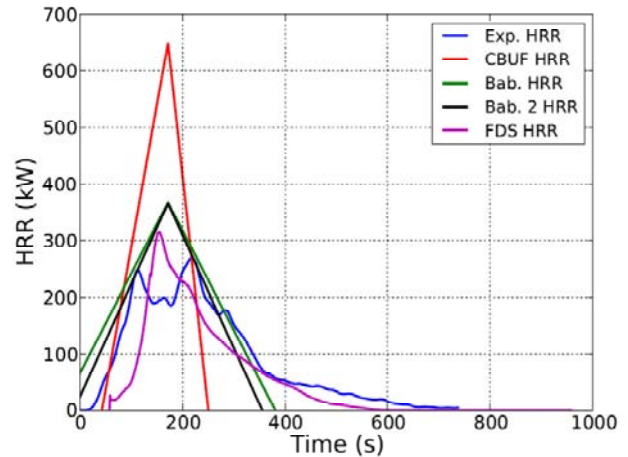


Figure I-14. SRM132CS1.

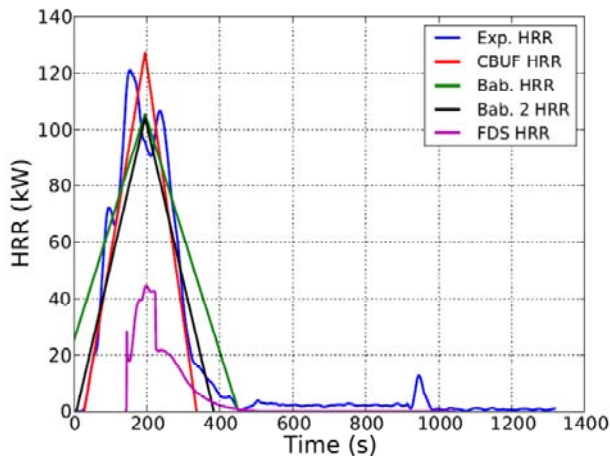


Figure I-15. SRM160CG1.

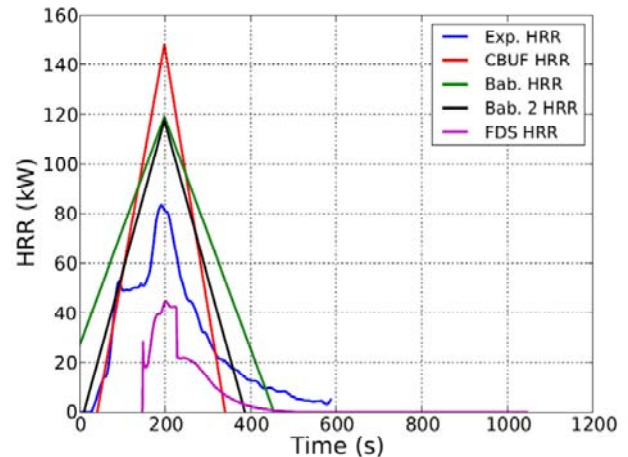


Figure I-16. SRM160CN1.

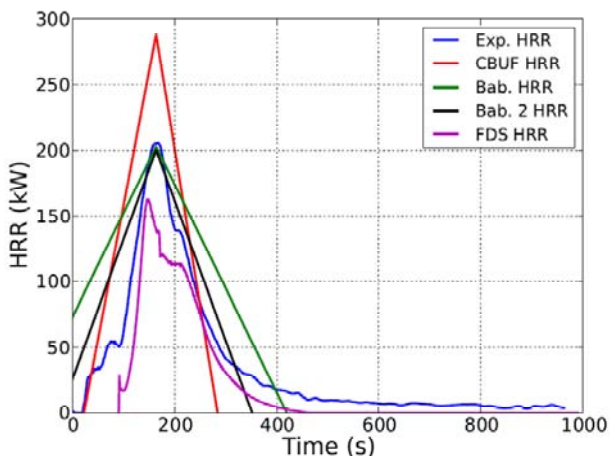


Figure I-17. SRM161AS1.

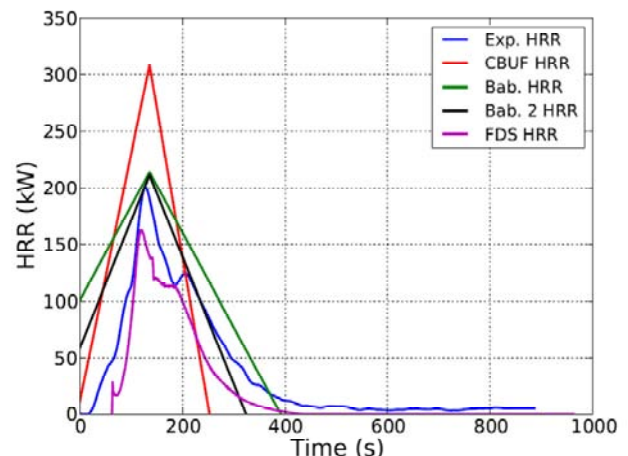


Figure I-18. SRM161CS1.

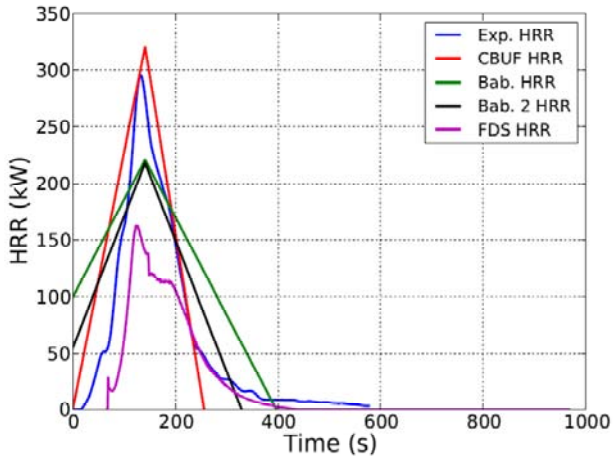


Figure I-19. SRM161CS2.

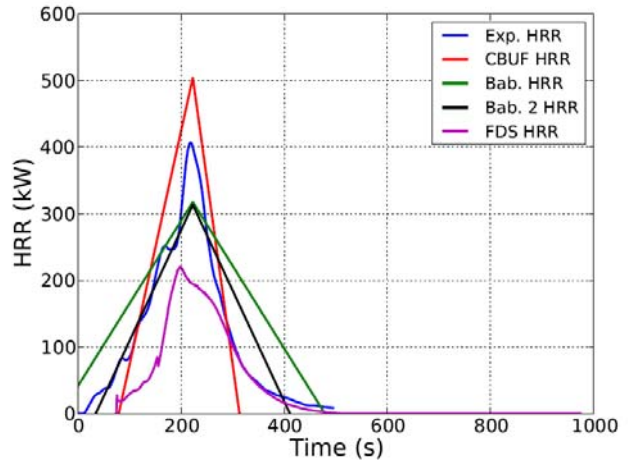


Figure I-20. SRM162CS1.

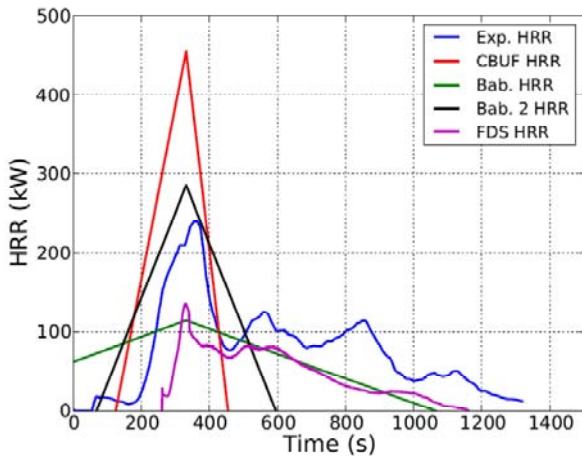


Figure I-21. SRM221AS1.

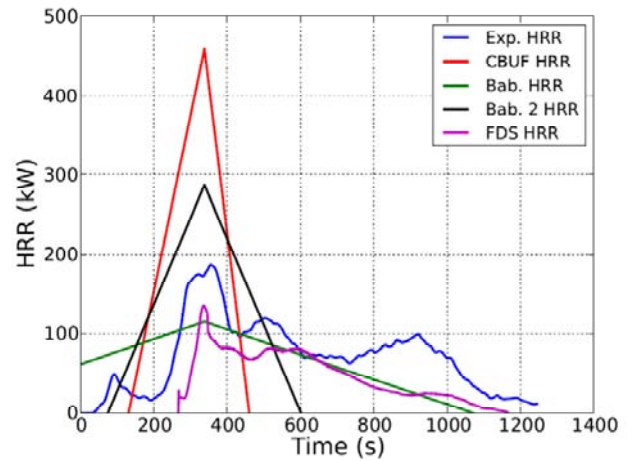


Figure I-22. SRM221CS1.

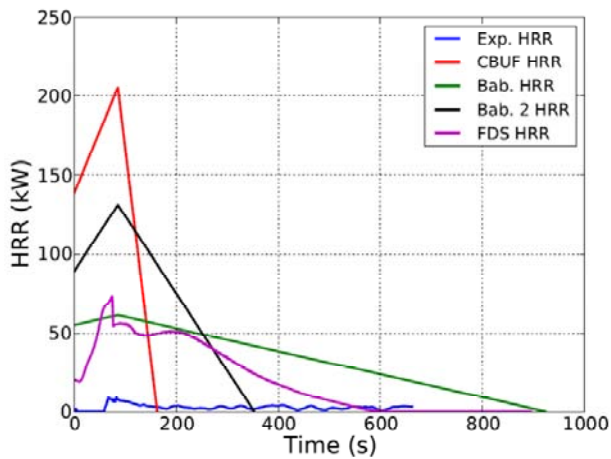


Figure I-23. SRM231AS1.

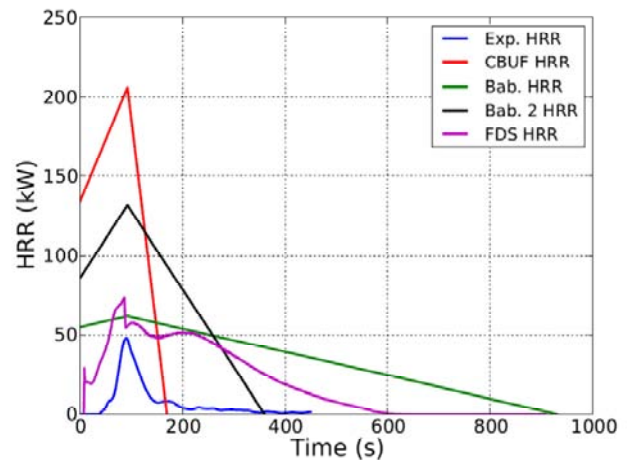


Figure I-24. SRM231CS1.

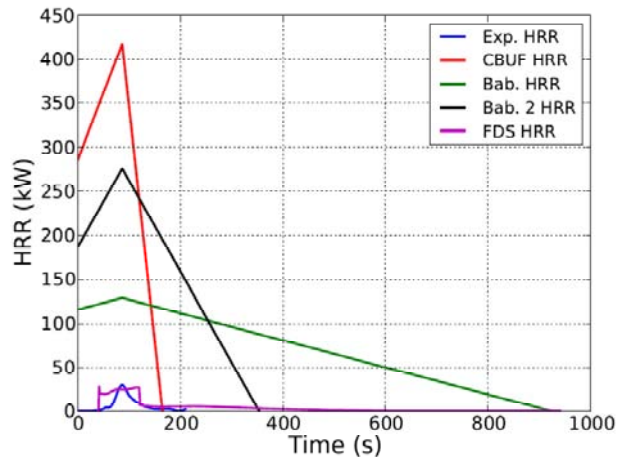


Figure I-25. SRM233CS1.

APPENDIX J

BURNING RATE PREDICTIONS FOR USED FURNITURE TESTS

(CONSISTING OF 5 PAGES)

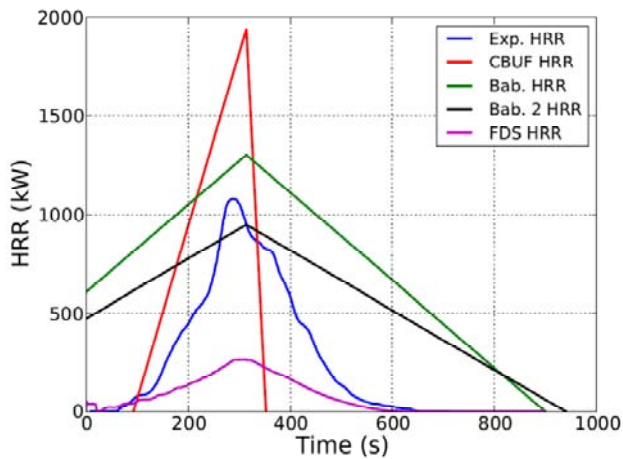


Figure J-1. LRU013AS1.

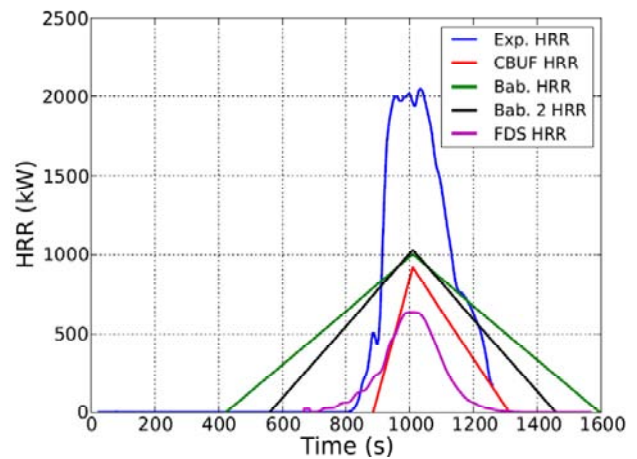


Figure J-2. LRU033BS1.

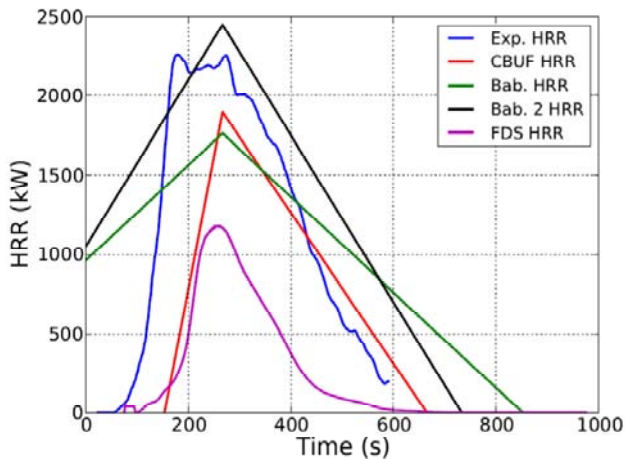


Figure J-3. LRU043AS1.

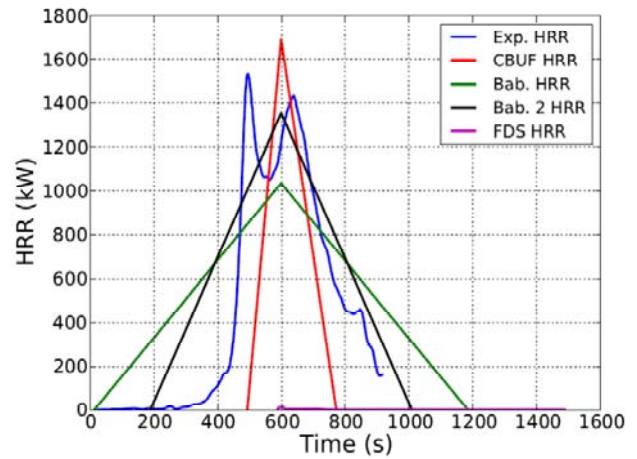


Figure J-4. LRU053BS1.

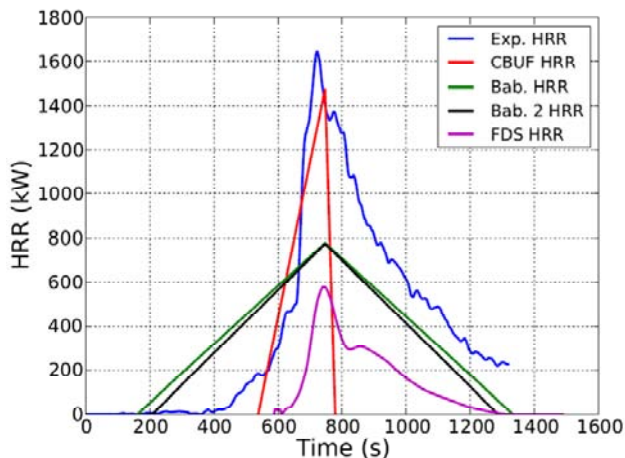


Figure J-5. LRU062BS1.

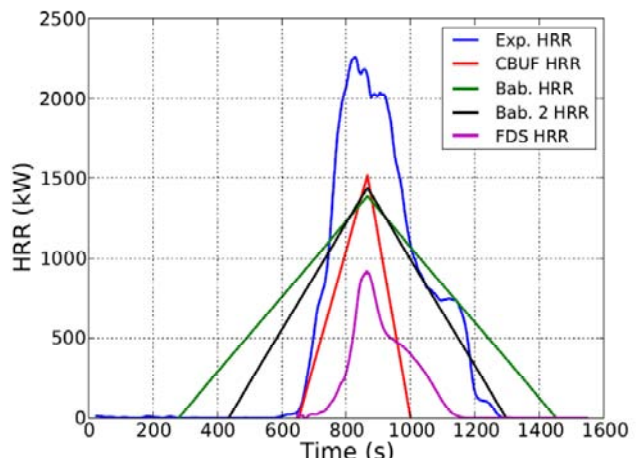


Figure J-6. LRU073BS1.

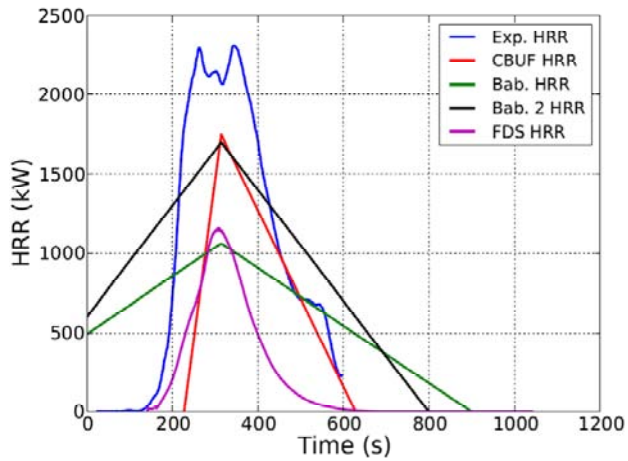


Figure J-7. LRU083BC1.

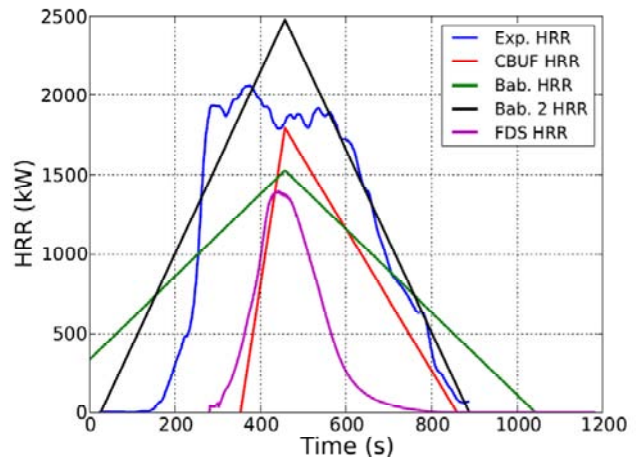


Figure J-8. LRU093BC1.

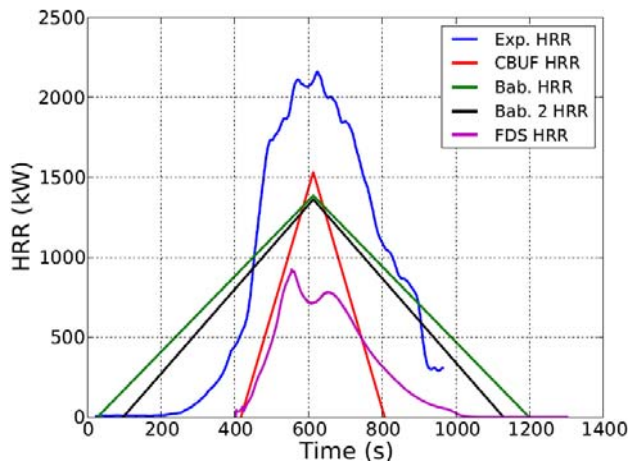


Figure J-9. LRU103BC1.

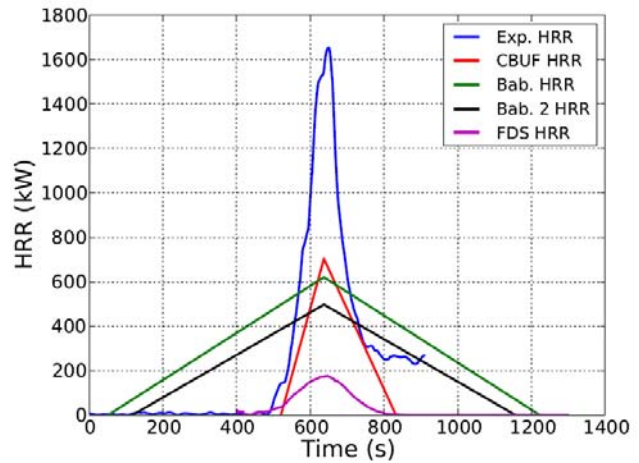


Figure J-10. LRU111BS1.

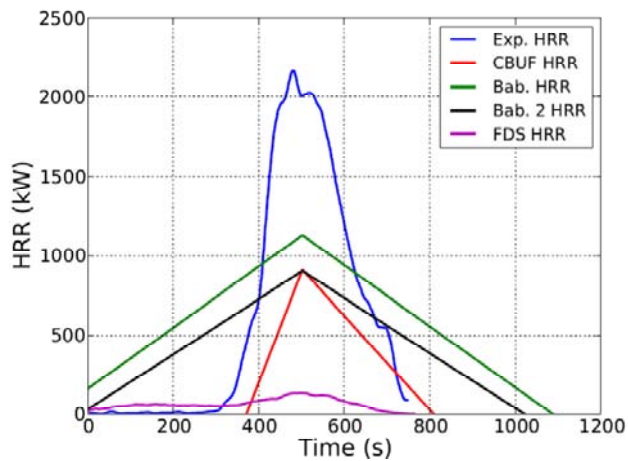


Figure J-11. LRU113BS1.

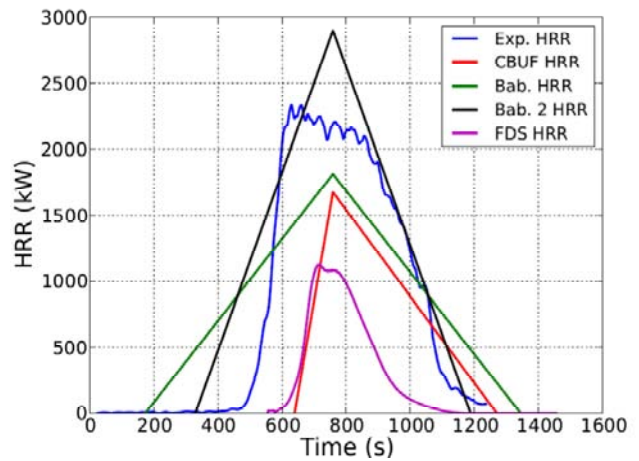


Figure J-12. LRU123BS1.

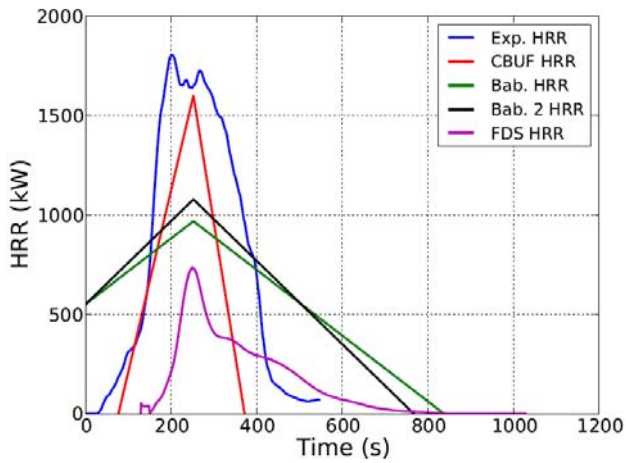


Figure J-13. LRU132AS1.

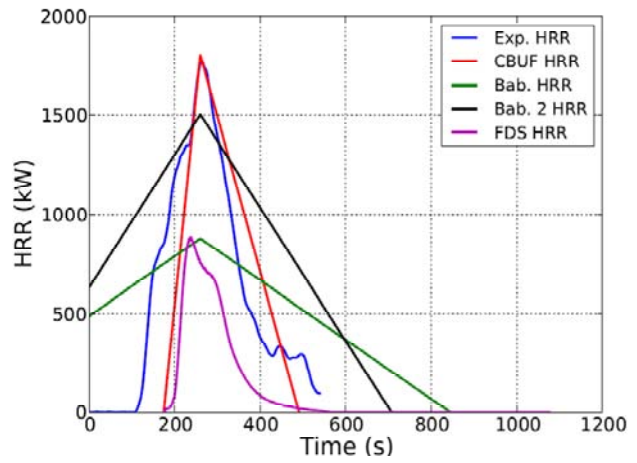


Figure J-14. LRU141BS1.

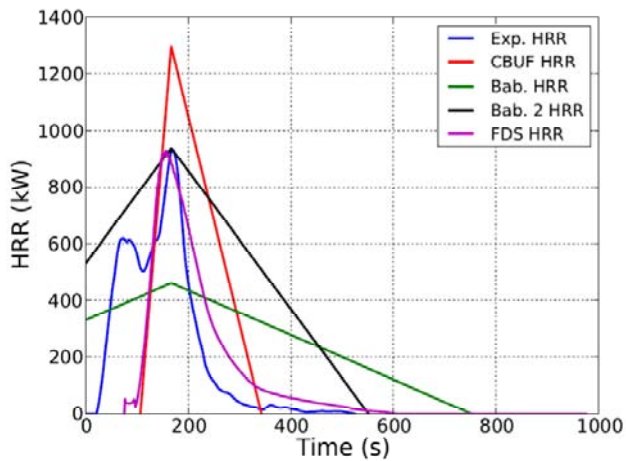


Figure J-15. LRU161AS1.

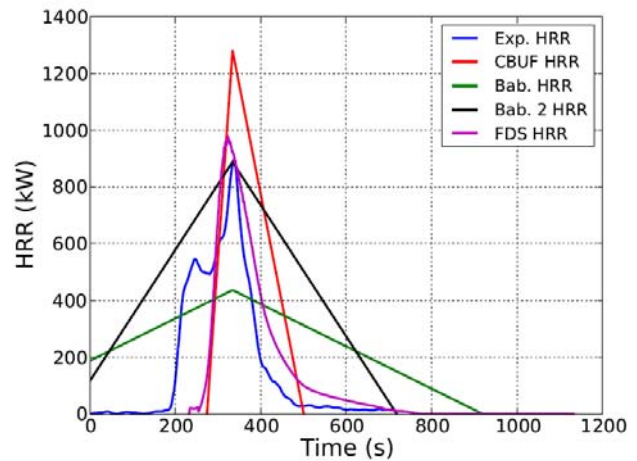


Figure J-16. LRU161BS1.

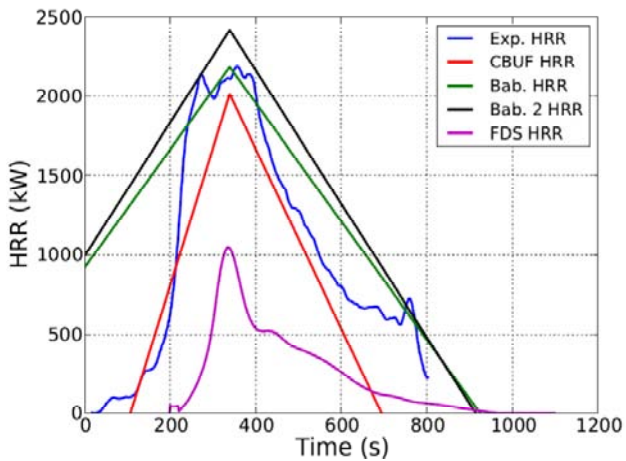


Figure J-17. LRU173AS1.

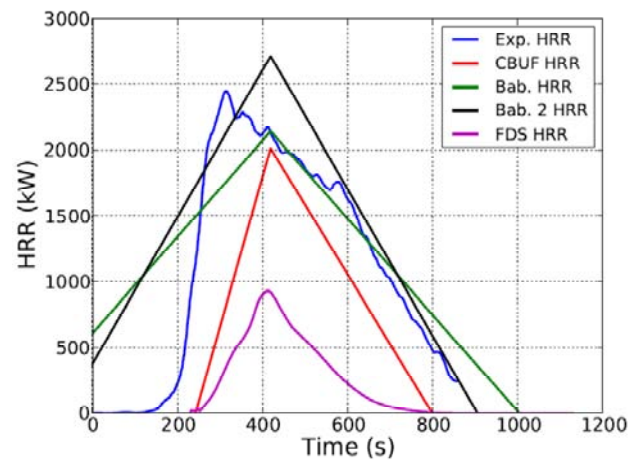


Figure J-18. LRU183BC1.

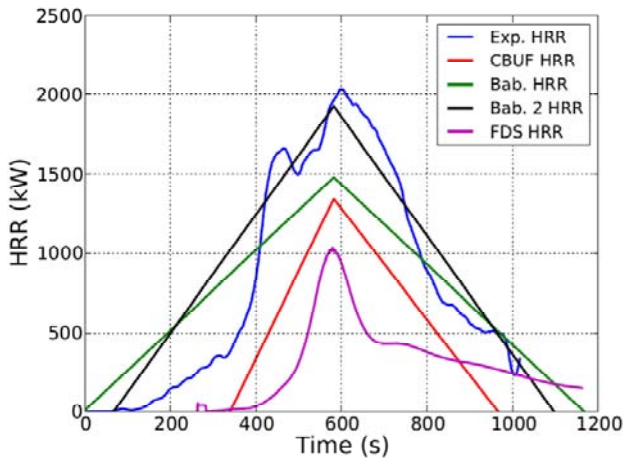


Figure J-19. LRU193AS1.

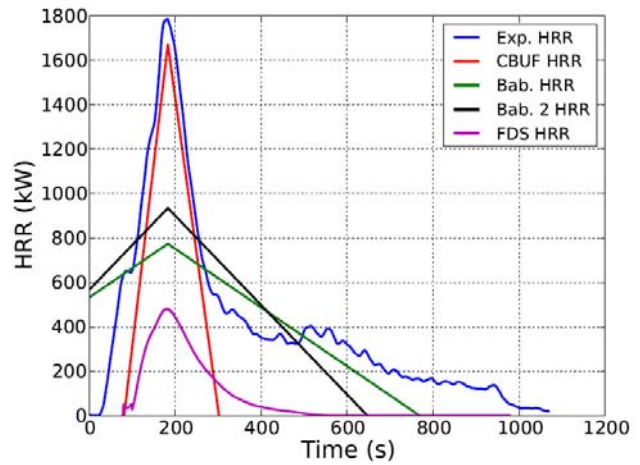


Figure J-20. LRU201AS1.

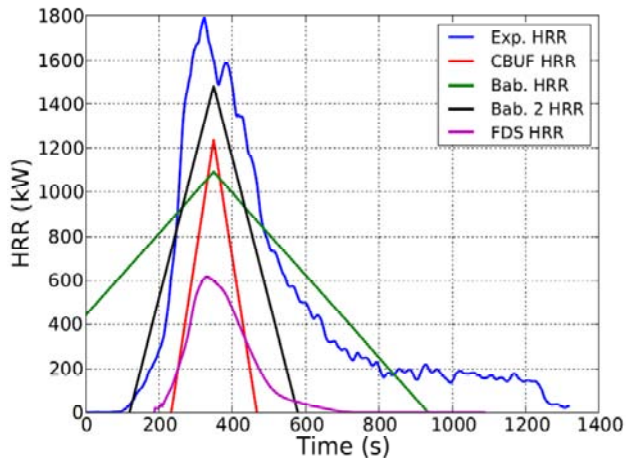


Figure J-21. LRU211BC1.

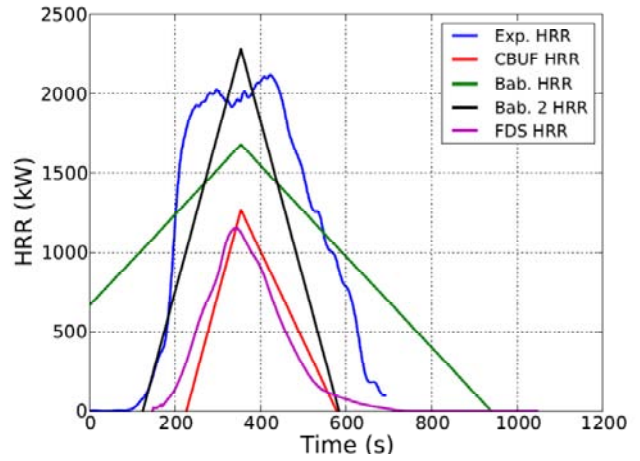


Figure J-22. LRU213BC1.

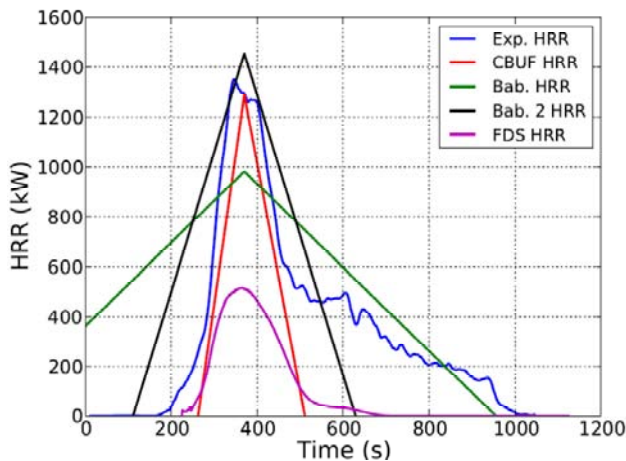


Figure J-23. LRU221BC1.

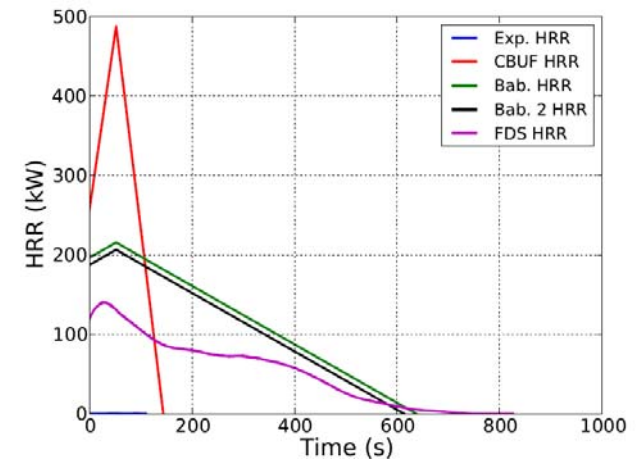


Figure J-24. SRU020BS1.

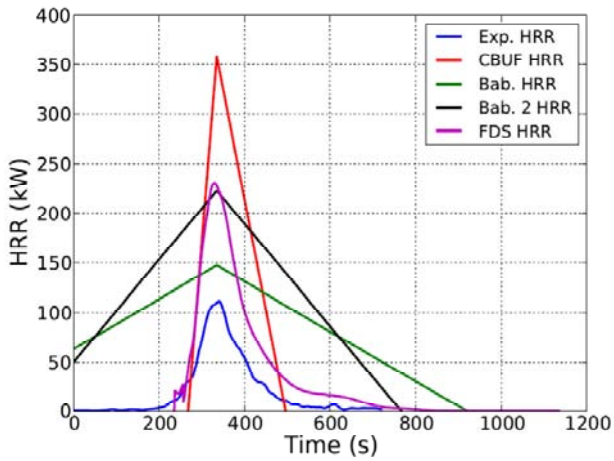


Figure J-25. SRU150BS1.

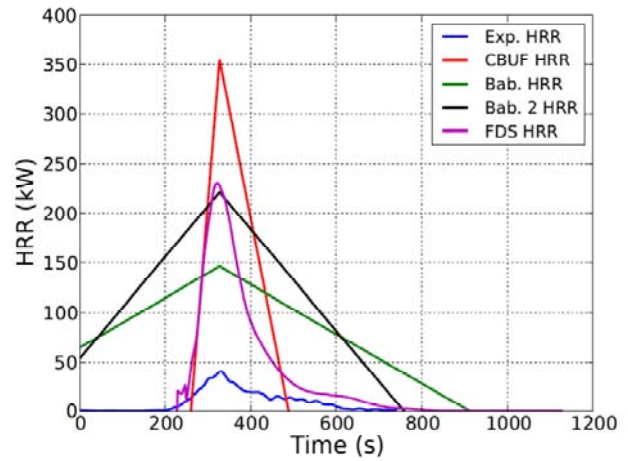


Figure J-26. SRU150BS2.

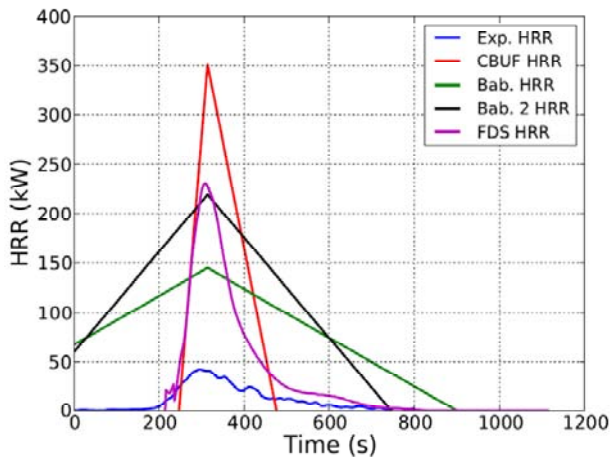


Figure J-27. SRU150BS3.